Dissertation zur Erlangung des Doktorgrades der Naturwissenschaften

(Dr. rer. nat) der Naturwissenschaftlichen Fakultät III -

Biologie und Vorklinische Medizin

der Universität Regensburg

DNA methylation in chromatin - complexes and mechanisms

durchgeführt am

Lehrstuhl für Biochemie III

der Universität Regensburg

vorgelegt von

Max F. Felle

aus Regensburg

Juni / 2009

TABLE OF CONTENT

LIST OF ABBREVIATIONS

Ax	absorbance at x nm
aa	amino acid
ACF	ATP-utilizing chromatin assembly and remodeling factor
Amp	ampicillin
APS	ammonium persulfate
ATP	adenosin-5´-triphosphate
bp	base pair
BRG1	Brahma-related gene product
BRM	Brahma protein
BSA	bovine serum albumine
°C	degrees Celsius
C-terminal	carboxy terminal
Ci	Curie
CpG	cytosine-phosphatidyl-guanosine
CHD	Chromodomain
CHIP	Chromatin Immunoprecipitation
CHRAC	Chromatin accessibility complex
Cpm	counts per minute
cryo-EM	cryo-electron microscopy
C-terminal	Carboxy-terminal
CV	Column volume
D	Drosophila
DEAE	Diethylaminoethyl
Da	Dalton
DMSO	dimethylsulfoxide
DNA	deoxyribonucleic acid
Dnmt1	DNA-cytosine-5-methyltransferase 1
Dnmt3a	DNA-cytosine-5-methyltransferase 3a
Dnmt3b2	DNA-cytosine-5-methyltransferase 3b2
dNTP	2'-deoxynucleotide triphosphate
DTT	dithiothreitol
DREX	Drosophila embryo extract
E. coli	Escherichia coli
EDTA	ethylenediaminotetraacetate
EGTA	ethylenglycole-bis(aminoethyleter)-N,N,N´,N´-tetra acidic acid
EMSA	electrophoretic mobility shift assay
EST	expressed sequence tag
EtBr	ethidium bromide
EYFP	enhanced yellow fluorescent protein

I

FCS	fetal calf serum
Fig.	Figure
His-tag	hexahistidine tag
IPTG	isopropylthiogalactoside
g	gram or relative centrifugal force
GST	glutathione-S-transferase
GOI	gene of interest
h	human
H1 / H2A / H2B / H3 / H4	histone proteins
HAT	Histone acetyl-transferase
HMT	Histone methyl-transferase
HDAC	histone deacetylase
Ig	immunoglobulin
IP	immunoprecipitation
ISWI	Imitation of switch
kDa	Kilo daltons
LB	Luria-Bertani
m	mouse
M	molar
MALDI	matrix-assisted laser desorption/ionization
MNase	Micrococcus Nuclease
MW	molecular weight
MWCO	molecular weight cut off
N-terminal	amino terminal
Ni-NTA	nickel-nitroacetic acid
NoRC	nucleolar remodeling complex
ODx	optical density at x nm
ORF	open reading frame
PAA	polyacrylamide
PBS	phosphate buffered saline
PCR	polymerase chain reaction
PEG	polyethylene glycol
pET	plasmid for expression by T7 RNA polymerase
POI	protein of interest
Pfu	Pyrococcus furiosus
rec	recombinant
RT	room temperature
rDNA	ribosomal DNA
PMSF	phenylmethylsulfonyl fluoride
RNA	ribonucleic acid
rpm	revolutions per minute
RT	room temperature
sec	second

Sf21	Spodoptera frugiperda 21 cells
Snf	Sucrose non-fermenter
Snf2h	Snf2 homolog protein
SWI	Mating type switching
SAM	S-adenosyl-methionine
SDS	sodium dodecyl sulfate
SDS-PAGE	sodium dodecyl sulfate polyacrylamide gel electrophoresis
Tab.	table
TBE	tris borate EDTA
Taq	Thermus aquaticus
TCA	trichloroacetic acid
TCS	tissue culture supernatant
TCL	tissue culture lysate
TE	Tris EDTA
TEMED	N,N,N',N'-tetramethylethylenediamine
Tip5	TTF-I interacting protein 5
Tris	tris(hydroxymethyl)aminomethane
TS domain	targeting sequence domain
TSS	transcription start site
U	unit
UV	ultraviolet
WCE	whole cell extract
wt	wild-type

The common abbreviations are used for prefices, chemical and physical units, chemical elements, essential amino acids as well as for the bases occurring in DNA.

SUMMARY

The DNA in the eukaryotic genome is packaged into chromatin whose basic repeating unit is the nucleosome consisting of 147bp of DNA wrapped around an octameric histone core. The histone octamer is composed of two copies of each of the four histone proteins H2A, H2B, H3 and H4.

DNA methylation is an epigenetic mechanism that is involved in various important processes in the cell such as differentiation and proliferation, transcriptional regulation, genomic imprinting, X-chromosome inactivation, silencing of repetitive elements, maintenance of genomic stability and DNA repair. In the mammalian genome, DNA methylation occurs almost exclusively in the context of CpG di-nucleotides and is brought about by three DNA cytosine-5-methyltransferases that use S'adenosyl-methionine (SAM) as methyl-group donor. Due to Dnmt1's preferential activity towards hemi-methylated DNA and the fact that it restores methylation patterns on the newly synthesized daughter strand during replication, it is referred to as the *maintenance* DNA methyltransferase, whereas the *de novo* DNA methyltransferases Dnmt3a and Dnmt3b introduce new methylation marks in the genome. Dnmt3L is structurally related but catalytically inactive and serves as a cofactor for Dnmt3a and Dnmt3b.

Importantly, DNA methylation is indispensible for mammalian embryogenesis and aberrant DNA methylation is often found concomitant with cancer. Dnmt1 was shown to be implicated in the formation of tumors, however the underlying mechanisms especially the question of Dnmt1 targeting remain largely unknown.

The goal of this thesis was to identify new Dnmt1 complexes from native tissues that would allow comparison of complex composition in tumors. ICBP90 (UHRF1) and USP7 were identified as interacting proteins from co-immunoprecipitation experiments. During the course of this study, UHRF1 was described not only to interact with Dnmt1 but to recruit Dnmt1 to replication foci during late S-phase. *In vivo* and *in vitro* immunoprecipitations revealed different possible complexes, namely Dnmt1/ICBP90, Dnmt1/USP7 and ICBP90/USP7. Furthermore, a possible trimeric complex of USP7 binding with two different domains to both Dnmt1 and ICBP90 was established. Notably, chromatin immunoprecipitation demonstrated the existence of different Dnmt1/ICBP90/USP7 complexes at four different loci *in vivo,* however the function in chromatin related processes awaits further investigation.

Interestingly, ICBP90 and USP7 are endowed with antagonistic enzymatic activities. ICBP90 exhibits autoubiquitinylation and ubiquitinylation activity towards histone H3, and USP7 *in vitro.* On the contrary, USP7 was able to target ICBP90 and histones H2A, H2B and H3 for deubiquitination *in vitro* whereas global levels of ubiquitinylated H2A and H2B were not changed upon knockdown or over-expression of USP7. Binding of ICBP90 and Dnmt1 to USP7 did not influence the *in vitro* activity of USP7. Moreover, Dnmt1 was ubiquitinylated by ICBP90 *in vitro,* but Dnmt1 protein or ubiquitinylation levels were not affected by USP7 over-expression or knockdown *in vivo.*

Future research will focus on the role of histone ubiquitinylation/deubiquitination in transcriptional repression and silencing of repetitive elements in heterochromatin.

SUMMARY

In another project, the properties of Dnmt binding to DNA and mono-nucleosomes and the principle mechanisms of DNA methylation in chromatin by the *de novo* DNA methyltransferases were in focus. It could be shown that Dnmt3a and Dnmt3b2 stably associated with DNA >35bp in length, albeit longer DNA fragments were preferred indicative of a cooperative binding process. Furthermore, binding to DNA or mono-nucleosomes was highly dynamic and the interaction of mono-nucleosomes with the *de novo* DNA methyltransferases did not disrupt mono-nucleosomes. Dnmt3a generally bound comparably well to DNA and mono-nucleosomes with different DNA linker length whereas Dnmt3b2 preferentially bound to free DNA and mono-nucleosomes with long linker DNA.

In vitro DNA methylation assays, either performed with radioactive SAM or non-radioactive one, but following single-molecule analysis with bisulfite treatment clearly demonstrated that Dnmt3a and Dnmt3b2 could not methylate DNA within the nucleosome but only linker DNA. This indicated that the DNA strand facing opposite the histone octamer did not represent a target for methylation and that nucleosomes constitute a major restriction for DNA methylation. Further experiments will address the role of chromatin remodeling enzymes in this process.

Dnmt3L, a stimulatory factor for Dnmt3a and Dnmt3b, was shown to bind to non-methylated H3K4. Therefore, the effect of Dnmt3L on binding to DNA and nucleosomes by Dnmt3a and Dnmt3b was analyzed. Dnmt3L itself neither bound to DNA nor to mono-nucleosomes in EMSA experiments. Addition of Dnmt3L to Dnmt3a and Dnmt3b enhanced DNA binding and modified the binding behavior towards nucleosomes.

Interestingly, recombinant Dnmt3L was tightly associated with nucleosomes when purified from Sf21 insect cells. Sucrose density gradient analysis confirmed this observation as Dnmt3L was distributed over the whole gradient with nucleosomal species of different weight. However, when endogenous nucleosomes were substituted for nucleosomal templates of various sizes or 'naked' DNA Dnmt3L entered the gradient by 1/3rd, although the peak fractions migrated at higher densities.

To unravel the reasons for the stable association of Dnmt3L with endogenous nucleosomes, future work will concentrate on the identification of possible loading factors, specific posttranslational histone modifications and nucleosomal architecture.

A INTRODUCTION

A.1 DNA and chromatin

The enormous length and complexity of eukaryotic genomes confronts the cells with several constraints. On the one hand, genomic DNA has to be compacted to fit into the nuclear sub-cellular compartment and on the other hand, genetic information has to be readily accessible. Furthermore, multi-cellular organisms require functional specialization of individual cells in united cell structures and thus differential gene expression. Cells meet these requirements by assembling the genome into a highly compact but dynamic structure termed chromatin, consisting of DNA and associated proteins (histones and non-histone proteins)(Olins and Olins 2003). The term chromatin (from the greek word 'chroma' for coloring) was first proposed in the 1880s when Walter Flemming observed a stainable substance in the cell nucleus. Noteworthy, there is evidence that besides proteins, RNA constitutes an integral component of chromatin regarding structure and stability (Rodríguez-Campos and Azorín 2007).

Chromatin presents the natural substrate for all kinds of DNA-dependent processes such as the control of gene expression as well as DNA replication, recombination and repair (Felsenfeld and Groudine 2003; Khorasanizadeh 2004). Changes to this highly organized structure are allowed through various related mechanisms such as post-translational modifications of histones (Vaquero et al. 2003; Fischle 2008), the exchange of canonical histones by histone variants (Bernstein and Hake 2006) and by energy-dependent alterations of the chromatin structure, a process called ATP-dependent nucleosome remodeling (Varga-Weisz and Becker 2006). These modulations influence the chromatin structure and therefore play a role in the regulation of gene accessibility and expression.

A.1.1   Chromatin structure

A.1.1.1   The nucleosome is the basic unit of chromatin

By different levels of compaction, the DNA of the human cell with 2m length is compacted to 10µm to fit into the nucleus. DNA compaction into chromatin is realized by several layers of structural hierarchy.

The nucleosome core particle (NCP) is the universal repeating unit in chromatin with a molecular weight of 210kDa (Kornberg 1974). The high-resolution crystal structure revealed an octameric histone core with 147bp of DNA wrapped around in 1.65 helical turns of a flat left-handed superhelix (Luger et al. 1997) (Figure 1). The histone octamer itself is composed of two copies of each of the four histone proteins H2A, H2B, H3 and H4 (Luger et al. 1997). The massive distortion of the DNA is brought about the tight interaction between the rigid framework of the histone proteins with the DNA at 14 independent DNA-binding locations (Luger and Richmond 1998). Noteworthy, the nucleosome exhibits a modular assembly in which the H2A-H2B dimers can be removed while interaction with the DNA and the $(H3-H4)_2$ tetramer is maintained (Luger 2003), reflecting assembly and disassembly pathways.

The four core histones are small basic proteins (11 - 16kDa), which are highly conserved throughout evolution. Structurally eukaryotic histones are bipartite proteins composed of a carboxy-terminal three-helix 'histone fold' domain and less structured N-terminal domains. These structural components organize the nucleosomal DNA and mediate intra-nucleosomal and secondary inter-nucleosomal interactions (Richmond and Davey 2003; Luger 2006).

The highly basic amino-terminal domains ('tails') extending from the surface of the nucleosome are thought to be mainly unstructured. These histone tails that exhibit numerous lysine, arginine and serine residues are targets for post-translational modifications (A.1.2).

Furthermore, nucleosomes not only contain the four canonical histones but also variants that either slightly differ in sequence or contain an additional domain or both. Histone variants are assumed to be involved in transcriptional regulation, development and tissue specific gene expression, thus adding another element of epigenetic regulation to chromatin (Bernstein and Hake 2006).
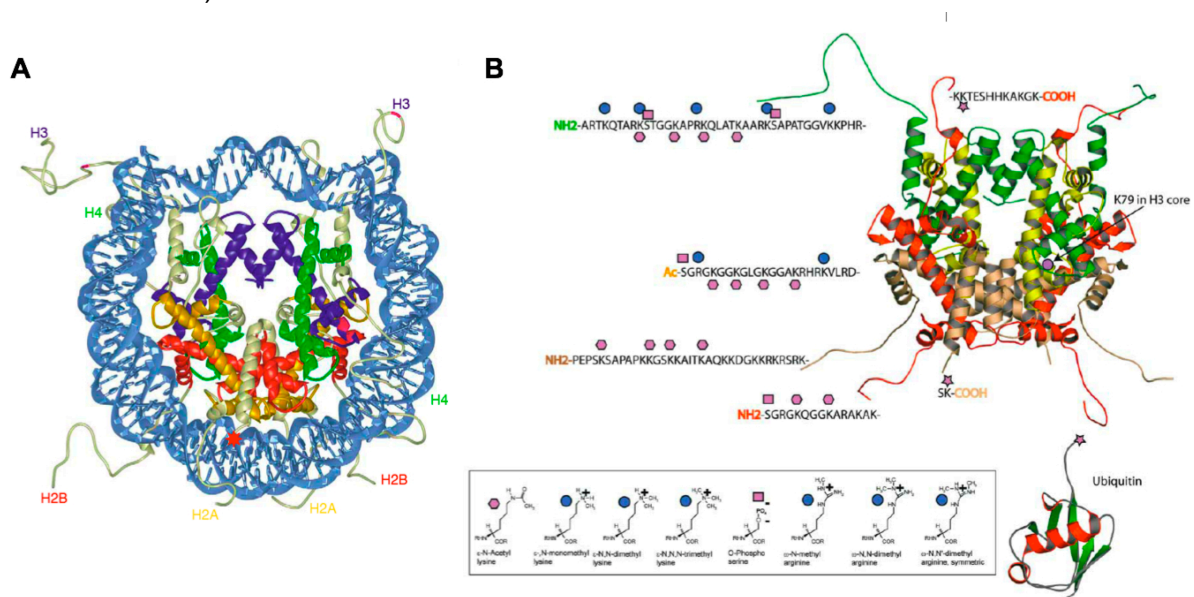
Figure 1 Structure of the nucleosome core particle and posttranslational modifications

A.) 147 bp of DNA (colored in light blue) are wrapped around the histone octamer in 1.7 turns. The histone octamer is composed of two copies of each histone H2A (yellow), H2B (red), H3 (blue) and H4 (green) and forms the nucleosome core particle. Histone tails protrude from the nucleosome core particle (white). The red star indicates the site of ubiquitination in yeast (taken from (Luger 2003). **B.)** The histone octamer of the nucleosome core particle is shown. H2A (red), H2B (brown), H3 (green), H4 (yellow) and the respective histone tails with the sites of modification are depicted. The covalent modifications of the amino acids are shown. Taken from (Khorasanizadeh 2004).

A.1.1.2   Structural organization of chromatin

DNA packaging into chromatin can be dissected into a structural hierarchy with several levels of organization (Woodcock and Dimitrov 2001; Horn and Peterson 2002; Woodcock 2006).

The succession of nucleosomes linked by short stretches of DNA (15-60bp) into a flexible chain, also referred to as 'pearls on a string', builds up the 10nm fiber of chromatin.

A fifth histone protein called linker histone H1/H5 is attached to the DNA situated at the entry/exit sites of the nucleosome. H1 was shown to control the nucleosomal repeat length (Woodcock et al. 2006) thereby facilitating and stabilizing inter-nucleosomal interactions and

establishing the second level of organization, the so-called '30nm fiber'. The structure of the 30nm fiber remains elusive despite of intensive work on the topic. Currently two architectural concepts on how nucleosomes are arranged within this fiber are under discussion. In the 'solenoid model' nucleosomes are spiraled into a one-start helix (Robinson and Rhodes 2006; Routh et al. 2008), wherein the nucleosomes are gradually coiled around a central axis (6-8 nucleosomes per turn) with the nucleosomes that are adjacent in the 10nm fiber are also situated next to one another in the helix. The other model proposed a 'zig-zag' packaging that features a two-start helix in which the 10nm fiber criss-crossed between two helical turns (Dorigo et al. 2004; Khorasanizadeh 2004; Schalch et al. 2005).
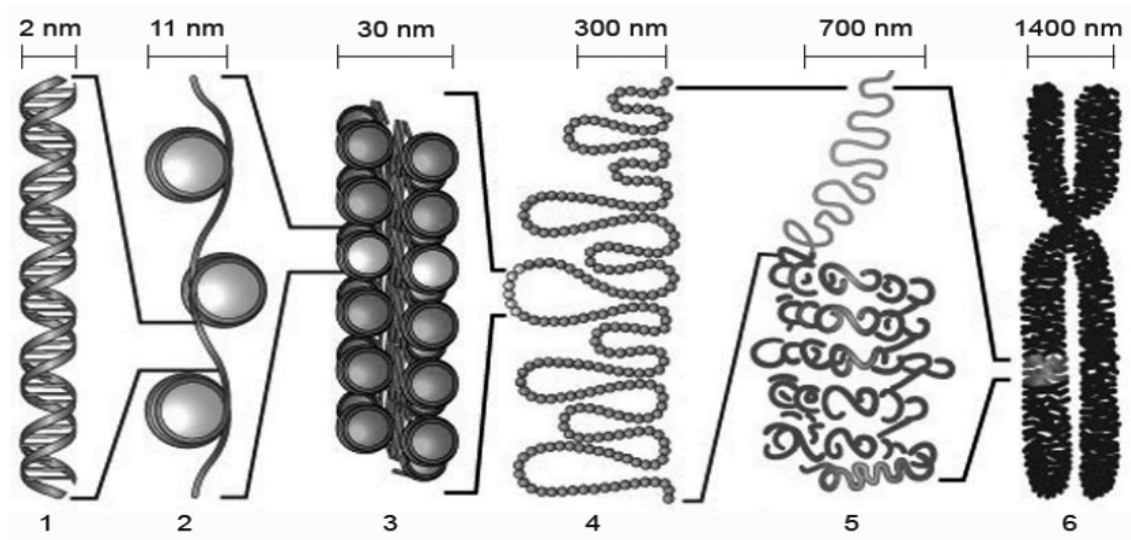
Figure 2 Model of hierarchical levels of DNA compaction

A linear DNA molecule (1) is compacted into a nucleosomal array (2). This 10nm fiber is believed to be wound into the 30nm fiber (3) that is depicted according to the solenoid model. Higher order chromatin structures (4 and 5) contribute to the formation of the highly organized structure of mitotic chromsomes. (modified from (Felsenfeld et al. 2004).

Very little is known about levels of organization above the 30nm fiber, i.e. higher order tertiary structures although there is accumulating evidence suggesting that chromatin fibers are organized into large domains potentially through interaction with a 'nuclear matrix' or 'scaffold' (Hancock and pm026 2000; Baxter et al. 2002; Cremer et al. 2004). Furthermore, these condensed sections appear to be even more organized and reach their highest level of compaction as visible chromosomes during metaphase in mitosis.

The spatial restricted structural elements are distinguishable by characteristic hallmarks like the incorporation of non-canonical histone variants, particular histone posttranslational modifications, chromatin compaction status and locally restricted non-histone protein components.

A.1.2   Histone posttranslational modifications and cross talk

Posttranslational modifications (PTM) of histones and other proteins are recognized as important regulators of protein function and stability, protein-protein interactions or sub-cellular localizations (Yang 2005). Histone proteins are subjected to a multitude of different

PTMs, also referred to as histone 'hall marks', including lysine acetylation, methylation, ubiquitinylation and SUMOylation, arginine methylation, serine and threonine phosphorylation, glutamate ADP-ribosylation and proline isomerization (Gelato and Fischle 2008). In addition, methylated lysines can exist in a mono-, di-, or tri-methyl state, whereas targeted arginine residues can be modified into symmetric or asymmetric di-methylated or a mono-methylated state.

Conventionally, chromatin can be categorized into two main classes, euchromatin and heterochromatin. The first one is characterized by a low condensation state and a more nuclease-sensitive configuration, making it poised for gene expression, although not necessarily transcriptionally active. In contrast, heterochromatic structures comprise highly condensed regions that are in general gene-poor and form mainly on repetitive sequences, such as satellite centromeric and pericentromeric repeats as well as telomers (Baxter et al. 2002; Grewal and Elgin 2002). These structures replicate late in S-phase and are accompanied by H3K9me3 and H4K20me3, whereas H3K9ac and H3K16ac and methylated H3K4 are often found within euchromatic sites.

The inactive X-chromosome contains several hallmark histone modifications such as H3K9me2, H3K27me3, H4K20me, H3K4 demethylation, general deacetylation, as well as the histone variant macroH2A and high level of DNA methylation (Brinkman et al. 2006).

Many covalent modifications alter the electrostatic charge of histones, thereby changing the structural properties of the histones or the chromatin environment. Some histone tail modifications serve as target sites for protein recognition modules. (A.1.2.1, A.1.2.2).

The temporal overlap of various PTMs on histone N-terminal tails discloses the possibility of combinatorial effects. Accordingly, the proposed 'histone code' postulates that a certain set of histone modifications dictates the recruitment of particular transacting factors to accomplish specific functions (Strahl and Allis 2000; Jenuwein and Allis 2001; Turner 2007). Several experimental data demonstrate indeed combinatorial effects of histone modifications, however the evidence for a 'universal code' still lacks. It rather seems that the interdependency of multiple histone PTMs refer to a 'cross-talk' promoting or antagonizing one another (Fischle 2008). Importantly, at present it is not clear which PTMs effectively lead to the establishment of a chromatin element, or whether an element with certain architectural features or protein composition enhance the addition or removal of certain marks (Khorasanizadeh 2004; Gelato and Fischle 2008).

In general, the inter-relationship between posttranslational histone modifications, special histone variants, chromatin remodeling (A.1.4), DNA methylation (A.3) and the RNAi machinery seem to be important for the establishment or maintenance of certain chromatin states (Narlikar et al. 2002; Robertson 2002; Hake et al. 2004; Vos et al. 2006).

A.1.2.1   Histone acetylation

Histone acetylation is set by histone acetyltransferases (HATs), which catalyze the transfer of acetyl groups from acetyl-CoA to the ε-amino terminal groups of specific lysine residues on all four core histones. This reaction is reversed by specific factors, the histone deacetylases (HDACs), which remove acetyl groups from lysines. Alterations of the histone

acetylation state appear to play an important role in chromatin assembly and gene regulation. Increased histone acetylation often correlates with transcriptional activity, whereas decreased acetylation correlates with a transcriptionally repressed state (Fischle et al. 2003a) (Gelato and Fischle 2008). The bromodomain, found in chromatin-associated proteins and HATs, functions as the sole protein module known to bind acetyl-lysine motifs (Mujtaba et al. 2007).

The first HAT identified was isolated from macronuclei from *Tetrahymena* (Brownell et al. 1996)*, and showed strong homology to Gcn5, a transcriptional co-activator in *S. cerevisiae.* Gcn5 as the catalytic subunit of the 'SAGA' transcriptional co-activator complex (Grant et al. 1997) clearly linked histone acetylation to gene regulation. In the past years, many HATs have been identified, often in multi-protein complexes and with different histone tail specificities (Glozak et al. 2005).

Histone acetylation is believed to primarily neutralize the positive charge of histones, thus decreasing their affinity for the DNA and altering nucleosome-nucleosome interactions (Vaquero et al. 2003). In fact, eviction of linker histone and H4K16 acetylation resulted in decompaction of the 30nm fiber *in vitro* (Robinson et al. 2008)*. The resulting permissive structure facilitates binding of proteins such as those of the transcriptional machinery (Khorasanizadeh 2004). In addition, acetylated tails can directly recruit components of chromatin associated factors via the bromodomain (Mujtaba et al. 2007), including the TBP associated factor $TAF_{II}250$ and the human SWI/SNF chromatin remodeling enzyme BrgI (A.1.4).

In general, histone acetylation plays an important role in nuclear processes like chromatin assembly, DNA repair and apoptosis, VDJ recombination and dosage compensation in Drosophila ((Iizuka and Smith 2003) and references therein).

Histone deacetylases, the enzymes that remove the acetyl groups, are generally suggested to play an important role in gene inactivation. Indeed, the first identified histone deacetylase (HDAC1), was shown to be a homolog of the yeast Rpd3p transcriptional regulator (Taunton et al. 1996). Several classes of HDACs were defined, according to their expression pattern, homology and their sensitivity against specific inhibitors. Very often, HDACs are found within large multi-subunit complexes, components of which serve to target enzymes to genes, leading to transcriptional repression. In agreement, many transcriptional repressors were found to be associated with histone deacetylases, and their activity was necessary for gene silencing (Vaquero et al. 2003). In particular, class I HDACs form complexes with the transcriptional co-repressor Sin3 (David et al. 2008), the ATP-dependent remodeling complex NuRD (Zhang et al. 1999), DNA methyltransferases Dnmt1, Dnmt3a/b (Fuks et al. 2000; Rountree et al. 2000; Fuks et al. 2001; Geiman et al. 2004b) and the histone methyltransferase Suvar39H1 (Czermin et al. 2001). Hence, HDACs are involved in multiple functions such as transcriptional and epigenetic silencing, development, cell differentiation, X-chromosome inactivation in mammalian females, and position effect variegation in *Drosophila.*

A.1.2.2 Histone methylation

Histone methylation occurs on both lysine and arginine residues on several histone tails, although it is best described for histone H3 and H4 (Lachner and Jenuwein 2002; Fischle 2008). Histone methyltransferases (HMT) catalyze the transfer of up to three methyl-groups form S-adenosyl-methtionine (SAM) to the ε-amino group of a single lysine residue. The protein arginine methyltransferase (PRMT) generates both mono- or di-methylated arginine residues, either symmetrically or asymmetrically by transferring methyl-groups to the guanidine-group.

Of the many known lysines residues methylated, six have been well characterized to date: five on H3 (K4, K9, K27, K36, K79) and one on H4 (K20) (Lachner and Jenuwein 2002). Although histone methylation has been largely associated with transcriptional repression and epigenetic regulation, it is also involved in transcriptional activation, dependent on the interplay with other histone modifications (Turner 2002). Methylation of K4, K36 and K79 of histone H3 are examples of transcriptional activation (Beisel et al. 2002; Fischle et al. 2003a; Santos-Rosa et al. 2003), whereas H3K9me3 and H3K27me3 are characteristic marks for silenced regions (Bannister et al. 2001; Lachner and Jenuwein 2002). In addition, H3K79me and H4K20me have been implicated in the process of DNA repair.

Probably one of the best-studied modifications, namely H3K9me2/3, functions as a 'docking site' for HP1 (heterochromatin protein 1), which is characteristic of inactive heterochromatic regions (Bannister et al. 2001). Similar, H3K27me3 is bound by the Polycomb group protein (PRC1 complex) (Cao et al. 2005), involved in maintaining the silenced state of homeotic genes during development and of the X-chromosome. Both proteins bind to the methylated lysines through a specific recognition module, the chromodomains (Fischle et al. 2003b). The PHD domain (Plant Homeodomain) is another prominent protein fold, found to specifically recognize H3K4me2/3 (Bienz 2005), thus reading part of the histone code (Jenuwein and Allis 2001; Wysocka et al. 2006). PHD fingers tend to be found in nuclear proteins that have a role in chromatin regulation and are involved in both gene activation and repression (Mellor 2006). In addition other protein domains such the Tudor domain (H3K79me, H4K20me), WD40-Repeat domain (H3K4me) are capable of specific interactions with methylated lysine residues (Martin and Zhang 2005).

In relation, Suvar3-9 and E(z) of PRC2 were the first SET domain (Suvar3-9, Enhancer-of-zeste, Trithorax domain) containing histone methyltransferases (HMT) described (Rea et al. 2000), specifically methylating H3K9 and H3K27 respectively. Subsequently, by homology search to the SET domain and functional assays other HMTs were identified (Vaquero et al. 2003).

Until recently, it was unclear whether histone lysine demethylation would take place in the cell, primarily through the observation, that methyl groups seemed to be very stable on heterochromatic regions. The discovery of the LSD1 protein, the first demethylase specific for methylated H3K4, dramatically changed the view on the dynamics of histone methylation (Shi et al. 2004). LSD1 is present in different repressor complexes and its substrate specificity was modulated from H3K4me to H3K9me when binding to the androgen receptor (Shi et al. 2005; Metzger et al. 2006), thus exerting a function in gene activation. Recently,

five new demethylases were identified that possess the JmjC-domain which is different from the LSD1 protein. Interestingly, these demethylases were found to demethylate specific methyl states (Culhane and Cole 2007; Swigut and Wysocka 2007). Of Importance are UTX (ubiquitously transcribed tetratricopeptide repeat, X chromosome) and JMJD3 (jumonji domain containing 3) that were found to specifically remove di- and tri-methyl marks on H3K27 *in vivo* (Hong et al. 2007; Lee et al. 2007b). Furthermore, UTX occupies promoters of *Hox* gene clusters and associates with MLL2/3 during retinoic acid signaling, resulting in H3K27 demethylation and H3K4 methylation respectively (Lee et al. 2007b).

A.1.2.3   Other histone modifications

All histones including H1 have been shown to be substrates for phosphorylation *in vivo.* In particular phosphorylation of H1 and H3 (S10, S28) have been associated with chromosome condensation and segregation (Wei et al. 1999; Vaquero et al. 2003). H3S10 phosphorylation appears early in G2 of the cell cycle, first in pericentromeric heterochromatin and then spreading, by metaphase to the rest of the chromosome (Hendzel et al. 1997). A 'methyl-phospho binary switch' has been proposed in that H3S10ph leads to ejection of HP1 from H3K9me3 (Fischle et al. 2005). Importantly, H3K10ph is regulated by Aurora-B a member of the Aurora/AIK kinase family that participates in mitotic regulation.

ADP-ribosylation implies the transfer of ADP-ribose molecules to either glutamic acids in a poly-glutamate stretch or single arginine residues with NAD^+ as the source for ADP-ribose. Thus, ADP-ribosylation is linked to the metabolic state of the cell. Although H1 and H2B are the most highly modified, all histones seem to be ADP-ribosylated (Golderer and Gröbner 1991). Interestingly, preferentially hyper-acetylated histones, especially H4, are found to be ADP-ribosylated. Due to its fast turn-over in the cells, it has been proposed to play a role in adaptation of the cell to environmental changes (Pieper et al. 1999).

A.1.3   Polycomb silencing

Polycomb group proteins (PcG) are epigenetic regulators that silence specific sets of genes through chromatin modifications. The most prominent function that can be assigned to PcGs is the involvement in X-chromosome inactivation (Xi) in female mammals, but also in germline development, stem cell identity, cell-cycle regulation and cancer (Schuettengruber et al. 2007). PcG proteins were originally identified in *Drosophila* as repressors of *Hox* genes based on mutant phenotypes involving posterior transformation of body segments. In vertebrates, this function is essentially conserved with several Polycomb mutants exhibiting skeletal malformations ((Sparmann and Van Lohuizen 2006) and references therein).

PcG proteins are classified into two groups on the basis of their association with distinct classes of multimeric complexes, termed Polycomb repressive complexes (PRCs) (classes of multimeric complexes, termed Polycomb repressive complexes (PRC). The PRC2 core complex consists of the mammalian homologs of the *Drosophila* proteins Enhancer of zeste (E(Z)), Suppressor of zeste12 (SU(Z)12), extra sex combs (ESC) and Nurf-55 (RbAp46/48 in human) and is involved in initiation of gene repression (Schuettengruber et al. 2007). E(Z) is

a SET containing HMT targeting H3K27 and to a lesser extent H3K9 for tri-methylation (Müller et al. 2002). PRC1 constitutes a more divers complex with the core components Polycomb (PC), Polyhomeotic (PH), Posterior sex combs (PSC) and Sex combs extra (SCE/RING). Importantly, PRC1 possess an E3 ubiquitin ligase activity towards H2AK119 and this modification is associated with gene repression and X-chromosome inactivation (de Napoles et al. 2004; Cao et al. 2005; Wu et al. 2008).

Studies in *Drosophila* have led to the identification of specific cis-regulatory sequences in *Hox* genes, termed Polycomb response elements (PREs) (Sengupta et al. 2004; Ringrose and Paro 2007). PREs are typically several hundred base pairs in length, function as potent transcriptional silencer elements and are bound, either directly or indirectly, by PcG proteins. The majority of PcG target genes hold extensive H3K27me3 that extends well beyond promoter regions (Schwartz et al. 2006). PRC1 was believed to be recruited to appropriate genomic loci, due to the recognition of H3K27me3 by Polycomb through its chromodomain (Min et al. 2003; Wang et al. 2004b; Fischle et al. 2005).
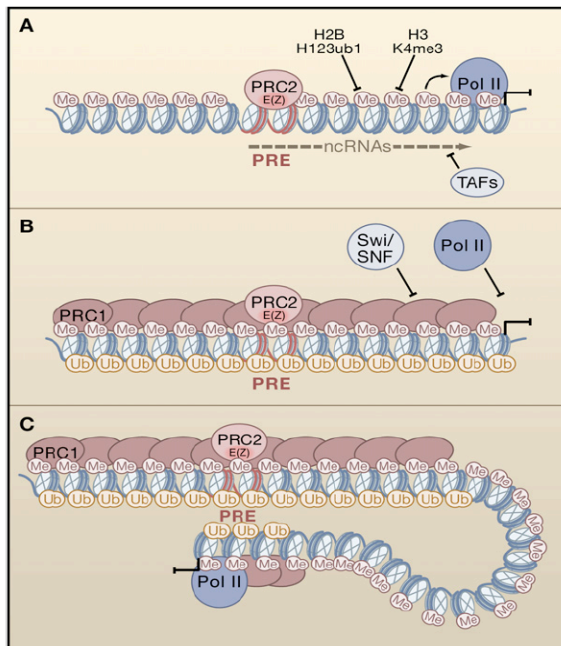
Figure 3 PRE - Polycomb regulation

A.) PRC2-mediated H3K27me3 might directly interfere with transcriptional activation and/or inhibit H2BK123ub1 or H3K4me3. Transcription of noncoding RNAs may mediate repression of a downstream gene by transcriptional interference. TAFs, TBP-associated factors. **B.)** H3K27me3 and PRC1 complexes spread from the PRE to a promoter located close to the PRE, interfering with ATP-dependent nucleosome remodeling activities (SWI/SNF) and RNA Pol II recruitment. The E3 ligase activity of dRing leads to H2A ubiquitinylation, contributing to silencing. **C.)** RNA Pol II can be recruited to a subset of PcG-silenced genes, suggesting a role for PRC1 in gene silencing downstream of RNA Pol II assembly at the promoter region. For promoters located far away from PRE sequences, PRC2 complexes bound at PREs may loop out and contact neighboring nucleosomes. (taken from (Schuettengruber et al. 2007))

Recently, a third PRC complex, namely Pleiohomeotic (PHO) repressive complex (PhoRC) was purified from *Drosophila* embryos (Klymenko et al. 2006). Interestingly, PHO bears DNA binding capability and therefore combines sequence specific DNA binding with a unique binding to mono- and di-methylated H3K9 and H4K20 through the dSfmbt subunit. Neither PRC1 nor PRC2 core complexes contain sequence specific DNA binding proteins, but Pho has been shown to bind to PRC2 subunits and to induce PRC2 recruitment at the PRE of the *ubx* gene in *Drosophila* (Schuettengruber et al. 2007).

The precise molecular mechanisms of PRC-mediated repression are still poorly understood, but it has been suggested that the complex can inhibit transcription by preventing ATP-dependent nucleosome remodeling by the SWI/SNF complex (Shao et al. 1999), as well as by directly blocking the transcription initiation machinery (Dellino et al. 2004). PRC2 mediated H3K27me3 and H1K26me3 serves as binding platform for PRC1 and HP1

respectively (Müller et al. 2002; Kuzmichev et al. 2004). In addition, EZH2 was shown to recruit the *maintenance* methyltransferase Dnmt1 to target genes (Viré et al. 2005) thereby setting another repressive mark. Furthermore, ubiquitinylation of H2AK119 by PRC1 together with H3K27me3 lead to gene repression by opposing histone marks associated with active transcription. USP7, a histone H2B deubiquitinase, was found to be associated with Polycomb protein on the *ubx* PRE and co-localized with homeotic genes in salivary gland polytene chromosomes in *Drosophila* (van der Knaap et al. 2005). Hence, one could envision a contribution to silencing through recruitment of USP7 by PRCs, since deubiquitination of H2BK120ub1 leads to low levels of active transcription marks H3K4 and H3K79 methylation (Sun and Allis 2002).

A.1.4 Chromatin remodeling

The packaging of chromosomal DNA by nucleosomes condenses and organizes the genome, but occludes many regulatory DNA elements. However, this constraint also constitutes a level of regulation by allowing accessibility to certain DNA sequences. In order to enable dynamic access to packaged DNA and to tailor nucleosome composition in chromosomal regions, cells have evolved a set of specialized ATP-dependent chromatin remodeling complexes (also referred to as remodelers) that use the energy of ATP hydrolysis to move, destabilize, eject or restructure nucleosomes (Becker and Hörz 2002). Remodelers were found to be involved in a wide range of processes that include the regulation of transcription, chromosome segregation, DNA replication and DNA repair (Clapier and Cairns 2009).
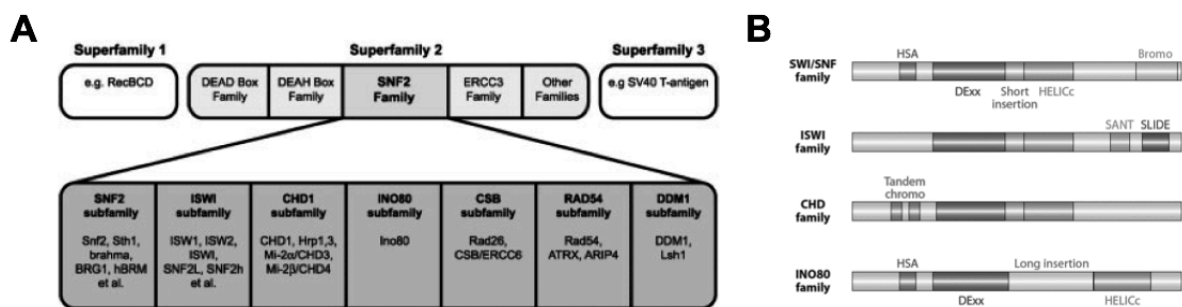
Figure 4 Snf2-like family of ATPases

A. Classification of ATPases in three different superfamilies. The Snf2-like family belongs to the DEAD/H superfamily of nucleic acid stimulated ATPases and can be further subdivided into subfamilies (Lusser and Kadonaga 2003). **B**. The four most prominent subfamily members of the Snf2-like family are depicted. Although they share an ATPase domain that is split into two parts: DExx and HELICc domain, they differ in unique domains residing adjacent to the ATPase domain. Bromo (bromodomaims recognize acetylated lysines) and HAS (helicase-SANT) domain for SWI/SNF family, SANT-SLIDE (SANT-like ISWI domain) module for ISWI family, tandem chromo domain (chromodomains recognize H3K4me2/3) for the CHD family and the HAS domain for the INO80 family (Clapier and Cairns 2009).

All ATP-dependent chromatin remodeling factors identified so far are multiprotein complexes consisting of 2-12 subunits, and contain a related motor protein subunit that belongs to the Snf2-like family of ATPases. The Snf2-like family belongs to the DEAD/H superfamily of nucleic acid stimulated ATPases and can be further subdivided into several subfamilies

according to the presence of protein motifs outside of the ATPase region (Figure 4) (Eisen et al. 1995; Flaus et al. 2006b). At least four major classes of catalytic subunits of chromatin remodeling complexes are distinguished: The Swi/Snf family, the Mi-2 / CHD family, the ISWI class and the Ino80 group (Figure 4). Several other Snf2-like proteins have been found or suggested to possess ATP-dependent chromatin-remodeling activity, such as Rad54, ATRX, CSB (Cockayne Syndrome protein B) and the plant protein DDM1 ((Lusser and Kadonaga 2003) and references therein).

In addition to their ATPase subunit and unique protein motifs, the particular function and the biological context of chromatin remodelers are selectively influenced by a great variety of associated subunits (Tsukiyama 2002; Lusser and Kadonaga 2003).

A.2 Ubiquitin and ubiquitin modifying enzymes

A.2.1 Modification of proteins by ubiquitin and ubiquitin-like proteins (ubl)

Ubiquitin (ub) is a polypeptide consisting of 76 amino acids and is highly conserved among eukaryotes but is absent from bacterial and archea. Among many functions of ubiquitin, the best understood is the targeting of proteins for degradation by the proteasome. Ubiquitin is attached to a substrate lysine side chain through an isopeptide bond via its C-terminal glycine residue in dependency of ATP consumption (Ciechanover et al. 1980; Wilkinson et al. 1980). Ubiquitinylation occurs through the sequential action of activating (E1), conjugation (E2), and ligase (E3) enzymes (Hershko et al. 1983). In detail, E1 activates ubiquitin by using ATP to synthesize a high-energy ubiquitin C-terminal adenylate that is needed for the formation of an E1-ubiquitin thiol-ester. The latter ubiquitin is passed to an E2 cysteine residue and from there, in an E3-dependent manner to the ε-amino group of a lysine in the substrate.

There are two main types of E3s for ubiquitin, the RING class and the HECT class. The RING E3's contain a subunit or domain with a zinc finger domain (RING domain, or the structurally related but zinc-free U-box E3's) and function as adaptors (Figure 5). They bind the ubiquitin thiol-ester-linked E2 and substrate proteins simultaneously and position the substrate lysine nucleophile in close proximity to the reactive E2-ub thiol-ester bond, facilitating the transfer of ubiquitin. Catalysis of ubiquitin-substrate modification by the HECT E3's follows a mechanism distinct from that of the RING E3s. The activated ubiquitin moiety is first transferred from the E2 conjugating enzyme to an active-site cysteine in the conserved HECT domain of the E3. The thio-ester – linked ubiquitin is subsequently transferred to the substrate (Kerscher et al. 2006).

Proteins can be modified on a single or on multiple residues by a single ubiquitin or by ubiquitin oligomers. The fate of an ubiquitin-protein conjugate depends in part of the length of the ubiquitin chain and on the configuration of the ubiquitin-ubiquitin linkages in the ubiquitin chain. In yeast, potentially all seven conserved lysines of ubiquitin itself (K6, 11, 27, 29, 33, 48, 63) are used as branching sites for the generation of ubiquitin polymers. K48-linked oligo-ubiquitin chains efficiently promote binding of the protein to the 26S proteasome, with subsequent degradation of the substrate but recycling of ubiquitins ((Amerik and

Hochstrasser 2004) and references therein). In contrast, mono-ubiquitinylation or attachment of short K63-linked ubiquitin marks target proteins not for proteasomal degradation, but for endocytosis, transcriptional control (histone mono-ubiquitinylation), vesicular trafficking and DNA repair respectively (Dupré et al. 2001; Hicke 2001; Clague and Urbé 2006; Huang and D'Andrea 2006; Osley 2006).
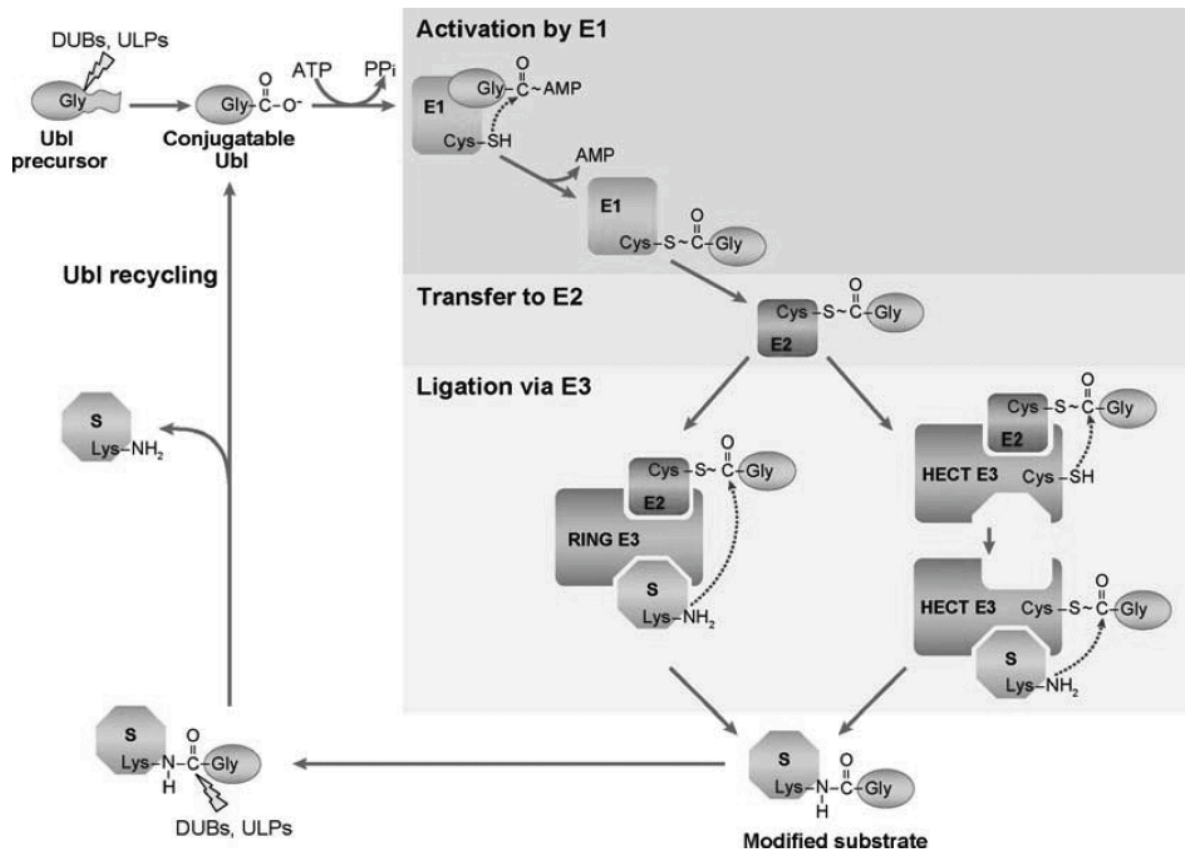
Figure 5 **Generalized ubiquitin/ ubiquitin-like conjugation pathway**

Ubiquitin (ub) or ubiquitin-like (ubl) precursors are processed to expose the C-terminal glycine in the mature ubl which can be activated with ATP by E1 to form a high-energy ubl-adenylate which is transferred to the catalytic cysteine of the E1. The ubl is then transferred via a transthiolation reaction to the E2 conjugating enzyme. The ubl can be ligated to a substrate with the aid of an E3 ligase enzyme. The adaptor-like RING E3s catalyze modification by binding simultaneously the ubl-E2 thio-ester complex and the substrate thereby bringing the substrate lysine and the thio-ester ubiquitin bond in close proximity for transfer. In contrast, the HECT E3s catalyze the substrate ligation in two steps. First, the ubl is transferred to a catalytic cysteine of the HECT E3 then the E3-ubl thio-ester complex transfers the ubl to the substrate. The DUBs (deubiquitinating enzyme) and the ULP (ubl specific protease) can remove ubls from substrates (Kerscher et al. 2006).

Since the discovery of ubiquitin, an entire family of small proteins related to ubiquitin (referred to as ubiquitin-like proteins; ubl) has been defined. Although not necessarily sharing high sequence similarity, the ubls all possess essentially the same three-dimensional structure, the ubiquitin or β-grasp fold (Hochstrasser 2000). Furthermore, all ubls are covalently attached via their C-terminal glycine residue to lysine target sites on substrate proteins resulting in an isopeptide bond between the ubl and substrate (Welchman et al. 2005; Kerscher et al. 2006).

Considering the large amount of ubls and the fact that ubl modifications are reversible, it was not a surprise that there has evolved a great variety of specific E1, E2 and E3 ubl ligases (Hochstrasser 2000; Welchman et al. 2005; Kerscher et al. 2006), as well as deubiquitinating enzymes (DUB) and ULPs (ubl specific protease) that remove ubls from substrates (Amerik and Hochstrasser 2004; Nijman et al. 2005; Kerscher et al. 2006).

A.2.2 UHRF1 – member of the ubiquitin PHD Ring Finger family

The first two members of the Ubiquitin PHD Ring Finger family that have been identified are ICBP90 in human (inverted CCAAT box binding protein of 90kDA) and NP95 in mouse (nuclear protein of 95kDa). ICBP90 was found by using the second inverted CCAAT Box (ICB2) of the human topoisomerase IIα gene as the DNA target sequence in a yeast 1-hybrid screen (Hopfner et al. 2000) whereas NP95 was discovered by engineering antibodies against murine thymic lymphoma (Fujimori et al. 1998). ICBP90 and NP95 are encoded by the *UHRF1* gene (Unoki et al. 2008) and NIRF and NP97 are encoded by the *UHRF2* gene (Bronner et al. 2007).

In addition, there is a third member encoded by the *UHRF3* gene, namely ICBP55 in human and NP55 in mouse, lacking the first N-terminal ubiquitin-like domain (also referred to as NIRF_N-domain) and a fourth member encoded by the *UHRF4* gene, namely ICBP87, lacking the C-terminal RING domain.

Phylogenetic studies showed that UHRF1 is highly conserved but restricted to vertebrates since UHRF1 equivalents were neither found in the fly- or worm-database nor in the *S. cerevisiae* database (Bronner et al. 2007). The author hypotheses that UHRF1 as an E3 ligase for histones and mono-ubiquitinylation of histones (at least for histone H3) have evolved phylogenetically with vertebrates.

In contrast, in *Arabidopsis thaliana* a protein that resembles hUHRF1 was found (Woo et al. 2007) but it differs from the former by the fact that it lacks the NIRF_N domain and by the location of the RING domain between the PHD and SRA domain. VIM1 (variant in methlyation 1) is able to bind *in vitro* to methylated DNA and recombinant histones, and associates *in vivo* with methylated genomic loci and chromocenters (Woo et al. 2007) - features that are shared by both human and mouse UHRF1 (Citterio et al. 2004; Unoki et al. 2004; Bostick et al. 2007; Sharif et al. 2007; Karagianni et al. 2008).

As depicted in Figure 6 UHRF1 consists of four conserved domains. Situated on the far N-terminus of UHRF1, the NIRF_N domain (also referred to as ubiquitin-like domain; ubl) exhibits a typical alpha/beta ubiquitin fold. It is 35% identical to ubiquitin (A.2.1) and the lysines K33 and K52 are structurally conserved with K29 and K48 of ubiquitin with poly-ubiquitinylation of the latter being the key signal for proteasomal degradation (Kerscher et al. 2006). Nevertheless, the role of the NIRF_N domain is less clear but recent data indicate protein-protein interactions. The ubiquitin-like domain (NIRF_N) of PLIC-1 (protein linking IAP to the cytoskeleton) is able to bind to the ubiquitin-interacting motif (UIM) of S5a, a proteasomal 19S cap subunit (Heir et al. 2006)
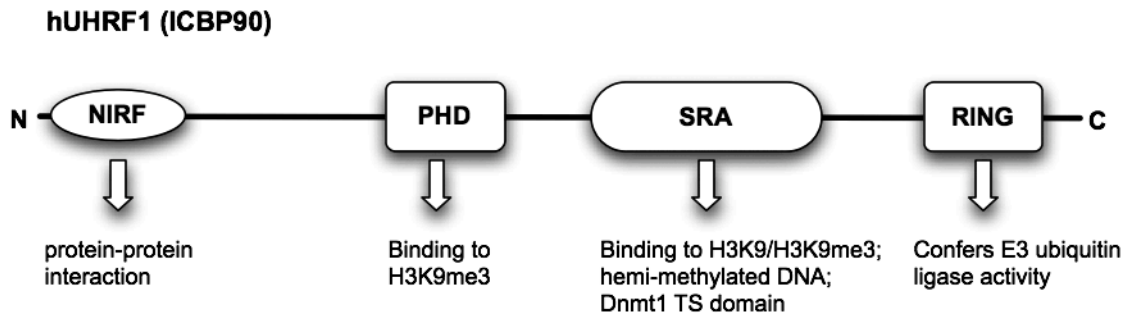
hUHRF1 (ICBP90)

Figure 6 Domain structure of UHRF1

The domain structure of human UHRF (ICBP90) and the function of the distinct domains are depicted. NIRF_N domain (ubiquitin-like domain), PHD domain (Plant Homeodomain), SRA domain (SET and RING Finger associated), RING domain (Really interesting new gene).

The PHD domain of ICBP90 was found to confer H3K9me3 specific binding, whereas the SRA domain bound equally well to methylated and non-methylated H3K9 (Karagianni et al. 2008).

The SRA domain (SET and RING finger associated domain) is a 170 amino acid long domain characterized by the conservation of up to 13 evenly spaced glycine residues and the VRV(I/V)RG motif (Baumbusch et al. 2001). Due to its YDG motif it is also referred to as YDG domain.

The SRA domain accounts for the high binding affinity of UHRF1 for methyl-CpG di-nucleotides (Unoki et al. 2004) and its preference for hemi-methylated DNA *in vitro* (Bostick et al. 2007). The structural basis for the recognition of hemi-methylated DNA via the SRA domain was recently elucidated revealing a base flipping mechanism of the 5-methyl-cytosine out of the double helix into a binding pocket of the SRA domain (Arita et al. 2008; Avvakumov et al. 2008; Hashimoto et al. 2008). In agreement, ICBP90 is associated with methylated promoter regions of various tumor suppressor genes, including $p16^{INK4A}$ and $p14^{ARF}$, in cancer cells (Unoki et al. 2004) and the localization of mUHRF1 on replicating heterochromatin is dependent on the presence of hm DNA (Sharif et al. 2007) (see below).

Besides methylated DNA binding properties, the SRA-domain was also found to interact with HDAC1 (Unoki et al. 2004) and Dnmt1 (Achour et al. 2007) (Bostick et al. 2007). By means of deletion studies and yeast-2-hybrid experiments, the TS domain of Dnmt1 could be identified as the region in Dnmt1 mediating this interaction.

UHRF1 with its RING Finger domain (Really interesting new gene) located at the C-terminus belongs to the class of Ring finger type E3 ubiquitin ligases (Chen et al. 2006; Kerscher et al. 2006). UHRF1 family members, like other Ring finger containing ligases, possess an *in vitro* autoubiquitinylation activity (Citterio et al. 2004; Mori 2004; Jenkins et al. 2005; Karagianni et al. 2008). UHRF1 is able to target histones for ubiquitinylation *in vitro* and *in vivo*, though with a preference for histone H3 (Citterio et al. 2004; Karagianni et al. 2008).

Northern Blot analysis of several human cancer cell lines revealed the existence of two mRNA species of 5.1 and 4.3 kb respectively which could account for the two bands that are often observed in Western Blot experiments for hUHRF1 (Bronner et al. 2007).

The expression of UHRF1 peaks in late G_1 and during the transition from G_2 to M phase in normal cells, whereas UHRF1 is continuously expressed at a high constant level in cancer cells (Mousli et al. 2003; Jeanblanc et al. 2005). UHRF1 mRNA is most abundant in proliferating tissues like thymus, fetal tissues, bone marrow, but low in quiescent cells, suggesting that UHRF1 is related to cell proliferation (Fujimori et al. 1998; Hopfner et al. 2000). This is in agreement with the observation of increased expression of UHRF1 in cancer tissues of breast cancer, rhabdomyosarcoma, pancreatic adenocarcinoma, prostata and lung cancers.

Both mRNA and protein levels of ICBP90 are down-regulated in response to DNA damage in human colon adenocarcinoma HCT-116 cells and lung carcinoma A549 cells (Jenkins et al. 2005). DNA damage activates the p53-dependent checkpoint pathway that induces the expression of p21$^{Cip1/WAF1}$ resulting in cell cycle arrest at G_1/S transition by inhibition of cyclin-dependent kinase (Cdk). Interestingly, the reduction of UHRF1 expression is inhibited by ATM kinase inhibitor and does not occur in p53-/- and p21-/- cells suggesting an ATM/p53/p21$^{Cip1/WAF1}$ dependent regulation of UHRF1 expression after DNA damage (Arima et al. 2004). NP95 depleted murine embryonic stem cells were more sensitive to X-ray radiation, UV light and DNA damaging agents proposing a role as a component in the DNA response pathway or in the maintenance of genomic stability (Muto et al. 2002).

Depletion of hUHRF1 using siRNA in Hela cells (Bronner et al. 2007) and NIH3T3 cells treated with shRNA to mUHRF1 (Bonapace et al. 2002) resulted in G_1 arrest. These findings suggest UHRF1 being essential for S-phase entry. The role of ICBP90 in the G_1/S transition seems to be controlled by the E2F1 transcription factor necessary for S-phase entry (Mousli et al. 2003).

Another important fact to mention is that NP95 is indispensible for proper mice development since mUHRF1-/- mice died in midgestation (Muto et al. 2002).

In immunoprecipitation UHRFBP1, a new 170kDa nuclear protein interacting with UHRF1 was found (Unoki et al. 2004). Although little is known, it also bound to HDAC1 and is believed to relocate UHRF1. In a yeast-two-hybrid screen, the RbAp48 (pRB binding protein (Qian et al. 1993)) was identified as potential interaction partner of ICBP90 (Bronner et al. 2002). This interaction is likely to occur in vivo, since HDAC1 interacts with UHRF1 and RbA48 (Nicolas et al. 2001). RbA48 binds directly to H4 (Nicolas et al. 2001) and could favor the deacetylation of histones. Accordingly, this association may link histone H3 ubiquitinylation and H4 deacetylation to DNA methylation considering that UHRF1 binds to H3 and Dnmt1 (Citterio et al. 2004; Achour et al. 2007; Bostick et al. 2007; Karagianni et al. 2008). Interestingly, RBAp46/48 are components of the human NURF remodeling complex (Clapier and Cairns 2009) and the PRC2 complex (Schuettengruber et al. 2007), hence are involved in both gene activation and repression respectively.

During the cell cycle, the location of NP95 is dynamically changed. Although the observations are to some extent contradictory, NP95 co-localized with chromatin-bound PCNA during mid S-phase (Uemura et al. 2000; Miura et al. 2001). Distinct localization of the two proteins, however, is evident in very early and late S-phase, suggesting that Np95 is not directly involved in the replication machinery, but in other DNA replication-linked nuclear events (Miura et al. 2001). Ablation of NP95 upon siRNA knock-down showed that replication

of heterochromatin was greatly impaired during mid S- and late S-phase, whereas replication of euchromatin was not affected (Papait et al. 2007). Depletion of NP95 also caused hyperacetylation of lysines 8, 12 and 16 of heterochromatin H4 (Papait et al. 2007) whose deacetylated state is essential to maintain the compacted and silenced condition of these regions (Agalioti et al. 2002). As a consequence, an increase of pericentromeric major satellite transcription (Papait et al. 2007) was observed, suggesting a role in regulating the low level RNA transcription from major satellite repeats whose RNAs are involved in heterochromatin formation (Reinhart and Bartel 2002).

Besides triggering deacetlyation of histone H4 probably through HDAC1 and thus conserving the integrity of heterochromatin, mUHRF1 was also found to be a factor responsible for maintaining global DNA methylation levels (Bostick et al. 2007; Sharif et al. 2007) since mUHRF1 knockout ES cells are characterized by massive global losses of DNA methylation. In addition, repetitive elements like LINEs, IAPs and SINEs, major and minor satellite repeats as well as imprinted regions (*Igf2*, *Cdkn1c*) were heavily affected by a decrease in methylation, although protein levels of *maintenance* and *de novo* methyltransferases were not altered.

Furthermore, both UHRF1 and Dnmt1 depleted ES cells fail to properly differentiate and show embryonic lethality (Li et al. 1992; Muto et al. 2006), but both remain proliferative as ES cells. Both are found during mid S-phase at replication foci, and in late S-phase both are associated with DAPI stained heterochromatin (Bostick et al. 2007; Sharif et al. 2007).

In NP95-/- ES cells the accumulation of Dnmt1 at replicating heterochromatin during mid S-phase was abolished and its binding to heterochromatin changed to a diffuse localization pattern compared to wild-type (Sharif et al. 2007). Interestingly, mUHRF1 is dependent on the presence of hm DNA since in Dnmt triple knockout ES cells (TKO) NP95 showed a diffuse localization pattern and almost no enrichment in the newly synthesized heterochromatin. When transiently introducing Dnmt3a/Dnmt3b, both of which methylate DNA at pericentromeric heterochromatin (Bachman 2001; Lehnertz et al. 2003; Ge et al. 2004), or their respective inactive mutants into TKO ES cells, NP95 localization to heterochromatin was restored whereas for the mutants not.

Upon mUHRF1 knockdown Dnmt1's association with chromatin was severely reduced in co-immnoprecipitation (Bostick et al. 2007), whereas vice versa mUHRF1 binding to chromatin was not affected. Disruption of the PCNA-Dnmt1 interaction resulted in only a small decrease in the efficiency of *maintenance* methylation (Schermelleh et al. 2007; Spada et al. 2007) confirming the existence of another Dnmt1 recruitment mechanism. Taken together, UHRF1 binds to hm DNA and Dnmt1 via its SRA-domain (Bostick et al. 2007) (Achour et al. 2007) thereby recruiting Dnmt1 and facilitating efficient maintenance of CpG methylation.

A.2.3   Histone ubiquitinylation

Ubiquitinylation of histone molecules was found for histones H2A, H2B, H3, H4, H2A.Z, macroH2A and H1 (Zhang 2003; Kinyamu et al. 2005; Osley 2006). In most cases only a single ubiquitin moiety is attached to histones, which is not sufficient for targeting proteins for degradation via the 26S proteasome. During mitosis the core histones are globally

deubiquitinated at metaphase and reubiquitinylated as cells enter anaphase (Goldknopf et al. 1980), indicating a continuous turnover of the ubiquitin mark during cell growth.

Histone H1 was shown to be ubiquitinylated by TAFII250, the largest subunit of TFIID comprising both E1 ubiquitin activating and E2 ubiquitin conjugating activities (Pham and Sauer 2000). H2A was the first protein found to be ubiquitinylated (Goldknopf and Busch 1975). The ubiquitinylation site was mapped to lysine K119 within the C-terminal histone fold domain. Interestingly, although H2Aub1 accounts for 5-15% of total H2A molecules it is restricted to higher eukaryotes and absent from *S. cerevisiae* (Osley 2006). In contrast, ubiquitinylated H2B (ubH2B) was also found in yeast at lysine K123 and K120 in higher eukaryotes and constitutes 1-2% of the total H2B pool (Osley 2006). H2A and H2B ubiquitinylation will be discussed in detail in the following sections.

H3 is ubiquitinylated in rat spermatids, although the site is unknown (Osley 2006). The ubiquitin E3 ligase UHRF1 (A.2.2) specific for H3 was identified (Citterio et al. 2004; Karagianni et al. 2008), but the function of H3 ubiquitinylation remains elusive. Recently, histone H4 was found to be mono-ubiquitinylated at lysines K31 and K91 in both human and yeast (Osley 2006) and the complex EEUC responsible for ubiquitinylation has been identified.

A.2.3.1   Histone H2A ubiquitinylation

Ubiquitinylated H2A (ubH2A) was long thought to play a role in activation and repression of genes due to its association with active and inactive regions of chromatin respectively. Nowadays, ubH2A is recognized as an epigenetic mark involved in silencing. First indications came from immuno-fluorescence studies with mouse spermatocytes that showed ubH2A being present in the heterochromatin XY body of meiotic prophase cells (Baarends et al. 1999). Additional cytological studies revealed that ubH2A is also present at the inactive X-chromosome in female mammals, at unpaired autosomal regions in male meiosis and at unpaired X and Y chromosomes in female meiosis ((Baarends et al. 2005). In proliferating cells, ubH2A is present throughout the cell cycle, but it is down-regulated during G_2/M transition and is not present on condensed chromosomes (Mueller et al. 1985; Joo et al. 2007).

The RING finger containing E3 ubiquitin ligases, namely mouse Ring1B, human Ring2, fly dRing, that target H2A for ubiquitinylation *in vitro* have been identified in both vertebrates and flies as components of the Polycomb group (PcG) complex PRC1 (A.1.3) (de Napoles et al. 2004; Wang et al. 2004a; Cao et al. 2005). In addition, PRC1 and ubH2A are enriched in regions of the genome that are subject to PcG-dependent transcriptional silencing such as the inactive X-chromosome and homeotic genes and the presence of the Ring E3 is required for H2A ubiquitinylation at these locations (de Napoles et al. 2004; Wang et al. 2004a).

Interestingly, PRC1 contains two additional RING domain - containing proteins, Ring1A and Bmi1, but unlike Ring1B, neither possesses a functional ubiquitin ligase. However, the two proteins stimulate the activity of Ring1B *in vitro*, and regulate the H2AK119ub1 levels at silenced *Hox* genes *in vivo* (Cao et al. 2005). Further evidence of PRC1 complexes and ubiquitinylated H2A playing direct roles in the control of transcriptional silencing came from

RNAi experiments directed against the RING E3's. In *Drosophila,* RNAi-mediated knockdown of dRing resulted in derepression of the homeotic gene *Ubx* (Wang et al. 2004a). Similarly, deprivation of cells of Bmi1 showed expression of a number of *Hox* genes that had been silenced before (Cao et al. 2005). In contrast, reactivation of the silenced X-chromosome did not occur upon depletion of ubH2a through double knockout of Ring1A and Ring1B in ES cells (de Napoles et al. 2004).

Besides silencing in heterochromatic regions, ubiquitinylated H2A is also involved in the transcriptional repression in euchromatin (Osley 2006). In addition, ubiquitinylation of H2A was found to be highly dynamic, as suggested from varying global changes of ubH2A during the cell cycle, indicating the involvement in the regulation of cell cycle progression (Joo et al. 2007). Accordingly, the existence of several mammalian H2A deubiquitinating enzymes belonging to the JAMM/MPN+ family (2A-DUB) and to the ubiquitin-specific protease family (USP3, USP16/Up-M, USP22) was reported (Joo et al. 2007; Nicassio et al. 2007; Zhu et al. 2007b; Nakagawa et al. 2008; Zhang et al. 2008b).

Recently, the deubiquitinase Ubp-M (also referred to as USP16) was identified to specifically target ubH2A but not ubH2B for deubiquitination *in vitro* and *in vivo* (Joo et al. 2007). Even more important, ablation of Ubp-M in Hela cells resulted in slow growth rates owing to defects in the mitotic phase of the cell cycle and showed that H2A deubiquitination is a prerequisite for H3S10ph and subsequent chromosome segregation. Furthermore, blocking the function of Ubp-M by injection of Ubp-M antibodies in *Xenopus laevis* embryos resulted in defects of posterior development indicating that *Hox* gene expression is regulated through H2A deubiquitination and counteracts the PcG mediated repression (Joo et al. 2007).

Moreover, it was shown that chromatin assembled *in vitro* with ubH2A, but not H2A, specifically repressed the di- and tri-methylation of H3K4 and thus transcriptional initiation, but not elongation (Nakagawa et al. 2008). Furthermore, USP21, an ubiquitin-specific protease, was found to catalyze the hydrolysis of ubH2A and to relieve ubH2A mediated repression. Over-expression of USP21 in the liver up-regulated a gene that was normally down-regulated during hepatocyte regeneration (Nakagawa et al. 2008).

A similar observation was made for the JAMM/MPN+ domain containing H2A deubiquitinase 2A-DUB that participated in the transcriptional regulation of the androgen receptor gene (Zhu et al. 2007a). 2A-DUB forms a protein complex with the HAT p300/CBP associated factor (p/CAF) thereby regulating transcriptional initiation by stepwise coordination of histone acetylation, H2A deubiquitination and linker histone H1 dissociation.

USP22 is the mammalian counterpart of the deubiquitinase Ubp8 in yeast specifically targeting ubH2B. As for Ubp8, USP22 is a component of the human co-activator complex SAGA (Zhang et al. 2008b; Zhao et al. 2008), but in addition to H2B, USP22 deubiquitinates H2A *in vitro.* Furthermore, USP22 was recruited to *myc* target genes through direct recruitment of the Myc transcription factor.

In agreement to the role of transcriptional regulation through ubH2A, it was shown that the N-CoR/HDAC1/3 repressor complex specifically recruited the E3 ubiquitin ligase 2A-HUB that catalyzed mono-ubiquitinylation of H2A and thus mediated a selective repression of a specific set of chemokine genes (Zhou et al. 2008b). In addition, H2A mono-ubiquitinylation

acted to prevent FACT recruitment at the transcriptional promoter region thereby blocking RNA polymerase II release at the early stage of elongation (Zhou et al. 2008b).

Latest data identified the existence of 'bivalent promoters' (Bernstein et al. 2006) that are associated with histone marks characteristic of both active (H3K4me3) and inactive (H2K27me3) chromatin. Low-level transcription of the 5' region of the coding region of these genes was detectable in WT cells, despite the presence of Ring1A/B and ubH2A (Stock et al. 2007). In fact, S5pCTD RNA polymerase II was situated at these promoters at levels comparable to actively transcribed genes, indicating that ubH2A hinders transcription at early stages of elongation.

As a summary, histone H2A ubiquitinylation is important for X-chromosome inactivation and *Hox* gene silencing mediated by Polycomb group proteins (A.1.3). Accumulating evidence indicates that H2A ubiquitinylation/deubiquitination through repressive and activating complexes regulate transcriptional silencing and activation respectively. The emergence of 'bivalent promoters' renders the picture even more complex and suggests that ubH2A may act as a platform for recruitment of regulatory factors responsible for the fine-tuning of transcriptional initiation and elongation processes. Among transcriptional regulation, H2A ubiquitinylation was found to be involved in cell cycle progression.

A.2.3.2   Histone H2B ubiquitinylation

Histone H2B mono-ubiquitinylation (H2BK123 in yeast and H2BK120 in vertebrates) has in general been linked to active transcription, although there is evidence for a possible role in silencing. It was shown that H2BK123ub1 was a prerequisite for H3K4me3 and H3K79me3 (Sun and Allis 2002; Wood et al. 2003a), whereas deubiquitination of H2BK123ub1 was necessary for methylation of H3K36 (Henry et al. 2003), indicative of a positive role in transcription.

In *S. cerevisiae,* H2B mono-ubiquitinylation is catalyzed by the enzymes Rad6 (E2) and Bre1 (E3) (Wood et al. 2003a)*.* Additionally, the PAF elongation complex was shown to be required for RAD6-Bre1 catalytic activity but not for recruitment to the promoter (Wood et al. 2003b).

The human homologs of yeast Bre1, RNF20 and RNF40, are two RING domain proteins that are 15% identical and 28% similar to yeast Bre1 (Hwang et al. 2003). The E2 UbcH6 has been shown to interact with RNF20/RNF40 and to mediate H2B mono-ubiquitinylation together with hPAF as a trimeric complex *in vitro*. Furthermore, knockdown of RNF20 or components of the hPAF complex decreased whereas RNF20 over-expression increased H2Bub1 levels *in vivo* (Zhu et al. 2005).

In *S. cerevisiae* H2B ubiquitinylation can be reversed by two deubiquitinating enzymes (USPs), namely Ubp8 and Ubp10. Ubp8 as a component of the Gcn5 (HAT) - containing co-activator complex SAGA efficiently deubiquitinates H2Bub1 *in vitro* and *in vivo,* therefore combining deubiquitination and acetylation activities (Daniel et al. 2004). In fact, both H2B ubiquitinylation and Ubp8-dependent deubiquitination are required for proper transactivation, owing to a correct balance of H3K4 and H3K36 methylation set by sequential addition and removal of ubiquitin (Henry et al. 2003) (Kao et al. 2004). USP22 was found as the human

homolog of Ubp8 as part of the hSAGA/TFTC/STAGA complex (Zhang et al. 2008a; Zhao et al. 2008).

In contrast, Ubp10 (Dot4) acts independently of SAGA and in contrast to Ubp8 that deubiquitinates H2B in transcriptionally active euchromatin, interacts with Sir4 to facilitate silencing of sub-telomeric regions and rDNA in *S. cerevisiae.* (Emre et al. 2005; Gardner et al. 2005). However, Ubp10 may also have a role in silencing of euchromatin as well, since Ubp10 deletion strains show derepression of a number of genes that are not in the vicinity of heterochromatin (Gardner et al. 2005). In relation, USP7 has been described as an H2Bub1 deubiquitinating enzyme in *Drosophila* that is associated with Polycomb group proteins at the *ubx*-PRE (Polycomb responsive element) and at telomeres and chromocenters (van der Knaap et al. 2005). In addition, mutations of USP7 enhanced developmental defects of Polycomb protein knockout, further suggesting a role in PRC mediated silencing. Like Ubp10, USP7 might help to maintain transcriptionally inactive chromatin by removing the potentially activating ubiquitin moiety from H2B.

Several lines of evidence further support a positive role for H2Bub1 in transcriptional regulation. Bre1/RNF20 are recruited to promoters by transactivators Gal4 in yeast and p53 in human respectively, and the following ubiquitinylation of H2B was indispensible for full gene activation (Henry et al. 2003; Hwang et al. 2003). Over-expression and knockdown of RNF20 enhanced and reduced the induction of p53 - regulated p21 and MDM2 target genes (Kim et al. 2005). Moreover, Csp35, a protein that interacts with H3K4 HMT COMPASS and H3K79 HMT Dot1, is recruited to promoters by H2Bub1 (Lee et al. 2007a).

CHIP-on-CHIP analysis of ubiquitinylated H2B in human cells revealed a predominant location of this modification in the intragenic region of highly expressed genes (Minsky et al. 2008). In agreement, Rad6/Bre1 mediated H2Bub1 was abolished by mutations in subunits of protein complexes involved in transcriptional elongation (Espinosa 2008). Furthermore, H2Bub1 is required for full recruitment of Spt16 (a subunit of FACT) to intragenic regions (Fleming et al. 2008) and cooperates with FACT to promote transcriptional elongation through nucleosomal arrays (Pavri et al. 2006). In addition, Ubp8 promotes phosphorylation of Ser2 at the C-terminal domain (CTD) of RNAPII (Wyce et al. 2007), which is required for transcription elongation and co-transcriptional recruitment of mRNA processing factors (Ahn et al. 2004). A more detailed analysis in Bre1 mutants revealed that H2Bub prevented the recruitment of the Ser2-kinase Ctk1.

MDM2 is a major negative regulator of the tumor suppressor p53 and uses its RING finger domain to ubiquitinylate p53 for proteasomal degradation (Michael and Oren 2003). Interestingly, MDM2 ubiquitinylated H2A and H2B *in vitro,* but predominantly H2B *in vivo.* In addition MDM2 and H2bub were localized to the p53 responsive gene p21. MDM2 binding to a promoter, following H2B ubiquitinylation showed silencing in a luciferase reporter assay (Minsky and Oren 2004). On the one hand this is in contrast to the above-mentioned observation that RNF20 over-expression led to increased expression of p21 (Kim et al. 2005), but on the other hand it is an indication that H2BK120ub is either not necessarily the sole determinate of active transcription or that other E3 ligases and DUB's might regulate transcription in a gene-specific context. Considering the necessity of deubiquitination on elongation, one could imagine that poised RNA Polymerase II is stalled at the p21 promoter

19

upon H2B ubiquitination by MDM2. Deubiquitination of H2B would allow phosphorylation of the CTD of RNAPII and subsequent promoter escape and transcriptional elongation. USP7, interacting with both p53 and MDM2 and regulating their stability via deubiquitination (Li et al. 2002; Cummins and Vogelstein 2004) could be a candidate fulfilling H2B deubiquitination (van der Knaap et al. 2005).

Taken together, ubiquitinylated H2B is required for different steps in the process of transcriptional activation and elongation suggesting a model that multiple rounds of ubiquitinylation and deubiquitination are required for full gene induction (Henry et al. 2003; Wyce et al. 2007). Alternatively, this mode of action was assigned to a 'checkpoint' model allowing for RNAPII pausing and coordination in early elongation with RNA processing (Espinosa 2008). The function of ubH2B in gene silencing seems to be restricted to the action of deubiquitinating enzymes, keeping low levels of ubH2B which in turn maintain low levels of histone marks associated with active transcription.

A.2.4 USP7 – a ubiquitin specific protease

Deubiquitinating enzymes (DUB's) constitute a superfamily of thiol- and metallo-proteases specialized in the processing of ubiquitin and ubiquitin-like proteins. They are responsible for the disassembly of ubiquitin chains and for the cleavage of mono- and oligomers of this molecule, either in precursor form or attached to small nucleophiles and proteins (Amerik and Hochstrasser 2004; Nijman et al. 2005). Among, the DUBs, the ubiquitin specific proteases (USPs) constitute the largest family with 58 cysteine petidases identified so far (Nijman et al. 2005). One of the most prominent members of this superfamily is USP7, also known as Herpes simplex virus associated ubiquitin specific protease (HAUSP) due to its discovery in the promyelocytic leukemia nuclear bodies (PML) of herpes simplex virus infected cells (Everett et al. 1997). USP7 comprises 1102 amino acids with a molecular weight of approximately 130kDa and is composed of three domains, an N-terminal TRAF domain, a proteolytic core domain and a C-terminal domain.
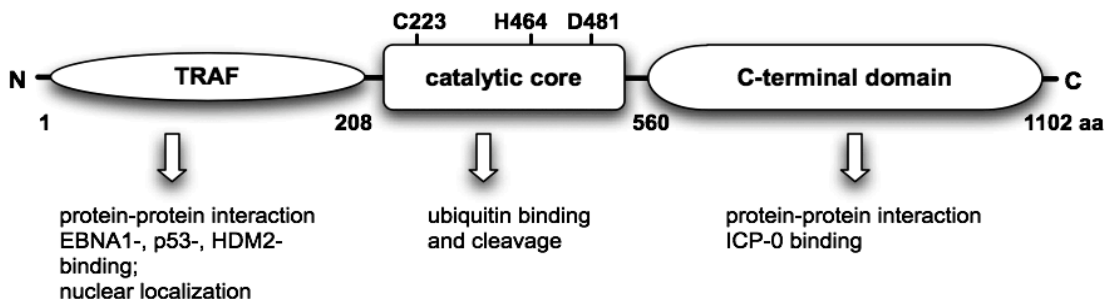
Figure 7 Domain structure of USP7 (HAUSP)

The domain structure of human USP7 (HAUSP) and the functions of the distinct domains are depicted. TRAF domain (TNF associated factor), catalytic core (catalytic residues are shown), C-terminal domain.

Due to the homology to the TNF receptor associated factors (TRAFs), the N-terminal domain of USP7 was named accordingly. The TRAF domain of USP7 is the interaction platform for several TRAF family proteins, EBNA1 nuclear antigen 1 (Holowaty et al. 2003), p53 (Hu et al. 2002) and was shown to be responsible for the nuclear localization of USP7, albeit no NLS sequence is present (Zapata et al. 2001; Fernández-Montalván et al. 2007).

Although the USPs make up for a highly divergent group, they all contain a catalytic core domain comprising eight conserved regions. The 3D crystal structure of the HAUSP core domain (aa208-560) was resolved and revealed an architecture composed of fingers, palm and thumb, which undergo dramatic conformational changes upon binding of the ubiquitin derivate Ubal (Hu et al. 2002). The C-terminal domain (aa560-1102) is composed of two domains (aa622-801 and aa885-1061) as determined through limited proteolysis mapping with the first of these polypeptides mediating the interaction of USP7 with the Herpes simplex virus protein ICP0 *in vitro* (Holowaty et al. 2003).

The tumor suppressor protein p53 was described as a direct target of USP7 *in vitro* and *in vivo* deubiquitinating and stabilizing p53 and thus antagonizing the MDM2 (HDM2 in human) mediated ubiquitin dependent degradation (Li et al. 2002). USP7 over-expression led to p53 accumulation and p53 mediated G_1 arrest and apoptosis. In colon adenocarcinoma HCT-116 cells, where both alleles of USP7 had been knocked-out, p53 displayed a much higher protein level (Cummins et al. 2004). This led to the observation that USP7 not only targets p53 but rather MDM2 for deubiquitination (Cummins and Vogelstein 2004). The current model for USP7 action indicates that in the absence of cellular stress, MDM2 is stabilized by the activity of USP7, maintaining low levels of p53. Upon cellular stress, the MDM2-USP7 interaction is impaired likely via posttranslational modifications, destabilizing MDM2 by auto-ubiquitinylation following proteasomal degradation. Free USP7 could eventually collaborate in stress-induced stabilization of p53 (Nijman et al. 2005).

Recently, the Chfr (checkpoint protein with FH and RING domains) E3 ubiquitin ligase, that was identified as a protein defining a mitotic checkpoint, that delays transition to metaphase in response to mitotic stress (Scolnick and Halazonetis 2000), was found to be regulated by USP7 (Oh et al. 2007). As mentioned earlier, USP7 was initially discovered as an interactor of ICP0, a Herpes simplex virus protein that plays a role in the switch between lytic and latent infection. ICP0 possesses an E3 ubiquitin ligase activity *in vitro,* mediated by its RING finger domain and induces the degradation of several cellular proteins including components of PML bodies and centromers. ICP0 is protected from autoubiquitinylation *in vitro* by USP7 and their interaction greatly increases the stability of ICP0 *in vivo* (Canning et al. 2004). Vice versa, ICP0 also targets USP7 for ubiquitination *in vitro* and proteasome dependent degradation *in vivo* (Boutell et al. 2005) suggesting a mutual regulatory mechanism on the activity and the stability of the two proteins. Recently the list of USP7 targets has been increased by the addition of FOXO4 transcription factor, which requires mono-ubiquitinylation for full trans-activation potential and is therefore deubiquitinated by USP7 resulting in exclusion of the nucleus (van der Horst et al. 2006).

Homeotic gene silencing in fly larve is mediated by the Polycomb silencing complex (Wang et al. 2004a). USP7 has been characterized as an ubH2B deubiquitinase *in vitro* and is involved in epigenetic silencing of homeotic genes in flies since USP7 mutations enhanced

Polycomb phenotypes (van der Knaap et al. 2005). Notably, the *USP7* gene is located on the X-chromosome and disruption of the gene is lethal to male and homozygous lethal in females. In addition, USP7 showed a distinct genome-wide distribution in larval salivary gland polytene chromosomes, suggesting potential functions in the regulation of multiple genes. Interestingly, USP7 was associated with several silenced regions including part of the chromocenter, telomeric regions and homeotic genes. The overall lack of co-localization with RNA Polymerase II suggested a role for USP7 in transcriptional silencing rather than activation. USP7 as an enhancer of Polycomb-mediated silencing deubiquitinating ubH2B would be in agreement with this notion (van der Knaap et al. 2005) .

Unexpectedly, biochemical purification of USP7 from *Drosophila* embryo extracts identified the metabolic enzyme GMP-synthase, as a strong interactor, required for enhanced deubiquitinase activity towards ubH2B and p53. GMP-synthase is required for synthesis of guanine nucleotides whose expression is strongly induced in rapidly proliferating cells (Boritzki et al. 1981) suggesting a link between the proliferative/metabolic state of the cell and histone modifications in analogous fashion to NAD^+-dependent histone deacetylases of the Sirtuin family (Holbert and Marmorstein 2005).

Related to this, it is of interest to note that all ubiquitinylated histones, including the four H2A variants and the H2Bs are absent from isolated metaphase chromosomes (Wu and Bonner 1981). Whether USP7 could be involved in this step is difficult to judge since no immunocytochemical data on the localization of USP7 during the cell cycle exist. Likewise, USP7 knockout cells (HCT-116 USP7-/- (Cummins and Vogelstein 2004)) are able to grow albeit slowly due to elevated p53 and p21 levels leading to G_1 arrest.

Ablation of USP7 by RNAi treatment had only marginal impact on the level of ubH2B in the total histone pool but H3K27me3 was strongly reduced (unpublished data, (van der Knaap et al. 2005). Hence, global changes in ubH2B levels probably require besides USP7 other USPs. The specific reduction of H3K27me3 that is mediated by the PRC2 component EZH2 (Viré et al. 2005; Wu et al. 2008) suggests that this modification is dependent on USP7 at certain chromosomal loci and confirms a functional role between USP7 and PcG silencing.

In summary, USP7 regulates the stability of factors that play a role in cell cycle checkpoints and progression and transcription through its deubiquitinating activity. The possible function of USP7 in gene silencing or activation correlated with H2B deubiquitination remains elusive.

A.3 DNA methylation

A.3.1   CpG methylation in eukaryotes

In terms of evolution, DNA methylation is old and can be found in bacteriophages, bacteria, fungi, plants and animals. In bacteria, DNA methylation can occur at the C-5 and the N-4 of cytosine as well as the N-6 of adenine, whereas DNA methylation at the C-5 position of cytosine in the context of CpG is the only covalent modification of DNA in higher eukaryotes (Hermann et al. 2004a). In any case, the methyl groups are positioned in the major groove of the DNA where they do not interfere with the Watson/Crick base-pairing capacities and where they can easily be detected by proteins interacting with the DNA. Thereby, methylation

adds extra information to the DNA that is not encoded in the sequence and C-5 methylation of cytosine was thus referred to as the 5th letter of the genetic alphabet.

Cytosine methylation accounts for 3-8% of all cytosine residues and for 60-90% of all CpG sites in mammalian genomes (Jeltsch 2002). Importantly, CpG sites are methylated on both strands of the DNA, resulting in a palindromically methlyated site. CpG sites in the genome are statistically underrepresented (5-10 fold) with respect to their expected normal frequency. This can be explained by the fact that deamination of 5-methyl-cytosine results in methyl-cytosine – thymine transition, whereas cytosine is deaminated to uracil which can be readily repaired by DNA repair mechanisms in the cell. As a result, CpG sites have been depleted from vertebrate genomes over evolutionary time and constitute for major hotspots of mutations in germlines and for acquired mutations in somatic cells (Hermann et al. 2004a). However, small regions of the genome, in which CpG di-nucleotides are not underrepresented, are known as 'CpG islands' (Cooper et al. 1983; Bird et al. 1985). Interestingly, CpG islands cover only 0.57 % of the genome and contain only 5.5% of the total number of CpG sites (Rollins et al. 2006), but over 50 % of the non-methylated CpG sites. Typically, they are found in promoter regions of about 60% of all genes including housekeeping genes and 40% of tissue specific genes and occur mostly unmethylated (Cross et al. 1994). Intriguingly, CpG islands can remain methylation-free even when their associated gene is silent (as seen for the β-globin gene) (Bird 2002). A small but significant proportion of all CpG islands become methylated during development thus rendering the promoter stably silent. Developmentally programmed CpG island methylation of this kind is involved in genomic imprinting and X- chromosome inactivation.

A.3.2 Biological role of DNA methylation

DNA methylation has a variety of important functions in mammals such as gene repression, control of cellular differentiation and development, preservation of chromosomal integrity, parental imprinting and X-chromosome inactivation (Bird 2002; Li 2002b) ((Hermann et al. 2004a) and references therein).

Although methylation of CpG sites regulates gene expression through several distinct mechanisms, it is generally associated with gene repression. First, CpG methylation induces changes in the interaction between DNA and DNA binding proteins. Binding of transcription factors such as E2F or NFκB, can be abolished, whereas recruitment of 5-methyl-cytosine binding proteins (MECP) that 'read' DNA methylation patterns, is enhanced. Besides DNA methyltransferases themselves (Robertson 2002) MECPs are also associated with HDACs, thereby inducing chromatin condensation and stable transcriptional repression (Ng et al. 1999; Zhang et al. 1999).

Interaction with other chromatin modifying proteins such as histone methyltransferases, heterochromatin protein HP1 and chromatin remodelers further contribute to this regulation (Robertson 2002).

The human genome contains approximately 40% of repetitive elements originating from transposons, retrotransposons and retroviruses (LTRs, LINEs, IAPs, SINEs) and are often referred to as 'parasitic' elements. Since random integration of transposable elements into

the genome constitutes for mutations, their spreading in the genome is inhibited by gene silencing and heterochromatin formation, mediated through extensive DNA methylation (Yoder et al. 1997; Smit 1999). In addition, repetitive DNA elements found in centromers, pericentromeric satellite repeats (minor and major α-satellites) and telomeres are highly methylated and densely packaged into heterochromatin, impairing homologous recombination events and thus providing chromosomal stability.

Genomic imprinting is a mammalian-specific phenomenon that refers to parental-origin-dependent mono-allelic expression in spite of identical nucleotide sequences (Li 2002b).

Early experiments with nuclear transfer of male and female pronuclei from fertilized eggs into enucleated fertilized eggs showed that both paternal and maternal genomes express different sets of genes that were required for complete embryonic development (McGrath and Solter 1984). Subsequently, two genomic regions on mouse chromosome 2 and 11 that showed opposite phenotypes when present as either two maternal or paternal copies respectively indicated parental-specific gene expression (Reik 1989). The existence of genomic imprinting in mammals was proven with the identification of the first imprinted genes. *Igf2r* (Insulin-like growth factor type 2 receptor) and the *H19* locus were identified as maternally expressed imprinted genes, whereas the *Igf2* gene was found to be a paternally expressed imprinted gene (Bartolomei et al. 1991; DeChiara et al. 1991; Wutz and Barlow 1998).

To date, there are about 80 imprinted genes known in mouse and many of these occur in clusters (3-10 genes, covering 100-3000kb) that are localized to imprinting regions found on eight mouse autosomes (Verona et al. 2003). Of the six imprinted clusters characterized so far, all share a common DNA sequence known as differentially DNA methylated region (DMR). Furthermore, DNA methylation generally suppresses the action of gametic DMR of the same parental chromosome that expresses the clustered mRNA genes. Thus, in the absence of methylation, the DMR cannot function appropriately leading to the repression of both copies of imprinted genes. Notably, some of the DMRs, like in the *Igf2r* region 2, present portable methylation signals that can direct specific DNA methylation even if they are moved to another chromosomal location (Herman et al. 2003). In addition, it was shown that non-coding RNAs, like the *AIR* RNA, are involved in targeting and activation of *de novo* DNA methylation (Sleutels et al. 2002) although the exact mechanism remains elusive.

Importantly, in germ cells, DNA methylation is removed in order to replace the existing methylation pattern by a gametic specific one that is maintained in somatic cells. In four clusters (*Ifg2r, Kcnq1, Gnas, Pws*), the gametic DMR has a maternal methylation imprint acquired during oogenesis whereas in two clusters (*Igf2, Dlk1*) it has a paternal imprint acquired during spermatogenesis. The DMR has been shown to control imprinted expression of the whole or part of the cluster and was therefore designated imprint control element (ICE) (Spahn and Barlow 2003). Interestingly, each cluster contains at least one non-coding RNA (ncRNA) that generally exhibits reciprocal parental-specific expression compared to the imprinted mRNA genes.

Over the years, data has accumulated that DNA methylation is involved in a number of diseases and that aberrant methylation patterns play a pivotal role in the genesis of cancer (Feinberg 2004), including defects in genome-wide hypo- and hypermethylation of specific

CpG islands, as well as loss of genomic imprinting (LOI). Global DNA hypomethylation, which promotes stimulation of oncogenes, reactivation of retrotransposons and genomic instability, occurs concomitantly with local hypermethylation of tumor suppressor genes leading to repression and is often found in a significant subset of melanomas and colon cancers ((Feinberg 2004) and references therein).

Furthermore, DNA methylation has been shown to be involved in ICF (Immunodeficiency, Centromeric instability, Facial abnormalities) and the Rett syndrome. ICF is an autosomal recessive disease characterized by hypomethylation of pericentromeric satellite repeats that is caused by a mutation in the Dnmt3b protein (Okano et al. 1999; Ehrlich et al. 2008). The Rett syndrome is an X chromosomal dominant disease that results from a mutation in the MeCP2 protein (Shahbazian and Zoghbi 2002; Kriaucionis and Bird 2003). MeCP2 is a 5-methyl-cytosine binding protein that fails to repress transcription in its mutant form.

Imprinting defects are found in solid tumors in childhood that arise from embryonic tissues. These so-called embryonal tumors comprising neuroblastoma (NB), Wilms tumor (WT), medulloblastoma (MB), rhabdomyosarcoma (RMS) and hepatoblastoma (HB) have been extensively studied in regard to epigenetic defects at the *Igf2/H19* locus. Interestingly, defective imprinting of *Igf2* and thus inappropriate activation of the maternal allele of the Igf2 gene are found in about 50% of all WT (Ogawa et al. 1993) and RMS cases (Zhan et al. 1994) as well as in about 25% of HB (Rainier et al. 1995; Hartmann et al. 2000).

In mammals, there are developmental periods of genome-wide reprogramming of methylation patterns *in vivo:* one during germ-cell development and one after fertilization. Typically, a substantial part of the genome is demethylated and after some time remethylated which occurs in a cell- or tissue-specific pattern (Reik et al. 2001; Li 2002a).

During gametogenesis, primordial germ cells undergo demethylation independent of replication, erasing parental imprinting marks (Oswald et al. 2000). In the course of oogenesis and spermatogenesis, maternal and paternal specific genomic imprints are re-established through *de novo* methylation activities of Dnmt3a and Dnmt3b and associated Dnmt3L (Hata et al. 2002; Hata et al. 2007). After zygote formation, the paternal DNA is demethylated by an active process (Oswald et al. 2000), while the maternal DNA is demethylated over several cell divisions by the lack of maintenance methylation (Rougier et al. 1998) resulting in global demethylation except for imprinted genes and retroviral sequences (Lucifero et al. 2004). After implantation, embryonic methylation patterns are reintroduced by a wave of *de novo* methylation. Genetic studies on zygote formation revealed that both *maintenance* and *de novo* methylation activities are indispensible for the formation of methylation patterns, and thus essential for embryonic development (Li et al. 1992; Okano et al. 1999).

A.3.3   The reaction mechanism of DNA methyltransferases.

DNA-cytosine-5-methyltransferases (Dnmts) must perform two functions. On the one hand they recognize a specific DNA sequence and on the other hand catalyze the transfer of the methyl-group from the substrate S-adenosyl-methinone (SAM) onto the C-5 position of

cytosine. Prokaryotic and eukaryotic C-5 methyltransferases comprise a large and a small domain with 10 conserved sequence motifs, six of which are highly conserved (I, IV, VI, VIII, IX and X) (Pósfai et al. 1989; Cheng et al. 1993; Kumar et al. 1994).

These motifs encompass the SAM binding pocket (I, IV, V, X) and the active site of the Dnmt (IV). The region between motifs VIII and IX is variable in different Dnmts and is believed to account for sequence specificity (Kumar et al. 1994). Notably, in contrast to other eukaryotic Dnmts, the catalytic domain of Dnmt1 is not catalytically active by itself, but requires allosteric activation by the N-terminal domain (Fatemi et al. 2001a).

Due to great sequence homology of C-5 DNA methyltransferases, the catalytic mechanism of methyl-group transfer is thought to be identical with a reaction pathway of Micheal addition and enzymatic release by β-elimination (Pradhan and Esteve 2003).
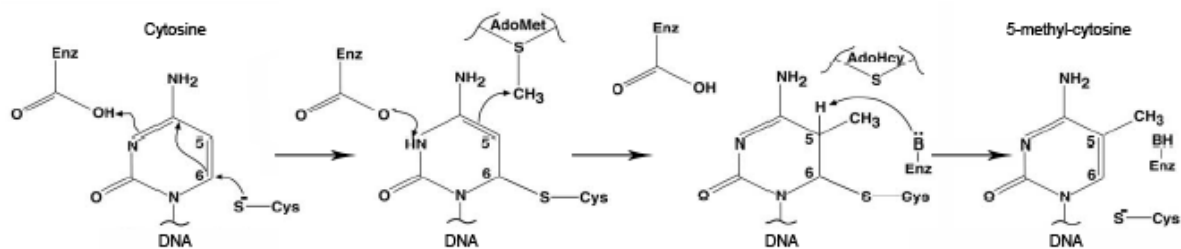
Figure 8 Reaction mechanism of C-5 DNA methyltransferases

The reaction mechanism as described for M. HhaI DNA methyltransferase. The carboxyl-group is provided by Glu 119 in the conserved sequence motif VI (ENV), the cysteine is provided by Cys 81 in sequence motif IV (PCQ). S-adenosyl methionine (adoMET) and S-adenosyl-homocysteine (AdoHcy) are the cofactor and the end product of the reaction respectively. (Pradhan and Esteve 2003).

After binding of DNA, recognition of the methylation site and binding of the co-substrate SAM, the DNA methyl-transfer reaction is initiated by nucleophilic attack of the cysteinyl thiolate of the Pro-Cys dipeptide in motif IV on the C6 position of the cytosine, resulting in a covalent complex intermediate between the enzyme and the DNA. The enzyme facilitates nucleophilic attack on the C6 by concomitant protonation of the N3 of the cytosine by a conserved glutamyl-residue in motif VI, forming a reactive enamine, which in turn attacks the sulphonium linked methyl-group of S-adenosyl-L-methionine. The methyl-group is subsequently transferred to the cytosine while simultaneously reprotonating the glutamyl-residue. After a proton is abstracted from the C5 position by a base in the catalytic center, the enzyme is released by expulsion of the cysteinyl-thiolate group and the C5-C6 double bond in the newly formed 5-methyl-cytosine is reconstituted. By transfer of a proton from the protonated base to the thiolate group, the cysteine in the Pro-Cys dipeptide is restored and the protein is ready for the next reaction cycle.

For all structures of C-5 methyltransferases in complex with target DNA, a base flipping mechanism was found as initially described for the uracil-DNA glycosylase in DNA repair ((Jeltsch 2002) and references therein). The target base is completely flipped out of the DNA helix and bound in a hydrophobic pocket in the large domain of the enzyme, allowing sterical accessibility to the cytosine. Interestingly, the SRA domain of ICBP90 was recently identified

as the first example of a DNA binding module using this mechanism for sequence-specific DNA recognition (Arita et al. 2008; Avvakumov et al. 2008; Hashimoto et al. 2008).

A.3.4 Identification of mammalian DNA methyltransferases

Genomic patterns of DNA methylation in higher eukaryotes were initially established using DNA-methylation sensitive restriction enzymes. When analyzing a particular DNA strand, it was found that methylated CpG sites were always either not methylated or symmetrically methylated indicating the existence of a DNA methyltransferase that would complement the DNA methylation mark of the parental stand on the newly synthesized daughter strand during replication (Bird and Southern 1978). Further evidence for the heritability of DNA methylation patterns was made by transfection of either non-methylated (nm) DNA or *in vitro* methylated DNA into cultured cells (Wigler 1981) showing the retention of the DNA methylation status for many generations.

Subsequently, Dnmt1 was the first cytosine-5 DNA methyltransferase to be isolated as a mammalian methyltransferase and identified via biochemical purification (Bestor and Ingram 1983; Bestor 1988). In addition, the DNA methyltransferase activity purified from murine erythroleukemia cells showed inefficient methylation towards non-methylated (nm) compared to hemi-methylated (hm) DNA (Bestor and Ingram 1983) arguing for the role in *maintenance* of DNA methylation. Strong support for this view was provided by the fact that inactivation of Dnmt1 in mouse ES cells led to genome-wide loss of CpG methylation (Li et al. 1992).

Table 1 Functions of mammalian DNA methyltransferases

Dnmt	Species	Major activity	Major phenotypes and loss-of-function mutations
Dnmt1	mouse	*maintenance* methylation of CpG sites	genome-wide loss of DNA methylation, embryonic lethality at embryonic day 9.5 (E9.5), abnormal expression of imprinted genes, ectopic X-chromosome inactivation, activation of silent retrotransposons
Dnmt2	mouse	weak activity	no change in CpG methylation, no obvious developmental phenotypes
Dnmt3a	mouse	*de novo* methylation of CpG	Postnatal lethality at 4-8 weeks, male sterility, and failure to establish imprints in both male and female germ cells
Dnmt3b	mouse	*de novo* methylation of CpG	Demethylation of minor satellite DNA, embryonic lethality around E14.5 days with vascular and liver defects (embryos lacking both Dnmt3a and Dnmt3b fail to initiate *de novo* methylation after implantation and die at E9.5
Dnmt3b	human	*de novo* methylation of CpG	ICF syndrome; loss of methylation in repetitive elements and pericentromeric heterochromatin

Early experiments showed that nm DNA transfected into somatic cells tended to remain in a non-methylated state after multiple cell divisions, whereas transgenes introduced into morula stage pre-implantation mouse embryos by infection with Moloney murine leukaemia virus (MML-V) became *de novo* methylated and were blocked in expression (Jähner et al. 1982).

Further studies with embryonal carcinoma cells (EC) infected with MML-V revealed that in contrast to differentiated cells, expression of viral DNA was low and that proviral genomes were highly methylated as seen by their resistance to cleavage by SmaI. However, the proviral genomes were potentially infectious in cells that were treated with 5-aza-2'-deoxycytidine – an inhibitor of DNA methyltransferases (Stewart et al. 1982). These results indicated that the process of *de novo* DNA methylation is confined to toti- and pluri-potent stages of embryogenesis and thus also embryonic stem cells, and that DNA methylation could silence expression of viral genome *in vivo.* Deletion of the Dnmt1 gene, however, did not interfere with *de novo* methylation of proviral DNA in ES cells, suggesting the existence of other DNA methyltransferases (Lei et al. 1996).

By means of database search with four bacterial DNA cytosine methyltransferases, two new classes of DNA methyltransferases, namely Dnmt2 and Dnmt3 were found (Okano et al. 1998). Although Dnmt2 contains all the conserved motifs shared by prokaryotic and eukaryotic DNA cytosine methyltransferases, inactivation of Dnmt2 in mouse ES cells neither perturbed *de novo* nor *maintenance* methylation of proviral DNA (Okano et al. 1998). In fact, several years later Dnmt2 was shown not to methylate DNA but the cytosine 38 in the anticodon loop of the tRNA(Asp) (Goll et al. 2006) and that this function is highly conserved from plant to human.
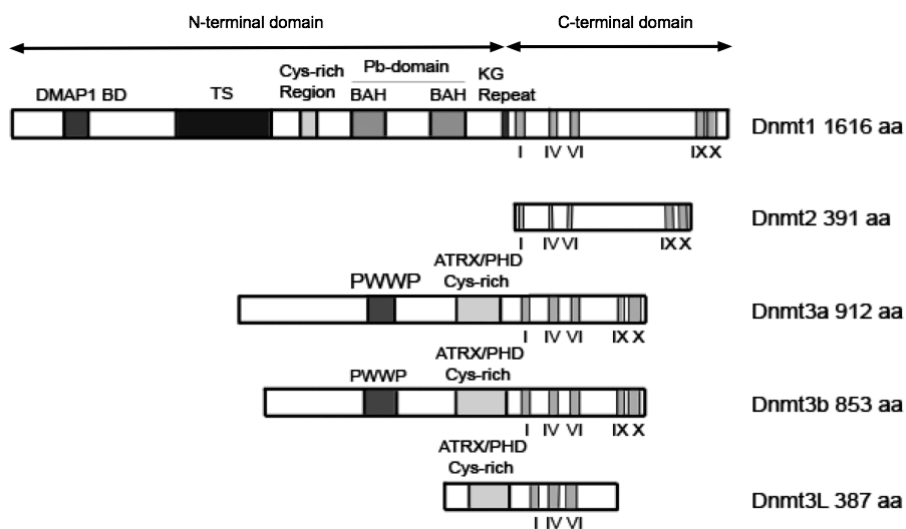
Figure 9 Domain structures of mammalian DNA methyltransferases

The mammalian DNA methyltransferases are divided into an N-terminal regulatory domain and a C-terminal catalytic domain with the latter showing strong amino acid sequence homology to prokaryotic DNA cytosine-5 methyltransferases (conserved motifs for catalysis are indicated). Dnmt1: DMAP1 (Dnmt1 associated protein 1) binding domain, TS (targeting sequence) domain, Cys-rich region (ATRX type zinc finger, DNA binding), Pb-domain (polybromo-1 protein homologous region containing two BAH domains) domains, GK (glycine-lysine) repeats. Dnmt3 family: PWWP domain, ATRX/PHD (cysteine-rich zinc finger domain of the ATRX/ plant homeo-domain type). Modified according to (Hermann et al. 2004a).

Dnmt3a and Dnmt3b were identified as the *de novo* methyltransferases in both mouse and human and cloned subsequently (Okano et al. 1998; Xie et al. 1999). Accordingly, unlike Dnmt1, these proteins showed no preference for hm DNA *in vitro* (Okano et al. 1998). Disruption of the genes for Dnmt3a and Dnmt3b blocked *de novo* methylation in ES cells and early embryos, but it had no effect on the maintenance of imprinted methylation patterns

28

(Okano et al. 1999). Interestingly, Dnmt3a and Dnmt3b exhibit non-overlapping functions in development, with Dnmt3b specifically required for methylation of pericentromeric minor satellite repeats. Furthermore, male and female germ cells lacking Dnmt3a or the associated regulatory factor Dnmt3L failed to establish distinct methylation patterns at imprinted genes (Bourc'his et al. 2001; Hata et al. 2002; Kaneda et al. 2004). Whereas inactivation of both Dnmt3a and Dnmt3b resulted in early embryonic lethality, loss of either gene caused severe defects in early embryonic development resulting in postnatal (Dnmt3a) or embryonic (Dnmt3b) lethality (Okano et al. 1999).

A.3.5 Dnmt1 – the *maintenance* methyltransferase

Dnmt1 is a 1616aa protein that comprises a large N-terminal regulatory domain (approximately 1100aa) that is linked via a glycine-lysine rich stretch (GK-repeats) to the conserved C-terminal catalytic domain (Figure 9). However, expression of either N- or C-terminus has not yielded an active enzyme (Fatemi et al. 2001b).

Enzymatic studies revealed a high preference of Dnmt1 towards hemi-methylated (hm) DNA and a high methylation processivity of hm DNA (Bacolla et al. 1999; Pradhan et al. 1999; Hermann et al. 2004b) reflecting the role of *maintenance* methylation *in vivo* (Bestor 2000). Analyses of its subnuclear localization is in agreement with this function. Dnmt1 shows a diffuse nuclear distribution during G_1 and G_2 phase, but associates with replication foci during S-phase (Leonhardt et al. 1992; Chuang et al. 1997).

Dnmt1 directly interacts with PCNA through the PCNA-binding domain (PBD, aa163-174) (Chuang et al. 1997), promoting DNA methylation of the newly synthesized daughter strand during replication (Iida et al. 2002). Nevertheless, Dnmt1 exhibits an intrinsic high processivity and fidelity towards hm DNA irrespective this interaction (Vilkaitis et al. 2004). Moreover, the interaction with PCNA is highly dynamic *in vivo* and constitutes for a 2-fold increase in methylation efficiency, but it is not strictly required for maintaining global DNA methylation (Schermelleh et al. 2007). In addition, replication takes place faster than methylation (Schermelleh et al. 2005) indicating other mechanisms for Dnmt1 recruitment. Hence, the Targeting sequence domain of Dnmt1 (TS; aa316-601) (Leonhardt et al. 1992) was found to recruit Dnmt1 to replication foci, especially to 'larger' foci during mid and late S-phase. This localization is mediated through the interaction of the TS domain with the SRA domain of UHRF1 (Achour et al. 2007), a heterochromatin associated protein (Karagianni et al. 2008) that binds preferentially to hm DNA (Unoki et al. 2004; Bostick et al. 2007; Arita et al. 2008) (A.2.2). The importance of the interaction with this factor becomes evident since UHRF1(-/-) ES cells revealed global and local hypomethylation and methylation defects of imprinted genes and retrotransposons (Sharif et al. 2007) – reflecting the situation of Dnmt1 knockout in ES cells and mice (Li et al. 1992). The preference of Dnmt1 for hm DNA is approximately 20-25-fold compared to nm DNA (Pradhan et al. 1999; Hermann et al. 2004b). In spite of this fact introduction of *de novo* methylation could occur during each round of replication. UHRF1 acting as a sensor for hm DNA and associating with Dnmt1 could contribute to the fidelity of complementing DNA methylation patterns.

As already mentioned, Dnmt1 is essential during early stages of embryogenesis represented by death of Dnmt1 knockout mice during midgestation (Li et al. 1992) but it is also required for proliferation and survival in somatic cells (Jackson-Grusby et al. 2001; Egger et al. 2006). Dnmt1 is down-regulated during G_0 and G_1 phase in normal and tumor cells, albeit slightly elevated levels in the latter one (Robertson et al. 2000b). Considering the major function of Dnmt1 in the involvement of the replication process, the expression level of Dnmt1 should correlate with the proliferative status of the cell. However, Northern Blot analysis revealed a somewhat paradoxical picture that Dnmt1 is highly expressed in lung and placenta, but also in low-proliferative tissues such as heart and brain (Robertson et al. 1999).

Three alternative splice variants of Dnmt1 exist, namely Dnmt1b, Dnmt1o and Dnmt1p, that are expressed in a tissue and development dependent manner.

The Dnmt1b isoform contains an additional 48 bp exon between exons 4 and 5 that codes for 16 additional amino acids (Hsu et al. 1999; Bonfils et al. 2001). Although Dnmt1b mRNA is ubiquitously expressed in all cell lines and the in vitro enzymatic properties of Dnmt1b are comparable to Dnmt1 (Bonfils et al. 2001), the exact function of Dnmt1b remains elusive.

Dnmt1o is a truncated isoform of Dnmt1, lacking the N-terminal 118aa due to a second in-frame start codon (Yoder et al. 1996). It is synthesized and stored in the cytoplasm of the oocyte and traffics to the eight-cell nucleus during preimplantation development, where it maintains DNA methylation patterns on alleles of imprinted genes (Ratnam et al. 2002). Notably, Dnmt1o is a degradation resistant form of Dnmt1 allowing for accumulation of high concentrations in non-cycling oocytes (Ding and Chaillet 2002). In accordance, the N-terminal 120aa of Dnmt1 are involved in ubiquitin dependent proteasomal degradation (Zhou et al. 2008a).

A larger form of Dnmt1 mRNA, referred to as Dnmt1p, was detected exclusively in pachytene spermatocytes (Mertineit et al. 1998), but it was not translated. An alternative Dnmt1 transcript resembling Dnmt1p was found in myotubes (Aguirre-Arteta et al. 2000) indicating a role of Dnmt1p during gametogenesis and myogenesis.

A.3.5.1 Interactions of Dnmt1

The N-terminus of Dnmt1 serves as a regulatory domain in the process of DNA methylation but also as a binding platform for numerous proteins.

The C-X-X-C domain of Dnmt1 is highly similar in sequence to zinc fingers and bound specifically to non-methylated CpG di-nucleotides (Pradhan et al. 2008). Deletion of this domain led to decreased activity *in vitro*, and over-expression of Dnmt1ΔCXXC resulted in partial loss of methylation on rDNA loci.

Recently another function was assigned to the TS domain. It was identified as the key determinate for dimerization of Dnmt1 in a head-to-head orientation (Fellinger et al. 2009) that could account for a possible prerequisite for recognition of hemi-methylated palindromic target sites.

The only Dnmt1 complex purified by means of chromatographic fractionation from Hela nuclear extracts was a complex consisting of Dnmt1, pRB, E2F1 and HDAC1 that was shown to repress transcription from promoters containing E2F1 binding sites (Robertson et

al. 2000a). In fact, both Dnmt1 and pRB were shown to interact with HDACs to induce gene silencing (Luo et al. 1998; Magnaghi-Jaulin et al. 1998; Fuks et al. 2000). Another effect of pRB binding to Dnmt1 was found. Overexpression of pRB using an adenoviral construct led to inhibition of global DNA methylation irrespective the phosphorylation status of pRB (Pradhan and Kim 2002). Addition of methylated ds DNA to a reaction containing unmethylated substrate led to catalytic activation of Dnmt1, suggesting the end product could function as a ligand for allosteric activation (Bacolla et al. 1999; Fatemi et al. 2001a). Deletion of the N-terminal 501aa abolished this activation (Pradhan and Estève 2003). Interestingly, the RB protein bound to the allosteric site of hDNMT1 (aa 284-287) and inhibited methylation, suggesting pRb may compete with DNA binding and thus regulate methylation spreading (Pradhan and Estève 2003). Furthermore, A similar regulatory mechanism was proposed for p21 mediated PCNA-Dnmt1 complex destabilization (Chuang et al. 1997).

Dnmt1 was also found to form another complex comprising HDAC2 and DMAP1 (Dmt1 associated protein1) (Rountree et al. 2000). DMAP1 binds to the far N-terminus of Dnmt1, exhibits intrinsic transcriptional repressive activity, binds to the co-repressor TSG101 and is targeted to replication foci throughout S-phase. In contrast, HDAC2 joins Dnmt1 and DMAP1 only during late S-phase providing for histone deacetylation and heterochromatin formation after replication. Further studies revealed the existence of two complexes, p33ING1-Sin3-HDAC and DMAP1-DNMT1, that physically interact with one another through p33ING1 and DMAP1 and that are recruited independently to pericentromeric heterochromatin regions during late S-phase (Xin et al. 2004). Importantly, they are required for histone deacetylation and H3K9me3 and binding of HP1. Recent data attributed DMAP1 an important role in specific gene silencing forming a complex with Bmi1 of PRC1 and Dnmt1 (Negishi et al. 2007). Knockdown of either Bmi1 or DMAP1 resulted in transcriptional derepression and loss of recruitment of the other factors. Moreover, the Bmi1 homologous polycomb protein NSPc1 (Nervous System polycomb1) was shown to promote H2A ubiquitination and to cooperate with PRC2 and Dnmt1 dependent DNA methylation in *Hox* gene silencing (Wu et al. 2008). Furthermore, the PcG protein EZH2 interacts within the context of PRC2/3 complexes with Dnmt1 and recruits Dnmt activity to EZH2 target promoters *in vivo* (Viré et al. 2005).

An example for specific transcriptional silencing in cancer is the recruitment of Dnmt1 and Dnmt3a to target sites by the leukemia-promoting PML-RAR fusion protein leading to promoter hypermethylation and silencing (Di Croce et al. 2002).

The physical interaction of Dnmt1 with the *de novo* methyltransferases has been described *in vitro* and *in vivo* (Kim et al. 2002). Both Dnmt3a and Dnmt3b interact with their N-terminus (but not PHD domain) with two different regions in the far N-terminus of Dnmt1. The functional relevance of this interaction was underscored by studies with Dnmt knockouts in HCT-116 colon adenocarcinoma cells. Dnmt1 knockout in HCT-116 cells revealed only a 20% reduction of global methylation (Rhee et al. 2000). Later studies revealed that the knockout strategy had failed and generated an active Dnmt1 hypomorph lacking a great part of the N-terminal domain (Li et al. 2007b). Nevertheless, double-knockout (DKO) of Dnmt1 and Dnmt3b almost eliminated methyltransferase activity and reduced DNA methylation to 5% showing demethylation of repeated sequences, loss of *Igf2* imprinting, abrogation of

silencing of the tumour suppressor gene $p16^{INK4a}$, and growth suppression (Rhee et al. 2002).

The 'real' Dnmt1 knockout in HCT-116 cells, that targeted the deletion of the catalytic domain, also showed only slight reduction of global methylation, suggesting a partial compensation of Dnmt3a and Dnmt3b, but led to G_2/M checkpoint activation and G_2 arrest (Li et al. 2007b). Furthermore, cells escaping this arrest showed severe mitotic defects and underwent cell death either during mitosis or after arresting in a tetraploid G_1 state.
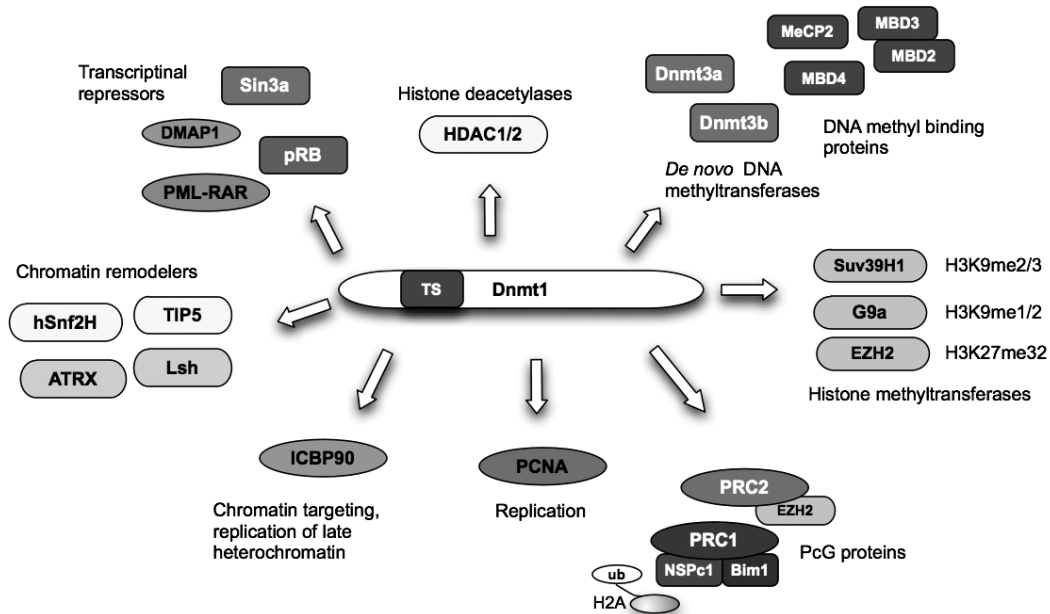
Figure 10 Proteins directly/ functionally interacting with Dnmt1

Dnmt1 interacts with various proteins generally involved in silencing. Specific functions are given in the text.

After replication, the DNA is assembled into chromatin. The histone methyltransferase G9a being specific for H3K9me1/2 especially in euchromatic regions, is targeted by Dnmt1 to replication foci (Esteve et al. 2006). *In vitro,* the complex of Dnmt1 and G9a led to enhanced DNA and histone methylation of assembled chromatin substrates. Notably, G9a-null mice display severe growth retardation and die during embryonic development (Tachibana et al. 2002) reminiscent of Dnmt1 knockout mice (Li et al. 1992). In agreement, ES cells lacking G9a showed a significant reduction in DNA methylation of retrotransposons, major satellite repeats and densely methylated CpG-rich promoters (Dong et al. 2008).

Similar to G9a, the HMT Suv39H1 specific for H3K9me2/3 and HP1 binding to H3K9me3 were both shown to interact with Dnmt1 (Fuks et al. 2003) indicating a functional connection between DNA and histone methylation.

Furthermore, the methyl-DNA-binding proteins MeCP2 and MBD2 were shown to mediate gene repression by recruiting histone deacetylase complexes to methylated genes (Ng et al. 1999). Dnmt1 was found to interact with the MBD2-MBD3 complex and co-localized to replication foci during late S-phase (Tatematsu et al. 2000). Importantly, the MBD2-MBD3 complex showed a hitherto unreported affinity to hm DNA suggesting a role in heterochromatin formation after replication through recruitment of HDACs. MeCP2 also bound to hm DNA and associated with Dnmt1 (Kimura and Shiota 2003). Interestingly,

Dnmt1 substitutes the mSin3A-HDAC1 complex indicating the absence of HDAC activity in the MeCP2-Dnmt1 complex. Therefore, MeCP2 was postulated to contribute to *maintenance* methylation – a function that today is assigned to UHRF1 (see above; A.2.2).

Besides the interaction of Dnmt1 with transcriptional regulators and chromatin modifying enzymes, ATP-dependent chromatin remodeling proteins (A.1.4) have been identified to play a role in DNA methylation (see section A.3.8).

Taken together, DNA methylation is highly coordinated together with other chromatin modifications and Dnmt1 is regulated in a tightly cross-linked network of interactions.

A.3.6 *De novo* DNA methyltransferases Dnmt3a and Dnmt3b

Dnmt3a and Dnmt3b were both identified by a database-search (Okano et al. 1998). They do not exhibit any preference for hemi-methylated DNA *in vitro* and were thus considered as *de novo* methyltransferases (Okano et al. 1998; Gowher and Jeltsch 2002; Suetake et al. 2003). Both proteins are able to methylate cytosine bases outside the context of CpG sites, but the biological function of this phenomenon remains unclear (Gowher and Jeltsch 2001; Gowher and Jeltsch 2002; Lin et al. 2002). In addition, Dnmt3a shows preference for CpG sites that are flanked by pyrimidines rather than purines (Lin et al. 2002). In a more detailed study the flanking sequences of up to four base pairs surrounding the central CpG site were analyzed showing preferred RCGY over YCGR (R = purine; Y= pyrimidine) methylation by Dnmt3a and Dnmt3b and a preference of AT-rich flanks over GC-rich ones (Handa and Jeltsch 2005). They share homologous C-terminal catalytic domains that in contrast to Dnmt1 are catalytically active (Gowher and Jeltsch 2002), homologous cysteine-rich regions (also referred to as PHD/ATRX domain) (Xie et al. 1999) and PWWP domains (Qiu et al. 2002) that are approximately 100-150 aa in length and are often found within chromatin associated proteins. The PWWP domain from mouse Dnmt3b (amino acids 223--357) has been structurally characterized (Qiu et al. 2002) and exhibits DNA binding properties. However, the affinity of the PWWP domain of Dnmt3a towards DNA is smaller than that of Dnm3b (Chen et al. 2004). Notably, disruption of the PWWP domain in both proteins abolishes their association with pericentromeric heterochromatin and their abilities to methylate this region (Chen et al. 2004).

Recently, the essential transcription factor SALL3 was identified as a novel inhibitor factor for Dnmt3a interacting via the PWWP domain (Shikauchi et al. 2009). Interestingly, SALL3 expression reduced Dnmt3a mediated CpG island methylation *in vivo* and *in vitro* and affected chromatin association of Dnmt3a.

The PHD/ATRX domain comprises approximately 50aa residues, is characterized by a conserved Cys_4-$HisCys_3$ zinc-binding motif and is found mainly in proteins involved in eukaryotic transcriptional regulation (Hermann et al. 2004a). Dnmt3a binds to RP58, a DNA binding transcriptional repressor found in heterochromatin, leading to methylation independent repression of genes (Fuks et al. 2001). Interestingly, this silencing was mediated by HDAC1 that associated with Dnmt3a through its PHD/ATRX-homology domain. Similar to Dnmt3a, Dnmt3b and Dnmt1 associate with HDAC1 leading to methylation

independent silencing (Rountree et al. 2000; Bachman 2001) although the latter does not share the PHD domain.

As seen for Dnmt1, Dnmt3a interacts through its PHD/ATRX-homology domain with the H3K9 specific HMT Suv39H1 and HP1 (Fuks et al. 2003) indicating cooperation in formation or maintenance of heterochromatin. Similarly, Dnmt3a associated *in vivo* and *in vitro* via the PHD domain with the euchromatic HMT SETDB1 that is specific for H3K9me3 (Li et al. 2006). Co-expression of both proteins was essential for recruitment to an artificial promoter and its repression. The list of proteins interacting with the PHD domain of Dnmt3a was recently expanded by the arginine methyltransferase PRMT5 that specifically promotes symmetric H4R3 di-methylation (Zhao et al. 2009). Interestingly, H4R3me2 serves as direct target for Dnmt3a through its PHD domain. Knockdown of PRMT5 and subsequent loss of H4R3me2 resulted in reduced Dnmt3a binding, DNA methylation and thus activation of the β-globin locus.
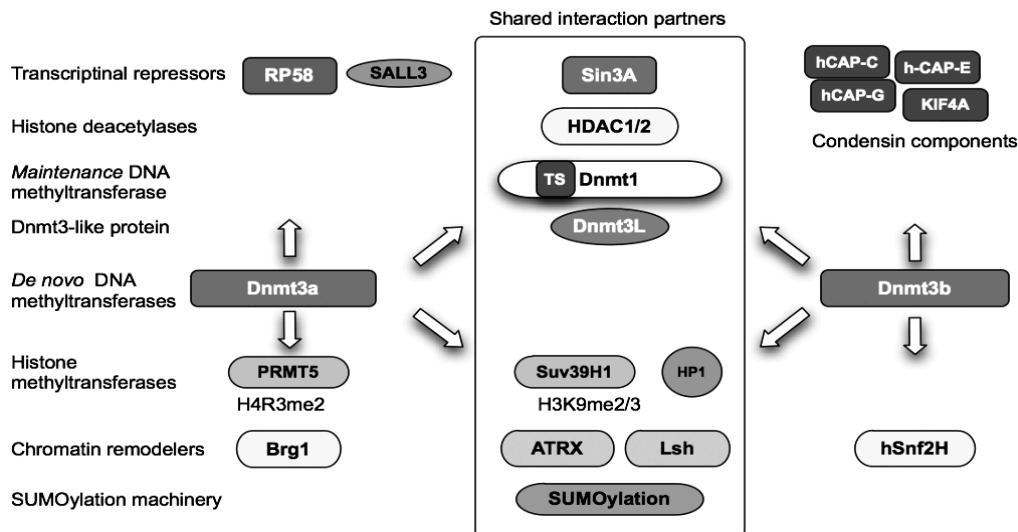
Figure 11 Interacting proteins of Dnmt3a and Dnmt3b

Dnmt3a and Dnmt3b interact with various proteins. In the middle panel shared interaction partners are depicted whereas proteins associating only with Dnmt3a or only Dnmt3b are shown to the left and the right respectively. Details of protein function are given in the text.

Like Dnmt3a, Dnmt3b has been shown to interact with factors involved in gene silencing such as HDAC1/2, Suv39H1, Hp1 and the ATP-dependent chromatin remodeling enzyme hSnf2H and to co-localize with these proteins to transcriptionally repressed, heterochromatic regions (Lehnertz et al. 2003; Geiman et al. 2004b). Moreover, Dnmt3b was purified via chromatographic fractionation from Hela nuclear extracts in a complex containing several components of the condensin complex (hCAP-C, hCAP-E and hCAP-G), KIF4A, HDAC1, the co-repressor SIN3A and hSnf2H (Geiman et al. 2004a). Dnmt3b co-localized with these components on condensed chromosomes throughout mitosis contrasting observations of Dnmt3b localization in murine ES cells and embryonic fibroblast cells (Bachman 2001).

The structure of the catalytic domain of Dnmt3a in complex with the C-terminal domain of Dnmt3L was solved by X-ray crystallography (Jia et al. 2007). Both the structure and mutagenesis experiments suggest that the interaction with Dnmt3L is required for full Dnmt3a activity and for formation of nucleoprotein filaments (Jurkowska et al. 2008).

Furthermore, Dnmt3a interacts with subunits of the SUMOylation machinery and undergoes this posttranslational modification both *in vivo* and *in vitro* (Ling et al. 2004). SUMOylation inhibits the interaction with HDAC1 and HDAC2 and abolishes transcriptional repression by Dnmt3a. Recently, the human polycomb group protein Cbx4 (HPC2) was identified as the SUNO E3 ligase for Dnmt3a, SUMOylating its target in the far N-terminus *in vivo and* in *vitro* (Li et al. 2007a). Likewise, Dnmt3b interacts and co-localizes with SUMO-1 and the E2 conjugating enzyme Ubc9, although the function remains elusive (Kang et al. 2001).

Dnmt3a is ubiquitously expressed in most adult tissues, whereas Dnmt3b is only detectable in testis, thyroid and bone marrow. In contrast, both Dnmt3a and Dnmt3b expression is elevated in several tumor cell lines to levels comparable to Dnmt1 (Xie et al. 1999) underscoring the notion of aberrant methylation in cancer cells.

Like Dnmt1, Dnmt3a and Dnmt3b were shown to exist in different splice variants. There are two isoforms of Dnmt3a, namely Dnmt3a1 and Dnmt3a2 that differ in the first 223aa (Chen et al. 2002). Dnmt3a1 is the major form in adult tissues, where it co-localizes with heterochromatin, whereas Dnmt3a2 is the predominant form in ES cells and embryonal carcinoma cells and can be detected in testis, ovary, thymus and spleen. Accordingly, Dnmt3a and Dnmt3a2 may have distinct DNA targets and different functions in development. To date, five human splice variants of Dnmt3b, Dnmt3b1 – Dnmt3b5 have been identified and were shown to be expressed in a tissue specific manner (Robertson et al. 1999). Dnmt3b1, 3b2, 3b3 represent the major slice variants (Okano et al. 1998). Dnmt3b1 is the longest form and is regarded as the typical gene product of *DNMT3B*. All other splice variants encode smaller proteins. Dnmt3b2 lacks approximately 25 aa between the PHD and the PWWP domain and was shown to be catalytically active (Qiu et al. 2002). Dnmt3b3 resembles Dnmt3b2 but lacks additional 63aa in the catalytic domain rendering the enzyme inactive (Aoki et al. 2001). Dnmt3b4 and Dmt3b5 are expected to be inactive due to truncations of the catalytic domain (Robertson 2002). Details about their functions remain unclear.

Unlike Dnmt1, which localizes to replication foci during S-phase in murine embryonic fibroblasts, Dnmt3a co-localizes with HP1α and MeCPs throughout the cell cycle to late-replicating pericentromeric heterochromatin (Bachman 2001). In contrast to Dnmt3a, Dnmt3b remained diffuse in the nucleus of embryonic fibroblasts at all cell cycle stages. However, Dnmt3a and Dnmt3b co-localized to these pericentromeric heterochromatin regions in murine ES cells – even in Dnmt1-null ES cells, that lose the majority of methylation in these regions. These results indicate that Dnmt3a and Dnmt3b acquire unique functions during the transformation from ES cells to embryonic fibroblast cells and that localization to heterochromatin is not dependent on preexisting methylation marks.

As already mentioned (A.3.4), both enzymes are crucial for development as indicated by the lethality of the respective knockout mice (Okano et al. 1999). Two revealing publications clearly underscore the functional differences of Dnmt3a and Dnmt3b. With conditional knockout technology, the effect of Dnmt3a and Dnmt3b ablation during gametogenesis was monitored (Kaneda et al. 2004). Offspring from Dnmt3a conditional mutant females died in

utero and lacked methylation and allele-specific expression at all maternally imprinted loci examined. Furthermore, Dnmt3a conditional mutant males showed impaired spermatogenesis and lacked methylation at two of three paternally imprinted loci. By contrast, Dnmt3b conditional mutants and their offspring showed no apparent phenotype. The phenotype of Dnmt3a conditional mutants was virtually indistinguishable from that of Dnmt3L knockout mice.

A detailed methylation analysis of the paternally methylated DMRs (*H19, Dlk1/Gtl2* and *Rasgrf1*), interspersed repeats (SineB1, IAP and LINE1) and satellite repeats (major and minor) in male germ cells from Dnmt3a and Dnmt3b knockout mice demonstrated that Dnmt3a mainly methylated DMRs of *H19* and *Dlk1/Gtl2* and SineB, whereas Dnmt3b exclusively methylated satellite repeats. Interestingly, both proteins were required for the methylation the *Rasgrf1* DMR and IAPs and LINEs showing some overlapping function. Importantly, all sequences analyzed showed moderate to severe hypomethylation in Dnmt3L-deficient prospermatogonia, indicating a critical role for both *de novo* methyltransferases (Hata et al. 2007).

The unique function of Dnmt3b methylating satellite repeats is reflected by the ICF syndrome (Okano et al. 1999; Ehrlich et al. 2008). In agreement, the catalytic domain of Dnmt3a methylates DNA in a distributive whereas Dnmt3b in a more processive manner accelerating methylation of macromolecular DNA *in vitro*.

As a summary, Dnmt3a and Dnmt3b are highly related proteins endowed with similar *in vitro* enzymatic properties and protein domains that generally direct interactions with chromatin associated factors. Nevertheless, *in vivo*, especially during gametogenesis and development they have unique and only minor overlapping functions.

A.3.7 Dnmt3L

The DNMT3L gene was initially found through homology search of zinc finger containing proteins (Aapola et al. 2000) and was isolated from mouse (Aapola et al. 2001). Both human and mouse Dnmt3L show similarity with zinc finger ATRX/PHD domains of proteins of the SNF2 family and the *de novo* methyltransferases Dnmt3a and Dnmt3b (Aapola et al. 2001). In addition, the C-terminal domain shares motifs of the catalytic domain of Dnmt3a and Dnmt3b but on the one hand is truncated and on the other hand lacks the consensus amino acid residues PC in motif IV and ENV in motiv VI which form the catalytic center of cytosine-5 methyltransferases (Hata et al. 2002) (Figure 9).

Although catalytically inactive, Dnmt3L was shown to repress transcription through recruitment and interaction of HDAC1 via its PHD-like domain (Aapola et al. 2002; Deplus et al. 2002). Dnmt3L was found to be essential for embryonic development due to the establishment of maternal imprints and the appropriate expression of imprinted genes (Bourc'his et al. 2001; Hata et al. 2002). Dnmt3L knockout mice failed to establish maternal methylation imprints as seen for Dnmt3a-/- and Dnmt3b+/- mice. In addition, both Dnmt3a and Dnmt3b interact with Dnmt3L *in vivo* and the lack of Dnmt3a, like the lack of Dnmt3L, resulted in disrupted spermatogenesis and thus male sterility (Hata et al. 2002). Latest studies revealed an important role of Dnmt3L in *de novo* methylation of long-terminal-repeats

(LTR) and non-LTR retrotransposons in precursors of spermatogonial stem cells (Bourc'his and Bestor 2004) whereas tandem repeats in pericentromeric regions were normally methylated.

In vivo analysis with replicating minichromsomes carrying various imprinting centers showed that co-expression of Dnmt3L and Dnmt3a resulted in a striking stimulation of *de novo* methylation whereas co-expression of Dnmt3L and Dnmt3b led to little changes in target methylation (Chedin et al. 2002).

In vitro studies revealed that Dnmt3L also had a stimulatory effect on the *de novo* methylation (Suetake et al. 2004; Gowher et al. 2005a). Through the interaction with Dnmt3L, the *in vitro* methylation activity of Dnmt3a and Dnmt3b on oligonucleotides was increased 15 fold whereas on longer DNA fragments >200bp only 1.5-3 fold. It was shown that the C-terminal domain was sufficient for stimulation (Suetake et al. 2004; Gowher et al. 2005a). In particular, association of Dnmt3L with Dnmt3a was proposed to induce a conformational change and thus to lower the K_M value for DNA and SAM. After DNA binding, Dnmt3L would dissociate from the Dnmt3a/DNA complex, suggesting a role for Dnmt3L as an exchange factor (Gowher et al. 2005a). By means of surface plasmon resonance and filter binding assays Dnmt3L was able to bind to DNA (Gowher et al. 2005a), contrasting gel retardation assays where no binding was observed (Suetake et al. 2004). Recently, the crystal structure of a Dnmt3a/Dnmt3L tetrameric complex of the respective C-terminal domains was solved (Jia et al. 2007). Dnmt3a forms a dimer with two catalytic centers at the interface and one helical turn of DNA apart, suggesting the periodicity of 8-10bp in methylation of maternally imprinted genes. The Dnmt3L/Dnmt3a interaction is required for the stability of the Dnmt3a dimer and thus the enzymatic activity (Jia et al. 2007). Rather than binding as individual tetramers, Dnmt3a/Dnmt3L complexes formed a nucleoprotein filament in vitro (Jurkowska et al. 2008).

Immunoprecipitation of Flag-tagged Dnmt3L from embryonic stem cells, showed association of Dnmt3a2, Dnmt3b and the four canonical histones (Ooi et al. 2007). Further studies on the association of Dnmt3L with histone tails identified the first seven N-terminal amino acids of histone H3 to be the target for binding. Interestingly, non-methylated H3K4 was indispensible for binding through the PHD-like domain of Dnmt3L whereas other modification such as H3K9me3 did not disturb the interaction (Ooi et al. 2007). Methylation of lysine 4 on histone H3 has recently been suggested to protect gene promoters from de novo methylation which is compatible with these findings.

A.3.8 DNA methylation in the context of chromatin

Both, *de novo* DNA methyltransferases Dnmt3a and Dnmt3b and the *maintenance* DNA methyltransferase Dnmt1 have been extensively studied with regard to their enzymatic properties ((Bacolla et al. 1999; Pradhan et al. 1999; Aoki et al. 2001; Gowher and Jeltsch 2001; Gowher and Jeltsch 2002; Yokochi and Robertson 2002; Suetake et al. 2003). All these results were obtained through in vitro studies involving naked DNA as a substrate. However, the DNA of eukaryotic cells is packaged into a compact nucleoprotein complex whose elemental structure is nucleosomes (Woodcock and Horowitz 1995).

Recently, DNA methylation activity towards reconstituted mono-nucleosomes as substrate was reported (see below).

Robertson showed that the catalytic efficiency of Dnmt1 and Dnmt3a towards mono-nucleosomes with linker DNA (5S rDNA) decreased 8 fold and 17 fold respectively, although binding to the substrate and maximal velocity was comparable to naked DNA (Robertson et al. 2004). Different observations were reported by Okuwaki who found out that Dnmt1 was intrinsically capable of methylation within the nucleosome core, but to a much lesser extent and in a sequence dependent manner (Okuwaki and Verreault 2003). On the contrary, H. Gowher (Gowher et al. 2005b) found comparable methylation efficiency for DNA and nucleosomal templates (147bp) for Dnmt1 and Dnmt3a irrespective the sequence. In contrast, distinct roles of Dnmt3a and Dnmt3b in the methylation of DNA and nucleosome were described. The methylation activity of Dnmt3a seemed to be inhibited by mono-nucleosomes whereas Dnmt3b showed low but significant methylation within the nucleosome (Takeshima et al. 2006). Moreover, Dnmt3a was shown to preferentially methylate linker DNA which is impaired by binding of histone H1 (Takeshima et al. 2008).

Interestingly, not only the enzymes' intrinsic properties seem to have an effect on the methylation in chromatin, but also components of ATP-dependent chromatin remodeling factors.

Deletion of *DDM1* in *Arabidopsis* or its mouse homolog *Lsh,* members of the SNF2 family of remodeling enzymes, resulted in global loss of methylation, especially in repetitive elements like satellites and rDNA (Bartee and Bender 2001; Dennis et al. 2001; Fan et al. 2005). Recently, it was shown that acquisition of DNA methylation of non-methylated episomes required Lsh and that Lsh interacted specifically with the *de novo* DNA methyltransferases (Zhu et al. 2006). In particular, Lsh was demonstrated to recruit Dnmt3b to some *Hox* genes and to regulate Dnmt3b dependent DNA methylation and PRC mediated histone modifications (Xi et al. 2007). In another study, the function of Lsh as a recruitment factor was further underscored showing the cooperation with Dnmt1, Dnmt3b and HDAC1/2 in gene silencing (Myant and Stancheva 2008).

Mutation in the ATRX gene, belonging to the Rad54 subfamily (Snf2 family) (Flaus et al. 2006a) results in a human genetic disease called X-linked α-thalassemia mental retardation (ATR-X) syndrome. Interestingly, unlike for *DDM1* and *Lsh,* methylation defects in ATR-X patients are restricted to selected regions of the genome such as rDNA repeats, and are characterized by both hypo- and hypermethylation (Gibbons et al. 2000).

NoRC, a nucleolar remodeling complex containing hSnf2H (ISWI – like subfamily) (Strohner et al. 2001), represses rDNA transcription by recruiting DNA methyltransferase and histone deacetylase (Santoro and Grummt 2005). Furthermore, interaction of Dnmt1 with hSnf2H has been shown to increase the affinity of Dnmt1 towards nucleosomes (Robertson et al. 2004).

In addition, Dnmt3b was shown to interact with hSnf2H (Geiman et al. 2004b) and Dnmt3a forming a complex with Brg1 (Snf2 like subfamily) in mouse lymphosarcoma cells (Datta et al. 2005).

B OBJECTIVES

B.1 Identification of new Dnmt1 interacting proteins

DNA methylation is an epigenetic modification that is integrated in a highly dense network of regulatory mechanisms that control a great variety of essential cellular processes such as cell differentiation and proliferation, genomic integrity, DNA repair, imprinting of genes during development and X-chromosome inactivation in females.

Aberrant methylation is a hallmark of many cancers leading to silencing of tumor suppressor genes, activation of oncogenes and retrotransposons and defective imprinting. Dnmt1 as the *maintenance* DNA methyltransferase was shown to be implicated in these processes. Albeit many interactors of Dnmt1 had been identified, the underlying mechanisms that result in 'mistargeting' of Dnmt1 or recruitment to specific methylation sites in tumors remain largely unclear.

In this study, the aim was to identify new Dnmt1 containing complexes from native tissue (human placenta as an extra-embryonal tissue) and the subsequent comparison of complex composition from embryonal tissues such as Wilms tumors. As a reference the human cervix carcinoma cell line Hela S3, growing in suspension, was chosen.

The presence or absence of specific factors could modulate Dnmt1's targeting to specific loci or its enzymatic activity. In addition, new proteins of unknown function could be identified and further characterized.

B.2 De novo DNA methylation in the context of chromatin

The human genome is highly compacted in the nucleus through package into chromatin. The basic repeating unit of chromatin is the nucleosome that consists of 147bp of DNA wrapped around a histone octamer. On the one hand nucleosomal DNA represents a constraint as DNA accessibility is impaired but on the other hand features a level of regulation.

Dnmt3a and Dnmt3b are *de novo* methyltransferases that introduce new methylation marks at specific sites and at specific time points in development. The DNA methylation enzymes also have to cope with nucleosomal substrates.

Although some data on DNA methylation in the context of chromatin exist, we sought to systematically address the properties of nucleosome and DNA binding of Dnmt3a and Dnmt3b2 and subsequently their methylation characteristics. With this information, the molecular function of ATP-dependent chromatin remodeling enzymes in DNA methylation could be further investigated.

Moreover, the Dnmt3L protein interacting with and positively affecting the activity of the *de novo* methyltransferases *in vitro* and *in vivo* was found to bind to non-methylated H3K4. Therefore the role of Dnmt3L in binding and methylation of nucleosomes by Dnmt3a and Dnmt3b was under investigation.

C RESULTS

C.1 Towards identifying new interaction partners of Dnmt1

C.1.1   MALDI analysis of putative Dnmt1 interaction partners

Nuclear extracts from human placenta and Hela S3 cells (E.1.11) were generated as described (E.2.9.2) and subjected to immunoprecipitation with the Dnmt1 specific antibody 2C1 cross-linked to proteinG sepharose (E.1.6; E.2.12.2). Through comparison of proteins pulled down with the 2C1-beads and proteins bound unspecifically to the proteinG sepharose used for preclearing, possible candidates only found in the "beads" lane were cut out and sent for MALDI analysis to the "Zentrallabor für Proteinanalytik" (Prof. A. Imhof) at the LMU in Munich (Figure 12).

Figure 12 MALDI analysis of proteins co-immunoprecipitated with Dnmt1

Dnmt1 was immunoprecipitated with the 2C1 antibody (E.1.6), coupled to 50µl proteinG sepharose from 9.0mg of human placenta nuclear extract, 4.5mg Hela S3 nuclear extract and 2.0mg MNase released nuclear extract (E.2.9.2). Beads were boiled in 40µl HU buffer and subjected to 4%-12% SDS-PAGE and Coomassie Blue staining. 'B' denotes 2C1 coupled proteinG sepharose, and 'P' proteinG beads used for preclearing of the extracts. Molecular weight marker and proteins bands cut out for MALDI analysis are indicated.
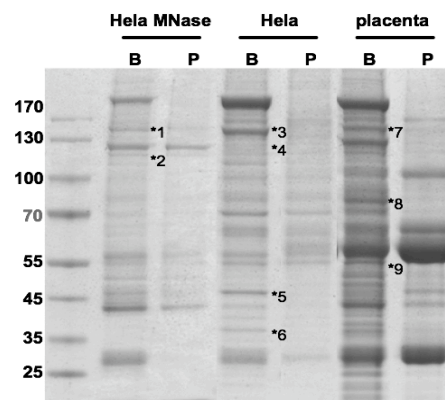
Although there was a lot of unspecific binding of proteins to proteinG sepharose under the IP conditions chosen, some bands could be well identified as unique for the specific IP reaction. Table 2 summarizes the MALDI results from the gel-bands. Proteins displaying possible candidates were shadowed in grey. ICBP90 (Bostick et al. 2007) and PCNA (Chuang et al. 1997) had already been described as Dnmt1 interaction partners. Dnmt1 was identified as bait protein before (data not shown). In addition, a prominent Dnmt1 degradation product was present in placenta nuclear extract. USP7 also known as HAUSP was found to be a new possible interaction partner of Dnmt1 in Hela S3 nuclear extracts. The IP reaction was repeated and more bands were sent for MALDI analysis (data not shown).

As a summary, USP7 was found as unique band in IP's from all extracts tested, whereas ICBP90 could only be confirmed as interaction partner from Hela MNase released nuclear extracts. This is in agreement with published data that ICBP90 is a chromatin - associated factor (Citterio et al. 2004; Bostick et al. 2007; Sharif et al. 2007; Karagianni et al. 2008). In vivo co-immunoprecipitation experiments with Hela S3 nuclear extracts and MNase released extracts suggest that most of ICBP90 is associated with chromatin (C.1.4). In WCE from HEK293 cells (E.2.6.3) over-expressing EGFP-tagged Dnmt1 or USP7 (E.2.6.5), ICBP90 was hardly present in the soluble fraction but resided in the pellet (data not shown). ICBP90 from mouse was only properly released from nuclei that had been treated with DNAseI before (Citterio et al. 2004) (Prof. H. Leonhardt, personal communication). Accordingly, it

seems as if the fraction of Dnmt1 interacting with ICBP90 was not properly released in placenta and Hela S3 nuclear extracts prepared according to the method of F. Pugh (E.2.9.2) and thus no prominent protein band was found in the respective 'bead' lane.

Table 2 MALDI results for Dnmt1 immunoprecipitation from nuclear extracts

#	name	score / alternate description
1	USP7	209 for gi|34851150, ubiquitin-specific protease 7 isoform [Homo sapiens]
2	ICBP90	138 for gi|6815251, transcription factor ICBP90 [Homo sapiens]
3	USP7	266 for gi|150378533, ubiquitin specific protease 7 [Homo sapiens]
4	CRA_E	87 for gi|119627830, splicing factor proline/glutamine-rich (polypyrimidine tract binding protein associated), isoform CRA_e [Homo sapiens]
5	Actin	178 for gi|32698757, actin-like 8 [Homo sapiens]
6	PCNA	77 for gi|4505641, proliferating cell nuclear antigen [Homo sapiens]
7	Dnmt1	176 for gi|6684525, DNA (cytosine-5)-methyltransferase [Homo sapiens]
8	HSP70	76 for gi|62897129, heat shock 70kDa protein 8 isoform 1 variant [Homo sapiens]
9	CRA_B	65 for gi|119616871, cytidine monophosphate N-acetylneuraminic acid synthetase, isoform CRA_b [Homo sapiens]

C.1.2   MALDI analysis with iTRAQ labeling

Gel-based MALDI evaluation has the disadvantage of proteins of interest being masked by unspecific proteins that show the same running behavior in SDS-PAGE. In addition, the visualization of proteins is limited to the detection limit of Coomassie Brilliant Blue or silver staining.

MALDI analysis using the iTRAQ labeling technique (Applied Biosystems) refers to a multiplexed protein quantitation strategy that provides relative and absolute measurements of protein in complex mixtures (Ross et al. 2004; Chen and Andrews 2009). The core of this methodology is a multiplexed set of isobaric reagents (iTRAQ, 114, 115, 116 and 117) that yield amine-derivatized peptides. The derivatized peptides are indistinguishable in MS, but exhibit intense low-mass MS/MS signature ions that support quantitation. Thus, differential labeling of peptides eluted from IgG control proteinG sepharose and from target protein directed antibodies, following separation of combined peptides on a reversed phase chromatography (Nano-HPCL) and MALDI analysis allows the determination of enrichment of specific peptides compared to IgG control.

Samples were digested in solution with trypsin following *in silico* differential isobaric labeling of peptides from IP sample and proteinG sample with different iTRAQ reagents (Applied Biosciences) (E.2.14.3). Labeled peptides were mixed and separated on a reversed phase chromatography (nano-flow HPLC-system Dionex) (E.2.14.3) applying a linear gradient from 5% - 95% of buffer B (80% acetone-nitril, 0.05% TFA) and spotted with 5 volumes of CHCA-matrix (2mg/ml in 70% acetonitrile, 0.1% TFA) on a MALDI-target by the probot-system (Dionex). Spotted fractions were analyzed with the 4700 series MALDI-TOF/TOF system (Applied biosciences) with the kind help of S. Jakob.
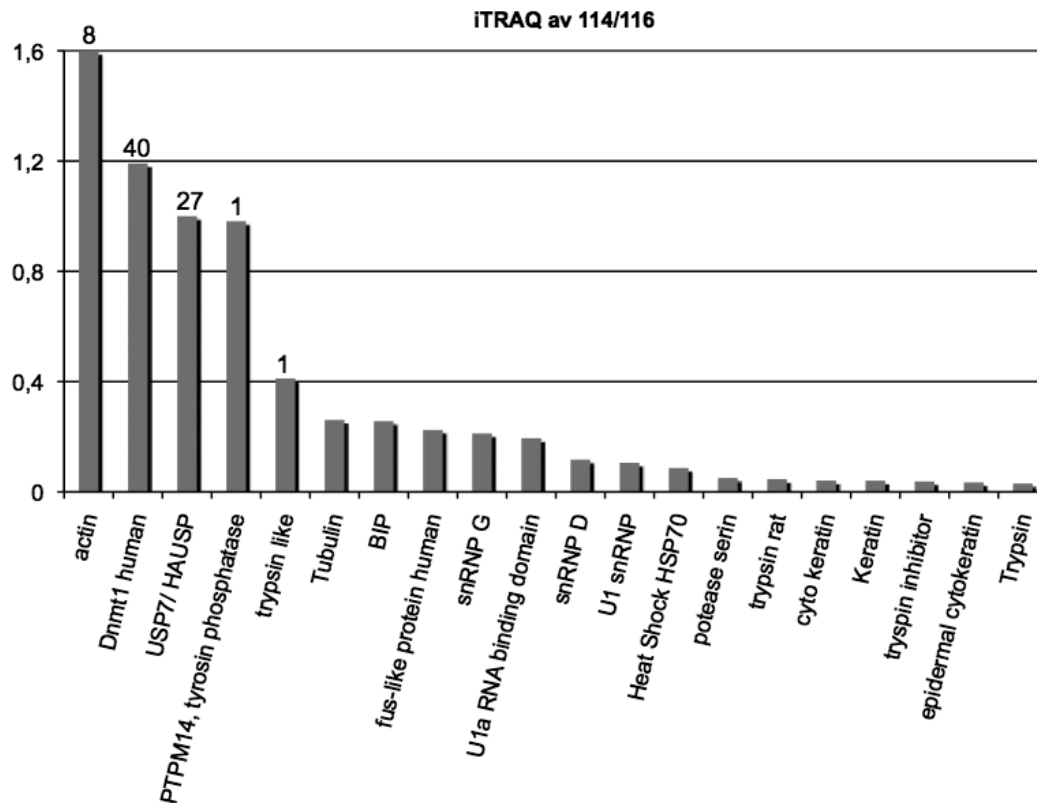
Figure 13 Dnmt1 co-immunoprecipitation – iTRAQ MALDI analysis

Dnmt1 specific immunoprecipitation with Hela nuclear extract was done as described (E.2.14.2). Trypsin digest of IP samples, *in silico* iTRAQ labeling of respective peptides and subsequent separation on a reversed phase chromatography (nano-flow HPLC) was performed (E.2.14.3). Separated peptides were spotted on MALDI targets and analyzed with a MALDI-TOF/TOF-system of the 4700 series (Applied Biosystems). Usually 6-7 peptides in each spot were further fragmented in MS/MS mode. The measured m/z ratios were assigned to the peptides and the respective proteins by MASCOT database search in the human database. The ratio of specific IP versus proteinG control (114/116) is plotted against the proteins identified. For the 5 strongest hits the amount of peptides identified are listed above the bars.

Although all three extracts (C.1.1) were analyzed, only results for the IP reaction from Hela S3 nuclear extracts were obtained (Figure 13). The signals of the Hela S3 MNase extract were not strong enough for adequate MALDI performance and the placenta nuclear extract was contaminated with vast amounts of parental IgG from the preparation. These peptides masked other relevant peptides and thus tainted the evaluation.

As shown in Figure 13, the ratio of specific IP versus proteinG control is plotted as iTRAQ labeling ratio 114/116 against the peptide hits acquired from the evaluation process. For the five highest score results, the number of peptides found are given. Accordingly, Dnmt1 as bait and USP7 as prey are highly enriched as seen with the gel-based MALDI analysis (C.1.1). Although actin and PTPM14 (protein tyrosine phosphatase) are better or equally well enriched compared to Dnmt1, less peptides were found and thus not considered as potential interaction partners of Dnmt1.

C.1.3 Dnmt1, ICBP90, USP7 co-migrate in gelfiltration

Nuclear extracts from human placenta and Hela S3 cells (E.2.9) were separated on a Superose6 gelfiltration column (GE Healthcare) (E.2.3.6). 500µl fractions were collected, TCA precipitated (E.2.3.4) and subjected to SDS-PAGE following either silver staining or Western Blot analysis.
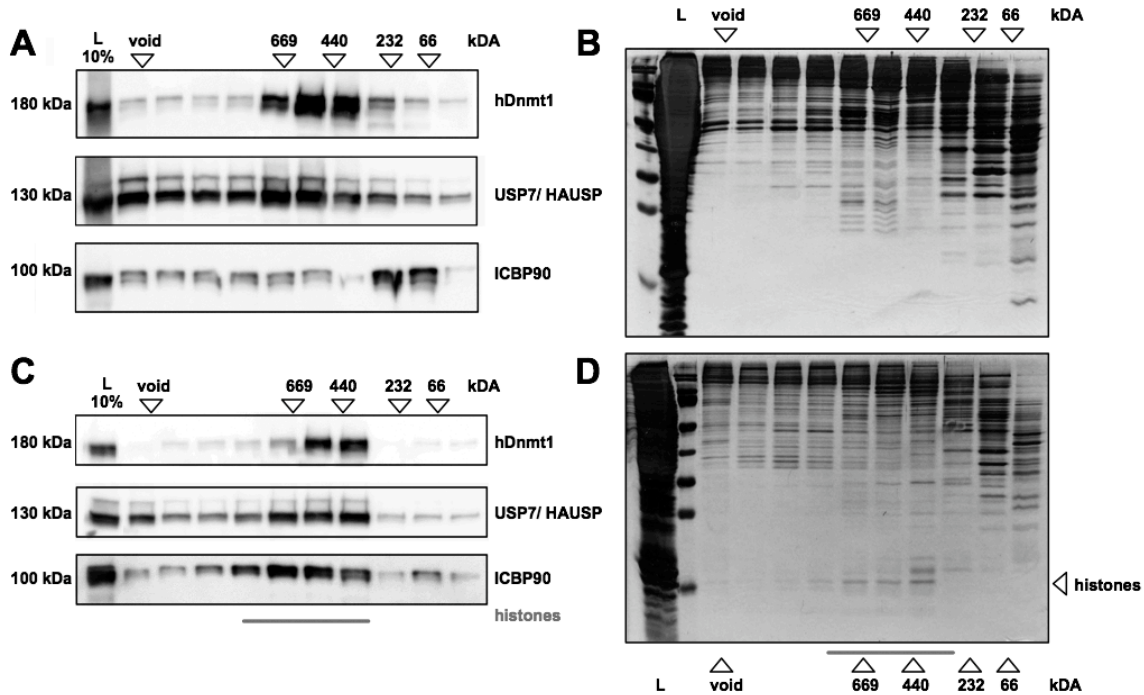
Figure 14 Gelfiltration analysis of nuclear extacts from Hela S3

500µl of Hela S3 nuclear extacts (4.5mg salt extracted, 2.0mg MNase released nuclear extract) were applied on a supererose6 gelfiltration column (GE Healthcare). 500µl fractions were collected, TCA precipitated (E.2.3.4) and subjected to SDS-PAGE following either silver staining (E.2.3.2) or Western Blot analysis (E.2.3.3). **A** WB analysis of every second fraction of Hela S3 nuclear extract with the antibodies indicated (E.1.6). **B** same as for A, but silver staining of respective fractions. **C** same as for A but for Hela S3 MNase released extract. Migration of histones as determined from D is indicated. **D** same as for C but Silver staining of respective fractions. Apparent molecular weight and SEC markers are indicated.

According to Figure 14, Dnmt1, ICBP90 and USP7 are present in all fractions. Dnmt1 and USP7 show a distinct peak between 440-669kDa for both salt extracted nuclear extract and MNase released nuclear extract. Interestingly, ICBP90's monomer peak between 66-232kDa is shifted to higher molecular weight and co-migrates with Dnmt1 and USP7 in the MNase released extract. As seen from the silver gel, this shift is accompanied by histones present in these fractions. Whether the co-migration of ICBP90 with Dnmt1 and USP7 is due to a specific interaction with these proteins, either directly or nucleosome - mediated, or whether a different histone containing ICBP90 complex with a similar molecular weight exists, cannot be concluded from the gelfiltration data alone. Considering the co-IP data (C.1.1; C.1.4) the gelfiltration data underscore the picture of a well extractable Dnmt1/ USP7 dimer and a possible trimeric complex of Dnmt1, ICBP90 and USP7 more tightly associated with chromatin.

Placenta nuclear extract separated on size exclusion chromatography (SEC) (Figure 15) shows a very similar result for Dnmt1, USP7 and ICBP90 as seen for the Hela S3 nuclear

extract. This is in accordance with the fact that the purification protocol after the step of nuclei preparation is virtually the same (E.2.9). Notably, ICBP90 is detected to a much lesser extent, although approximately double the amount was loaded. This reflects the observation that the expression level and protein level is low in quiescent cells and high in proliferating cells (Jenkins et al. 2005) and the fact that only a sub-population of the cells of placenta is in S-phase. In addition, in cancer cells ICBP90 is highly expressed throughout the cell cycle whereas its expression peaks during late G_1 and the transition of G_2 – M-phase in lung fibroblast cells (Mousli et al. 2003).
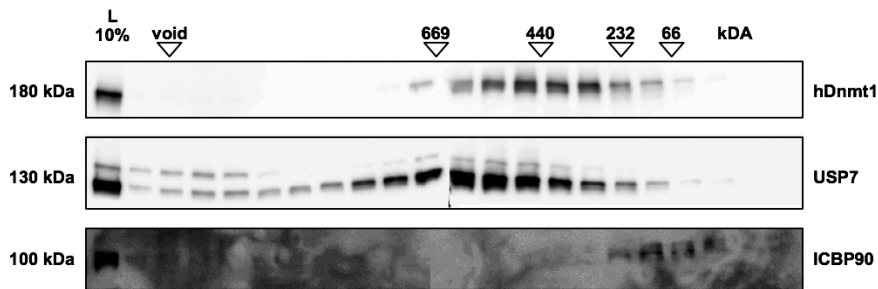
Figure 15 Gelfiltration analysis of nuclear extracts from human placenta

500µl of placenta nuclear extract (9.0 mg/ml) (E.2.9) were applied on a superose6 gelfiltration column (GE Healthcare). 500µl fractions were collected, TCA precipitated (E.2.3.4) and subjected to SDS-PAGE following Western Blot analysis (E.2.3.3). Immuno-detection of all fractions with the antibodies as indicated (E.1.6). Apparent molecular weight and SEC markers are given.

C.1.4   Dnmt1, ICBP90 and USP7 interact with one another *in vivo*

In order to investigate the possible existence of a trimeric complex, co-immunoprecipitations with Dnmt1, ICBP90 and USP7 as bait from Hela S3 MNase released nuclear extracts were performed. The immunoprecipitation was done as described (E.2.12.1) with the following modifications: 50µl slurry proteinG sepharose was used for the specific IP and preclearing reactions. 2.0µg of anti-USP7 antibody, anti-ICBP90 antibody (Hopfner et al. 2000) and irrelevant anti IgG antibody control (E.1.6) and 50µl of anti-Dnmt1 2C1 cross-linked proteinG beads (E.2.12.2) were used.

Samples were separated on 6% SDS-gels and subjected to Western Blotting following immuno-detection with the respective antibodies. LaminA/C served as control for a nuclear protein that should not interact with the POIs.

All antibodies chosen not only immunoprecipitate their target protein but also co-immunoprecipitate the other two proteins of interest (Figure 16). The MALDI result for the immunoprecipitation of Dnmt1 with the same extract is confirmed (C.1.1). LaminA/C as a nuclear protein is not precipitated and serves as a control for the specificity of the interaction. Together with the gelfiltration data (C.1.3), it cannot be ruled out that the observed interaction is truly protein-protein based but mediated via DNA or nucleosomal interactions.
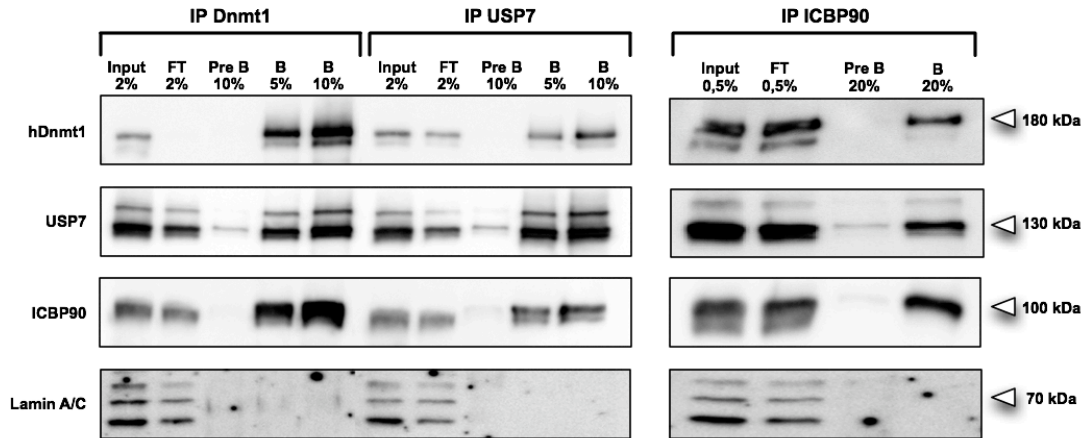
Figure 16 Co-immunoprecipitation of Dnmt1, ICBP90, USP from Hela S3 MNase released extracts

POIs were subjected to immunoprecipitation with 200µl of Hela S3 MNase released extract (2.0mg/ml) (E.2.9.3) with 2.0µg of USP7 and ICBP90 antibodies (E.1.6) and 50µl slurry proteinG sepharose and 50µl anti Dnmt1 2C1 cross-linked proteinG sepharose. Prior to immunoprecipitation, extracts were precleared with 50µl slurry proteinG beads supplemented with 2.0µg irrelevant IgG control antibody (E.1.6). Input, flowthrough (FT), preclearing beads (pre B), 'specific' beads (B), molecular weight markers and antibodies used for immuno-detection (E.2.3.3) are indicated.

In order to further pursuit this aspect, 3.0mg of high salt extracted Hela S3 nuclear extract (E.2.9.2) were treated with 60U DNAseI (Roche) while performing the immunoprecipitation procedure as mentioned above (Figure 17).
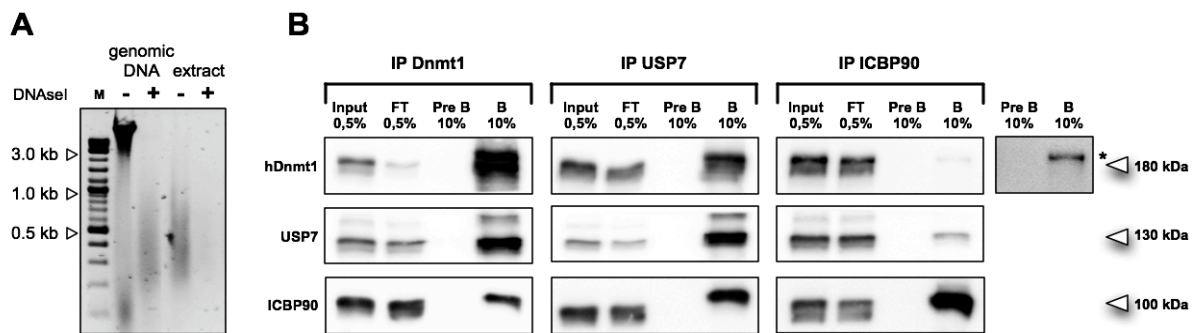
Figure 17 Co-immunoprecipitation of Dnmt1, ICBP90, USP from Hela S3 nuclear extracts treated with DNAseI

A.) DNAseI digest (Roche, 10U) of 15µg of Hela genomic DNA and 50µl of Hela S3 nuclear extract (3.0mg/ml) for 5 hours at 4°C. Samples were proteinaseK digested, ethanol precipitated (E.2.2.2) and subsequently the DNA was analyzed on a 1% agarose gel with SYBR Safe staining (Invitrogen). Molecular weight marker (NEB) is indicated. **B.)** POIs were subjected to immunoprecipitation with 300µl of Hela nuclear extract (10mg/ml) (E.2.9.2), supplemented with 1x DNAseI reaction buffer and 60U of DNAseI (Roche). 2.0µg of USP7 and ICBP90 antibodies (E.1.6) and 50µl slurry proteinG sepharose and 50µl anti Dnmt1 2C1 cross-linked proteinG sepharose were used. Prior to immunoprecipitation, extracts were precleared with 50µl slurry proteinG beads supplemented with 2.0µg irrelevant IgG control antibody (E.1.6). Input, flowthrough (FT), preclearing beads (pre B), 'specific' beads (B), molecular weight markers and antibodies used for immuno-detection (E.2.3.3) are indicated. * denotes modulation of the immunoblot signal to a stronger contrast.

Although the better control experiment would have been the DNAseI digest of the MNase released nuclear extract, several conclusions can be drawn. First, all three proteins seem to

interact with one another, indicating a protein-protein based interaction. Especially the Dnmt1 and USP7 IP do not differ from the results seen for the MNase released extract (Figure 16). Second, ICBP90 is well precipitated but only little amounts of Dnmt1 and USP7 are co-precipitated. Thus, besides a protein-protein interaction, the greater part of a possible trimeric complex might exist in the context of chromatin.

C.1.5 Dnmt1, ICBP90 and USP7 interact with one another *in vitro*

Direct interactions were tested with co-immunoprecipitation experiments (E.2.12.1) using recombinant proteins, either expressed from bacteria or insect cells (E.2.8; E.2.7).

Dnmt1 was demonstrated to be recruited to hemi-methylated DNA via ICBP90 (Bostick et al. 2007; Sharif et al. 2007). By deletion studies and yeast-2-hybrid experiments, the TS domain of Dnmt1 could be identified as the region in Dnmt1 mediating the interaction with the SRA domain of ICBP90 (Achour et al. 2007; Bostick et al. 2007).
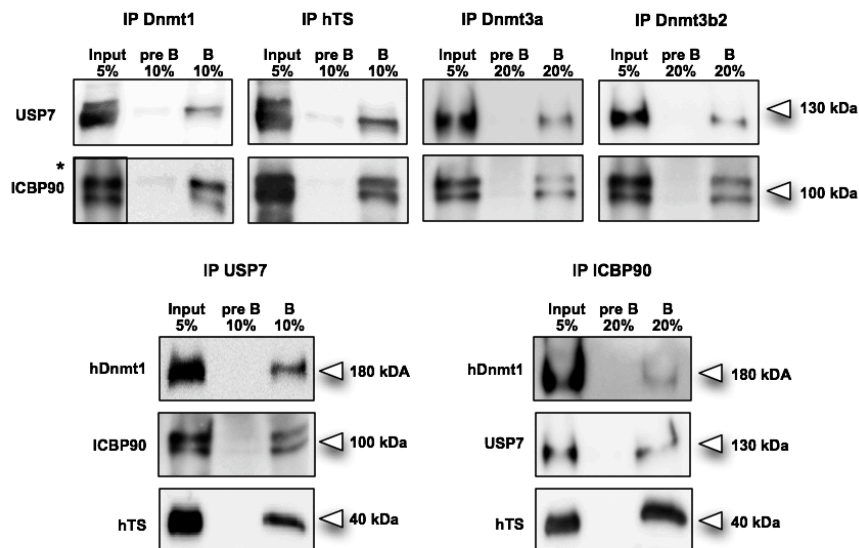
Figure 18 Co-immunoprecipitations of recombinant proteins

Recombinant proteins were expressed in bacteria or Sf21 insect cells as described (E.2.8; E.2.7). 50µl slurry proteinG beads coupled with the specific antibodies (E.1.6) were incubated with 2.5µg of bait protein in 200µl IP buffer (50mM Tris ph 7.5, 150mM NaCl, 1mM EDTA, 0.05%NP-40) for 2h at 4°C on a rotating device. After washing, 2.5µg of prey protein was added and further incubated for 2 hours. Beads were washed and resuspended in 50µl HU buffer. Samples were subjected to SDS-PAGE and Western Blot analysis following immuno-detection with the indicated antibodies. Molecular weight marker, input, preclearing beads (pre B) and specific beads (B) are indicated. * denotes modulation of the immunoblot signal to a stronger contrast.

As shown in Figure 18, the *in vitro* interaction of Dnmt1 and the TS domain with ICBP90 and vice versa can be confirmed. In addition, Dnmt1, its TS domain and ICBP90 also interact with USP7. These results argue against a sole trimeric complex since Dnmt1 interacts with its TS domain with both ICBP90 and USP7. It rather suggests the existence of three different dimer complexes namely Dnmt1/ICBP90, Dnmt1/UP7 and ICBP90/USP7.

For reasons of curiosity, the co-immunoprecipitations of ICBP90 and USP7 were also done for the *de novo* methyltransferases Dnmt3a and Dnmt3b2. At least under the *in vitro* conditions tested, they both interact with ICBP90 and USP7.

In order to further map the interaction surface of USP7, USP7 domains (roughly 200-300aa in length, E.2.8.4) fused to GST were expressed in *E. coli* and bound to gluthatione sepharose (GE Healthcare). GST-USP7 domains or GST were incubated with the recombinant proteins of interest (E.2.12.1) and subsequently analyzed with SDS-PAGE and Western Blot (Figure 19).

The results obtained are very conclusive. First, Dnmt1 and its hTS domain interact strongest with USP7 domain 3 (aa561-916), whereas ICBP90 interacts with the TRAF domain (aa1-215) of USP7. Hence, a trimeric complex with USP7 being the interaction 'platform' is in principle possible. Second, the *de novo* methyltransferases Dnmt3a and Dnmt3b2 bind to USP7 domains 1-3, but clearly, the TRAF domain seems to exert the strongest interaction.

Furthermore, a similar experiment with the SRA domain of ICBP90 fused to GST was bound to glutathione sepharose and pull-down experiments performed as described above (Figure 19). The interactions of the SRA-domain with Dnmt1 and the TS domain are in line with the results obtained (C.1.4, Figure 18) as well as published data (Achour et al. 2007; Bostick et al. 2007). In addition, the SRA domain seems to be sufficient for the interaction with USP7 and the *de novo* methyltransferases.
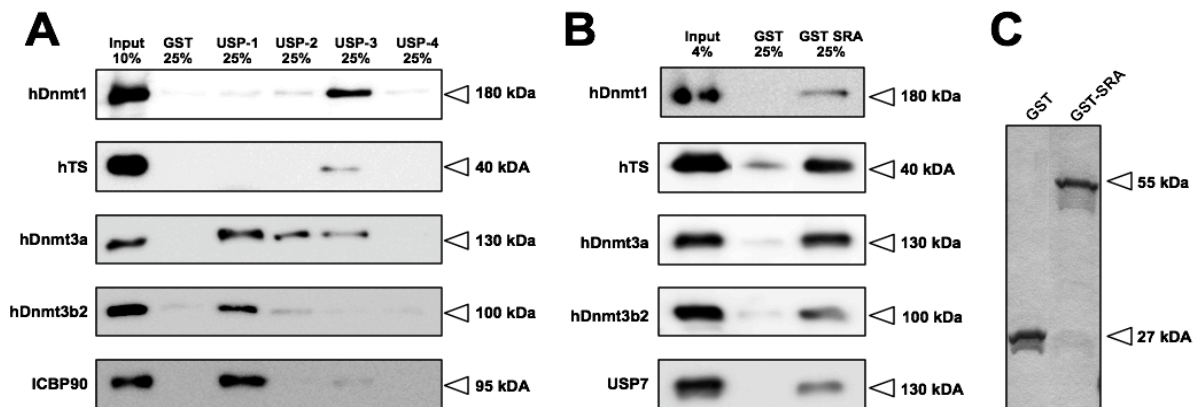
Figure 19 Interaction map of USP7 domains and the SRA domain of ICBP90

GST and USP7-domains fused to GST were purified from *E. coli* as described (E.2.8.4). GST-SRA expressed in Sf21 insect cells was kindly provided by A. Neu. Purification via glutathione sepharose was done as for the GST-USP7 domains. Recombinant proteins of interest (2.5-3.0µg) were incubated with 2.5µg of glutathione sepharose bound bait protein in 200µl IP buffer (50mM Tris ph 7.5, 150mM NaCl, 1mM EDTA, 0.05%NP-40) for 2h at 4°C on a rotating device. After washing 3x with IP buffer, beads were resuspended in 50µl HU buffer. Samples were subjected to SDS-PAGE and Western Blot analysis following immuno-detection with the indicated antibodies. Molecular weight marker, input and GST-beads are indicated.

Taken together, although no other domains had been tested, the TS domain of Dnmt1 and the SRA domain of ICBP90 are sufficient for the interaction with the other proteins of interest. In contrast, USP7 preferentially binds ICBP90 via its TRAF domain whereas Dnmt1 (and TS domain) is bound by domain 3. Accordingly, a trimeric complex with USP7 binding to Dnmt1 and ICBP90 as well as three different combinations of dimeric complexes are possible.

C.1.6   Dnmt1 and histones impair the autoubiquitinylation activity of ICBP90

ICBP90 and ICBP90ΔRING which lacks ubiquitinylation activity, were expressed as C-terminal His-tagged proteins in *E. coli* (E.2.8.3). In order to verify the enzymatic activity, *in vitro* auto-ubiquitinylation reactions were performed (Figure 20) (E.2.11.3). Furthermore, the effect of Dnmt1, inactive USP7 C223S, histones from *Drosophila* and hTS added at the onset of the reaction was examined.

ICBP90 and ICBP90ΔRING were detected as double bands in Western Blot with both anti-ICBP90 antibody and anti-His antibody (Figure 20). This is in agreement with the two bands visible after the Ni-NTA purification on SDS-PAGE and Coomassie Blue staining (E.2.8.3). Considering the C-terminal His-tag, detection with the anti-His antibody suggests an N-terminal degradation product. ICBP90ΔRING shows a weak band running slightly higher in SDS-PAGE reflecting ubiquitinylation. As stated in the manual, the E2 conjugating enzyme (UbcH5c, Biomol) is also capable of ubiquitinylation of certain target proteins and thus could be responsible for the low background detected.
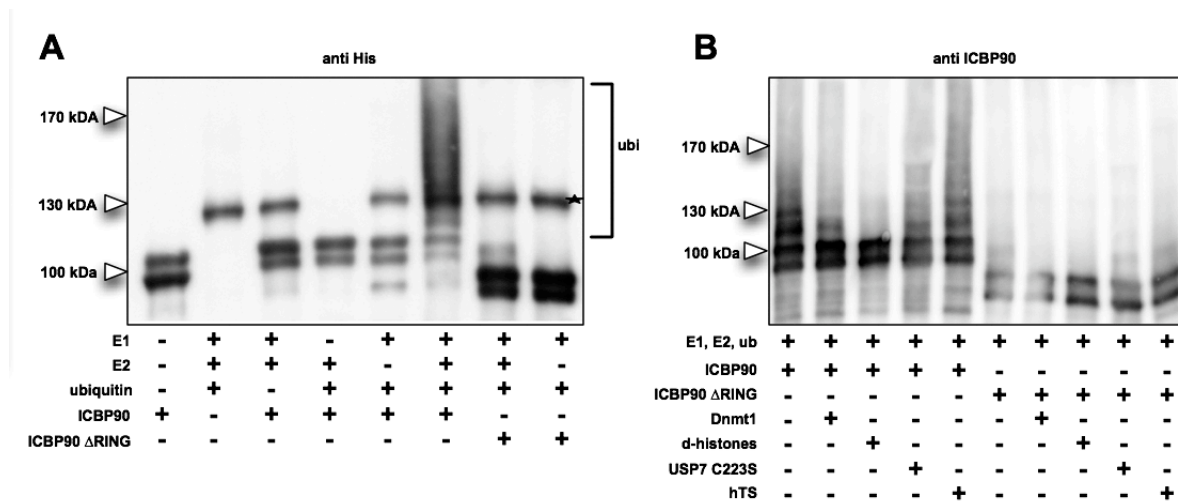
Figure 20 Autoubiquitinylation of ICBP90

A. ICBP90 activity assay is performed with 500ng ICBP90 or ICBP90ΔRING and 10µg ubiquitin (bovine, Sigma) for 1h at 37°C (E.2.11.3). Samples were analyzed by Western Blot and immuno-detection with anti-His antibody (Dianova). * indicates immuno-signal from His-tagged E1 conjugating enzyme, ubi marks ubiquitin adducts. **B**. ICBP90 activity assay performed as in A but in the presence of 1.0µg of Dnmt1, USP7 C223S, 2.0µg hTS or 2.0µg histones from drosophila. Immuno-detection was performed with anti-ICBP90 antibody (E.1.6).

Nevertheless, it is evident that ICBP90 exerts autoubiquitinylation activity that is mediated by its RING domain. When incubated with histones from *Drosophila* this activity was completely abolished. Dnmt1 and USP7 C223S seemed to impair autoubiquitinylation, whereas hTS did not have any effect. Whether these changes in activity were due to sole protein interactions and thus conformational changes or sterical hindrance, or whether Dnmt1, USP7 C223S and histones represented competing targets for ubiquitinylation remains to be clarified.

C.1.7   ICBP90 ubiquitinylates histone H3 – a substrate for USP7

In order to detect only ubiquitinylation products, the ICBP90 activity assay was performed in the presence of Flag-tagged ubiquitin (Figure 21). As already seen before, Dnmt1 and USP7

C223S show a weak, histone octamers a strong reduction of ubiquitinylation of ICBP90. Interestingly, the histones by themselves do not impair the auto-ubiquitinylation reaction as strong as the octamers. One explanation could be a salt dependent inhibitory effect, since recombinant human octamers (stored in a 1M NaCl containing buffer) raise the salt concentration in the reaction by 200mM.

The histone containing reactions were also loaded on a 17% SDS-gel and subjected to Western Blotting followed by immuno-detection with antibodies directed against each histone (Figure 21, B). As already described, ICBP90, in contrast to NP95, only ubiquitinylates histone H3 (Citterio et al. 2004; Karagianni et al. 2008).

In another ICBP90 activity assay containing histone H3, either no protein, USP7 or the inactive site mutant USP7 C223S were added at the onset of the reaction. USP7 was able to deubiquitinate histone H3, whereas USP7 C223S or Mock control were not (Figure 21, C).

To summarize, histone H3 is targeted *in vitro* by ICBP90 for ubiquitinylation and by USP7 for deubiquitination. ICBP90 did not ubiquitinylate the other histones *in vitro*.
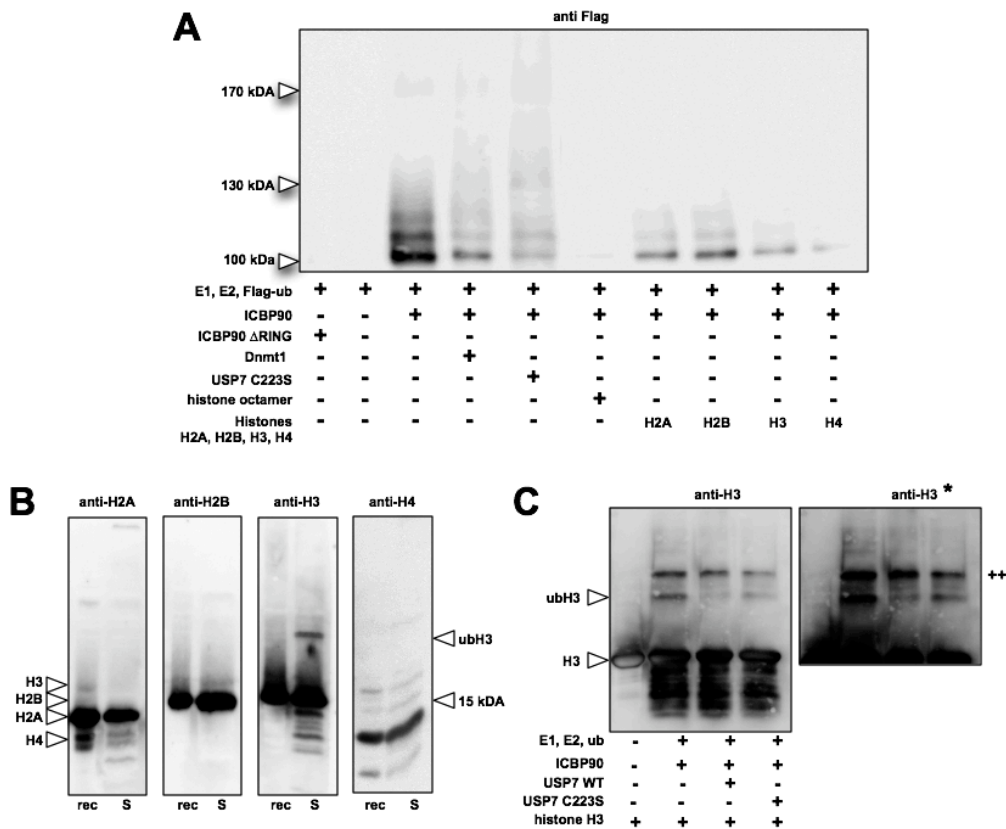
Figure 21 Histone H3 is mono-ubiquitinylated by ICBP90 and deubiquitinated by USP7

A. ICBP90 activity assay (E.2.11.3) was performed with 500ng ICBP90 or ICBP90ΔRING and 100ng Flag-ubiquitin in the presence of 1.0µg of Dnmt1, USP7 C223S, 2.0µg histone octamer or 2.0µg histones for 2h at 37°C. Recombinant human histones were expressed in *E coli*. Histones and octamers were kindly provided by C. Huber. Samples were analyzed by Western Blot and immuno-detection with anti-Flag antibody. **B.** Histone reaction from A. subjected to SDS-PAGE on a 17% gel following Western Blot and immuno-detection with histone specific antibodies (E.1.6). For comparison, recombinant histones (rec) and sample (s) are shown. **C.** Reaction as for B but in the presence of 10mM DTT, 1.0µg Flag-ubiquitin, 500ng USP7 or USP7 C223S catalytic site mutant and 5.0µg histone H3. Molecular weight markers are indicated. * indicates modulation of immuno-blot signal to stronger contrast. ++ marks unknown signal.

C.1.8 USP7 and Dnmt1 are targeted for ubiquitinylation by ICBP90

Dnmt1, ICBP90 and USP7 are able to interact with one another *in vivo* as well as *in vitro* (C.1.4, C.1.5). Besides recruitment to certain loci or the concomitant action of three different enzymatic activities in gene regulation, one could also speculate that ICBP90 regulates Dnmt1's and USP7's specific activity or protein turnover by ubiquitinylation.

To follow up this idea, ICBP90 activity assays with either no additional protein, Dnmt1 or USP7 C223S in the presence or absence of Flag-ubiquitin were performed, following an immunoprecipitation with antibodies directed against ICBP90, Dnmt1 and USP7 respectively. Preclearing beads and 'specific' beads were boiled in Lämmli dye, subjected to SDS-PAGE and Western Blotting. Ubiquitinylated species were detected with an anti-Flag antibody and subsequently reprobed with protein specific antibodies (Figure 23).
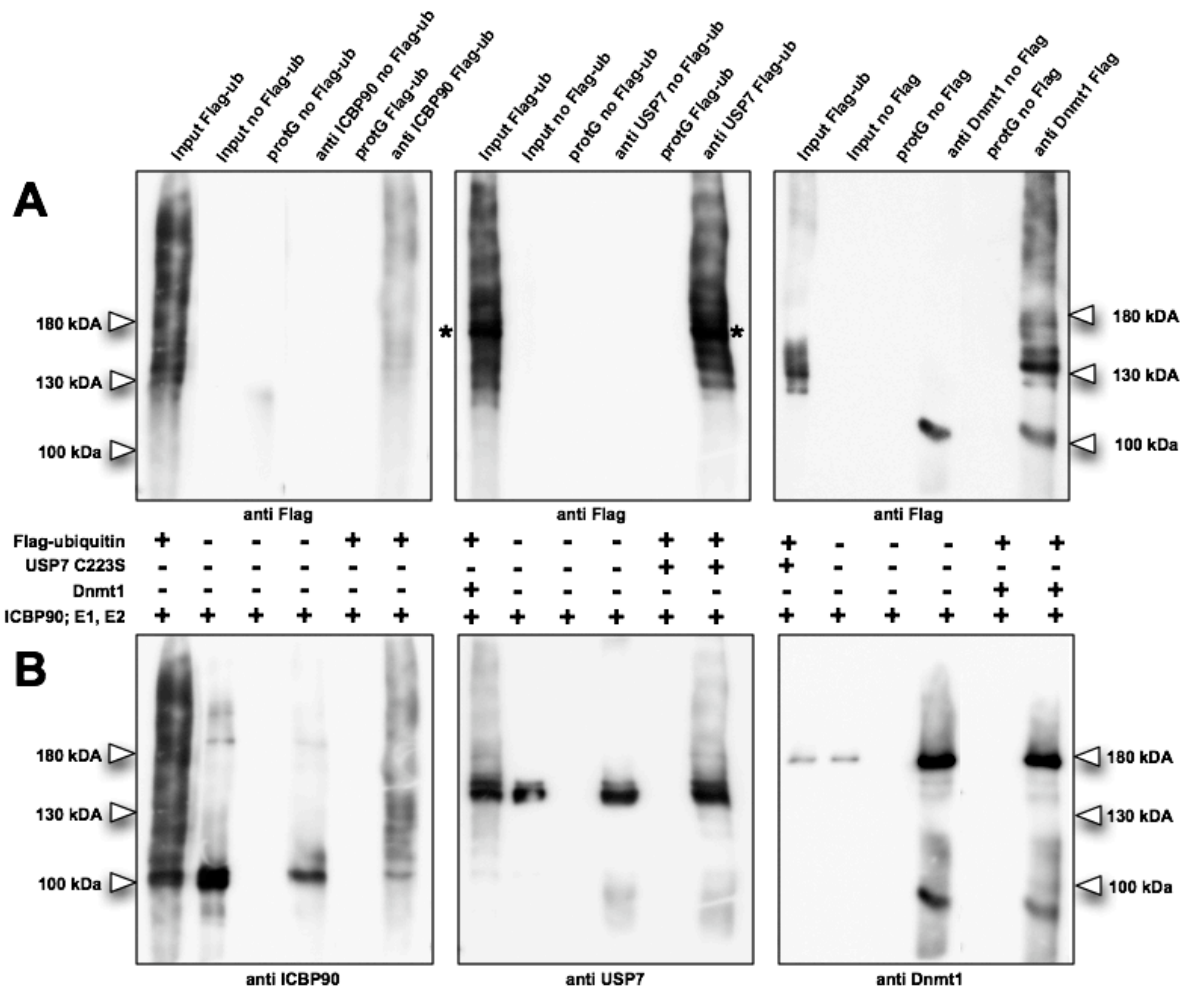
Figure 22 ICBP90 ubiquitinylates USP7 and Dnmt1 *in vitro*

A) ICBP90 activity assay (5x) was performed (E.2.11.3) in the presence of 5.0µg Flag-ubiquitin, 2.5µg Dnmt1 or 2.5µg USP7 C223S for 3h at 37°C. A control reaction in the absence of Flag-ubiquitin was run in parallel. The reactions were filled up to 200µl with IP buffer (50mM Tris pH7,5, 150mM NaCl, 0,1mM EDTA, 0,05% NP40), precleared with 20µl proteinG beads for 1h at 4°C, following incubation with 20µl proteinG beads coupled with 1.0µg of the indicated antibodies for 2 hours. The beads were washed 3x with EX-300 and boiled in 20µl HU buffer at 65°C for 10min. Samples were separated on a 6% SDS-PAGE, following Western Blot and immuno-detection with anti-Flag antibody to screen for ubiquitinylated species. 5% Input and 25% beads were loaded. **B**) The same blots were reprobed with protein specific antibodies as indicated. Molecular weight markers are indicated. * marks ubiquitinylated USP7.

ICBP90 induced its own ubiquitinylation as seen before (C.1.6). According to the Western Blot signal, it seemed as if ICBP90 and its ubiquitinylated species were co-immunoprecipitated by USP7 C223S and Dnmt1. Nevertheless, USP gives a unique signal (*) at roughly 140-150kDa, which is not present in the Input or IP lanes of ICBP90. When reprobing the blot with anti-USP7 antibody, no other signals but the signal at 140-150kDa appear. This suggests USP7 being mono- possibly to some extent oligo-ubiquitinylated. The increase in molecular weight of 10kDa for Flag-ubiquitin cannot be properly displayed in the molecular weight region of USP7. In addition, if only a subpopulation is mono- or di-ubiquitinylated and immuno-detection is performed with a POI specific antibody, the signal of the unmodified protein usually covers the much weaker signal of the modified protein. Hence, detection is not possible.

Dnmt1, although extremely well precipitated, does not show any significant signal of correct size that could account for a specific ubiquitinylated species. But a 'smear' of poly-ubiquitinylated proteins is clearly enriched in the Dnmt1 immunoprecipitation lane compared to Input, although considering different loading. Therefore, it could well be that Dnmt1 was poly-ubiquitinylated, however not very efficiently.

The results presented lead to the conclusion that ICBP90 targets USP7 and probably Dnmt1 for ubiquitinylation *in vitro.* The question whether this situation is also relevant *in vivo* is an interesting aspect to follow up.

C.1.9   USP7's *in vitro* activity is not influenced by Dnmt1 and ICBP90

USP7's activity was tested with an ubiquitin specific cleavage assay on an ubiquitin-like substrate fused to GST (GST-Ub52, (Baker and Board 1991)) as essentially established in the laboratory of R. D. Everett (Canning et al. 2004) (E.2.11.4). In order examine whether the binding of ICBP90 or Dnmt1 to USP7 could affect conformational changes and thus have an effect on the activity of USP7 *in vitro*, USP7 and the model substrate GST-UB52 were incubated with increasing amounts of either ICBP90 or Dnmt1 (Figure24).

Although interactions of Dnmt1 and ICBP90 with USP7 were shown (C.1.5), the binding did not impair USP7's activity on the model substrate GST-Ub52 whereas the activity is inhibited by NEM.
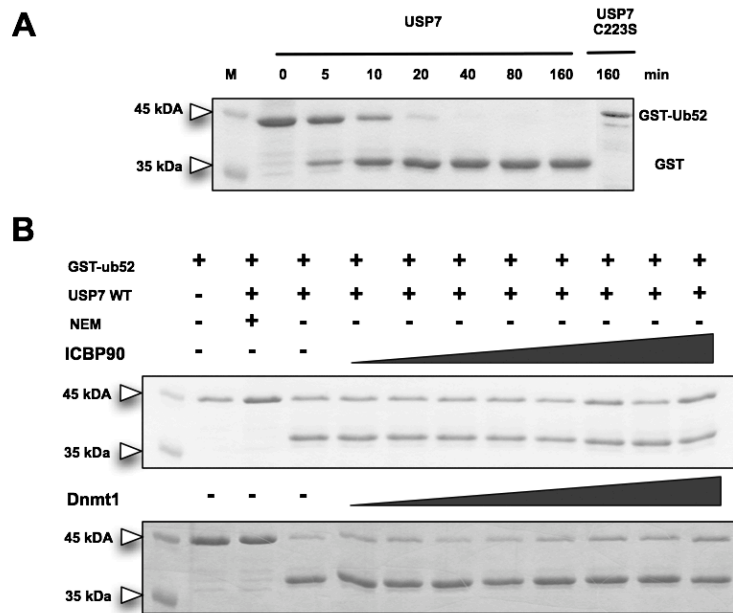
Figure 23 Dnmt1 and ICBP90 do not influence USP7's activity *in vitro*

A. 5.0ng of USP7 were incubated at 37°C with 1.0µg GST-UB52 linear model substrate for increasing time (E.2.11.4). USP7 C223S (inactive mutant) was used as control with the longest time point. Reactions were stopped after the indicated time points with the addition of Lämmli dye and boiling at 95°C. **B.** 5.0ng of USP7 were incubated with increasing amounts of Dnmt1 (10-800ng) and ICBP90 (3-500ng) for 10min at 37°C. As control either no protein or 10mM NEM DUB inhibitor was added. After the addition of 1.0µg GST-ub52, the reactions were stopped after 10min. Samples were analyzed by SDS-PAGE (15% gel) and Coomassie Blue staining. Molecular weight markers are indicated.

C.1.10 USP7 deubiquitinates ubiquitinylated histones and ICBP90 *in vitro*

In *Drosophila melanogaster,* the essential USP7 protein was found to contribute to epigenetic silencing of homeotic genes by Polycomb (PC) and to selectively deubiquitinate histone H2B but not H2A (van der Knaap et al. 2005). ICBP90 and its mouse homologue NP95 contain a RING finger domain that confers E3 ubiquitin ligase activity which induces their own ubiquitinylations (C.1.6). Besides autoubiquitinylation, NP95 ubiquitinylates recombinant histones H2A, H2B and H3 *in vitro* but only histone H3 when precipitated from WCE together with NP95 (Citterio et al. 2004). In contrast, ICBP90 was shown to ubiquitinylate only histone H3 *in vitro* (C.1.7) (Karagianni et al. 2008).

Interestingly, USP7 and ICBP90 form a complex, although they possess antagonistic enzymatic activities (C.1.4, C.1.5). In order to investigate the role of human USP7 in histone deubiquitination, histones were purified from HEK293 cells by acidic extraction (E.2.3.5) in the presence of 10mM NEM – an inhibitor of deubiquitinating enzymes (DUB). Extracted histones were subjected to the USP7 specific activity assay (E.2.11.4) with either no enzyme (Mock), USP7 or inactive USP7 C223S. Samples were analyzed by Western Blot following immuno-detection with histone specific antibodies (E.1.6).
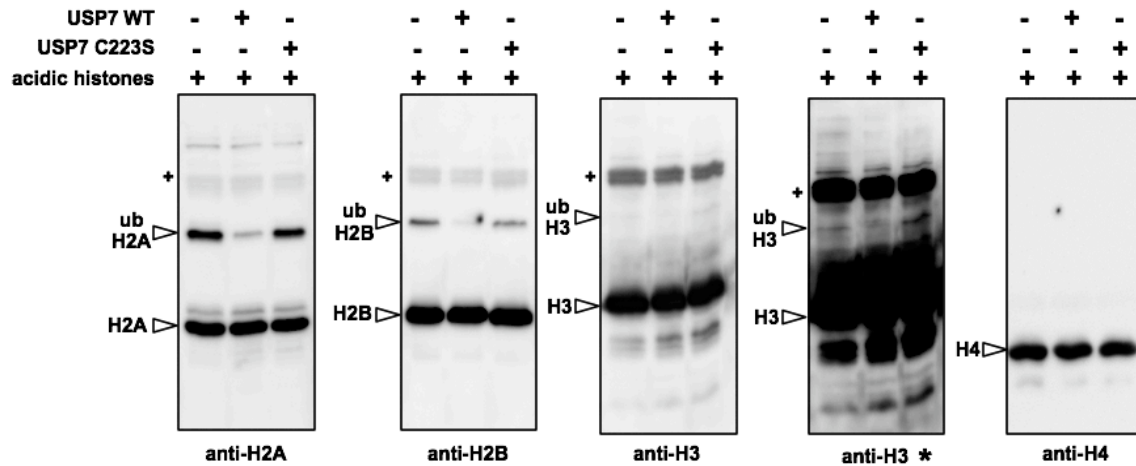
Figure 24 USP7 deubiquitinates histones *in vitro*

Total histones were purified from HEK293 cell by acidic extraction (E.2.3.5) and 10µg subjected to the USP7 activity assay (E.2.11.4) with either no USP7, 1.0µg of USP7 or 1.0µg of the inactive USP7 C223S mutant. Samples were boiled in Laemmli dye, separated on a 17% SDS-gel and Western Blot was performed. Immuno-detection was done with the indicated histone specific antibodies. * indicates modulation of the immuno-signal to a stronger contrast. + marks an unknown background signal.

Mono-ubiquitinylated H2A and H2B comprise 5-15% and 1% of the total H2A and H2B pool respectively (Vissers et al. 2008). Although not clearly stated, mono-ubiquitinylated H3 seems to be less abundant than mono-ubiquitinylated H2A and H2B. As seen in Figure 24, the proportion of mono-ubiquitinylated histones is reflected as described before. In addition, USP7, but not USP7 C223S and Mock control, exerts deubiquitination activity towards ubiquitinylated histones H2A, H2B and H3. Whether histone H4 is ubiquitinylated *in vivo* and whether it would be a potential target for USP7 cannot be judged due to the weakness of the antibody.

Last, an ICBP90 activity assay was performed (E.2.11.3) in the presence of Flag-ubiquitin and 10mM DTT for 2 hours at 37°C. USP7 or USP7 C223S were added in substoichiometric amounts compared to ICBP90 either at the onset of the reaction or added after stopping the auto-ubiquitinylation reaction with 20mM EDTA. The total reaction was stopped by adding Lämmli dye and boiling at 95°C. Samples were analyzed by Western Blot and immuno-detection with anti-Flag antibody (Figure 25).

As seen before, ICBP90 possesses autoubiquitinylation activity (C.1.6) that is impaired by binding of inactive USP7 C223S even when substoichiometric amounts of USP7 C223S are used. Interestingly, USP7 C223S partially prevents the formation of higher oligo- and poly-ubiquitin chains indicating that the ubiquitin moiety is bound to the catalytic domain and protected from further ubiquitinylation. Active USP7 efficiently removes ubiquitin moieties from ICBP90 when added at the beginning of the reaction, whereas when added after the reaction has been stopped, only the signal corresponding to the mono-ubiquitinylated species disappears. This observation suggests that USP7 preferentially removes mono-ubiquitins which is in agreement with previous data (Canning et al. 2004).
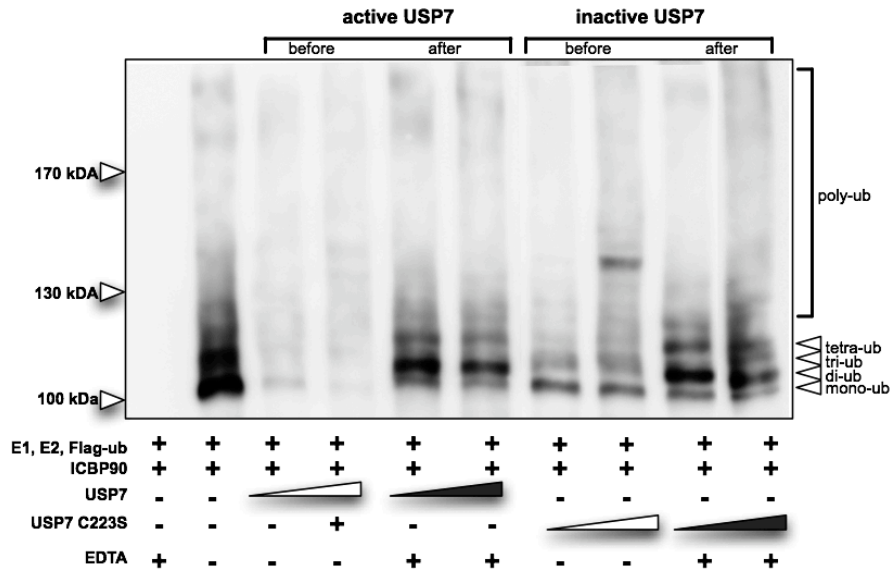
Figure 25 USP7 prevents ICBP90 from autoubiquitinylation

ICBP90 activity assay was performed with 250ng ICBP90, 100ng flag-ubiquitin and 100mM DTT for 2h at 37°C (E.2.11.3). USP7 or USP7 C223S (5ng and 50ng each) were added either at the onset (**white triangle**) of the reaction or after having stopped the reaction with 20mM EDTA (**grey triangle**). The reaction was allowed to continue for 2h at 37°C. Samples were boiled in Lämmli dye, subjected to SDS-PAGE (6% gel) and Western Blot analysis with anti-Flag antibody (M2, Sigma). Molecular weight marker and ubiquitin adducts are indicated.

C.1.11 USP7, Dnmt1, ICBP90 are ubiquitinylated *in vivo*

Recombinant ICBP90 and ICBP90 over-expressed in mammalian cells were shown to induce their own ubiquitinylation *in vitro* (Karagianni et al. 2008) (Jenkins et al. 2005). It was reported that Dnmt1 was selectively degraded by a proteasomal pathway upon 5-aza-2'-deoxycytidine treatment (Ghoshal et al. 2005) and inhibition of HDAC1 (Zhou et al. 2008a). In order to study the role of USP7 on the *in vivo* ubiquitinylation levels of Dnmt1 and ICBP90 upon knockdown and over-expression, the ubiquitin binding protein Dsk2p from *S. cerevisiae* fused to GST (E.2.8.6) (Anindya et al. 2007) was used for the purification of ubiquitinylated proteins from WCE.

All three proteins under investigation are ubiquitinylated *in vivo* (Figure 26). The specific binding of ubiquitinylated proteins to GST-dsk2p was confirmed by reprobing the Western Blot with an anti-ubiquitin antibody. Curiously, only a single ubiquitin signal was detected, although one would expect a smear to higher molecular weight indicating poly-ubiquitinylation. Typically, *in vivo* ubiquitinylation studies are performed with over-expressed POIs and tagged-ubiquitin (HA-tag or His tag; (Treier et al. 1994)). This is due to the fact that on the one hand good antibodies against ubiquitin do not exist and on the other hand ubiquitinylated proteins present a subpopulation. Since ubiquitinylation of endogenous proteins was pursued with the dsk2p-system, it might well be that only the most prominent ubiquitinylated species, namely mono- or di-ubiquitin, were detectable.
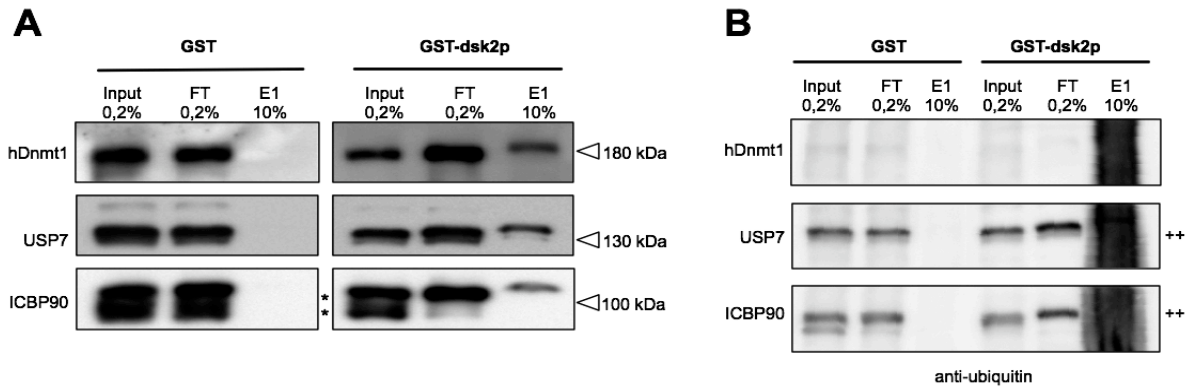
Figure 26 Dnmt1, ICBP90, USP7 are ubiquitinylated *in vivo*

A. WCE from Hela cells were prepared in 1xPBS+0.3% Triton-X-100 supplemented with 10mM NEM (E.2.6.3). 50µl of GST or GST-dsk2p (ubiquitin binding protein, (E.2.8.6) were incubated with 5.0mg of WCE in 1.0ml MobiCol columns at 4°C overnight. After centrifugation the flowthrough was collected and the beads washed 3x times with 500µl lysis buffer and 3x with EX-300+0.05%NP40 with 5min incubation steps in between. Bound proteins were eluted together with GST or GST-dsk2p from the glutathione sepharose with 50µl elution buffer (50mM Tris pH 8.0, 150mM NaCl, 10mM reduced glutathione) for 1h at 16°C shaking at 1300rpm. Samples were analyzed by Western Blot following immuno-detection with antibodies directed against the proteins of interest. ** indicate two bands for ICBP90 as seen *in vitro* (C.1.6) **B.** Western Blots from A were reprobed (++) with an ubiquitin specific antibody (E.1.6). Input, flowthrough (FT), elution (E) and molecular weight markers are indicated.

C.1.12 Effects of USP7 levels on Dnmt1 and ICBP90 *in vivo*

ICBP90 ubiquitinylated USP7 and vice versa USP7 was able to deubiquitinate ICBP90 *in vitro* (C.1.8, C.1.10). Dnmt1 was shown to be ubiquitinylated *in vivo* (see above) and represented a target for ubiquitinylation by ICBP90 *in vitro*, albeit not very efficiently (C.1.8).

In the following three experiments, the effects of USP7 knockdown and over-expression were examined in regard to the following aspects.

a.) Does USP7 have a regulatory effect on the protein levels of Dnmt1 and ICBP90?

b.) Are ICBP90 and Dnmt1 targets of USP7 and thus does their ubiquitinylation status change upon USP7 knockdown or over-expression (C.1.13)?

c.) Do levels of ubiquitinylated H2A and H2B change upon USP7 knockdown or over-expression globally (C.1.12)?

For USP7 knockdown and over-expression studies, cell lines based on the colorectal adenocarcinoma cell line LS174T, carrying plasmids with either shRNA (LS88) or N-myc-USP7 (LS89) under the control of a tetracycline/doxycycline inducible promoter were kindly provided by M. Maurice (E.1.11) (Van De Wetering et al. 2003; Meulmeester et al. 2005; Kessler et al. 2007). For doxycycline treatment, cells were grown as described (E.2.6.6) and seeded on tissue culture plates with a cell number giving rise to 50-60% confluency on the day of harvest. WCE were prepared in the presence of 10mM NEM (E.2.6.3) and used for both Western Blot analysis and the purification of ubiquitinylated proteins (C.1.13). From the residual pellet histones were purified by the method of acidic extraction (E.2.3.5) and analyzed for changes in ubiquitinylation (C.1.14).
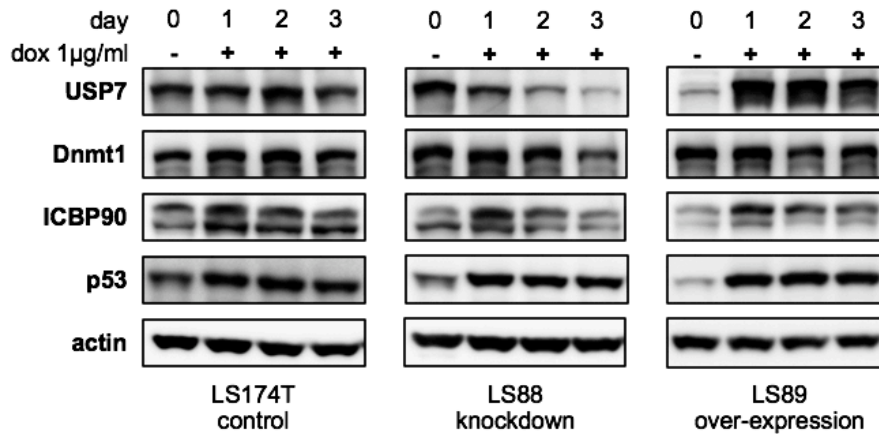
Figure 27 USP7 knockdown and over-expression upon doxycycline treatment

LS cell lines (E.1.11) were grown in RPMI1640/Hepes (GIBCO) supplemented with blasticidin (10µg/ml), zeocin (200µg/ml; normally 500µg/ml) and TET-FBS (clonetech #631106). Cells were seeded on tissue culture plates with a cell number giving rise to 50-60% confluency on the day of harvest. Doxycycline induction was performed with the addition of doxycycline to a final concentration of 1µg/ml. Cells were harvested (indicated days post-induction) and WCE prepared (E.2.6.3) in the presence of 10mM NEM. 30µg of WCE of the cell line LS89 and 50µg of the cell lines LS174T and LS88 were taken for Western Blotting following immuno-detection with the indicated antibodies.

Whereas USP7 was over-expressed up to 4-fold in LS89 cells already after 24 hours of induction, endogenous USP7 levels could be reduced to 25% after 3 days of doxycycline treatment in the LS88 cell lines (Figure 28).

The stability of the tumor suppressor p53 is directly controlled through the interaction with USP7 and its deubiquitination activity (Li et al. 2002). However, USP7 also indirectly affects p53 stability and activity by associating with and deubiquitinating Hdm2 leading to Hdm2 stabilization (Meulmeester et al. 2005). USP7 ablation results in a phenotype opposite to predicted. Rather than decreasing p53 levels associated with increased p53 ubiquitination, the absence of USP7 resulted in p53 accumulation accompanied by decreased p53 ubiquitination. The basis for this phenotype was traced to the increased ubiquitinylation of MDM2 (mouse homologue of Hdm2), a negative regulator of p53 levels (Cummins and Vogelstein 2004).

In the knockdown cell line LS88, p53 levels were slightly, in LS89 cells stronger increased reflecting the dual regulatory mechanism by Hdm2 and USP7. In contrast, Dnmt1 levels were unaffected by changes in USP7. Although the effects were quite low, ICBP90 levels seemed to be reduced upon USP7 knockdown owing to possible higher auto-ubiquitinylation and thus degradation. ICBP90 was demonstrated to be down-regulated by p53/p21[Cip1/WAF1]-dependent DNA damage checkpoint signals (Arima et al. 2004). In order to exclude a p53/p21 dependent down-regulation, p21 protein levels should be analyzed.

Upon doxyclycline treatment, USP7 levels were already up-regulated by a factor of 4 after 24 hours and then slightly decreasing the following days (LS89). ICBP90 levels were also increased which could be a direct effect of deubiquitination by USP7.

C.1.13 Effects of USP7 levels on ubiquitinylated Dnmt1 and ICBP90 *in vivo*

WCE (3.0mg) derived from LS cell lines treated with doxycycline (C.1.12) were incubated with either 50µl ubiquitin binding protein Dsk2p from *S. cerevisiae* fused to GST or GST (E.2.8.6) (Anindya et al. 2007). Ubiquitinylated proteins were eluted as described and subjected Western Blotting following immuno-detection with antibodies directed against proteins of interest.

As seen before (C.1.12), USP7 levels were decreased and increased upon doxycycline induced knockdown and over-expression. The level of ubiquitinylated USP7 seemed to follow this observation leading to the effect that in LS88 cells less ubiquitinylated USP7 was present. Curiously, in LS89 cells more ub-USP7 was precipitated although equal amount of total USP7 was present. Dnmt1, whose protein level was not affected by alterations in the amount of USP7 (Figure 28), did not show any difference in the degree of ubiquitinylation, indicating no direct regulation of stability by USP7 *in vivo* (Figure 29). As discussed above, USP7 knockdown led to an increase of p53 but the predicted increase of ubiquitinylated p53 could not be confirmed (Cummins and Vogelstein 2004). It rather seemed that the amount of ubiquitinylated p53 was the same compared to untreated cells, which might be due to the fact that USP7 levels were reduced the most to 25% (LS88) compared to total ablation in HCT-116 USP7 -/- cells. In contrast, USP7 over-expression not only led to increased p53 levels but also to increased ubiquitinylated p53. Hdm2 mediated p53 ubiquitinylation and USP7 dependent deubiquitination would be balanced on higher p53 protein level.
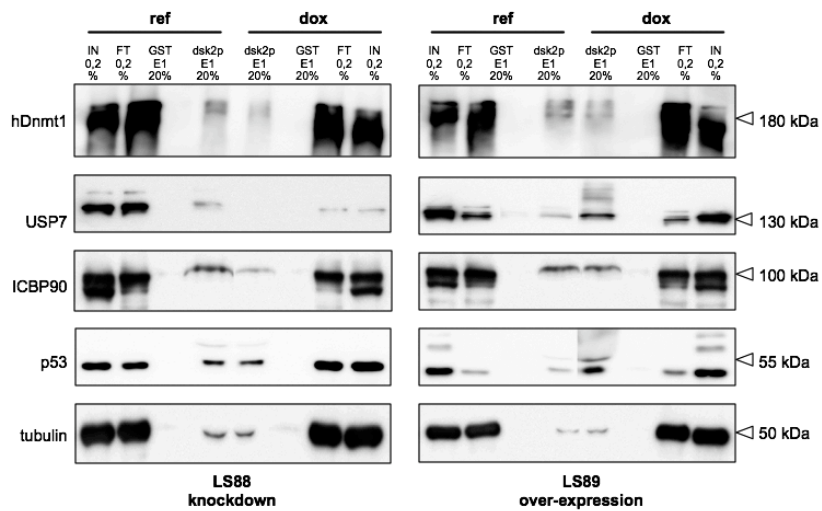
Figure 28 Ubiquitinylation status of Dnmt1 and ICBP90 upon USP7 knockdown or overexpression

WCE were prepared in 1xPBS+0.3% Triton-X-100 supplemented with 10mM NEM (E.2.6.3) and incubated with 50µl of GST or GST-dsk2p (E.2.8.6) (3.0mg WCE) in 1.0ml MobiCol columns at 4°C overnight. Beads were washed 3x times with 500µl lysis buffer and 3x with EX-300+0.05%NP40 with 5min incubation steps in-between. Bound proteins were eluted together with GST or GST-dsk2p from the glutathione sepharose with 50µl elution buffer (50mM Tris pH 8.0, 150mM NaCl, 10mM reduced glutathione) for 1h at 16°C shaking at 1300rpm. Samples were analyzed by Western Blot following immuno-detection with antibodies directed against the proteins of interest. Antibodies, molecular weight and cell lines are indicated.

ICBP90 as observed to slightly decrease upon USP7 knockdown (Figure 28) showed reduced levels of ubiquitinylated ICBP90 although expected the other way round. If ICBP90

is deubiquitinated by USP7, a respective over-expression of USP7 should lead to increased ICBP90 protein levels and less ubiquitinylated ICBP90. For the latter there is almost no difference to Mock control detectable.

Importantly, it has to be taken into account that the cells were treated with DUB inhibitor NEM upon cell harvest and WCE preparation, but that no proteasome inhibitor (like MG132) had been added to the culture medium prior to cell harvest. This could have been helpful to stabilize ubiquitinylated intermediates and thus to better evaluate such weak effects.

Taken together, neither the Dnmt1 protein level nor the ubiquitinylated Dnmt1 level were affected by changes in the amount of USP7 in the cell. ICBP90 protein level showed an up- and down-regulation in dependence of increased or decreased levels of USP7. The ubiquitinylation status of ICBP90 was altered but not necessarily according to the expectation. In order to verify the direct effect of USP7 on the ubiquitinylation status of ICBP90, it would be better to work with cells that are transfected with three plasmids, carrying for example Flag-tagged ICBP90, HA-tagged ubiquitin and USP7 (WT or active site mutant). With the prerequisite of almost complete transfection efficiency, the amount of ubiquitinylation could be detected with an anti-HA antibody after Flag-purification.

C.1.14 USP7 levels have no global effect ubiquitinylated H2A and H2B *in vivo*

USP7 was capable of removing the ubiquitin moiety from histones H2A, H2B and H3 *in vitro.* In the course of analysis on the effects of knockdown and over-expression of USP7, also ubiquitin levels of histones H2A and H2B were under investigation.

Histones were purified with the method of acidic extraction (E.2.3.5) from $2x10^7$ LS cells either treated with doxycycline or untreated. 10µg of histones were subjected to SDS-PAGE and Western Blot analysis with histone specific antibodies.

As shown before (C.1.10), USP7 deubiquitinates H2A and H2B *in vitro* (Figure 30). Although NEM, inhibitor of deubiquitination enzymes, was present in the histone purification procedure, no difference in the global ubiquitinylation levels of H2A and H2B upon knockdown and over-expression were detectable. Histone H3 could not be included in the analysis due to the weak signals of apparent ubiquitinylated H3.

Ablation of USP7 in *Drosophila* upon siRNA treatment had only marginal impact on the level of uH2B in the total histone pool but strongly reduced the level of H3K27 methylation (unpublished data; (van der Knaap et al. 2005)). This indicates a probable redundancy of H2B deubiquitination by more deubiquitinating enzymes and possibly strong involvement of USP7 in PRC mediated silencing.

If USP7 dependent histone deubiquitination plays a role in gene regulation together with ICBP90 and Dnmt1, the analysis of changes in histone modifications and DNA methylation patterns at specific loci should be in focus.
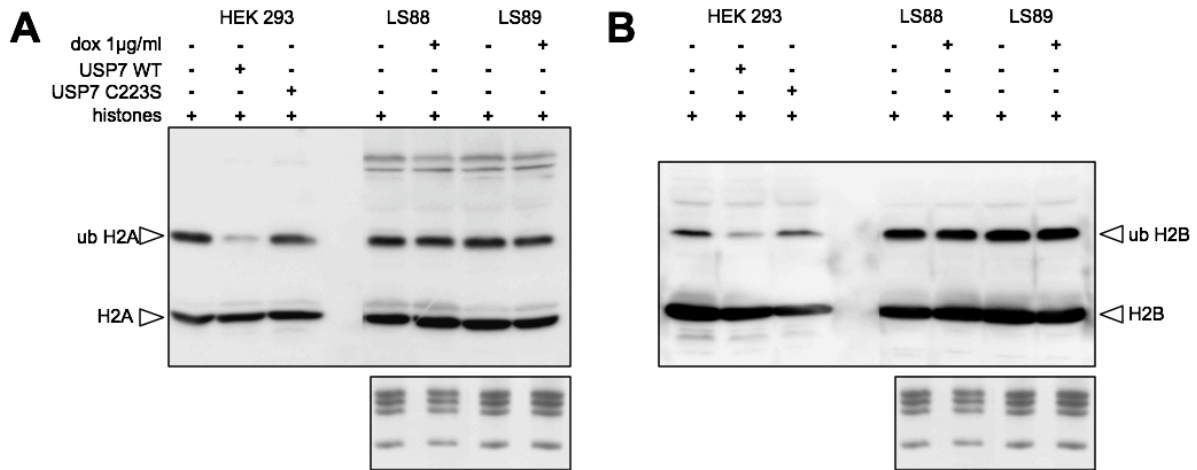
Figure 29 Ubiquitinylation status of H2A and H2B upon USP kd or over-expression

LS cell lines (E.1.11) were grown for subsequent doxycycline treatment as described (E.2.6.6). Doxycycline induction was performed with the addition of doxycycline to a final concentration of 1.0µg/ml. Cells from the LS88 cell line were harvested 3 days post-induction and cells from LS89 cell line 24 hours post-induction. WCE preparation and acidic extraction of histones (E.2.3.5) were performed in the presence of 10mM NEM. Non-induced cells were treated in parallel. **A.** Western Blot of extracted histones (10µg load) with anti-H2A antibody. Samples from non-induced cells are loaded next to samples from doxycycline induced cells. Deubiquitination reaction of histones from HEK293 cells by USP7 (C.1.10) serves as a control for the detection of ubiquitinylated H2A. **B.** same as for A but immuno-detection with an anti-H2B antibody. Coomassie Blue staining of extracted histones serves as loading control.

C.1.15 CHIP analysis of Dnmt1, ICBP90 and USP7

Dnmt1, ICBP90 and USP7 exert enzymatic activities that can affect chromatin composition and structure and thus accessibility. DNA methylation and histone ubiquitinylation could also serve as binding platforms for other modulating factors to be recruited (Vissers et al. 2008).

In search for genomic regions that are targeted by Dnmt1 or ICBP90, three genes were finally chosen for a more detailed analysis with chromatin immunoprecipitation (CHIP) (E.2.16.5, see below).

Dnmt1 was found to interact with Polycomb group protein (PcG) EZH2 (enhancer of zeste homolog 2) and localized to several target promoters in dependency of EZH2 (Viré et al. 2005). In addition for the identified target gene *WNT1* (wingless-type MMTV integration site family, member 1), it was shown that the CpG methylation status was controlled by EZH2 through direct recruitment of Dnmt1.

In another publication (Wu et al. 2008), NSPc1, a component of the PRC1 complex, promotes H2A ubiquitinylation and cooperates with Dnmt1 in *HoxA7* gene silencing. Interestingly, both are directed by EZH2 (PRC2) but NSPc1-mediated H2A ubiquitination and Dnmt1 dependent DNA methylation are interdependent in gene silencing.

In the group of Dr. R. Kappler, the CpG island of the *IGFBP3* gene promoter was methylated as seen with methylation specific PCR (MSP) and was found to be partially demethylated upon ICBP90 knockdown (personal communication).
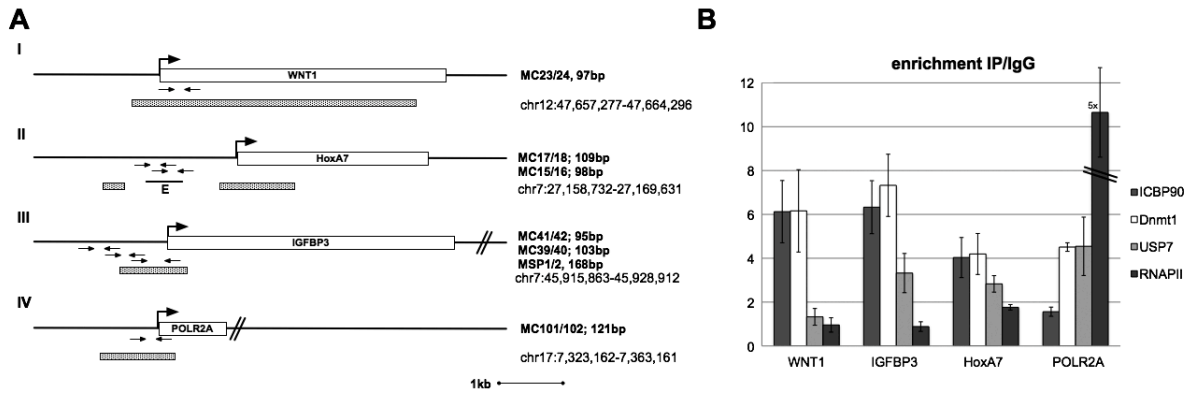
Figure 30 Gene targets for chromatin immunoprecipitation

A.) Genomic regions of target genes chosen for CHIP analysis are displayed. CpG islands are depicted in grey shading. Locations of qPCR primers (E.2.16.5) are depicted with black arrows. Their names and amplicon sizes as well as the genomic region are given. '//' denotes partial presentation of the gene. **B.**) Chromatin immunoprecipitations were performed with $2.0x10^7$ HCT-116 cells, formaldehyde cross-linked for 20min (E.2.15.3). Cross-linked chromatin was solubilized and DNA fragments with an average size of 500-1000bp generated through sonication (E.2.15.4). Chromatin was subjected to immunoprecipitation with the antibodies of interest (E.1.6), the precipitated DNA subsequently purified (E.2.15.6) and qPCR analysis performed (E.2.16.1). A detailed description of the evaluation is given (E.2.16.6). The average of three independent CHIP experiments for Dnmt1, ICBP90 and USP7 and the average of two CHIP experiments for RNAPII are shown. Standard deviations, target genes of interest (Figure 30) and antibodies used for CHIP (E.2.15.2) are indicated. The enrichment of specific IP versus IgG background is plotted against the genes under investigation. Note that the RNAPII enrichment at the *POLR2A* locus is displayed as $1/5^{th}$.

The *POLR2A* gene is highly expressed in proliferating cells and was therefore chosen as a reference for silenced genes.

In Figure 30, the target genes that were chosen for CHIP analysis are displayed. CpG islands as determined with the UCSC genome browser, locations of qPCR primers (E.2.16.5) and the chromosomal regions are indicated.

Dnmt1 and ICBP90 are associated with the three repressed genes *WNT1*, *IGFBP3* and *HoxA7* (Figure 30) whereas RNAPII is absent. This is in agreement with the observation that RNAPII is found at transcriptionally active loci as seen for the *POLR2A* gene promoter. Albeit different functions, ICBP90 was described as a chromatin associated factor responsible for Dnmt1 recruitment (Bostick et al. 2007; Sharif et al. 2007). Hence, the association of ICBP90 together with Dnmt1 at loci that are silenced or maintained in a repressed state is in accordance with the CHIP data obtained.

In contrast to Dnmt1 and ICBP90, USP7 that was neither described as a DNA binding factor nor harboring a DNA binding domain, is not associated with the *WNT1* promoter but found enriched at the *IGFBP3* and *HoxA7* genes together with Dnmt1 and ICBP90. Interestingly, besides RNAPII, USP7 and Dnmt1 are present at the *POLR2A* gene promoter, contradicting the general belief of DNA methylation solely associated with repression and silencing.

The CHIP data suggest the existence of three different complexes located at different loci:
at the *WNT1* gene, a Dnmt1/ ICBP90 dimer, at the *IGFBP3* and *HoxA7* loci a trimer complex of Dnmt1/ ICBP90 and USP7 and last a Dnmt1/ USP7 dimer at the *POLR2A* gene can be observed.

On the first glance, the possible function of these complexes is not conclusive and will need further investigation (see discussion).

C.2 Characterization of Dnmt3b complexes

Besides Dnmt1 which showed an elution profile between 440 and 230 kDa, placenta nuclear extracts (E.2.9.1) were also screened for larger Dnmt3b complexes on size exclusion chromatography.

Different antibodies directed against Dnmt3b recognized proteins of different size in Western Blot analysis. The first immunoblot was performed with a mouse monoclonal anti-Dnmt3b antibody (abcam, ab13603; E.1.6) that recognized a signal of approximately 65kDa compared to the expected signal of 95-100kDA. Since Dnmt3b splice variants cannot account for the observed difference in size and placenta nuclear extracts were more prone to protein degradation than nuclear extracts from Hela cells (data not shown), the detected Dnmt3b elution profile was verified with the DNA methyltransferase specific activity assay (E.2.11.1) with nm and hm oligonucleotides as substrate.

As seen in Figure 31, the activity profile of the fractions with nm DNA corresponds to the Western Blot signals detected for Dnmt3b (ab 13604). A higher activity can be observed in the elution fractions of Dnmt1, reflecting Dnmt1's preference for hm DNA whereas it is not present in the fractions that only contain Dnmt3b.

Another commercial antibody (ab 2851) and the rat monoclonal antibody D3b2-2C1 (E.1.6) directed against Dnmt3b detect signals of 50 kDa and 120 kDA respectively. Interestingly, the signals reflect the elution profile with a 1MDa Dnmt3b complex but not for mid-weight complexes (440-230 kDa). This discrepancy could be explained with a possible cross reactivity of the mouse monoclonal anti-Dnmt3b antibody (abcam, ab13603) with Dnmt1 degradation products that are not recognized by the rat monoclonal anti D3b2-2C1 antibody and the anti-Dnmt3b antibody (ab2851; E.1.6).

Accordingly, higher molecular weight complexes of Dnmt3b seem to exist in extracts of human placenta. So far, the establishment of Dnmt3b specific antibodies capable of immunoprecipitation has failed (data not shown). Thus, a straight-forward approach for identifying Dnmt3b protein complexes and new interaction partners has moved beyond reach.
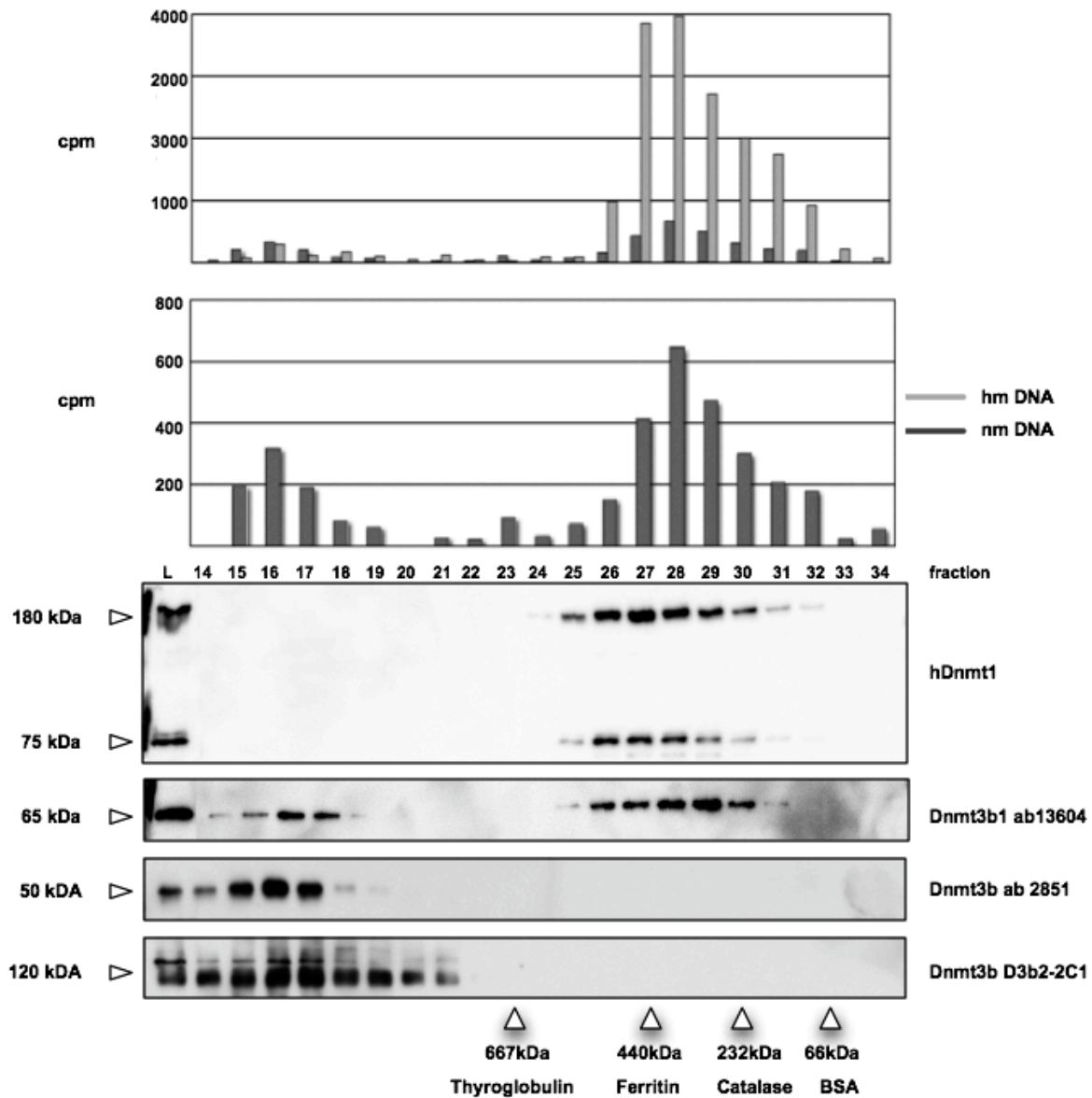
Figure 31 Dnmt3b and Dnmt1 from placenta extracts on SEC

Placenta nuclear extract (500µl, 18,5mg/ml; E.2.9.1) was separated on a Superose6 gelfiltration column (GE Healthcare) in 20mM Tris pH 8.0, 150mM NaCl, 1mM MgCl$_2$, 10% glycerol, 1mM DTT. 500µl fractions were collected and 30µl of each fraction was subjected to SDS-PAGE and Western Blot analysis. Immunodetection was performed with the following antibodies (E.1.6): Dnmt1 (2G3, rat monoclonal), Dnmt3b (D3B2-2C1, rat monoclonal), Dnm3b1 (mouse monoclonal, ab13604), Dnmt3b (rabbit polyclonal, ab2851). Molecular weight marker, fractions and gelfiltration standards are indicated. DNA methyltransferase assay was performed with 10µl of each fraction for 1 hour at 37°C as described (E.2.11.1) in the presence of 1µM oligonucleotide (either non-methylated (nm) or hemi-methylated (hm)).

C.3 Dnmt3a/b2 dependent de novo DNA methylation in the context of chromatin

Recently, DNA methylation activities towards DNA reconstituted into nucleosomes have been examined. However the results from the literature were rather contradictive (see introduction, A.3.8). Therefore, we sought to examine in detail the conditions of DNA and

nucleosome binding, followed by single molecule analysis of DNA methylation of nucleosomal matrices.

C.3.1   Minimal DNA binding length of Dnmt3a and Dnmt3b2 *in vitro*

Prior to experiments regarding the methylation of mono-nucleosomes with different linker lengths, basic characterization on DNA binding properties was performed. Despite the capability of Dnmt3a and Dnmt3b2 to methylate oligonucleotides *in vitro* (20-30nt, E.2.11.1), the minimal DNA length for proper binding was determined. Dnmt3a (N-His, Sf21 cells) and Dnmt3b2 (C-His, *E. coli*) were purified (E.2.7.3; E.2.8.2) and increasing amounts of protein were incubated with an Ultra low range DNA marker (Fermentas). Reactions were loaded on a 12% PAA gel and stained with ethidium bromide (Figure 32). Both Dnmt3a and Dnmt3b2 bind first to the longest DNA fragments, although the DNA amount (weight) per lane is almost the same (exception: 50bp; 2.5x as much), suggesting a cooperative binding mechanism resulting in binding preferentially to longer DNA. In accordance, the C-terminal domain of mouse Dnmt3a oligomerized on DNA to form a nucleoprotein filament (Jia et al. 2007; Jurkowska et al. 2008). According to the EMSA analysis, only DNA fragments >35bp are stably bound (Figure 32). In gelfiltration experiments with the C-terminal domain of mDnmt3a incubated with DNA fragments of different size (12, 20, 30, 45bp), Dnmt3a C-terminal domains partially shifted with DNA >20bp to higher molecular weight corresponding to 2, 3-4, and 5 five proteins bound respectively (Jia et al. 2007). EMSA studies performed with fluorescently labeled annealed oligonucleotides (15, 30, 45, 60bp) revealed weak association with DNA fragments of 45bp and 60bp of size, whereas DNA fragments 15bp and 30bp long were not shifted at all (data not shown).
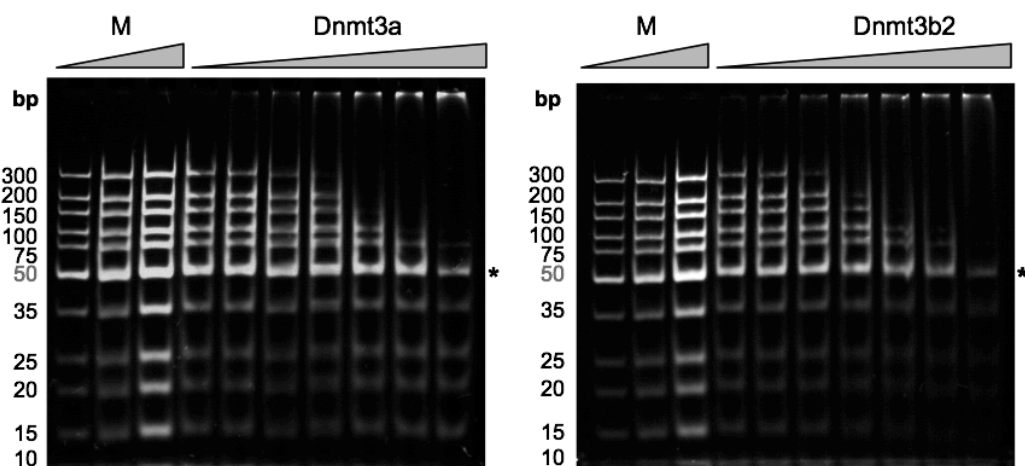
Figure 32 Minimal DNA length required for binding of Dnmt3a and Dnmt3b2

Dnmt3a (N-His, Sf21 cells) and Dnmt3b2 (C-His *E. coli*) were purified as described (E.2.7.3; E.2.8.2), incubated for 15min at 26°C with 125ng of an Ultra low ranger DNA marker (Fermentas) in binding buffer (20mM Tris pH 7.6, 30mM KCl, 5mM EDTA, 1mM DTT, 5µM SAM, 20% glycerol) and loaded on a 12% PAA gel in 0.4x TBE. The gel was subsequently stained with ethidium bromide. Dnmt3a titration was performed with 75ng – 2.4µg, Dnmt3b2 titration with 62.5ng – 4.0µg respectively. DNA molecular weight marker is indicated. * indicates minimal DNA length that is required for binding.

As a summary, although DNA fragments of 20bp and 30bp are methylated *in vitro* (E.2.11.1), stable protein-DNA interactions are observed with DNA fragments >35bp with EMSA. A co-operative binding effect of the *de novo* methyltransferases Dnmt3a and Dnmt3b2 is reflected by DNA binding preferences for longer DNA fragments

C.3.2 Dnmt3a and Dnmt3b2 show binding mobility towards naked DNA *in vitro*

In order to see whether Dnmt3a and Dnmt3b2 stay stably bound to DNA *in vitro* and thus reflect a DNA/protein filament (Jurkowska et al. 2008), proteins were incubated with a 342bp DNA fragment (20ng; MF79/80) for 15min at 26°C to allow for complex formation. Linearized competitor DNA was added, mixed, placed on ice and immediately loaded on a 12% PAA gel. Dnmt3a and Dnmt3b2 almost completely shift the 342bp DNA fragment with raising amounts of protein (Figure 33, lane 2,3; A and B) resulting in DNA/protein complexes at the top of the gel. When adding increasing amounts of linearized competitor DNA, complex formation with the other DNA strand occurs, releasing the shorter DNA fragment. In a time course experiment with the addition of competitor DNA in the range of 3-20sec and immediate loading on a 'running' gel led to the same observation (data not shown). Accordingly, DNA binding *in vitro* of both Dnmt3a and Dnmt3b2 is a highly dynamic process.
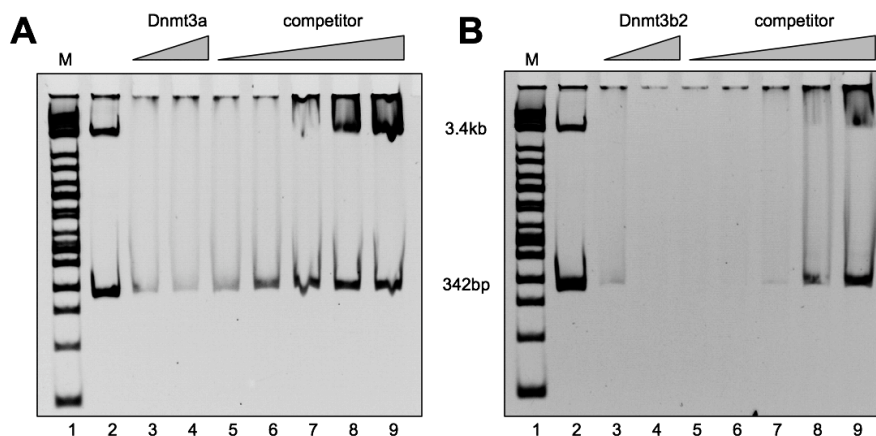
Figure 33 Binding mobility of Dnmt3a/b2 towards DNA

Dnmt3a (N-His, Sf21 cells) and Dnmt3b2 (C-His *E. coli*) were purified as described (E.2.7.3; E.2.8.2), incubated for 15 min at 26°C with 20ng of MF79/80 DNA fragment (342bp) in binding buffer (20mM Tris pH 7.6, 30mM KCl, 5mM EDTA, 1mM DTT, 5µM SAM, 20% glycerol). Competitor DNA (linearized DNA 2890bp) was added in increasing amounts (5-80ng) following incubation for 5min. The reaction mix was loaded on a 12% PAA gel in 0.4x TBE. The gel was subsequently stained with ethidium bromide. Lane (1); DNA (342bp) and competitor DNA are loaded **A.** Dnmt3a titration with two concentrations of Dnmt3a (lane 2 an 3). With the highest concentration, the competition reaction with competitor DNA is performed (lane 4-9). **B.** same as for A but with Dnmt3b2.

C.3.3 *In vitro* binding of mono-nucleosomes by Dnmt3a and Dnmt3b2

DNA templates with the 601 nucleosome positioning sequence ((Thåström et al. 2004a); referred to as WID, 147bp) flanked either on one side (asymmetric) or on both sides (symmetric) with DNA linkers of different size were PCR amplified (E.2.10.4) and partially assembled with *Drosophila* histones by salt dialysis (E.2.10.2). Figure 34 displays the

different partially assembled mono-nucleosomes that were used for binding studies with Dnmt3a and Dnmt3b2.

It is important to note that for comparative analysis the amount of DNA and nucleosomes loaded were adjusted to ethidium bromide staining. Of course, ethidium bromide staining depends on intercalation into dsDNA that is certainly impaired in DNA wrapped around a histone octamer. In addition, the number of molecules differs from DNA/nucleosomal template to another. Nevertheless, qualitative differences on DNA/protein or nucleosome/protein associations can be seen and thus conclusions on the binding properties towards DNA and nucleosomes of Dnmt3a and Dnmt3b2 can be drawn (Figure 35).

In Figure 35, partially assembled symmetric and asymmetric mono-nucleosomes with different lengths of linker DNA were incubated with rising amounts of Dnmt3a and Dnmt3b2 and subsequently loaded on a 5% PAA gel. Dnmt3a preferentially bound to the 77WID77 mono-nucleosome over symmetric nucleosomes with shorter linker DNA as well as free DNA (Figure 35 A, lanes 3-5). Interestingly, asymmetric nucleosomes and free DNA revealed equal binding by Dnmt3a (Figure 35 B, lanes 3-5). In another experimental setup, increasing amounts of Dnmt3a were incubated with a mixture of different nucleosomal species, namely 77WID77, 77WID and WID, and DNA (210bp) (Figure 35 C, lanes 3-5). Again, Dnmt3a first bound to nucleosomes 77WID77 followed by DNA and the 77WID nucleosome.
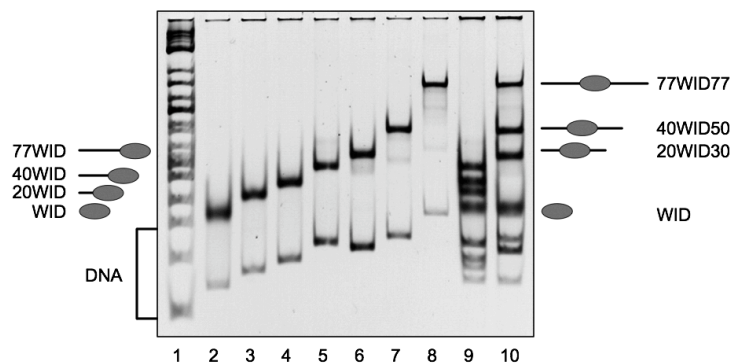
Figure 34 Symmetric and asymmetric mono-nucleosomes with different linker length

DNA fragments of different length with the 601 nucleosome positioning sequence ((Thåström et al. 2004a); referred to as WID, 147bp) situated at different positions were PCR amplified as described (E.2.10.4) and partially assembled with *Drosophila* histones by salt dialysis (E.2.10.2). Assembled nucleosomes were analyzed on a 5% PAA gel in 0.4x TBE following staining with ethidium bromide. DNA linker lengths are indicated. M indicates DNA marker. Lane 9 asymmetric mono-nucleosomes and lane 10 symmetric mono-nucleosomes as a mixture with the WID mono-nucleosome.

Dnmt3b2 behaved differently in a way that preferentially DNA and nucleosomes with longer DNA overhangs were favored over nucleosomes with short linker DNA (Figure 35 A, lanes 7-9; B lanes 7-9) indicating that DNA is the first and DNA linker length the second determinant of nucleosome binding. When Dnmt3b2 is incubated with the mixture of different nucleosomal templates and DNA (Figure 35 C, lanes 7-9), Dnmt3b2 bound to 77WID77 equally well as to free DNA followed by 77WID. As seen before, DNA seems to be the preferred substrate of binding and not the nucleosome itself.

65
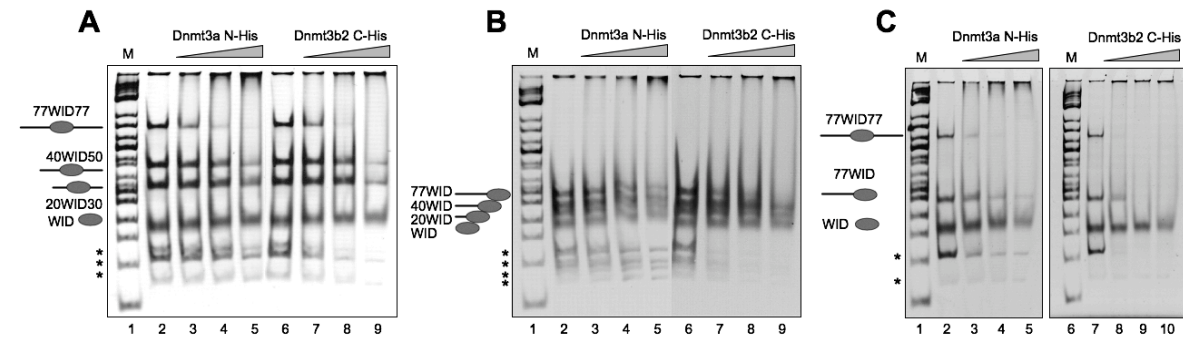
Figure 35 Binding behavior of Dnmt3a and Dnmt3b2 to mono-nucleosomes with different linker length

DNA fragments of different length with the 601 nucleosome positioning sequence ((Thåström et al. 2004a); referred to as WID, 147bp) situated at different positions were PCR amplified as described (E.2.10.4) and partially assembled with *Drosophila* histones by salt dialysis (E.2.10.2). Indicated assembled nucleosomes were incubated with Dnmt3a (N-His, Sf21 cells, 0.6-2.4µg, lanes 3-5) or Dnmt3b2 (C-His *E. coli,* 1.0-4.0µg, lanes 7-9) in binding buffer (20mM Tris pH 7.6, 30mM KCl, 5mM EDTA, 1mM DTT, 5µM SAM, 20% glycerol) for 15 min at 26°C. The reaction was stopped on ice and loaded immediately on a 5% PAA gel in 0.4x TBE. The gel was subsequently stained with ethidium bromide. **A.** Dnmt3a/b2 are incubated with symmetric nucleosomes of different linker length. **B.** same as in A but with asymmetric nucleosomes. **C.** same as in A but with mixture of DNA and symmetric and asymmetric nucleosomes. * marks free DNA; M indicates DNA molecular weight marker.

Therefore, generally Dnmt3a binds DNA and mono-nucleosomes comparably well, whereas Dnmt3b2 shows higher affinity to free/accessible DNA than to the nucleosomal core.

Although not shown, in individual reactions both Dnmt3a and Dnmt3b2 were able to bind to the 147bp mono-nucleosome comparable to mono-nucleosomes with linker DNA, indicating that it can serve as substrate.

C.3.4 Mono-nucleosomes are not disrupted by Dnmt3a and Dnmt3b2 *in vitro*

Dnmt3a and Dnmt3b2 associate with nucleosomal templates *in vitro* (C.3.3) albeit probably by different means. In order to test whether binding of Dnmt3a/b2 disrupts the nucleosome, nucleosome binding was competed with linear DNA (Figure 36).
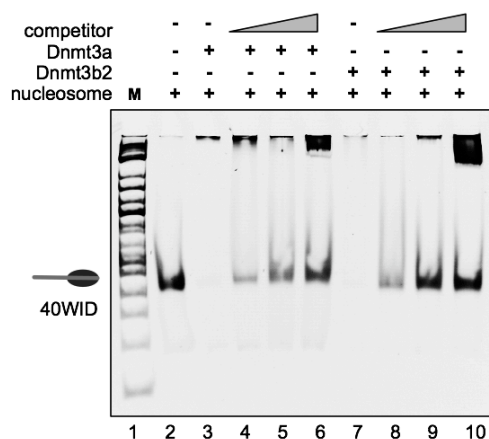
Figure 36 Dnmt3a/b2 do not disrupt mono-nucleosomes upon binding

Dnmt3a (N-His, Sf21 cells) and Dnmt3b2 (C-His *E. coli*) were purified as described (E.2.7.3; E.2.8.2), incubated for 15 min at 26°C with 80ng of the 40WID fragment (187bp, E.2.10.4) fully assembled with drosophila histones by the method of salt dialysis in binding buffer (20mM Tris pH 7.6, 30mM KCl, 5mM EDTA, 1mM DTT, 5µM SAM, 20% glycerol). Competitor DNA (linearized DNA 2890bp) was added in increasing amounts (50-200ng) following incubation for 5min. The reaction mix was loaded on a 5% PAA gel in 0.4x TBE. The gel was subsequently stained with ethidium bromide. M indicates DNA marker.

Without competitor DNA, the nucleosome is well bound by Dnmt3a and Dnmt3b2 and shifted to the top of the PAA gel (Figure 36, lane 2 and 7). Upon addition of increasing amounts of competitor DNA, both Dnmt3a and Dnmt3b2 dissociated from the 40WID nucleosome. The released mono-nucleosomes (lane 4-6 and lane 8-10) migrated in the gel as the unbound reference 40WID nucleosome (lane1) indicating that no loss of histones or changes in the position of the nucleosome occurred.

C.3.5   *In vitro* methylation of DNA and mono-nucleosomes by Dnmt3a and Dnmt3b2

In vitro methylation of nucleosomes by the *maintenance* and *de novo* DNA methyltransferases have already been under investigation, although the results were rather inconsistent (Robertson et al. 2004; Gowher et al. 2005b) (Takeshima et al. 2006).

Two DNA templates (MF79/80 342bp; MF124/125 147bp, (E.2.13.1) harboring an altered 601 nucleosome positioning sequence were amplified by PCR (pGA-BN601 Mr Gene; E.1.8) and assembled into nucleosomes (E.2.10.2) (Figure 37, A). *In vitro* DNA methyltransferase assays (E.2.11.1) with 100nM of Dnmt3a and Dnmt3b2, 480nM SAM (1.5µCi) and 480nM CpG sites of either the free DNA or the nucleosomal DNA were performed. 'Naked' DNA and accessible DNA in the linker region of mono-nucleosomes were equally well methylated, whereas the 147bp nucleosome was almost not methylated at all (Figure 37, B). Although the overall methylation efficiency of Dnmt3a and Dnmt3b2 differed (different protein preparations), methylation of the nucleosome (MF124/125 nuc) was decreased 35-fold and 27-fold compared to 'naked' DNA for Dnmt3a and Dnmt3b2 respectively (as determined from the 40min timepoint).
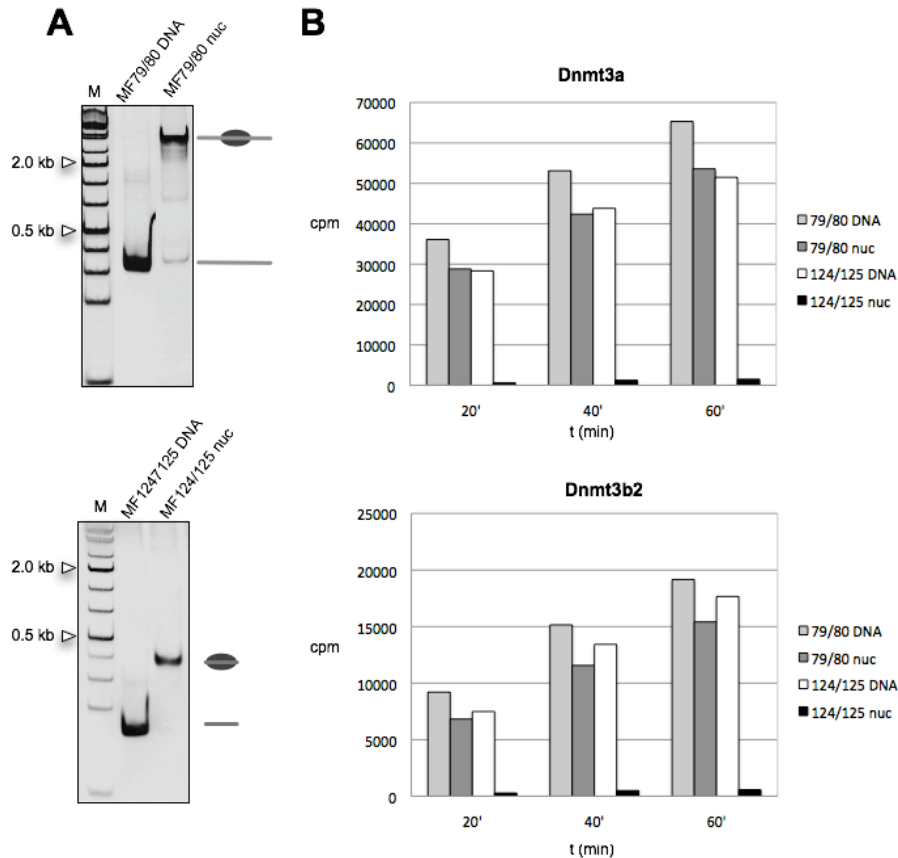
Figure 37 Radioactive DNA methylation assay with DNA and mono-nucleosomes

A. DNA fragments and mono-nucleosomes used for Dnmt specific radioactive methylation assay. The MF79/80 (342bp) and MF124/125 (147bp) DNA fragments that bear a modified 601 nucleosome positioning sequence (from pGA BN601 Mr Gene) were PCR amplified as described (E.2.13.1) and fully assembled with *Drosophila* histones by salt dialysis (E.2.10.2). Analysis on a 5% PAA gel in 0.4x TBE with ethidium bromide staining. Molecular weight marker is indicated **B.** Radioactive DNA methylation assay was performed (E.2.11.1) in the presence of 480nM SAM (1.5µCi), 100nM N-His Dnmt3a (Sf21 cells) and C-His Dnmt3b2 (*E. coli*), 480nM CpG sites of the indicated templates. At the given time points samples were withdrawn, stopped and treated as described (E.2.11.1). Radioactivity (cpm) was determined in a scintillation counter and plotted against the individual samples for each time point.

C.3.6   Bisulfite analysis of *in vitro* methylated DNA and mono-nucleosomes

In order to study in detail *in vitro* DNA methylation of Dnmt3a and Dnmt3b2 towards mono-nucleosomes, the PCR-fragment MF79/80 (342bp, 27 CpG sites, amplified on pGA BN601 Mr Gene E.1.8) was reconstituted with *Drosophila* histones by the method of salt dialysis (E.2.10.2) (Figure 38, A). The assumed position of the nucleosome was verified by restriction enzyme digesting analysis (Figure 38, B).
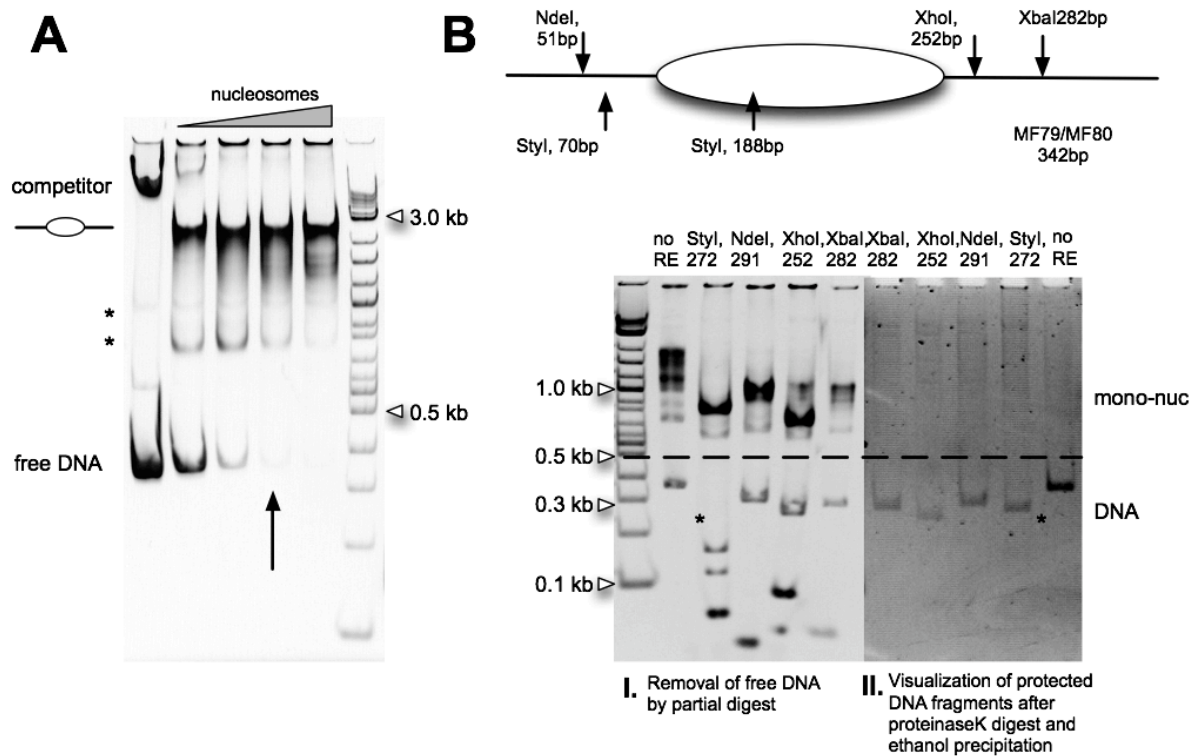
Figure 38 Reconstitution and mapping of the nucleosome binding site

A. The MF79/80 (342bp) DNA fragment that bears a modified 601 nucleosome positioning sequence (from pGA BN601 Mr Gene) was PCR amplified as described (E.2.13.1) and assembled in different ratios with *Drosophila* histones by salt dialysis (E.2.10.2) in the presence of competitor DNA (pCpGL basic, 250ng). Analysis on a 5% PAA gel in 0.4x TBE with ethidium bromide staining. Molecular weight marker is indicated. Arrow denotes nucleosomal template used for non-radioactive *in vitro* DNA methylation assay **B.** Although the high-affinity 601 nucleosome positioning sequence is present, its location was mapped. Partially assembled nucleosomes were digested with the indicated restriction enzymes (RE) and either directly (**I.**), or after proteinaseK digest and ethanol precipitation (Xref) (**II.**) loaded onto a 5% PAA gel. StyI cuts within the proposed nucleosomal region. In **I.** the 342bp DNA fragment is cut and shifted to smaller sizes (* denotes the theoretic position). After proteinaseK treatment, the DNA fragment (*) that had been protected from RE digest appears. Smaller fragments are no longer visible due to inefficient ethanol precipitation.

Non-radioactive DNA methylation reactions with Dnmt3a, Dnamt3b2 and the bacterial methyltransferase M.SssI as control were performed as described (E.2.11.1) and methylated DNA subjected to bisulfite treatment (E.2.13.3). Bisulfite converted DNA was PCR amplified using two different primer pairs for the sense and the anti-sense strand respectively. PCR products were cloned into pGEM-T-EASY vector (Promega) and transformed into chemically competent Xl1 Blue *E. coli* cells following Blue/White selection on Bluo-Gal/ampicillin LB-plates. DNA was isolated and sent for sequencing. Analysis of bisulfite converted DNA was done with BiQ ANALYZER software (http://biq-analyzer.bioinf.mpi-inf.mpg.de/) that had been provided by C. Bock (Bock et al. 2005).
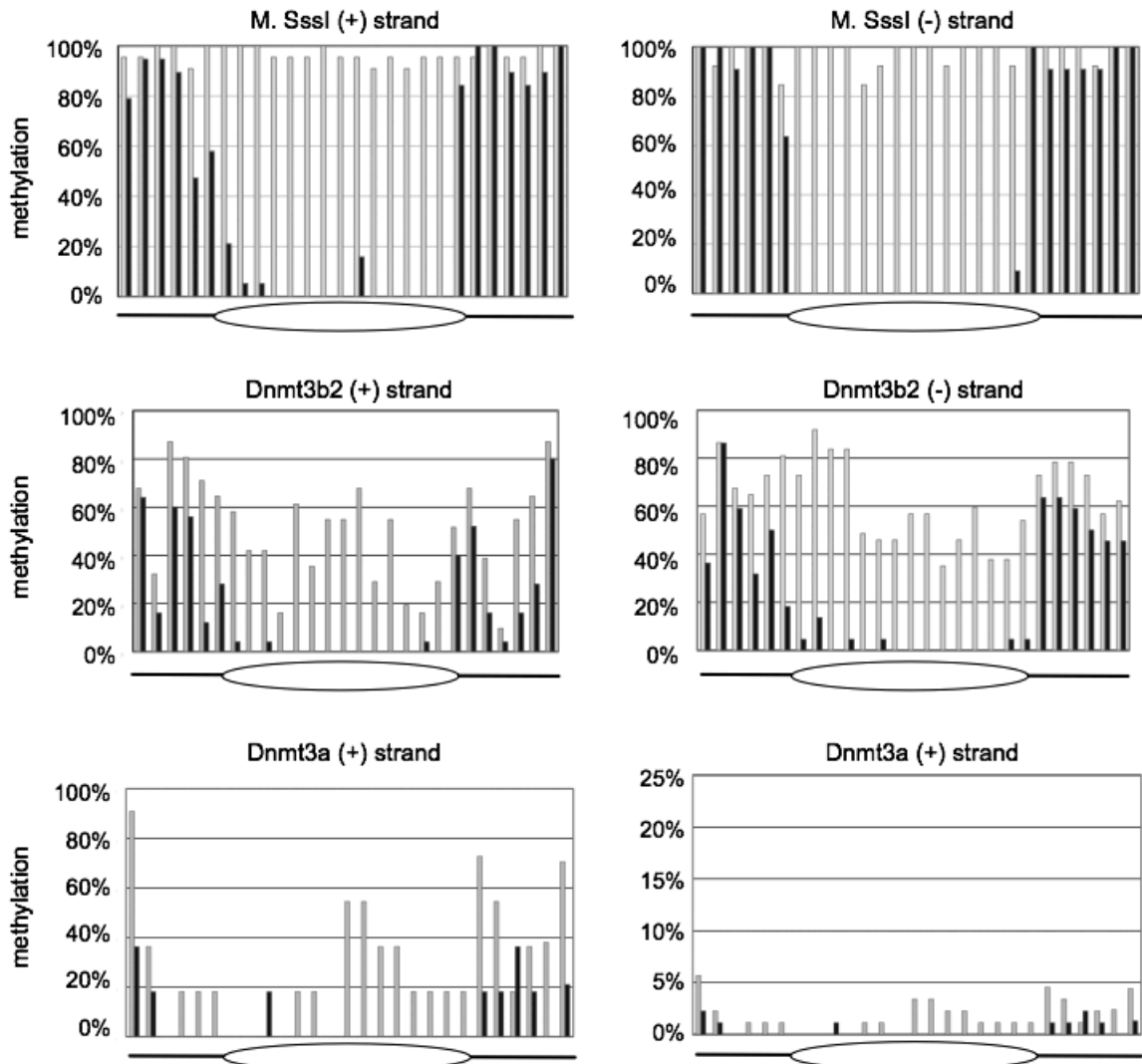
Figure 39 Bisulfite analysis of nucleosomal methylation by M.SssI, Dnmt3a and Dnmt3b2

The DNA methylation reaction with Dnmt3a/b was carried out in a reaction volume of 40µl in DNA methyltransferase buffer (20mM Hepes, pH 7.6, 1mM EDTA, 1mM DTT). Dnmt3a and Dnmt3b2 were used at a concentration of 600nM and 200nM, DNA or nucleosomal DNA (MF79/80 on pGA BN601 Mr Gene, 27 CpG sites) between 12.5 and 20nM CpG sites, BSA at 0.2µg/µl and SAM (Sigma A7007, 10mM) at 250µM. M.SssI was used as control in a separate reaction with 1x NEB buffer 2 and 4U M.SssI. The reactions were mixed well and incubated for 1 hour at 37°C. Another 250µM SAM were added following incubation for 1-1,5 hours. This step was repeated twice. The reactions were heat-inactivated at 65°C for 20min. and 40µl of the reaction were directly subjected to bisulfite conversion (E.2.13.3). After bisulfite conversiton, the (+) strand and the (-) strand were PCR amplified with the primer pairs MF89/90 and MF112/113 respectively. PCR products were cloned into the pGEM-T-EASY vector (Promega) following transformation into Xl1Blue *E.coli* cells. Isolated DNA from positive clones selected by Blue/White screening were sent for sequencing. Evaluation of the data was described elsewhere (E.2.13.6). M.SssI DNA(+) 22clones, M.SssI DNA(-) 13clones, M.SssI nuc (+) 19clones, M.SssI nuc (-) 11clones, D3b2 DNA (+) 31clones , D3b2 DNA (-) 37 clones, D3b2 25nuc (+) 25clones, D3b2nuc (-) 22clones, D3A DNA (+) 23clones, D3A nuc (+) 22clones. Black bars denote nucleosomal, light grey bars represent DNA templates.

The bacterial methyltransferase M.SssI (NEB) efficiently methylated both the upper and lower DNA strands whereas the DNA protected by the nucleosome was almost not accessible for methylation (Figure 39). Dnmt3b2 methylated the sense and anti-sense DNA strands, but to a lower extent compared to M.SssI and with an apparent sequence specificity, since some CpG sites were more frequently methylated than others. Analysis of the (+) and

the (-) strands was intended to see whether the DNA strand facing outwards of the nucleosome could be accessible for DNA methylation. As seen for M.SssI, Dnmt3b2 was also not able to methylate the DNA within the nucleosomal region except for some CpG sites situated at the entry/exit sites of the nucleosome indicating that nucleosomes represent a barrier for *de novo* methylation and the need for other mechanisms such as moving of histones or disassembly of histones to allow for DNA methylation.

The reaction efficiency of Dnmt3a was extremely low, for both the naked DNA and the nucleosomal template, although the picture of methylation, as for Dnmt3b2 and in comparison to the radioactive data (C.3.5), can be envisioned. After having recapitulated enzymatic prerequisites of Dnmt3a, it seemed that the amount of DNA/nucleosmal template with 20nM CpG sites was extremely below the K_M value of 250nM-2500 CpG sites as reported in the literature (Aoki et al. 2001; Gowher and Jeltsch 2001; Yokochi and Robertson 2002; Suetake et al. 2003). Latest results by C. Neuhäuser showed an increase of DNA methylation by Dnmt3a in a reaction setup with 600nM CpG sites to meet the K_M value requirements.

As a summary, Dnmt3a and Dnmt3b2 are able to methylate DNA and linker DNA, but hardly within the nucleosome suggesting the need for enzymatic activities like chromatin remodeling enzymes moving the histone octamer and thus providing accessibility.

C.4 Dnmt3L is associated with histones

Dnmt3L functions *in vivo* and *in vitro* as a stimulatory factor for *de novo* methylation (Chedin et al. 2002; Suetake et al. 2004; Gowher et al. 2005a). The interaction with Dnmt3a is of particular interest as the crystal structure of a tetrameric complex was solved (Jia et al. 2007) and Dnmt3L and Dnmt3a knockout mice showed the same methylation defects of maternally and paternally imprinted genes (Bourc'his et al. 2001; Hata et al. 2002).

The co-purification of Dnmt3L with Dnmt3a2, Dnmt3b and histones and the interaction with non-methylated H3K4 tails (Ooi et al. 2007) raises the question which effects Dnmt3L exerts on the methylation of nucleosomes by the *de novo* methyltransferases.

C.4.1   Dnmt3L is associated with histones *in vivo*

hDnmt3L was purified from Sf21 cells via its C-terminal Flag-tag (E.2.7.6). Interestingly, large amounts of DNA were co-purified (Figure 40, A). Further analysis showed the presence of histones (Figure 40, B) confirming the observation that Dnmt3L co-purified histones from ES cells (besides Dnmt3a2 and Dnmt3b) (Ooi et al. 2007) through the specific interaction of non-methylated lysine 4 on histone H3. The DNA fragment size of 500-1000bp reflects the sonication procedure during protein purification rather than putative binding to higher order chromatin structures. Applying a second purification step with an anion exchange matrix (Q-FF, GE Healthcare), histones and DNA could be well separated from Dnmt3L (Figure 40).

Figure 40 hDnmt3L purification from Sf21 insect cells

A. Protein samples after Flag and Q FF purification (E.2.7.6) (50µg each) were treated with proteinaseK and DNA was phenol chloroform extracted followed by ethanol precipitation. Analysis on a 1% agarose gel and ethidium bromide staining. **B.** SDS-Page analysis of the hDnmt3L two-step purification with 1.) Flag-tag and 2.) Q-FF column (E.2.7.6). Recombinant human histones (kindly provided by C. Huber) were loaded as reference.
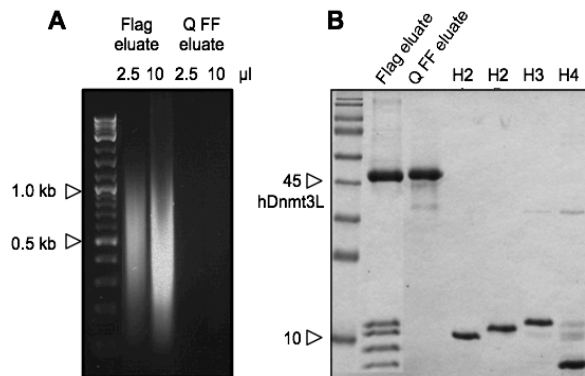
C.4.2 *De novo* DNA methyltransferases and the effect of Dnmt3L

Dnmt3L was purified from Sf21 cells via Flag-tag following a second purification step on an anion exchange column (C.4.1). The protein's integrity, although no precipitation occurred during purification, was verified by monitoring the stimulatory effect on DNA methylation for Dnmt3a and Dnmt3b (Suetake et al. 2004; Gowher et al. 2005a). Dnmt3a and Dnmt3b2 (100nM each), 480nM CpG sites (342bp) and 480nM SAM (1.5µCi) were incubated either alone or with increasing concentrations of Dnmt3L (108-1740nM) at 37°C for 30min. Reactions were stopped, spotted on a DE81 filter (Whatman) and subjected to scintillation counting. With rising concentrations, Dnmt3L exerted a stimulatory effect on the *in vitro* DNA methylation efficiency of Dnmt3a and Dnmt3b (Figure 41).
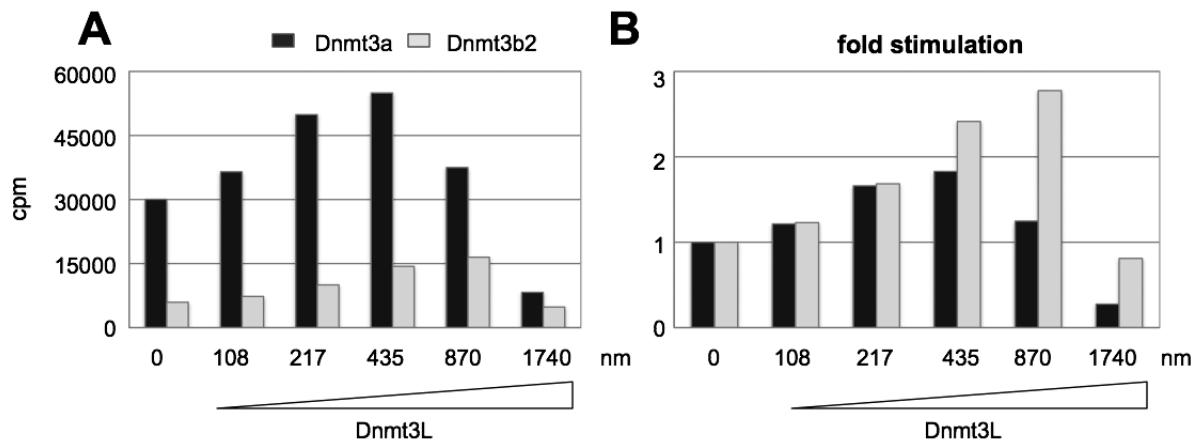
Figure 41 Dnmt3L stimulates the *in vitro* methylation activity of Dnmt3a and Dnmt3b2

In vitro methylation reaction was performed (E.2.11.1) with 100nM N-His Dnmt3a (Sf21 cells) and C-His Dnmt3b2 (*E.coli*), 480nM SAM (1.5µCi), 480nM CpG sites (200ng of 342bp MF79/80 PCR fragment) and rising amounts of hDnmt3L (Q-FF purified; 108-1740nM) for 30min at 37°C. The reactions were stopped with the addition of 10µM 'cold' SAM and spotted onto a DE81 filter (Whatman). After washing and drying, the filters were subjected to scintillation counting for 1min. **A.** Cpm of each sample is plotted against the Dnmt3L concentration. Black bars represent Dnmt3a samples whereas light grey represent Dnmt3b2 samples. **B.** The stimulatory effect of Dnmt3L is shown as ratio of each Dnmt3L reaction/Dnmt3L-free reaction plotted against the Dnmt3L concentration.

In agreement with previous data on DNA fragments >200bp (Suetake et al. 2004), the DNA methylation efficiency was increased 1.6-fold to almost 3-fold for Dnmt3a and Dnmt3b

respectively. Interestingly, high concentrations of Dnmt3L seemed to have an inhibitory effect although Dnmt3L was titrated up to 15µM with no apparent inhibitory effect (Gowher et al. 2005a). Dnmt3L was described as an exchange factor for SAM and DNA thus accelerating the methylation efficiency Dnmt3a (Gowher et al. 2005a). Considering the SAM concentration and Dnmt3L concentrations, it might well be that the methylation system was depleted of the substrate SAM, hence DNA methylation declined. Nevertheless, Dnmt3L had the expected stimulatory function and the proteins integrity was confirmed.

As Dnmt3L was described to form nucleoprotein filaments in cooperation with Dnmt3a and to bind to nucleosomes via non methylated H3K4 tails (A.3.7), Dnmt3L was tested for its ability to bind to DNA and nucleosomes in EMSAs. Furthermore, the effect of Dnmt3L on DNA and nuclesome association by the *de novo* DNA methyltransferases was examined.

In Figure 42 increasing amounts of Dnmt3L (Q-FF, no DNA/histones present) were incubated with DNA alone (342bp) or together with Dnmt3a or Dnmt3b2. In accordance with data from Suetake (Suetake et al. 2004), Dnmt3L could not bind to DNA in EMSA, contrasting results obtained through surface plasmon resonance and filter binding assays (Gowher et al. 2005a) When Dnmt3a and Dnmt3b were incubated with DNA and increasing amounts of Dnmt3L (molar ratio approximately 1:1 – 1:16, 1:2 – 1:10 respectively) a little increase on DNA binding in EMSA could be observed (Figure 42), In agreement, Dnmt3L was required for the stability of the Dnmt3a dimer and thus for DNA binding (Jia et al. 2007). Moreover, one could imagine that nucleoprotein filament formation with Dnmt3a/Dnmt3L or Dnmt3b2/Dnmt3L tetramers requires less complexes than Dnmt3a or Dnmt3b2 potential dimers. Therefore, addition of Dnmt3L leads to more DNA molecules bound.
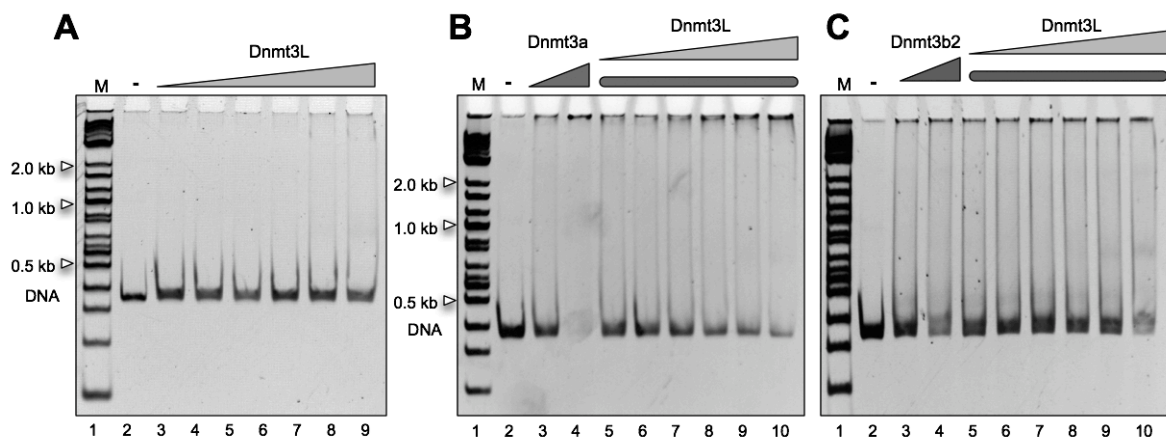
Figure 42 Effects of Dnmt3L on DNA binding

EMSA of 20ng of 342bp DNA fragment with Dnmt3L alone (**A**), Dnmt3a/Dnmt3L (**B**) or Dnmt3b2/Dnmt3L (**C**). **A)** Increasing amounts of hDnmt3L (0.15-2.4µg) (two step purification, E.2.7.6) were incubated with DNA. After incubation for 15min at 26°C in binding buffer (20mM Tris pH 7.6, 30mM KCl, 5mM EDTA, 1mM DTT, 5µM SAM, 20% glycerol), samples were loaded onto a 5% PAA 0.4xTBE and stained with ethidium bromide. **B/C.)** Two different amounts of N-His Dnmt3a (300ng, 600ng, B, lane 2-3) and C-His Dnmt3b2 (500ng, 750ng, C, lane 2-3) as indicated that led to increased DNA binding respectively. The lower amount of Dnmt3a/b2 was incubated with rising amounts of Dnmt3L (0.15-2.4µg, lanes 5-10).

In a similar experimental setup, increasing amounts of Dnmt3L or Dnmt3L with Dnmt3a and Dnmt3b2 were incubated with a mixture of mono-nucleosome of varying DNA linker length (Figure 43). Unexpectedly, Dnmt3L did not bind to mono-nucleosomes although tight

association was observed during purification (C.4.1). According to Prof. Dr. A. Imhof (personal communication), non-methylated H3K4 accounts for at least 50% of the histones isolated from *Drosophila,* hence partial binding should be observed. EMSA with nucleosomes composed of recombinant human histones (kindly provided by C. Huber) as well did not show any shift (data not shown).

Therefore, either other histone tail modifications (Jenuwein and Allis 2001) in cis or trans might influence directly the interaction with Dnmt3L or the structural architecture of a nucleosomal region might provide a platform for Dnmt3L binding. Furthermore, an unidentified transient loading factor could have been responsible for the recruitment and deposition of Dnmt3L onto chromatin.

In contrast to DNA, Dnmt3L does not positively affect the binding of Dnmt3a and Dnmt3b2 to nucleosomal substrates. It rather seems that binding affinities are somehow affected, thus leading to an unclear binding phenomenon.
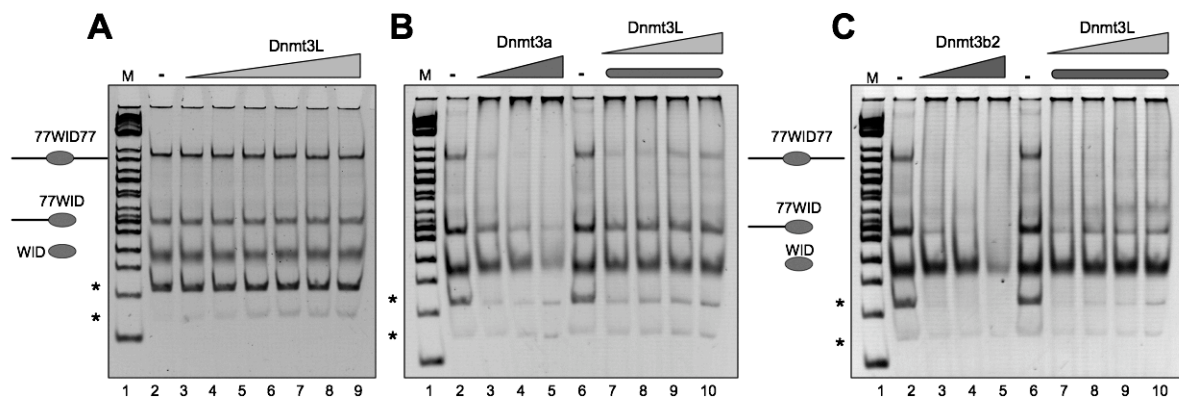
Figure 43 Effects of Dnmt3L on nucleosome binding by Dnmt3a and Dnmt3b2

EMSA of a mixture of mono-nucleosomes with different linker length and free DNA (*) with Dnmt3L alone (**A**), Dnmt3a and Dnmt3a/Dnmt3L (**B**) or Dnmt3b2 and Dnmt3b2/Dnmt3L (**C.**). **A)** Increasing amounts of hDnmt3L (0.15-2.4µg) (two step purification, E.2.7.6) were incubated with mono-nucleosomes. **B/C.)** Incubation of mono-nucleosomes with Dnmt3a/Dnmt3b2 alone (0.6-2.4µg; 1.0-4.0µg, lanes 2-5) or with Dnmt3a/Dnmt3b2 (0.6µg; 1.0µg) and rising amounts of Dnmt3L (0.15-2.4µg, lanes 7-10). After incubation for 15min at 26°C in binding buffer (20mM Tris pH 7.6, 30mM KCl, 5mM EDTA, 1mM DTT, 5µM SAM, 20% glycerol), samples were loaded onto a 5% PAA 0.4xTBE and stained with ethidium bromide.

C.4.3 Analysis of chromatin binding by Dnmt3L *in vivo* and *in vitro*

As Dnmt3L associated with endogenous nucleosomes but did not bind to mono-nucleosomes in EMSA, the question of association to higher chromatin structures was addressed.

First, Dnmt3L associated with endogenous nucleosomes (C.4.1) (40µg) was applied onto a 15%-45% sucrose density gradient (Figure 44). After centrifugation, fractions were taken and analyzed for the distribution of the nucleosomal species, Dnmt3L and histone H3 (E.2.10.6). Nucleosomes were separated according to their size (1n, 2n, 3n). Interestingly, Dnmt3L stayed tightly associated with chromatin, as it is distributed over the whole gradient. Although the immuno-blot signals were very weak, histone H3 could also be detected in some

fractions confirming association with nucleosomes. Nevertheless, a substantial part of the Dnmt3L population ran in fractions 15-17 where almost no DNA/chromatin was detectable. But it has to be kept in mind that the DNA/chromatin constituted of fragments of different size rather than distinct bands, making detection at low concentrations very difficult.
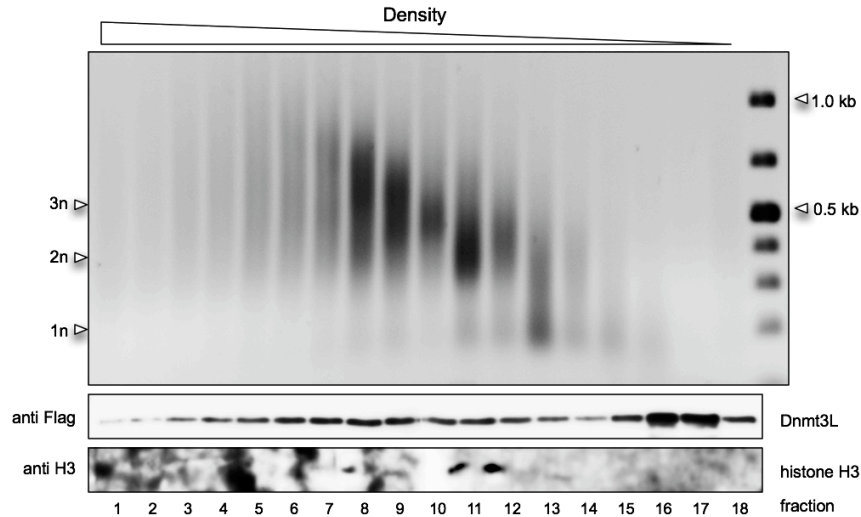
Figure 44 Recombinant Dnmt3L from Sf21 cells is tightly associated with nucleosomes

40µg of Dnmt3L (Flag-tag purification; roughly 6-7µg DNA; E.2.7.6) associated with nucleosomes was subjected to 10%-45% sucrose density gradient separation. After centrifugation (18h, 30,000rpm, SW40, no brake) 400µl of the 600µl fractions were collected, ethanol precipitated overnight with ammonium-acetate (E.2.2.2), loaded onto a 1.3% agarose gel and stained with ethidium bromide. 20µl of each fraction were subjected to SDS-PAGE (12%) following Western Blot analysis. Immuno-detection was performed with an antibody directed against the C-terminal Flag-tag of Dnmt3L and histone H3 (E.1.6).

In order to prove the hypothesis of recombinant Dnmt3L binding to larger nucleosomal templates, 5µg of a mixture of plasmid DNA, linearized plasmid DNA and 200bp DNA fragments fully assembled with *Drosophila* histones by salt dialysis (E.2.10.2) were dialyzed together with Dnmt3L against EX-100 buffer (no glycerol) and loaded onto a 15%-45% sucrose density gradient as described above. After centrifugation, fractions were taken and analyzed for the distribution of the nucleosomal species and Dnmt3L (E.2.10.6). Poly-glutamic acid (PGA) generally facilitates nucleosome assembly and generates salt assembled chromatin with more uniform spacing. Hence, in order to provide a regular nucleosomal array that might affect Dnmt3L binding, PGA (2mg/ml) was added to the dialysis step prior to loading. For comparison, Dnmt3L alone and Dnmt3L with DNA not assembled into nucleosomes were analyzed as well (Figure 45).

The major fractions of different nucleosomal templates applied could be well separated with the nucleosomal plasmid running in various DNA topologies at highest density (fr. 1-7, >3kb), followed by assembled linear DNA (fr. 9-13, 3.0kb) and mono-nucleosomes (fr. 12-13, 200bp) (only one run is shown since no difference between the runs could be observed).
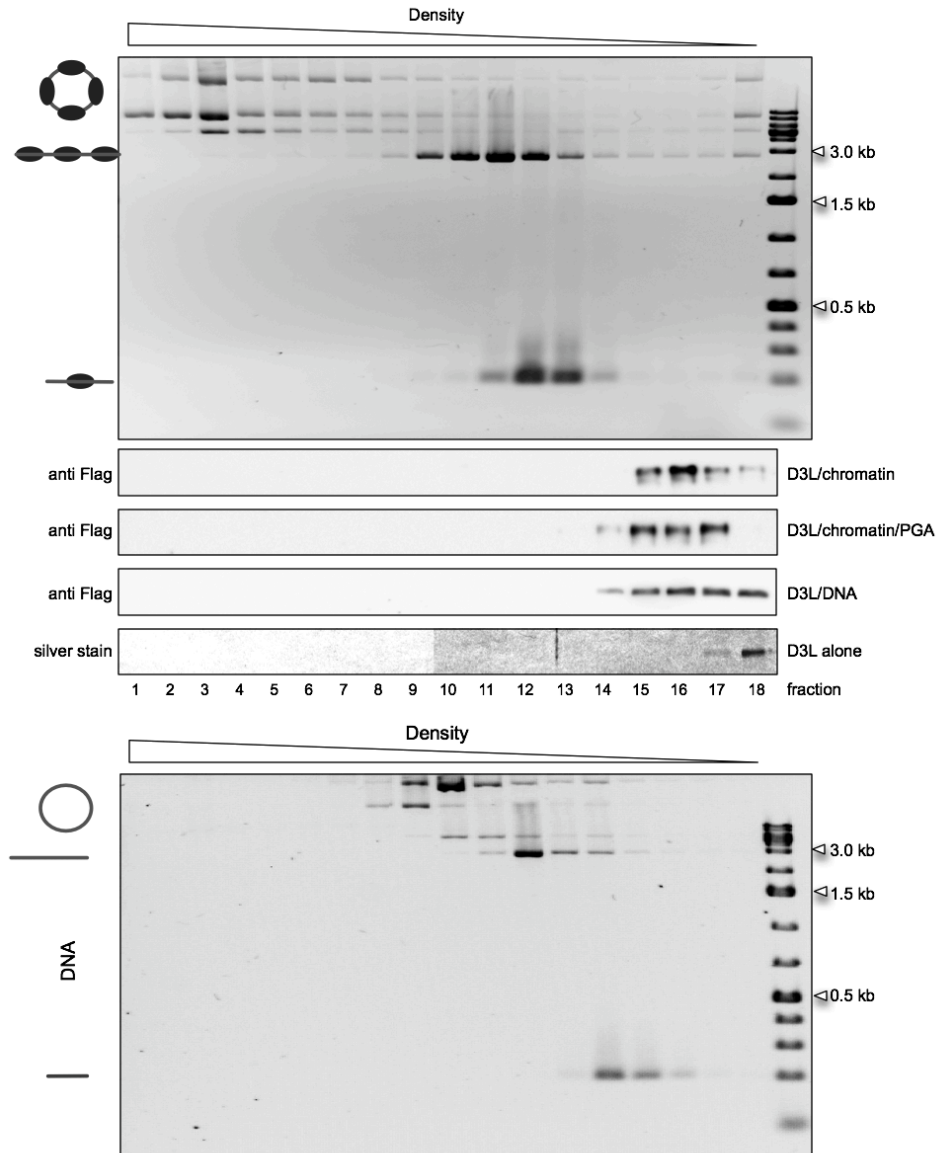
Figure 45 Sucrose gradient analysis of Dnmt3L and chromatin

Different nucleosomal species were separated on a 10%-45% sucrose gradient in EX-50 buffer (without glycerole) during centrifugation (18h, 30,000rpm, SW40, no brake) (E.2.10.6). Circular and linear plasmid DNA as well as 200bp DNA fragments (including the 601 nucleosome positioning sequence) were fully assembled into chromatin with histones from *Drosophila* by salt dialysis (E.2.10.2). 10µg Dnmt3L were either loaded alone, together with 5µg DNA or together with 5µg chromatin or in combination with 5µg chromatin and PGA (2mg/ml). Prior to loading, samples (100µl) were dialyzed for 1.5 hours against Ex-100 buffer (without glycerol). Analysis of chromatin and DNA was done as described (figure xx). Since no significant differences were visible, only one agarose gel for the nucleosomal derived DNA and one agarose gel for the DNA are shown.

Mono-nucleosomes migrated in fraction 13 as seen for the endogenous mono-nucleosomes co-purified with Dnmt3L (Figure 44). Importantly, some residual templates were also found in the other fractions. This is either due to chromatin interactions and thus co-migration with other chromatin templates or partial disassembly resulting in an altered running behavior of

free DNA in the density gradient. The latter cannot be completely excluded since direct analysis of the DNA/chromatin could not be performed due to low concentrations of DNA in the fractions.

Dnmt3L alone hardly entered the sucrose gradient and was present in fraction 17 and 18 (Figure 45). Dnmt3L together with chromatin entered the gradient further to fraction 14/15. Addition of PGA did not significantly change the running behavior of Dnmt3L. Notably, no Dnmt3L associated with the major nucleosomal fractions. Considering fast on/off rates of Dnmt3L binding to chromatin, it is well conceivable that Dnmt3L co-migrates with nucleosomes, but loses contact that cannot be reestablished due to further migration of the higher molecular weight nucleosomal matrices.

When applying Dnmt3L in combination with free DNA onto the sucrose gradient (Figure 45), the DNA species entered the sucrose gradient not as far as observed for their nucleosomal counterparts which is in agreement with the absence of the additional molecular weight of histones. In addition, a 'smeary' running behavior of the free DNA could be seen, suggesting this to be a property of the sucrose gradient. Hence, the separated chromatin was intact and did not partially disassemble during the run in the sucrose gradient. Interestingly, Dnmt3L associated with free DNA entered the gradient (fractions 14-18) comparable to Dnmt3L with nucleosomes. However, the distribution of Dnmt3L along these fractions is different indicating different binding properties towards DNA and nucleosomal matrices.

C.5 Structural analysis of Dnmt1

Through the interaction of the SRA domain with the targeting domain (TS) of Dnmt1 (Leonhardt et al. 1992; Achour et al. 2007), ICBP90 facilitates the loading of Dnmt1 to replicating regions (Bostick et al. 2007; Sharif et al. 2007).

However, the molecular mechanism that controls the activity of Dnmt1 and the recognition of hemi-methylated DNA remains largely unknown.

C.5.1   Dnmt1 – disruption of a protein dimer

Recombinant Dnmt1 was subjected to size exclusion chromatography (E.2.3.6) on a Superdex200 gel filtration column (GE Healthcare) followed by immunoblot analysis (E.2.3.3). Dnmt1 runs at an apparent molecular size of 400kDa which corresponds approximately to twice the molecular weight of Dnmt1 (183 kDA). The presence of 2M NaCl in the running buffer could not disrupt the intramolecular protein interaction, indicating a probable hydrophobic interaction domain (Figure 46).
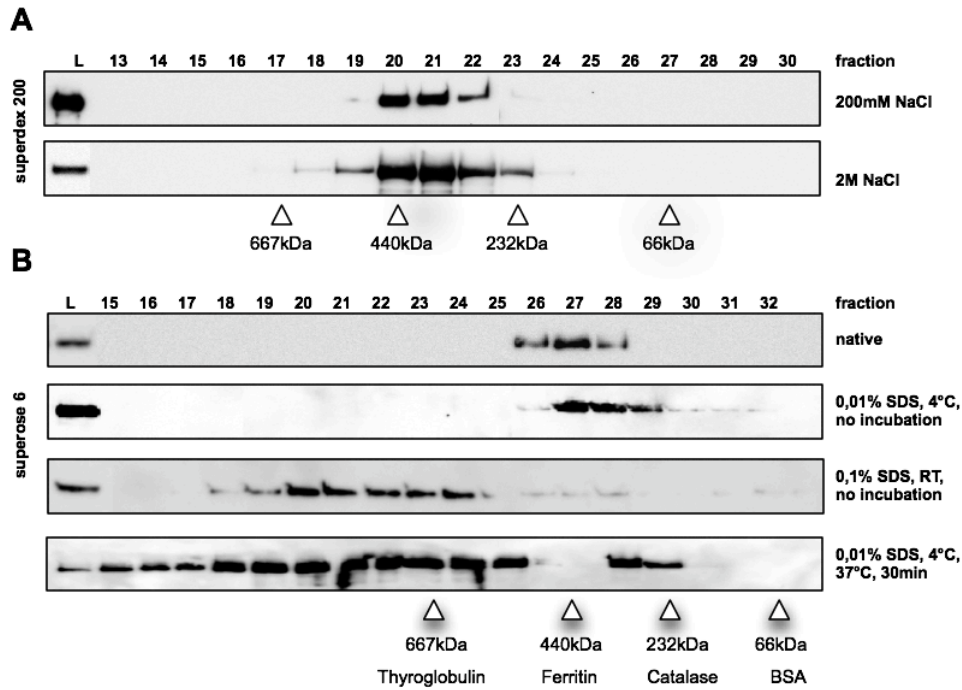
Figure 46 Recombinant Dnmt1 – an apparent dimer

A.) Recombinant Dnmt1 was loaded on a Superdex200 gelfiltration column (GE Healthcare) in running buffer (200mM NaCl/2M NaCl, 20mM Tris, pH 8.0; 1mM $MgCl_2$, 10% glycerol). Upper panel. Dnmt1 in running buffer supplemented with 200mM NaCl. Lower panel. Dnmt1 in running buffer with 2M NaCl. **B.)** Dnmt1 (30µg) was adjusted to the indicated SDS concentration and either incubated for 30min at 37°C or directly loaded on a Superose6 gelfiltration column (GE Healthcare) in running buffer (150mM NaCl, 20mM Tris, pH 7.5; 1mM EDTA, 10% glycerol) supplemented with the indicated concentrations of SDS. For both columns, 500µl fractions were collected, TCA precipitated and subjected to SDS-PAGE and Western Blot analysis (detection with D1-2G3 rat monoclonal antibody; E.1.6). Molecular weight standards and fractions are indicated

To further test this assumption, Dnmt1 was run on a Superose6 gelfiltration column in the presence of 0,01% SDS at 4°C and 0,1% SDS at room temperature. SDS seemed to partially disrupt the Dnmt1 dimer (Figure 46). Higher concentrations of SDS or incubation of the sample at 37°C for 30min prior to loading dramatically enhanced this effect. Not only the dimer peak vanished and Dnmt1 was shifted to fractions of lower molecular weight, but also multimerization could be observed. Tertiary structure and intramolecular interactions were disturbed allowing for intermolecular hydrophobic interactions to occur.

Taken together, these data indicate a Dnmt1 dimer, whose interaction might be mediated by a hydrophobic part of multiple parts of the protein.

C.5.2 Dnmt1 interacts with the TS domain

The human TS domain was expressed as MBP fusion construct and purified as described (E.2.8.7). Dnmt1 was purified from baculovirus infected Sf21 cells (E.2.7.2). Individual proteins together with BSA or Dnmt1 and hTS in a 1:6 molar ratio were incubated for 1h at 30°C and loaded on a gelfiltration column. Immunoblot analysis of collected fractions showed that Dnmt1 eluted in a fraction corresponding to a molecular mass of about 400 kDa (Figure 47, A). This is approximately two-fold the molecular weight of Dnmt1 (183 kDa) indicating the

presence of a dimeric complex. The hTS domain eluted with a distinct peak at about 65 kDa corresponding to a TS dimer and higher molecular weight complexes in the size range above 500 kDA indicating multimerization of the TS domain (Figure 47).

Dnmt1 incubated with hTS showed partial disruption of both Dnmt1 and hTS dimers. Dnmt1 was shifted to higher molecular weight driven by multimerization together with hTS and a downshift of multiple fractions of lower molecular weight suggesting Dnmt1-hTS heterodimers. Signals of Dnmt1 in fractions smaller than its own molecular weight can be explained by an altered structural conformation together with the hTS resulting in a different running behavior. In contrast, the hTS domain showed an altered distribution over the fractions of the column, directly inverse to the observation of Dnmt1. Incubation of TS with Dnmt1 led to a downshift of multimerized TS domains and a peak broadening in the low molecular weight region.

Accordingly, the hTS domain which by itself can form a stable dimer, seems to be the determinant of dimerization of Dnmt1.

In order to further test the interaction properties of Dnmt1 with the TS domain, a co-immunoprecipitation was performed. Dnmt1 was bound to proteinG sepharose coupled with Dnmt1 specific antibody 2E8 (E.1.6) and incubated with an excess of hTS. As indicated in Figure 47 (B), Dnmt1 is able to interact with and precipitate the TS domain.

In a recent publication, K. Fellinger (Fellinger et al. 2009) provides evidence by means of biochemical characterization that Dnmt1 forms a stable dimer. The parallel orientation of the Dnmt1 dimer is mediated by the interaction of the TS domain.
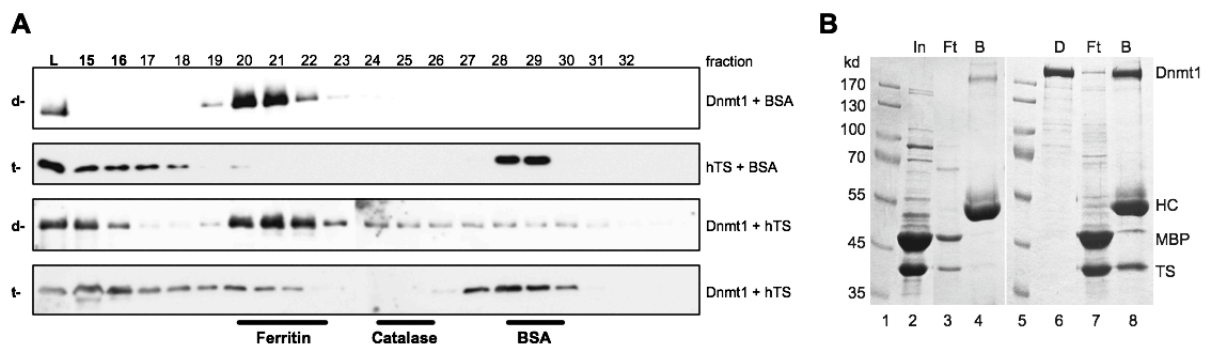
Figure 47 Dnmt1 interacts with hTS domain – gelfiltration analysis

A.) Molecular interactions between Dnmt1 and the TS domain were analyzed by gelfiltration on a Superdex200 column in 20mM Tris, pH 7.5, 150mM NaCl, 1mM EDTA, 1mM DTT. Dnmt1 and the TS domain were analyzed after mixing both proteins for 1 h at 30°C in a 1:6 ratio. For reference, individual proteins were incubated together with BSA. The proteins were visualized by Western blot with the 2C1 rat monoclonal antibody recognizing both, Dnmt1 and the TS domain (E.2.8.7, E.2.7.2). The proteins (Dnmt1 : d and hTS : t) and the migration of the size standards are indicated. **B.)** Dnmt1 co-immunoprecipitates the TS domain. MBP-TS was cleaved with TEV Protease (lane 2) and incubated with the Dnmt1 specific antibody 2E8 coupled to proteinG beads. 2% of the flowthrough and 50% of the beads were loaded (lanes 3 and 4). Recombinant Dnmt1 (lane 6) was incubated with a 50 fold excess of the hTS domain for 1h at 30°C. The reaction was incubated with the 2E8 antibody coupled to beads and 10% of the flowthrough and 50% of the beads were loaded on a 6% SDS-PAGE (lane 7 and 8). Proteins were stained with Coomassie Blue and the position of Dnmt1, the antibody heavy chain (HC), the Maltose Binding Protein (MBP) and the human TS domain are indicated

C.6 Phosphokanamycin – inhibitor of Swi/Snf remodeling enzymes

Chromatin remodeling complexes are implicated as positive and negative regulators of transcription, replication and repair (Schnitzler 2008).

Due to their ability to read out DNA sequence/structure elements that direct nucleosome positioning (Rippe et al. 2007a), they might provide for an additional mechanism that defines the chromatin structure of the genome.

Phosphokanamycin (PK) was described as a specific inhibitor of the Swi/Snf remodeling complex (Muthuswami et al. 2000). ATP- dependent changes of nucleosome positions can be assessed in *in vitro* nuclesome sliding reactions as initially established by Längst (Langst et al. 1999). PK was shown to inhibit the remodeling machines ACF and Mi2 (Langst et al. 1999; Brehm et al. 2000) as well as the activity of Snf2H and the chromatin remodeling complex NoRC in a dose dependent manner (Santoro et al. 2002; Strohner et al. 2004a)(Felle et al., manuscript in preparation), whereas kanamycinA did not affect nucleosome remodeling.

C.6.1   PK does not globally inhibit ATPases or affect the integrity of chromatin

In order to exclude a global inhibitory effect of PK, the ATPase activities of chromatin assembly (E.2.10.1) and murine transcription extracts (Langst et al. 1997) were monitored in the presence of 500µM of PK or kanamycin A respectively (Figure 48, A). The rate of ATP hydrolysis was followed by an enzymatic assay that couples ATP hydrolysis to NADH synthesis (Lindsley 2001)(E.2.11.5). No obvious differences in ATP hydrolysis rates were observed with PK compared to kanamycinA or Mock control, indicating that PK selectively inhibits ATPases that belong to the Snf2 family and does not globally affect ATPases present in the partially purified extracts.

Notably, a bi-phaseal course of ATP consumption could be observed for both DREX and mouse transcription extract (Figure 48, A). A scenario in which at first the nucleosomes would be loaded onto the DNA and moved to their final positions could account for the higher ATP hydrolysis rate at the onset of the reaction. At later time points, the slower ATP consumption rate could derive from continues interactions of remodeling enzymes and nucleosomes situated at their final positions.

One model system to study chromatin dynamics and molecular mechanisms of gene regulation in chromatin is the *Drosophila* chromatin assembly extract (Becker and Wu 1992). Chromatin reconstitution with this extract results in efficient nucleosome deposition with regular spacing (Figure 48, B). As Phosphokanamycin might affect the chromatin assembly function of the extract by inhibiting the remodeling complexes, PK was included once chromatin assembly was completed. The addition of kanamycinA and PK after 4 hours did not change the chromatin structure of the rDNA minigenes, as revealed by MNase digestion and visualization of the nucleosomal ladder (Figure 48, B).
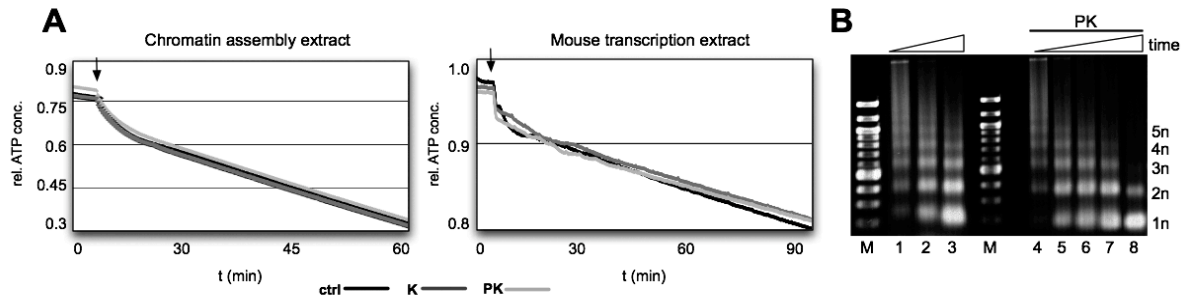
Figure 48 Effect of PK on chromatin assembly and transcription extracts

A.) Measurement of ATP hydrolysis rates in the Drosophila embryo extract and the murine transcription extract. Extracts were incubated with 500µM kanamycin A or PK and the rate of ATP hydrolysis was measured as described in (E.2.11.5). Arrow indicates addition of 0.3mM ATP. **B.)** PK does not impair the integrity of chromatin. MNase digestion of chromatin assembled on plasmid DNA (E.2.10.3). Chromatin reconstituted with the *Drosophila* extract (E.2.10.1) was digested with MNase for 0.5 to 3min (lanes 1-3) or for 0.5 to 6min (lanes 4-8) in the presence of 600 µM PK. The nucleosomal ladder (1n .. 5n) and the DNA marker (M; 1kb ladder) are indicated.

C.7 Dnmt1 antibody epitope mapping

A classical approach in the purification of nuclear multi protein complexes comprises the preparation of nuclear extracts of high protein concentration and subsequent multiple column purifications using matrices with different chemical characteristics that eventually enrich one's POI together with interacting proteins while depleting protein contaminations.

The composition of purified protein complexes and the identity of the proteins can then be analyzed with the MALDI technique (Matrix assisted laser desorption/ionization).

Another method that facilitates this often laborious process is the use of antibodies that specifically immunoprecipitate one's POI out of a complex protein mixture. This technique can be applied either on cell lysate, nuclear extracts or protein samples that had already been purified with one or two column purification steps.

In order to ease SDS PAGE based protein identification or to perform *in vitro* activity assays, the aim is to release one's POI from the antibody by competition with peptides that correspond to the epitope the target protein.

In the course of this study, the epitopes for four rat monoclonal antibodies directed against full length Dnmt1 (2C1, 2G3, 2E8, 2G3; E.1.6) was mapped and peptide elution of antibody bound Dnmt1 performed.

C.7.1 Antibody domain mapping

For a rough survey which domains of Dnmt1 are recognized by the individual antibodies, six different domains were expressed in bacteria and subjected to Western Blot analysis (E.2.3.3) using the respective antibodies.
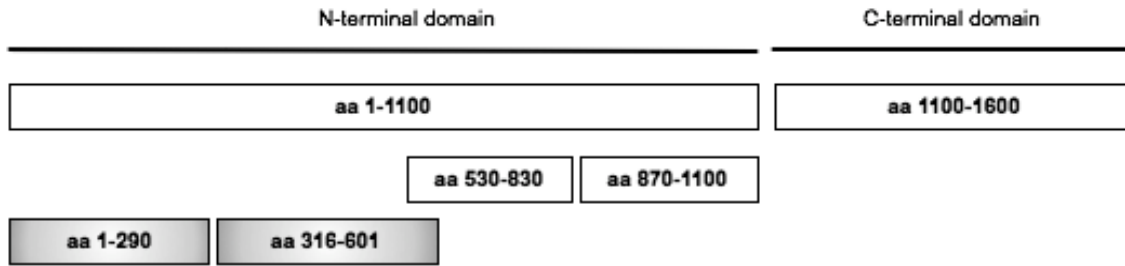
Figure 49 Protein domains of Dnmt1 for antibody mapping

Schematic overview of the Dnmt1 domains used. N-terminal and C-terminal (catalytic domain) domain are indicated. White colored domains were cloned into pRSETa expression vector (Invitrogen), grey colored domains were expressed as MBP fusion proteins (E.2.8.7).

According to Western Blot analysis, the epitope for the Dnmt1 antibodies 2C1 and 2C12 lies within the TS domain (aa 316-601) and for the antibodies 2E8 and 2G3 within the first 290 amino acids of Dnmt1.
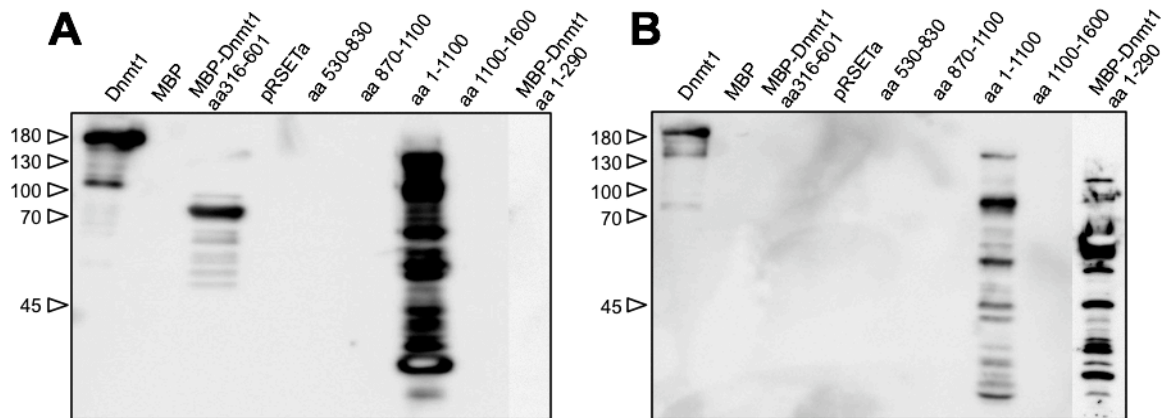
Figure 50 Western Blot analysis and immunodetection of Dnmt1 domains

Dnmt1 domains cloned into pRSETa vector were transformed into Bl21 E. coli cells and protein expression induced. Cells were lysed in Laemmli buffer and boiled at 95°C for 10min. MBP-Dnmt1 aa 1-290 was handled as the other domains, whereas MBP-Dnmt1 aa 316-601 was purified via amylose resin (E.2.8.7). Recombinant human Dnmt1 was purified as described (E.2.7.2). All samples were resolved on a 15% SDS-PAGE, subjected to Western Blot following immunodetection. A.) Immunodetection with 2C1 antibody (2C12 shows the same result; not shown). B.) Immunodetection with 2E8 antibody (2G3 is the same, not shown).

C.7.2   Epitope mapping of anti-Dnmt1 2C1 and 2C12

The exact epitope that is recognized by the antibodies 2C1 and 2C12 was mapped applying a limited proteolysis approach with V8 serine protease from *Staphylococcus aureus* (E.2.12.3). The purified native MBP-hTS C-Flag (E.2.8.7) was digested with V8 protease which cleaves after glutamyl residues. Only accessible sites that lie in the linker regions between protected protein domains are cleaved. Western Blot analysis following comparison of immunodetected (anti-Flag antibody serves as control) cleavage products allows a rough estimation of the epitope region.
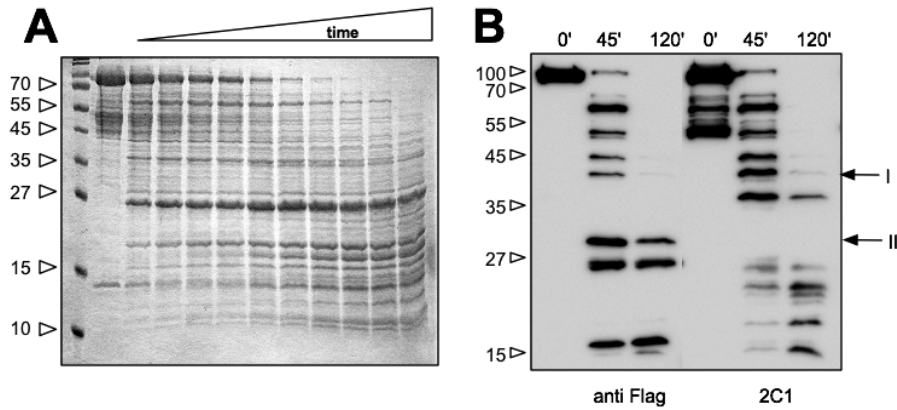
Figure 51 Limited proteolysis of MBP-hTS C-Flag and immunodetection

A.) Limited proteolysis of MBP-hTS C-Flag with V8 protease in a 200:1 molar ratio in 100mM Tris pH 7.8, 0,2% SDS. The reaction mixture was incubated at 37°C. Samples were withdrawn at different time points (0, 5', 10', 15', 20', 30', 45', 60', 75', 90', 120'), boiled in Laemmli buffer at 95°C and subjected to SDS PAGE (15%). **B.)** Samples from 0', 45' and 120' time points were further analyzed by Western Blot and immunodetection with anti Flag (4H3, 1:2000) and anti Dnmt1 2C1 and 2C12 (1:20; result for 2C12 not shown since the same). Position I denotes fragment that is recognized by both 2C1 and Flag antibody whereas cleavage fragment at position II is not detected by 2C1 suggesting that the epitope of 2C1 lies between the last 30-35kDa corresponding to roughly 60-70 aa, thus aa 316-376/386 of hDnmt1.

The epitope region for 2C1 and 2C12 (aa 316- 376/ 386 of hDnmt1) was further narrowed by expression of MBP fusion proteins with 14 amino acids with 7 amino acids overlap and again Western Blot analysis. The epitope recognized best in immunodection corresponds to aa 316-330 (DEDEKEEKRRKTTP).

Limited proteolysis of the MBP-Dnmt1 aa 1-290 construct could not be performed since its purification failed.

Figure 52 Epitope fine mapping of anti Dnmt1 2C1 antibody

MBP fusion proteins with 14aa of Dnmt1 starting at position aa 316 (with a 7aa overlap) were expressed in E. coli as described for MBP-hTS (E.2.8.7). Induced cells were lysed in SDS sample buffer and boiled at 95°C for 10min. Samples were immunodetected with antibody 2C1 after SDS PAGE on a 15% gel and Western Blot. The result for antibody 2C12 is not shown since it recognizes the same epitope.
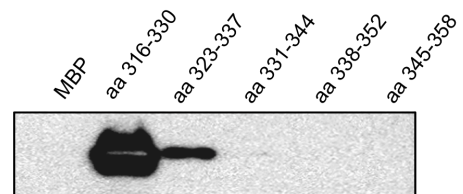
The following peptides were ordered and dissolved in 50mM Tris pH 7.5, 150mM NaCl at concentrations of 5-10mg/ml (P1:DEDEKEE, P2:KRRKTTP, P3: DEKEEKRRK, P4: KDEDEKEEKRRKTT). Peptide release of immunoprecipitated recombinant hDnmt1 in IP-buffer (50mM Tris pH 7.5, 150mM NaCl, 0,05%) supplemented with 2,5mg/ml peptide failed (data not shown).

As a summary, Dnmt1 specific antibodies 2E8 and 2G3 recognize aa 1-290 and antibodies 2C1 and 2C12 aa 316-330 of hDnmt1 respectively. Only the antibody 2E8 recognizes mouse Dnmt1 (data not shown).

D DISCUSSION

D.1 Dnmt1 interacts with ICBP90 and USP7

In search of new interaction partners of Dnmt1, ICBP90 (also referred to as UHRF1) and USP7 were identified by co-immunoprecipation with Dnmt1 from Hela S3 and human placenta nuclear extracts following MALDI analysis (C.1.1,C.1.2). Gelfiltration chromatography (C.1.3), *in vivo* pull-down experiments (C.1.4) as well as *in vitro* interaction studies with the recombinant proteins or protein domains (C.1.5) revealed a Dnmt1/ICBP90 (Achour et al. 2007; Bostick et al. 2007) and a Dnmt1/USP7 interaction. Furthermore, the data point out that UHRF1 directly interacts with USP7 and that a trimeric complex could exist with USP7 binding to ICBP90 and Dnmt1 with domains 1 (aa1-215) and 3 (aa651-916) respectively. Chromatin immunoprecipitation of these proteins and subsequent qPCR analysis confirmed the observation of different combinations of Dnmt1/ ICBP90/ USP7 occupying four different gene loci *in vivo* (C.1.15).

Furthermore, the RING-type E3 ubiquitin ligase ICBP90 promotes autoubiquitinylation (C.1.6), and ubiquitinylation of histone H3 (Karagianni et al. 2008) (C.1.7) and USP7 (C.1.8) *in vitro.* Notably, binding of either the inactive USP7 C223S or Dnmt1 impaired autoubiquitinylation of ICBP90 *in vitro* (C.1.6) whereas active USP7 prevented autoubiquitinylation by removing ubiquitin moieties from ICBP90 (C.1.10). Although the results are not absolutely conclusive, USP7 might also be involved in regulating the stability of ICBP90 *in vivo* (C.1.12).

USP7 deubiquitinated H2A, H2B and H3 *in vitro* (C.1.10) but knockdown or over-expression of USP7 did not affect global levels of ubiquitinylated H2A and H2B *in vivo* (C.1.14). Binding of ICBP90 and Dnmt1 to USP7 did not influence the *in vitro* activity of USP7 (C.1.9). Moreover, Dnmt1 seemed to be a target for ubiquitinylation by ICBP90 *in vitro* (C.1.8) but was not affected *in vivo* in regard to protein stability (C.1.12) and ubiquitinylation (C.1.13) upon knockdown or over-expression of USP7.

We have purified a new complex consisting of Dnmt1/ICBP90/USP7 but are still lacking knowledge about its biological functions. The aim of this discussion is to address the roles of histone ubiquitinylation/deubiquitination and DNA methylation in epigenetic regulation.

D.1.1 Dnmt1, ICBP90 and USP7 form multiple complexes *in vitro* and *in vivo*

In vivo immunoprecipitation studies as well gelfiltration chromatography point out the existence of different complexes, namely Dnmt1/ICBP90 and Dnmt1/USP7 and possible trimeric complex of Dnmt1, ICBP90 and USP7. Moreover, the data suggest that the interactions are stabilized on chromatin.

In order to test chromatin association of complexes/interactions and recruitment *in vitro, a* biotinylated nucleosomal array could be coupled to streptavidin coated beads following

binding of either Dnmt1, ICBP90 and USP7. Retention of proteins-of-interest either alone or in different combinations could be analyzed. Differences in binding to purified and crude chromatin could account for possible other recruitment or stabilizing factors.

Different nucleosomal substrates could be applied providing for optimal initial binding. A nucleosomal array consisting of hemi- or fully methylated DNA might present a better substrate for ICBP90 (Unoki et al. 2004). Dnmt1 was immobilized on DNA (Schermelleh et al. 2005). Reconstituted nucleosomes with chemically linked ubH2B might target USP7 (McGinty et al. 2008).

In vitro studies (C.1.5) further dissected the interrelation of Dnmt1, ICBP90 and USP7 revealing interaction of all proteins with one another indicating the following dimeric complexes: Dnmt1/ICBP90, Dnmt1/USP7, and ICBP90/USP7 (Figure 53). Interaction of Dnmt1 with ICBP90 and respectively the interaction of the TS domain with the SRA domain confirm published data (Achour et al. 2007). Second, ICBP90 binds via its SRA domain and Dnmt1 binds through its TS domain to domain 1 (TRAF domain, aa1-215) and domain 3 of USP7 (aa561-916) respectively, suggesting a trimeric complex of USP7 simultaneously associating with Dnmt1 and ICBP90 (Figure 53). Third, the *de novo* methyltransferases also precipitated ICBP90 and USP7 but in contrast to Dnmt1 bound preferentially to the TRAF domain of USP7.

Chromatin immunoprecipitations (CHIP) with antibodies directed against Dnmt1, ICBP90, USP7 and RNA polymerase II following the analysis on the occupation of four different loci (C.1.15) are in agreement with the concept of dynamic complexes.

Although the absolute or relative amounts of the protein-of-interests in the cell are difficult to judge, the gelfiltration data (C.1.3) suggest a larger population of Dnmt1/USP7 dimers (compared to ICBP90). ICBP90 as a tightly chromatin associated factor could be the recruitment factor of Dnmt1/USP7 to either sites of replication or sites of specific gene regulation (Unoki et al. 2004; Bostick et al. 2007). Different models on how dynamic Dnmt1/ICBP90/USP7 complexes may act are discussed below.
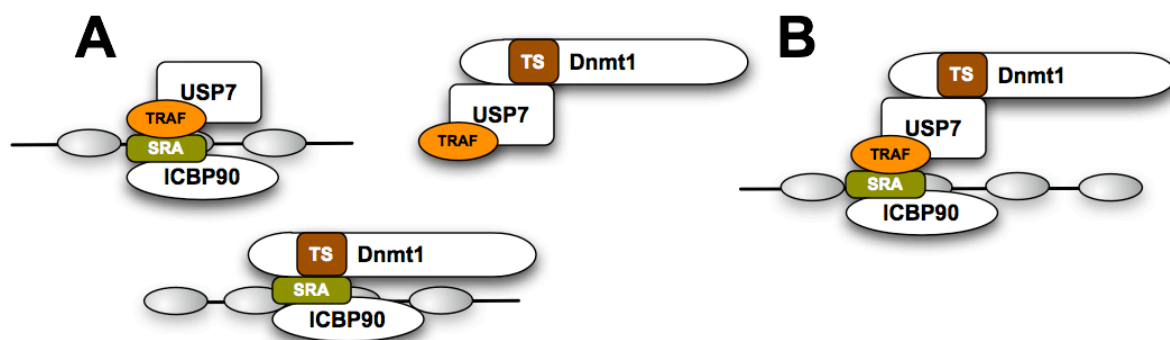
Figure 53 Complex formation of Dnmt1, ICBP90 and USP7

Possible complex formations as deduced from *in vitro* and *in vivo* studies (C.1.5). **A.)** Dimeric complexes, namely ICBP90/USP7, Dnmt1/USP7, Dnmt1/ICBP90. ICBP90 containing complexes are chromatin associated **B.)** Possible trimeric complex of Dnmt1/ICBP90/USP7. TRAF domain (TNF associated factor, orange, aa1-215), SRA domain (SET and RING finger associated, green, aa 409-616), hTS domain (Targeting domain, brown, aa316-601).

In one model, ICBP90 is bound to a promoter or a genomic region through interaction with a specific sequence or methylated CpG sites. ICBP90 would promote its own and/or histone H3 ubiquitinylation (C.1.7). The Dnmt1/USP7 complex would be targeted by ICBP90 to direct DNA methylation and deubiquitination of ubiquitinylated ICBP90 and ubH3 by USP7 (C.1.10).

USP7 may change the enzymatic properties of Dnmt1. Therefore, Dnmt1 would be inactive in a Dnmt1/USP7 complex until recruited to a specific target site. This potential function could easily be tested *in vitro.* As long as USP7 is engaged with removing ubiquitin moieties from H3, possible inhibition could be relieved and Dnmt1 could act together with ICBP90 in DNA methylation. Interestingly, so far it has not been shown whether ICBP90 is able to directly stimulate Dnmt1's activity towards DNA or nucleosomes. Therefore, besides a recruitment factor, ICBP90 could also act as an activator of DNA methylation.

In a second model, ubH3 could be the targeting signal for USP7 delivering Dnmt1 for ICBP90 mediated DNA methylation. Whether ICBP90 or ubH3 is the major target for USP7 could be tested on *in vitro* ubiquitinylated nucleosomal arrays. Inactive ICBP90∆RING associated with the array would not promote H3 ubiquitinylation (C.1.6) but could recruit USP7 as the SRA domain was shown to be the interacting domain of ICBP90 (C.1.5).

Considering the bulky ubiquitin moieties on histones H3, DNA methylation could take place in a more open chromatin structure. Ubiquitin from H3 would be removed by USP7 leading to possible chromatin rearrangements that could limit DNA methylation.

It is unclear whether Dnmt1, ICBP90 and USP7 would stay associated as a trimeric complex or as a Dnmt1/ICBP90 dimer and free USP7.

Both Dnmt1 and ICBP90 could maintain in cooperation with other factors a repressive chromatin state. Notably, ICBP90's ubiquitinylation activity was reduced upon binding of Dnmt1 (C.1.6), hence new H3 ubiquitinylation could be impaired. Moreover, a trimeric complex could also be stably associated within a heterochromatin environment. DNA methylation would be maintained and the activity of ICBP90 controlled by USP7 (C.1.6; C.1.10).

D.1.1.1   USP7 is absent from the *WNT1* gene locus

Dnmt1 and ICBP90 were present at the *Wnt1* locus (C.1.15) that had previously been described to be silenced in dependency of the H3K27me3 HMT EZH2 of PRC2 and Dnmt1 mediated DNA methylation (Viré et al. 2005). Dnmt1 was absent from the *Wnt1* locus upon knockdown of EZH2. It is well conceivable that ICBP90 is targeted by H3K27me3 in analogous fashion to H3K9me3 (Karagianni et al. 2008), directly by EZH2 or by a methylated CpG mark as mentioned above. The first notion could be tested with a peptide binding assay on H3K27me3 tails, the second with *in vitro* interactions studies and the last one with knockdown of the *de novo* DNA methyltransferases following CHIP. Dnmt/USP7 could be recruited either through ICBP90 or ubH3. Upon 'delivery' of Dnmt1 USP7 would remove ubH3 and dissociate whereas Dnmt1 interacting with EZH2 and ICBP90 would stay at the *Wnt1* locus.
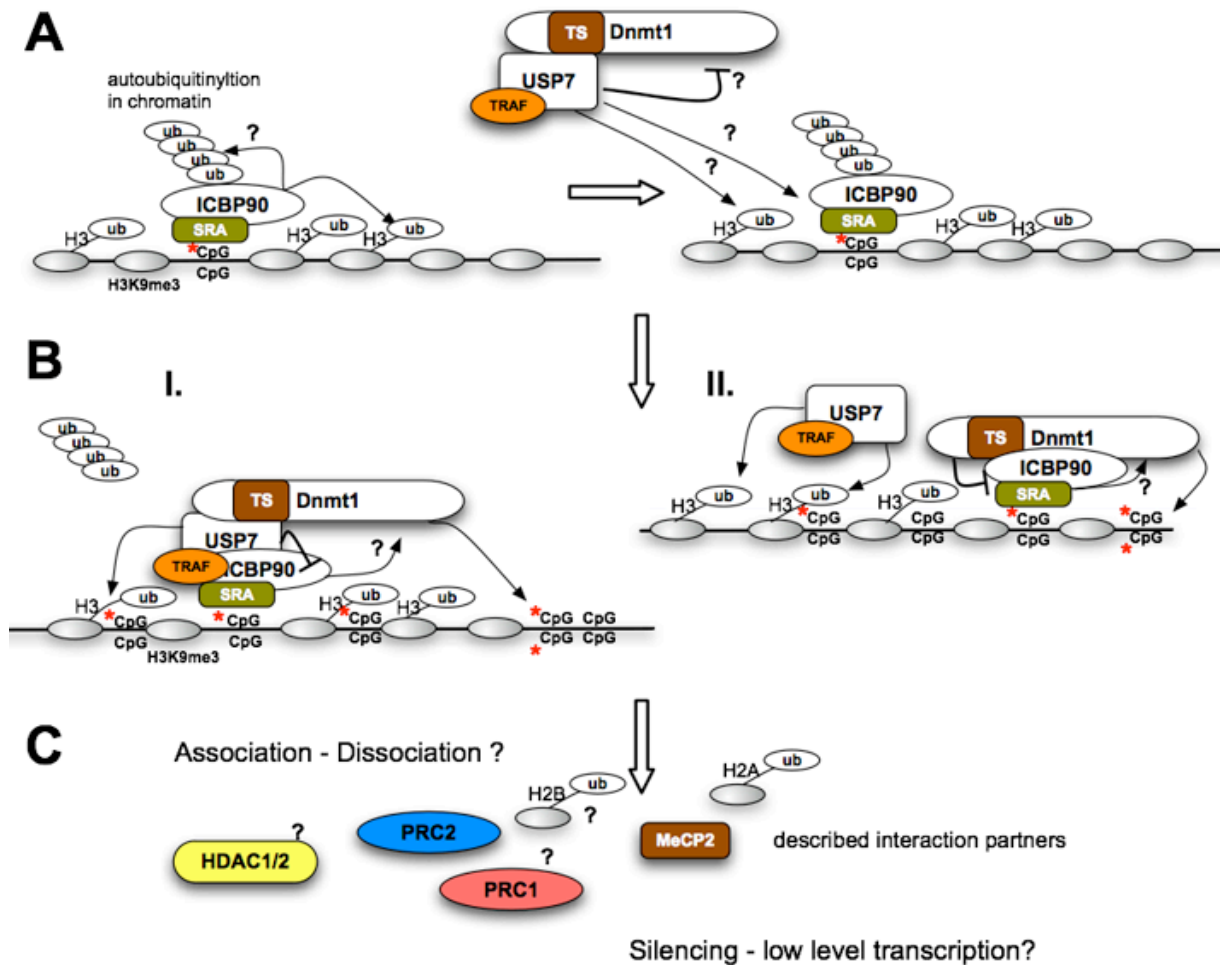
Figure 54 Possible mechanisms in transcriptional regulation

Possible mechanism on how Dnmt1, ICBP90 and USP7 could function in gene silencing. **A.)** ICBP90 binding to hemi-methylated DNA (red *) or H3K9me3 ubiquitinylates itself and histone H3. USP7 might inhibit Dnmt1's activity. The Dnmt1/USP7 complex might be recruited either by ICBP90 or ubH3. **B-I.)** USP7 might bind to ICBP90 forming a possible trimeric complex. USP7/Dnmt1 impair ubiquitinylation activity of ICBP90. USP7 removes ubiquitin from ubH3 and ICBP90. ICBP90 might stimulate Dnmt1 for DNA methylation. **B-II.)** USP7 delivers Dnmt1 which interacts with ICP90 (TS-SRA binding). Relieve of possible inhibition of Dnmt1 and stimulation of DNA methylation activity by ICBP90. USP7 removes ubiquitin from H3 and ICBP90. **C.)** Depending on the genomic context, the association of different factors (HDACs, PcG complexes. MeCP2) or the presence of ubiquitinylated H2A/H2, USP7 might stay associated or dissociate.

D.1.1.2   Dnmt1, ICBP90 and USP7 form a trimeric complex at the *IGFBP3* gene

Dnmt1, ICBP90 and USP7 occupied the *IGFBP3* gene promoter in CHIP analysis (C.1.15), an observation that could be explained with the above-mentioned model. Interestingly, *IGFBP3* was found to be mostly hyper-methylated in lung cancer cells (Chang et al. 2004) concomitant with association of HDAC and MeCP2. Both, Dnmt1 and ICBP90 interact with HDAC1 in gene regulation (Robertson et al. 2000a; Unoki and Nakamura 2003) and Dnmt1 with MeCP2 (Kimura and Shiota 2003). Therefore, the occupancy of Dnmt1 and ICBP90 at the *IGFBP3* gene agrees with this observation. Additionally, association of HDAC1/2 could be tested in CHIP.

The possible regulatory mechanism that could account for the *IGFBP3* gene is difficult to decipher *in vivo*. Albeit knockdown of USP7 is efficient, it is not complete and thus (C.1.12) residual Dnmt1/USP7 complexes could be recruited. In order to verify USP7's role as a targeting and inhibitory factor *in vivo* total ablation of USP7 in knockout cells could prove this assumption. Over-expression of USP7 could lead to competition of free USP7 and Dnmt1/USP7 complexes. Hence, H3 deubiquitination without concomitant Dnmt1 mediated methylation could occur which should be seen in reactivation of gene expression and at least partial demethylation.

Such a recruitment competition could also be analyzed using a biotinylated nucleosomal array system. Although this would be a sophisticated experimental setup, the biotinylated array system could be used to address the question of interrelation of DNA methylation and H3 deubiquitination.

D.1.1.3 Dnmt1/ICBP90/USP7 might be involved in 'bivalent' gene regulation

As for the *IGFBP3* gene, the three proteins also occupied the *HoxA7* gene (C.1.15). This gene was shown to be silenced by the action of both Polycomb repressive complexes PRC1 and PRC2 as well as Dnmt1 (Wu et al. 2008). Association of ICBP90 could occur in a similar fashion as just outlined for the *Wnt1* gene or ICBP90 could be recruited by some other unidentified transcriptional repressor. Dnmt1/USP7 would be recruited and function as pointed out before, with the exception that USP7 would stay associated either with Dnmt1/ICBP90 or components of the PRC1 complex. USP7 associated with the Polycomb protein (dPRC1) on the *Ubx* PRE in *Drosophila* (van der Knaap et al. 2005).

Ubiquitinylated H2A plays a role in gene silencing as knockdown of RING E3s resulted in re-expression of a number of *Hox genes* in both flies and human (Wang et al. 2004a; Cao et al. 2005). Therefore, on the first glance it seems rather unlikely that USP7 would deubiquitinate H2A.

In contrast, *Hox* genes were found in clusters of highly conserved non-coding elements (HCNE) that constitute 'bivalent domains' in ES cells (Bernstein et al. 2006). 'Bivalent domains' combine both large regions of repressive (H3K27me3) and smaller regions of activating (H3K4me3) modifications. These domains tend to coincide with genes expressed at low levels and assembled RNAP II – S5P–CTD indicative of transcription initiation competent. Conditional deletion of RING1A/B led to sequential loss of ubH2A, release of poised RNAPII and subsequent gene de-repression (Stock et al. 2007).

Importantly, also *HoxA7* was found to be controlled by such a bivalent promoter mechanism (Stock et al. 2007). Unphosphorylated RNA Polymerase II (antibody 8GW16 (Thompson et al. 1989; Xie et al. 2006)) was not bound to the *HoxA7* locus which is in agreement with the CHIP data from HCT-116 cells (C.1.15). Accordingly, besides Dnmt1 'delivery' and controlling ICBP90 and H3 deubiquitination, USP7 could possibly remove ubiquitin from H2A in a PcG regulated environment and thus contribute to low-level transcription.

Considering this function, over-expression and knockdown of USP7 would lead to reduced and increased ubH2A levels respectively concomitant with elevated and decreased gene expression. It is important to note that 'bivalent domains' are replaced by either active or

repressive gene configurations in differentiated cells (Bernstein et al. 2006). Therefore, although very attractive, the question remains whether USP7 functions as a H2A deubiquitinase in differentiated HCT-116 cells.

Another scenario also considering a bivalent regulation strategy would take up the idea of ubiquitinylated H2B (A.2.3.2). USP7 could help to maintain a transcriptionally 'low-active' chromatin state or assist in gene repression by constantly removing the activating ubiquitin moiety from H2B. Considering this idea, USP7's function would not be restricted to homeotic gene regulation but affect gene regulation in general or in response to cell signaling due to extracellular stimuli, stress response or cell damage.

However, a different observation was made in *Drosophila* that pointed towards a specific role in homeotic gene regulation. Global H3K27me3 levels were strongly reduced upon knockdown of USP7 whereas global ubH2B levels were not affected ((van der Knaap et al. 2005), unpublished data; C.1.14). Importantly, the histone demethylase UTX associates with promoters of *Hox* gene clusters and interacts with the HMT MLL2/3 during retinoic acid signaling, resulting in H3K27 demethylation and H3K4 methylation respectively (Lee et al. 2007b). An increase of ubH2B would induce a chromatin environment prone to active transcription concomitant with H3K27 demethylation.

As speculated for ubH2A, USP7 could assume additional functions dependent on the gene context and other transcription/repressive factors associated besides regulation of Dnmt1/ICBP90 activity.

D.1.1.4   Dnmt1 remains inactive at the *POLR2A* gene

USP7 and Dnmt1, but not ICBP90 were associated with the actively transcribed *POLR2A* gene. As depicted before, USP7 could inhibit the enzymatic activity of Dnmt1 - an idea that we will address in the future. Furthermore, ICBP90 as a possible activator of Dnmt1 is absent from the *POLR2A* promoter resulting in impaired DNA methylation. The association of Dnmt1/USP7 further suggests that there are other targeting mechanisms besides ICBP90. Therefore, targeting of Dnmt1/USP7 could be mediated by either an unknown factor or possibly even ubiquitinylated H2B. USP7 could act like USP21, being involved in the gene transactivation processes that require multiple rounds of histone H2B ubiquitinylation and H2B deubiquitination (A.2.3.2) or gene repression.

D.1.2   USP7 could be involved in mammalian development

The associations of USP7 with DNA methyltransferases and UHRF1 point towards a role in epigenetic regulation. Moreover, USP7 is essential in *Drosophila* and mutations enhance defects of Polycomb mutations (van der Knaap et al. 2005). Since USP7 interacts with UHRF1 and Dnmt1 but as well with Dnmt3a and Dnmt3b (C.1.5), it would be interesting to unravel the role of USP7 during mammalian development especially in regard to DNA methylation.

With conditional knockout mice, the effect of USP7 on imprinting and methylation of repetitive elements during gametogenesis could be monitored. The effect of USP7 knockout on DNA

methylation could also be analyzed in ES cells. The localization of USP7 to certain genomic regions in a Dnmt double-knockout (DKO; Dnmt3a/b(-/-)) or triple-knockout background (TKO, Dnmt1, 3ab (-/-)) could be studied to answer whether Dnmts represent major recruitment factors for USP7 to heterochromatic regions. Importantly, studies on the cellular localization of all three proteins have not been performed yet but would give intriguing answers on the possible function.

Moreover, although DNA methylation is absent from *Drosophila*, USP7 localized to silenced homeotic gene clusters and CHIP analysis demonstrated occupancy of USP7 and Polycomb (PRC1 component) at the *ubx* PRE (van der Knaap et al. 2005). All three proteins were bound at the *HoxA7* locus (C.1.15) and Dnmt1 had been shown to interact with components of PRC1 and PRC2 complexes (Viré et al. 2005; Negishi et al. 2007; Wu et al. 2008) indicating a function in a PcG dependent context.

Thus, direct interaction of USP7 with prominent factors of PcG and analysis on the co-localization with *Hox* gene clusters either with FISH or PcG proteins could shed light into this particular aspect of USP7 *in vivo* function.

D.1.3   USP7 could regulate the stability of ICBP90

ICBP90 and USP7 are endowed with two antagonistic enzymatic activities (A.2.2, A.2.4) that suggest reciprocal regulation (D.1).

Dnmt1 is recruited to sites of hemi-methylated DNA by ICBP90 (Bostick et al. 2007; Sharif et al. 2007). The expression of ICBP90 peaks during G_1/S-phase transition and is down-regulated during G_0 and G_1 (Fujimori et al. 1998; Hopfner et al. 2000), although it is expressed at slightly elevated levels throughout the cell cycle in cancer cells . As seen *in vitro* (C.1.10), USP7 could prevent the poly-ubiquitinylation of ICBP90 and possibly of Dnmt1 during S-phase by constantly removing ubiquitin moieties. After replication, USP7's activity could be impaired by several means such as posttranslational modification {(Fernández-Montalván et al. 2007)}, binding of an inhibitor protein or exclusion from the nucleus (Zapata et al. 2001), eventually leading to degradation of ICBP90. Subsequently, Dnmt1 would dissociate from ICBP90 consistent with its diffuse localization in the nucleoplasm during G_1 and G_0 (Leonhardt et al. 1992).

The *in vivo* studies on ICBP90 protein levels and ubiquitinylation status upon knockdown and over-expression of USP7 were difficult to interpret (C.1.12, C.1.13), firstly due to the fact that MG132 - a potent proteasome inhibitor – was not added prior to cell harvest and thus ubiquitinylated species were not properly accumulated. Secondly, ubiquitinylated species do only account for a subpopulation of the target protein, making purification of sufficient amounts with the dsk2p ubiquitin binding protein a bold venture.

A probably better method for investigation of the reciprocal activities of ICBP90 and USP7 *in vivo* are transfection experiments that should be performed with HA-tagged ubiquitin (Treier et al. 1994) and the two POIs expressed with different tags. Flag-ICBP90 could be immunoprecipitated from WCEs and the effect of USP7 or its inactive site mutant USP7 C223S on deubiquitination detected with an anti HA-antibody. Vice versa, the ubiquitinylation status of USP7 C223S could be monitored when either co-transfecting with ICBP90 or the

inactive ICBP90ΔRING. The ubiquitinylation/deubiquitination of Dnmt1 by ICBP90 and USP7 could be revised as well. For optimal results, transfection efficiency must be close to 100% which can be visually checked with fluorescence microscopy or when the gene of interest precedes an internal ribosome entry site (IRES) and a *GFP* gene. Alternatively, transfected cells could be sorted with FACS. In order to express the two effector proteins in equal amounts, an expression vector with a bidirectional promoter should be used.

The method of 'pulse-chase' with ^{35}S-labeled methionine could also be applied to examine protein stability. Cells deprived of methionine are treated with medium containing radioactive methionine ('pulse'). After incubation for 30-40min, the medium is removed, fresh medium added and cells harvested at given timepoints ('chase'). WCE are prepared and proteins subjected to SDS-PAGE following radiography. The decline of radioactively labeled proteins is a degree for the half-life thus stability of the protein. When comparing cells either transfected with USP7 or USP7 C223S, the effect on the protein stability of tagged-ICBP90 could be monitored. In order to circumvent p53 dependent G_1 arrest upon over-expression of USP7, it would be advisable to work with HCT-116 p53 (-/-) cells.

If ubiquitinylated H3 represents a binding platform for other factors or affects chromatin structure or formation especially during replication, loss of ubH3 could result in possible severe effects that could be visible in immunocytochemistry. By use of a knock-down-knock-in system (Hölzel et al. 2007), the endogenous ICBP90 could be down-regulated and replaced by the inactive ICBP90ΔRING (or a point mutation in the RING domain). Besides localization and possible effects on genomic stability or cell cycle, inactive ICBP90 could be purified (by Flag-tag) and associated histones analyzed for ubiquitinylated H3. Furthermore, changes on global ubH3 levels could be analyzed by Western Blot for acidic extracted histones.

D.1.4   Is USP7 involved in silencing of telomeres and rDNA genes?

As summarized in the introduction, ubiquitinylated H2A is generally associated with gene silencing and ubiquitinylated H2B with gene activation (A.2.3.1; A.2.3.2) (Osley 2006; Shilatifard 2006). In *S. cerevisiae,* Ubp10 was found to deubiquitinate H2B at telomers thus providing for an environment devoid of histone marks associated with active genes and allowing for Sir4 spreading and silencing (Emre et al. 2005; Gardner et al. 2005). In addition, a function in silencing of genes that are not in the vicinity of heterochromatin was found. Although not investigated in detail, Utp10 was also enriched at the rDNA locus which is silenced in dependency of Sir2 (Rusche et al. 2003) and Utp10-knockout increased H3K4me3 in these regions (Emre et al. 2005). Recently, the importance of DNA methylation of subtelomeric regions for telomere length and telomere recombination was demonstrated (Gonzalo et al. 2006; Benetti et al. 2007). In human cells lacking Dnmt1 but not Dnmt3b, a decrease in DNA methylation and an increase in H4K16ac at the rDNA genes could be observed (Espada et al. 2007) concomitant with the absence of SirT1 (the homolog of yeast Sir2) from the rDNA.

From these observations, one could outline a function of USP7 related to Ubp10 in *S. cerevisiae.* In this scenario, not USP7 but Dnmt1 would be recruited, hence in Dnmt1

knockout cells, USP7 would no longer be targeted to the rDNA genes following increasing levels of ubH2B. Ubiquitinylated H2B in turn would affect increase of H3K4me3 and H3K79me3 that counteract SirT1 binding and spreading.

Localization of USP7 to telomeric regions and rDNA repeats on acrocentric chromosomes (Henderson et al. 1972) in combination with FISH should give an idea of this possible function. Chromatin immunoprecipitation would be another method to prove occupancy at these genomic regions. In order to elucidate the functional importance in silencing and nucleolar and telomeric stability together with SirT1, knockdown of USP7 might affect SirT1 recruitment and spreading, although it is not known whether DNA methylation and other heterochromatic marks are sufficient to maintain the heterochromatic state. Disruption of telomeric and nucleolar structures would not be visible. Local analysis of alterations of histone modifications and occupancies of factors with chromatin immunoprecipitation would probably display a more detailed picture and could probably unravel less severe effects of USP7 ablation.

D.1.5   USP7 – the next steps

Considering the above-mentioned data and the interaction of USP7 with Dnmt1 and ICBP90, both being heterochromatin associated factors, it is intriguing to analyze the role of factor recruitment, regulation of enzymatic activity and thus regulation of transcription.

The order of factor binding to DNA/nucleosomal templates as well as the effect on DNA methylation, H3 ubiquitinylation/deubiquitination by ICBP90 and USP7 could be verified *in vitro* on reconstituted biotinylated DNA.

The question of protein ubiquitinylation/deubiquitination could be revised and possible consequences on enzymatic activity tested, especially in regard to DNA methylation. Above all, the notion of a possible inhibitory effect of USP7 and a stimulatory effect of ICBP90 towards Dnmt1 mediated DNA methylation should be answered. In regard, a Dnmt1/ICBP90/USP7 complex could be reconstituted *in vitro* and the activity analyzed. The intriguing role of ubH3 could be addressed with the knock-down-knock-in system, replacing active ICBP90 by its inactive counterpart.

In order to reveal the function of USP7 in silencing, future work should predominately address localization by means of microscopy and chromatin immunoprecipitation.

USP7 was shown to localize to the nucleus via its N-terminal TRAF-domain (Zapata et al. 2001). However, the distribution of USP7 within the nucleus and the localization to specific regions such as telomeres, centromers or other regions of heterochromatin have not been analyzed although they could already be indicative of possible functions. In particular, the localization of USP7 during the cell cycle and the question of its co-localization with Dnmt1 and ICBP90 during S-phase are important clues of functional relevance.

In order to verify a possible co-localization or even interaction with certain factors *in vivo*, analysis by means of chromatin immunoprecipitation would be the method of choice. In regard to the role of ubiquitinylated H2A and H2B in gene silencing, antibodies directed against H2AK119ub1 (Vassilev et al. 1995) and H2BK120ub1 (Minsky et al. 2008), histone marks for repression (H3K9me3, H3K27me3) or activation (H3K4me3, H3K36me3,

H3K79me3, H4K20me3) and specific proteins associated with certain genomic regions or transcriptional states should be applied. Of particular interest are the changes in occupancy of factors or histone marks at a certain gene loci upon over-expression or knockdown of USP7. Further elucidation of possible mutual regulatory mechanisms, order of factor recruitment or the interdependency of histone marks would require the knockdown/over-expression of co-localizing factors.

D.2 DNA methylation in chromatin

D.2.1 Binding of DNA and nucleosomes by Dnmt3a and Dnmt3b2 *in vitro*

The minimal DNA length that was required for stable binding of the *de novo* DNA methyltransferases in EMSA was found to be >35 bp (C.3.1). In contrast, studies with C-terminal domains of mouse Dnmt3a revealed partial binding to DNA >20bp of size in gelfiltration chromatography (Jia et al. 2007), suggesting that the N-terminal domain might affect protein conformation and thus DNA binding properties. Furthermore, a preference of binding to longer DNA fragments was observed, indicating a mechanism of cooperative binding of the *de novo* DNA methyltransferases. Recently, the C-terminal domains of Dnmt3a and Dnmt3L were found to form nucleoprotein filaments that are in agreement with the notion of cooperative binding (Jurkowska et al. 2008). Albeit the feature of cooperative binding association with DNA was shown to be highly dynamic (C.3.2). This observation may reflect a property of distributive DNA methylation that has been assigned to Dnmt3a and Dnmt3b compared to processive *maintenance* DNA methylation by Dnmt1 (Gowher and Jeltsch 2001; Hermann et al. 2004b).

In accordance with previous data Dnmt3L stimulated the activity of Dnmt3a and Dnmt3b roughly 1.6- and 3.0-fold respectively (Suetake et al. 2004). Dnmt3L could not bind to DNA (C.4.2) confirming previous EMSA data (Suetake et al. 2004), but contrasting results that were obtained by surface plasmon resonance and filter binding assays (Gowher et al. 2005a). In agreement with the observation of filament formation, Dnmt3L enhanced binding of free DNA by Dnmt3a and Dnmt3b2 (C.4.2).

Is there a biological relevance of filament formation on 'naked' DNA, taking into account that DNA is packaged into chromatin *in vivo*? As already outlined in the introduction (A.3.7), the Dnmt3a/Dnmt3L tetrameric complexes that form nucleoprotein filaments (Jia et al. 2007; Jurkowska et al. 2008) could explain the periodical DNA methylation pattern of 8-10bp of maternally imprinted DMRs. This would imply either complete eviction of nucleosomes in the region to be imprinted or a mechanism such as FACT for RNA Polymerase II transcription (LeRoy et al. 1998) that removes or partially disassembles nucleosomes for the 'growth' of the D3a/D3L or possible D3b/D3L filament.

The aspect of filament formation could be addressed *in vitro* with chromatin reconstitution on circular DNA with *Drosophila* embryonic extract (DREX), reflecting dynamic properties of cellular chromatin (E.2.10.1)*.* The Dnmt3a/Dnmt3L dependent removal of nucleosomes could be analyzed with a DNA supercoiling assay revealing the number of nucleosomes present on the DNA. Filament formation could be monitored *in vivo* when either Dnmt3a or Dnmt3L

fused to a DNA binding domain was tethered to a specific site. DNA methylation, endonuclease digestion and indirect endlabeling experiments could reveal potential spreading of Dnmt3a/Dnmt3L tetramers.

Although the interaction of the *de novo* DNA methyltransferases with free DNA might function similarly, different nucleosomal matrices with different lengths of linker DNA and linker DNA on either one or both sides demonstrated differences in the binding behavior of Dnmt3a and Dnmt3b2 (C.3.3).

Except for preferential binding to the 77WID77 nucleosome, Dnmt3a generally bound to mono-nucleosomal substrates and DNA equally well (C.3.3). Studies on the 5S rDNA fragment (208bp) revealed a similar behavior for Dnmt3a with comparable effects on 'naked' DNA and mono-nucleosomes (Robertson et al. 2004). Although examined in individual EMSA reactions rather than in an internally controlled mixture, DNA and nucleosomal templates (MMTV-A145/242bp, 5S rDNA 155/220bp) were all shifted with equal amounts of Dnmt3a, indicating no preference for either substrate.

Dnmt3b2 behaved differently in a way that free DNA and nucleosomes with longer DNA linkers were preferred over mono-nucleosomes with shorter linker DNA. These observations point out that DNA is the preferred substrate by Dnmt3b2. In accordance, EMSAs with Dnmt3b together with different DNAs and a mixture of nucleosomal templates revealed preferential binding to nucleosomes with linker DNA compared to nucleosomes without linker DNA (Takeshima et al. 2006). Moreover, the PWWP domain of Dnmt3b showed higher DNA binding affinities than the one of Dnmt3a (Chen et al. 2004) reflecting different binding characteristics.

Considering the difference of binding between symmetric and asymmetric nucleosomes, one could imagine two possible modes of binding. Either two linker DNAs provide double the amount of binding sites and possibly binding of one strand by Dnmt3 somehow facilitates binding of another Dnmt3 protein to the second linker DNA or the DNA at the entry/exist site of the nucleosome, forming a cruciform-like structure, is preferentially bound. With the latter mechanism and the difference of DNA affinity exhibited by the PWWP domain of Dnmt3a and Dnmt3b, the observations could be explained.

With regard to this idea, Dnmt3b2's binding affinity towards a potential cruciform DNA would be comparable to that of the PWWP domain towards free DNA whereas for Dnmt3a the latter would be lower. Hence, symmetric mono-nucleosomes with long linker DNA and free DNA would represent comparable binding substrates for Dnmt3b2. In contrast, Dnmt3a would rather bind to mono-nucleosomes with long linker DNA than to DNA. When comparing binding properties of Dnmt3b2 towards 'naked' DNA and asymmetric nucleosomes without potential cruciform structure, the amount of free DNA available for binding would become the key determinant. In contrast Dnmt3a's DNA binding affinity is lower, thus free DNA and asymmetric mono-nucleosomes would be shifted comparably well in EMSA.

The potential binding of Dnm3a and Dnmt3b2 to cruciform structures could be tested with *in vitro* formed cruciform DNAs that could be verified with antibodies directed against cruciform structures or cruciform binding proteins. Moreover, the DNA length for optimal binding to a nucleosomal cruciform could be analyzed. Linker histone H1, located at the entry/exit sites of the nucleosome (Woodcock et al. 2006), was shown to inhibit DNA methylation of di-

nucleosomes by Dnmt3a (Takeshima et al. 2008). Therefore, potential binding of Dnmt3a and Dnmt3b to the entry/exit sites of nucleosomes could be inhibited by H1.

Another approach to elucidate the binding mechanism of Dnmt3s to nucleosomes would be the determination of the exact binding sites of Dnmt3a and Dnmt3b2 on different nucleosomal templates. Footprint assays could be performed on distinct Dnmt3/nucleosome complexes.

D.2.2 Dnmt3L is stably associated with endogenous nucleosomes

Dnmt3L did not bind to nucleosomal templates in EMSA experiments (C.4.2) despite of stable association during purification from Sf21 cells (C.4.1). Furthermore, EMSAs with nucleosomes assembled with recombinant histones from *E. coli* constituting 100% of non-methylated H3K4 showed the same behavior. Accordingly, the data suggest either an unknown loading factor or a possible set of specific histone modifications to a specific sequence or structure that could serve as a stable binding platform for Dnmt3L. When the *de novo* methyltransferases were incubated with nucleosomal templates and Dnmt3L, an altered binding behavior was observed, although the results were not conclusive (C.4.2). Therefore, changes in binding behavior to different nucleosomal species should be analyzed individually.

Interestingly, Dnmt3L remained associated with endogenous nucleosomes when separated on a sucrose density gradient whereas 'free' Dnmt3L incubated with DNA or reconstituted chromatin (C.4.1) entered approximately one third of the gradient suggesting that DNA and reconstituted chromatin do not represent the optimal binding substrate.

Hence, the question remains why Dnmt3L stays stably associated with endogenous nucleosomes from Sf21 cells. In order to address these questions in the future, the following experiments could be envisioned.

First, Dnmt3L should either be stably or transiently transfected into mammalian cells and the association with endogenous histones should be verified. Comparison of posttranslational modifications of co-purified histones with histones obtained through acidic extraction would allow determination of modifications being responsible for potentially binding of Dnmt3L.

Second, although no other prominent proteins except for histones were detected during the Dnmt3L purification procedure, a possible loading factor that either transiently interacts with Dnmt3L or is present in substoichiometric amounts could be imagined. Formaldehyde cross-link of cells following Dnmt3L purification and SDS-PAGE analysis could disclose temporarily associated factors. Third, to test for sequence dependent binding or specific chromatin structures, mammalian nuclei could be exposed to different MNase conditions following purification of Dnmt3L. In addition, it would be interesting to find out which regions of the genome are associated with Dnmt3L. Chromatin immunoprecipitation following Micro-Array analysis (CHIP-on-CHIP) could reveal whether Dnmt3L is associated with imprinted DMRs and retrotransposons (LINEs) or randomly distributed.

Fourth, in order to examine the role of RNA in the Dnmt3L/nucleosome interaction, Dnmt3L and co-purified chromatin could be treated with RNAse.

Another approach that could be applied is chromatin assembly with the DREX system in the presence of Dnmt3L following analysis on the sucrose gradient. If stable association occurred, one could address whether Dnmt3L is an integral part of the reconstituted chromatin and therefore, needs to be added at the onset of the reaction, or tightly associates to chromatin structure, hence addition after assembly should be sufficient.

D.2.3 DNA methylation of mono-nucleosomes

Radioactive DNA methyltransferase assays with Dnmt3a and Dnmt3b2 were performed with three different substrates: free DNA (MF79/80; 342bp), mono-nucleosomes with symmetric linker DNA (MF79/80; 342bp) and mono-nucleosomes without linker DNA (MF124/125; 147bp) (C.3.5).

In a reaction setup with substrate saturating conditions, both Dnmt3a and Dnmt3b2 methylated free DNA and mono-nucleosomes with linker DNA equally well although the overall methylation efficiency differed from Dnmt3a to Dnmt3b2. This is in agreement with the notion that DNA and mono-nucleosomes with long linker DNA were bound similarly well (C.3.3).

Affirmative, comparable maximum velocities for the methylation of DNA and mono-nucleosomes with linker DNA (220bp, 5S rDNA) were found for Dnmt3a and Dnmt3b (Robertson et al. 2004; Takeshima et al. 2006). However, the amount of CpG sites applied were 5-15 fold higher for mono-nucleosomes indicative of different K_M values for DNA and mono-nucleosomes although similar association constants for both substrates were determined in EMSA experiments (Robertson et al. 2004; Takeshima et al. 2006).

Interestingly, nucleosomal DNA was hardly methylated at all (C.3.5). Quantitative analysis revealed a 35-fold and a 27-fold reduction of absolute DNA methylation towards mono-nucleosomes (147bp) of Dnmt3a and Dnmt3b2 respectively. This clearly indicates that DNA wrapped around the histone octamer represents a major obstacle to DNA methylation by the *de novo* DNA methyltransferases. From the extremely low activity of mono-nucleosomes (roughly 3% compared to 'naked' DNA), it is hard to judge whether it is caused by residual free DNA from the nucleosome assembly or from specific methylation within the nucleosome. Therefore, a detailed single-molecule analysis of DNA methylation with the method of bisulfite conversion (E.2.13) was performed (C.3.6). In contrast to the incorporation of [3]H- or ^{14}C labeled methyl-groups, following scintillation counting or PAGE-based quantitation respectively, this technique allows both analysis of each potential CpG target site and discrimination between sense and anti-sense strands.

The bacterial DNA methyltransferase M.SssI which served as a reference, efficiently methylated both the (+) and the (-) strand of the 'naked' and the nucleosomal template. DNA methylation did not occur within the nucleosomal core which in accordance with previously described data (Kladde et al. 1999) (Okuwaki and Verreault 2004).

Similarly, Dnmt3b2 methylated both the upper and the lower strand, but less efficient than M.SssI indicating possible sequence preferences (Handa and Jeltsch 2005). Residual DNA methylation was found at CpG sites located at the entry/exist sites of the nucleosome and for

two positions within the nucleosome. The methylation pattern suggests that residual methylation in the ^{3}H-assay originates from a low-level of nucleosomal methylation.

Other data on the methylation of nucleosomes by Dnmt3b pointed out that Dnmt3b was able to methylate within the nucleosome (Takeshima et al. 2006). However, the DNA methylation read-out was based on an error prone radioactive assay analyzing MNase treated and gel-purified nucleosomal fragments. The method of bisulfite treatment is superior since single molecules can be analyzed and possible contamination of free DNA directly be seen.

The reaction efficiency of Dnmt3a towards DNA and nucleosomal matrices was extremely low which originated from a non-saturated reaction setup regarding the amount of template used. Nevertheless, the overall picture of DNA methylation in chromatin by Dnmt3a resembles the results given by Dnmt3b2. In fact, latest DNA methylation experiments using optimal reaction conditions (data not shown) reveal a similar picture of nucleosomal DNA methylation by Dnmt3a.

In contrast, published data claimed equal methylation efficiencies of Dnmt3a towards free DNA and mono-nucleosomes (147bp) (Gowher et al. 2005b) as determined from gel separation based quantitation. However, their bisulfite analysis of nucleosomal DNA showed a methylation efficiency comparable to that of Dnmt3b2, indicating that indeed DNA methylation is restricted within the nucleosome.

In agreement with my results, recent data showed that Dnmt3a scarcely methylated the DNA within the core region, but preferentially methylated the linker DNA between two nucleosomes *in vitro* (Takeshima et al. 2006; Takeshima et al. 2008).

Our data suggest that DNA methylation within nucleosomes does not occur *in vivo* at all considering nucleosomal arrays and higher order chromatin structures. In addition, histone H1 was found to inhibit DNA methylation of linker DNA by Dnmt3a (Takeshima et al. 2008).

Nucleosomes represent a major barrier for *de novo* DNA methylation *in vitro* indicating that enzymatic activities like chromatin remodeling enzymes that move or assemble/disassemble nucleosomes are required.

As described in the introduction, Dnmt3a and Dnmt3b were found in complexes with remodeling enzymes (A.3.8). Recently, it was demonstrated that different chromatin remodeling machines with intrinsic binding preferences of nucleosomes establish specific nucleosome positioning patterns (Rippe et al. 2007b). Accordingly, *in vivo* distinct chromatin structures could be created defining DNA accessibility for DNA methyltransferases and other chromatin associated factors. In fact, nucleosome remodeling dependent silencing by NoRC was shown to be a prerequisite for histone H4 deacetylation, H3K9 methylation and DNA methylation at a defined CpG site in the upstream control element of the rDNA gene promoter (Santoro and Grummt 2005).

From a mechanistic point of view, it will be interesting to decipher the underlying molecular mechanisms of chromatin remodeling and DNA methylation.

Since DNA methylation does not occur within the nucleosome, the first question to follow up is whether moving of histones by chromatin remodeling enzymes is sufficient to create accessibility for CpG site methylation. DNA methyltransferase assays with simultaneous

nucleosome 'sliding' could be performed. *In vitro* chromatin remodeling reactions are substoichiometric in regard to remodeling enzymes, hence once the nucleosome is moved, the remodeler should dissociate and not interfere with binding of Dnmts. This notion would imply that the reaction would follow an endpoint and therefore, the released nucleosome position would represent a low-affinity target for the remodeler. With a different chromatin remodeling enzyme, the remodeling reaction could be much more dynamic, i.e. the adjusted nucleosome position also serves as a substrate for the remodeling enzyme and is then moved back to its original position. Whether a 'window of opportunity' for DNA methylation between the forward and reverse reaction exists remains elusive. In this regard, it would be intriguing to see whether DNA methylation can affect the DNA sequence/nucleosome affinity of the remodeling machine. If the affinity was lowered by DNA methylation, the nucleosome would be moved back to its original position but would not be relocated again, leading to an equilibrium on the side of the 'starting' position but with methylated DNA. If the affinity was increased, the equilibrium would be shifted to the side of the second nucleosome position.

Therefore, modulation of substrate affinities of chromatin remodeling machines through DNA methylation could be a trigger to adjust certain nucleosome positions conferred with a certain transcriptional state. So far unknown active DNA demethylation enzymes or other remodelers with a different substrate affinity could reverse this process.

Alternatively to nucleosome 'sliding', disassembly of the nucleosome could be required for full methylation, following nucleosome assembly analogous to chromatin formation after replication.

E MATERIALS AND METHODS

E.1 Chemicals, radioactive material, enzymes and media

Unless otherwise stated, all common chemicals and materials were ordered at Merck, Roche, Roth and Sigma. Radioactive S'adenosyl methionine was ordered at GE Healthcare/ Amersham (TRK581-250UCi, 9.25MBeq with 1.0mCi/ml 63.0Ci/mmol).

E.1.1 Chemicals

BSA (albumin fraction V)	Genaxxon
BSA (fatty acid free; CHIP)	SIGMA A-7511
Bluo-Gal	Invitrogen
P-Per (bacterial protein extraction Kit)	Pierce
Bromphenolblue	Serva
Dimethylsulfoxid (DMSO)	Merck
Dithiothreitol (DTT)	Merck
Ethidiumbromide 10 mg/ml	Roth
Glycogen (CHIP)	Roche (901-393)
β-Mercaptoethanol (14,3 M)	Sigma
Milk powder	Sucofin
Protein A/G sepharose	GE Healthcare; E. Kremmer GSF
Phenylmethylsulfonylfluoride (PMSF)	Roth
Phenol/ Cholorform/ Isoamylalcohol 25/ 24/ 1	Roth
Polyethyleneglycol 8000	Roth
RNasin 40U/µl	NEB
S'adenosly methionine (SAM)	Sigma A7007
Salmon Sperm DNA (CHIP)	Invitrogen Gibco (15632-011)
SYBR Safe	Invitrogen
N,N,N',N'-Tetramethylethylendiamine (TEMED)	Roth

E.1.2 Standard solutions

Stock solutions, buffers and bacterial growth media were made according to standard protocols (Sambrook and Russel 2001; LabFAQS, Roche). Additional buffers are described in the individual method sections. If not stated differently, all buffers are stored at room temperature

E.1.3 Enzymes

Restriction endonucleases were purchased from New England Biolabs if not stated differently. Other enzymes used are given in the respective section.

E.1.4 Protease inhibitors, antibiotics

Aprotinin bovine	Genaxxon (M6361.01)
Ampicillin	Sigma
Kanamycin	Sigma
Tetracycline	Sigma
Blasticidin S hydrochloride	Invivogen
Gentamycin sulfate	Genaxxon (M3121)
Leupeptin hemisulfate	Genaxxon (M6100.0100)
MG132 (Z-Leu-Leu-Leu-al)	Sigma (C2211)
N-Ethylmaleimide (NEM)	Sigma (E3876)
Pepstatin A	Genaxxon (M6359.01)
Penicillin/Streptomycin	Invitroge/ Gibco (15140)
Zeocin	Invivogen

E.1.5 Software and online tools

Application	Author
Biq Analyzer	Bock, 2005 #1802} www.biq-analyzer.bioinf.mpi-inf.mpg.de/
NEB double digest finder	New England Biolabs (www.neb.com)
Oligo Perfect designer	Invitrogen (www.invitrogen.com)
PeptideCutter	Gasteiger et al., 2005(www.expasy.org)
Phyre	Benett-Lovsey *et al.* (2008) (http://www.sbg.bio.ic.ac.uk)
Primer 3	www.primer3.sourceforge.net/webif.php
Reverse Complement	(www. bioinformatics.org)
VectorNTI	Invitrogen (www.invitrogen.com)
Netprimer	Premierbiosoft (www.premierbiosoft.com)

E.1.6 Antibodies

List of antibodies used for Western Blot analysis and immunoprecipitation

.

Table 3 antibodies

antibody	source	species	application	comment
anti actin	Sigma A2066	rabbit polyclonal	WB: very good signal on HeLA WCE 30µg with 1:2500 dilution	Antigene: the C-terminal actin fragment (C11 peptide, Ser-Gly-Pro-Ser-Ile-Val-His-Arg-Lys-Cys-Phe) attached to Multiple Antigen Peptide (MAP) backbone.
anti Dnmt1 2G3-1	E. Kremmer, Helmoltz Gesellschaft	rat monoclonal, IgG2a	TCS, WB 1:20-1:100, IP 20µl proteinG beads + 400µl TCS	recognizes aa 1-300 of human Dnmt1.
anti Dnmt1 2E8-1	E. Kremmer, Helmoltz Gesellschaft	rat monoclonal, IgG2b	TCS, WB 1:20-1:100, IP 20µl proteinG beads + 400µl TCS	recognizes aa 1-300 of human Dnmt1. Also recognizes mouse Dnmt1 (acc. To U. Rothbauer)
anti Dnmt1 2C1	E. Kremmer, Helmoltz Gesellschaft	rat monoclonal, IgG2b	TCS, WB 1:20-1:100, IP 20µl proteinG beads + 400µl TCS	recognizes aa 316-330 of human Dnmt1. Does not recognizes mouse Dnmt1.
anti Dnmt1 2C12-1	E. Kremmer, Helmoltz Gesellschaft	rat monoclonal, IgG2b	TCS, WB 1:20-1:100, IP 20µl proteinG beads + 400µl TCS	recognizes aa 316-330 of human Dnmt1. Does not recognizes mouse Dnmt1.
anti - Dnmt3a	abcam ab16704	rabbit polyclonal IgG	WB, use at 1:1000 dilution	raised against human Dnmt3a aa 10-118
anti - Dnmt3a	abcam ab2850	rabbit polyclonal IgG	WB, use at 1:1000 dilution	raised against mouse Dnmt3a aa 86-100.
anti D3A2 6A4	E. Kremmer, Helmoltz Gesellschaft	rat monoclonal	TCS, WB 1:20-1:100, IP 20µl proteinG beads + 400µl TCS	raised against peptide KRKRDEWLARWKREAE of human Dnmt3a1 conjugated to BSA. Does not recognize Dnmt3a2 (mistake).
anti Dnmt3b1	abcam ab 13604	mouse monoclonal, IgG1	WB, use at 1:500 dilution	raised against histagged recombinant Dnmt3b
anti Dnmt3b	abcam ab 2851	rabbit polyclonal, IgG	WB, use at 1:1000 dilution	raised against mouse Dnmt3b aa 1-14, might cross react with D3a in WB
anti D3B2-2C1	E. Kremmer, Helmoltz Gesellschaft	rat monoclonal	TCS, WB 1:20-1:100, IP 20µl proteinG beads + 400µl TCS	raised against peptide CYNNGKDRGDEDQS of human Dnmt3b conjugated to BSA. Recognizes Dnmt3b1(aa 403- 416) and Dnmt3b2 (aa383-396).
anti Flag M2	Sigma	mouse monoclonal	WB, use at 1:3000 dilution	raised against Flag-epitope DYKDDDD
anti H2A	upstate 07-146	rabbit polyclonal	WB, use at 1:1000 dilution	epitope: KLH-conjugated, synthetic peptide corresponding to amino acids 88-97 (IRNDEELNKL-C) of human Histone H2A; used by (Nicassio et al. 2007)
anti H2B	upstate-07371	rabbit polyclonal	WB, use at 1:1000 dilution	epitope: peptide corresponding to amino acids 118-126 (CG-AVTKYTSSK) of human Histone H2B (used by (van der Knaap et al. 2005; Nicassio et al. 2007))
anti H3	abcam ab 1791	rabbit polyclonal	WB, use at 1:1000 dilution	epitope: synthetic peptide conjugated to KLH derived from within residues 100 to the C-terminus of Human Histone H3 (used by (Nicassio et al. 2007; Németh et al. 2008)
anti H4	upstate 07-108	rabbit polyclonal	WB, use at 1:1000 dilution	

anti HAUSP/ USP7	Bethyl laboratories	rabbit polyclonal	WB, use at 1:5000 dilution	raised against human HAUSP aa 1-50, tested in Hela extracts; WB testet 1:5000- 1:10000 with 10-20µg of extract. (1µg/µl concentration). IP on recombinant and endogenous protein (2µg antibody/ 1-2mg WCE from HeLa or HEK 293 cells)
anti HDAC1	Santa Cruz; sc-7872	rabbit polyclonal	WB, use at 1:500 dilution	HDAC1 (H-51) is a rabbit polyclonal antibody raised against amino acids 432-482 of HDAC1
anti His	Qiagen	mouse monoclonal	WB, use at 1:3000 dilution	anti-penta His antibody
anti ICBP90/ NP95	BD Transduction laboratories 612264	mouse monoclonal, IgG2a	WB, use at 1:1000-2000 dilution	Immunogen raises against human ICBP90 aa 199-298. According to the references (Hopfner et al. 2000),(Hopfner et al. 2001) it might be the same antibody sent by C. Bronner. (Used in CHIP (Unoki et al. 2004; Jeanblanc et al. 2005))
anti ICBP90	C.Bonner, Hopfner et al 2000	mouse monoclonal	WB, use at 1:5000 dilution	mouse monoclonal antibody 1RC1C-10, raised against C-term starting from D263.(1µg/µl) WB recognizes both recombinant and endogenous ICBP90 in 10µg WCE at 100kDA. IP on recombinant and endogenous protein (2µg antibody/ 1-2mg WCE from HeLa or HEK 293 cells)
anti Lamin A/C	Santa Cruz, sc-20681	rabbit polyclonal	WB, use at 1:500 dilution	WB on Hela nuclear extract
anti p53 (DO-1)	Santa Cruz, sc-126	mouse monoclonal, IgG2a	WB, use at 1:1000 dilution	(conc: 0,2mg/ml), recognizes well p53 in Hela and LS174T cell extracts
anti Sp1	Upstate 07-645	rabbit polyclonal		Used for CHIP
anti ubiquitin	Covance P4G7	mouse monoclonal, IgG1	WB, use at 1:1000 dilution	WB on recombinant ubiquitin works fine. On Extract and purified histones cross reaction with histones.

Commercial standard secondary antibodies (anti-rat, anti-mouse, anti rabbit, horseradish peroxidase conjugate) were used at a 1:3000 dilution.

E.1.7   Oligonucleotides

Oligonucleotides were all purchased from Eurofins MWG Operon and diluted with MilliQ-water to a final 100µM solution. Oligonucleotides for PCR amplification and sequencing reactions were designed to show a minimum of secondary structure, primer dimerization and with a melting temperature Tm of 60°C with the freely available *netprimer* software provided by *premierbiosoft* (http://www.premierbiosoft.com).

Oligonucleotides used for cloning, sequencing and colony PCRs are deposited on the Längst account on addgene (www.lablife.org) and named MF (number). Oligonucleotides used for the amplification of nucleosomal fragments, denoted, AP (number), were deposited by Anna Schrader on addgene (www.lablife.org)

E.1.8   plasmids

List plasmids used for the experiments shown. A complete list of all plasmids generated, acquired or requested during this study is available on the Längst account on addgene (www.lablife.org).

Table 4 plasmids

#	name	vector backbone	N-TAG	C-TAG	bacterial resistance	cloning strategy	created by
8	pRSETa human Dnmt1 aa1100-1600 HindIII	E. coli, T7 Promotor, N-6xHis, EK recognition site	N-His		Ampicillin, ORI (E.coli)	HindIII fragment of C-terminus of Dnmt1from pEGFP-C1 Dnmt1 cloned into pRSETa single cut HindIII	M. Felle; E. Silberhorn
9	pRSETb human Dnmt1 aa 1-1100	E. coli, T7 Promotor, N-6xHis, EK recognition site	N-His		Ampicillin, ORI (E.coli)	KpnI /HindIII fragment of pEGFP-C1 Dnmt1 human fl (first KpnI, then HindIII) inserted into pRSET KpnI/HindIII	M. Felle; E. Silberhorn
10	pRSETb human Dnmt1 aa 870-1100	E. coli, T7 Promotor, N-6xHis, EK recognition site	N-His		Ampicillin, ORI (E.coli)	BamHi/HindIII fragment /735bp) of pEGFP-C1 Dnmt1 human fl inserted into pRSEtb BamH/HindIII	M. Felle; E. Silberhorn
11	pRSETb human Dnmt1 aa 530-830	E. coli, T7 Promotor, N-6xHis, EK recognition site	N-Flag		Ampicillin, ORI (E.coli)	BamHI fragment 1080bp) of pEGFP-C1 Dnmt1 human fl inserted into pRSEtb BamH	M. Felle; E. Silberhorn
15	pMal c2x TEV human Dnmt1 TS aa 316-601-Flag	cytoplasmic expression of MBP fusion protein with TEV, altered MCS	N-MBP TEV		Ampicillin, ORI (E.coli)	Amplification of the hTS with Primer MF26 and MF27 to give insert with N-terminal EcoRI and C-terminal Flag STOPP XhoI and HindIII. Cloning into MCS of pMAL c2x cut with EcoRI and HindIII	M. Felle; E. Silberhorn
17	pMal c2x TEV -C-Flag human Dnmt1 aa 1-290	cytoplasmic expression of MBP fusion protein with TEV	N-MBP TEV	C-Flag	Ampicillin, ORI (E.coli)	KpnI/BglII fragment (aa1-290) of pRSETb hDnmt1 ligated into pMalc2x TEV C-Flag cut with KpnI/BamHI	M. Felle; E. Silberhorn
21	pENTR3C -Dnmt3a	shuttle vector for Baculoviros expression			Kanamycin; ORI E.Coli	BamHI/EcoRI fragment of pRSETa Dnmt3a is ligated into pENTR3C cut with BamHI/EcoRI	M. Felle; E. Silberhorn
22	pENTR3C -Dnmt3b2	shuttle vector for Baculoviros expression			Kanamycin; ORI E.Coli	BamHI/EcoRI fragment of pRSETa Dnmt3b2 is ligated into pENTR3C cut with BamHI/EcoRI	M. Felle; E. Silberhorn
35-43	pMal c2X TEV -C-Flag hDnmt1 aa 316-386,ab mapping 2C1/2C12	cytoplasmic expression of MBP fusion protein with TEV, altered MCS	N-MBP TEV	C-Flag	Ampicillin, ORI (E.coli)	Cut pMal c2x TEV C-Flag with EcoRI and NheI and ligate oligonucleotide duplex coding for respective aa 316-386, 323-337, 331-344, 338-352, 345-358, 353-366, 359-372, 367-378, 373-386	M. Felle; E. Silberhorn

46	pETM Dnmt3a N-Flag C-His	E. coli, T7 Promotor, N-Flag; C-Thrombin 6xHis	N-Flag	C-His	Ampicillin, ORI (E.coli)	Cut pet 11 N-Flag Dnmt3a (#12) with Nhe/Nsi (removes Stop codon) and ligate C-Thrombin -6x His fragment iincluding Sall.	M. Felle; E. Silberhorn
47	pETM Dnmt3b2 N-Flag C-His	E. coli, T7 Promotor, N-Flag; C-Thrombin 6xHis	N-Flag	C-His	Ampicillin, ORI (E.coli)	Cut pet 11 N-Flag Dnmt3b2 (#13) with Nhe/Nsi (removes Stop codon) and ligate C-Thrombin -6x His fragment including Sall.	M. Felle; E. Silberhorn
48	pGEX 4 N-GST Dnmt3a-Do2	E. coli, tac Promotor, N-GST, lac operator; thrombin cleavage site	N-GST Thrombin		Ampicillin, ORI (E.coli)	Dnmt3a Domain2 (aa386-616) was amplified with primer MF46/46and cloned in frame after the N-terminal GST and Thrombin of pGEX 4t-1 with a C-terminal Flag tag.	M. Felle; E. Silberhorn
51	pENTR3C hTS aa316-601 C-terminal Flag	shuttle vector for Baculoviros expression		C-Flag	Kanamycin; ORI E.Coli	hTS is PCR amplified with MF60/61 with a C-terminal Flag and KpnI and EcoRV sites on pMal c2x TS C-Flag. Digested and cloned in pENTR3C.	M. Felle; E. Silberhorn
56	pGA4 BN-601-m1	carries mod. 601 seq for Bisulfite sequencing; T7 promotor, T3 termination			Ampicillin, ORI (E.coli)	the modified 601 sequence can be amplified with MF77/78	MR Gene
61	pGEX-ub52	Amp, GST N-terminal	N-GST		Ampicillin, ORI (E.coli)	(Everett), EcoRI/XhoI insert sequence verified	(Canning et al. 2004)
69	pGEX USP7-2 aa212-561	E. coli, tac Promotor, N-GST, lac operator; thrombin cleavage site	N-GST		Ampicillin, ORI (E.coli)	quired form Barbara Härtl (Dobner lab->MTA) BamHI/XhoI cloning of fragment	B. Härtl (Dobner lab)
70	pGEX USP7-3 aa561-916	E. coli, tac Promotor, N-GST, lac operator; thrombin cleavage site	N-GST		Ampicillin, ORI (E.coli)	aquiredf orm Barbara Härtl (Dobner lab->MTA) BamHI/XhoI cloning of fragment	B. Härtl (Dobner lab)
71	pGEX USP7-3 aa913-1102	E. coli, tac Promotor, N-GST, lac operator; thrombin cleavage site	N-GST		Ampicillin, ORI (E.coli)	aquired form Barbara Härtl (Dobner lab->MTA) BamHI/XhoI cloning of fragment	B. Härtl (Dobner lab)
73	pCpGL-basic	R6P origin, only in cells with pir gene			Zeocin, for PIR1 cells	Michael Rehli, Maja Klug	(Klug and Rehli 2006)
85	pGEX 4T1 USP7 TRAF aa1-215	E. coli, tac Promotor, N-GST, lac operator; thrombin cleavage site	N-GST		Ampicillin, ORI (E.coli)	generated using the LR recombinase reaction between pGEX 4T1 stopp DEST and pENTR USP7 TRAF domain	Max Felle
90	pDONOR221_Dnmt3L human	attL sites, ENTRY clone			Kanamycin; ORI E.Coli	form Dirk Kuck, from RZPD, Dnmt3L human full length, no stopp	Dirk Kuck

92	pDEST10 Dnmt3b2 human	ori, Amp resistance, gentamicin resistence,	N-His, TEV		Ampicillin, gentamycin, ORI (E.coli)	LR clonase reaction of pENTR3C Dnmt3b2 and pDEST10	Max Felle
94	pDEST10 USP7 fl stopp	ori, Amp resistance, gentamicin resistence,	N-His, TEV		Ampicillin, gentamycin, ORI (E.coli)	LR clonase reaction of pDONR USP7 fl stopp and pDEST10	Max Felle
97	pDM7 C-His ICBP90	bacterial expression, Amp		C-His	Ampicillin, ORI (E.coli)	LR reaction with pENTR SD ICBP90 no stopp, pDM7 C-His	Max Felle
99	pDM7 C-His ICBP90 ∆RING	bacterial expression, Amp		C-His	Ampicillin, ORI (E.coli)	LR reaction with pENTR SD ICBP90 ∆RING no stopp, pDM7 C-His	Max Felle
101	pDFB6 C-Flag Dnmt3L	ori, Amp resistance, gentamicin resistence,		C-Flag	Ampicillin, gentamycin, ORI (E.coli)	LR clonase reaction of pDONR Dnmt3L no stopp and pDFB6 C-flag	Max Felle
105	pGEM -T-EASY-BN601 MF79/80	pGEM-T-EASY, Amp, pUC origin for TA-cloning			Ampicillin, ORI (E.coli)	BN601 sequence Bisulfite experiments was amplified with MF79/80 on pGA-Vector BN601(Mr Gene), cloned into pGEM-T-EASY Promega	Max Felle
107	GST-Dsk2p	pGEX (Amersham)	N-GST		Ampicillin, ORI (E.coli)	(Anindya et al. 2007), Dsk2p ubiquitin binding protein from S.cerevisiae	Robert Steinbauer

E.1.9 GATEWAY vectors

The GATEWAY plasmids used for the experiments are listed. A complete list of all GATEWAY plasmids generated, acquired or requested during this study is available on the Längst account on addgene (www.lablife.org).

Table 5 GATEWAY vectors

#	name	gene/ protein	vector backbone	TAG	selection	strategy	created by
GW 2	pDONR222	Entry vector	ORI (E.coli), T7 promotor,		Kanamycin, chloramphenic ol, ccdB gene		Invitrogen, K. Rippe
GW 3	pDEST10	Viral destination vector for Bac to Bac	ORI (E.coli), polyhydrin promotor	N-His 6x, TEV	Ampicillin, chloramphenic ol, gentamicin, ccdB gene,	Stopp codon has to come from donor vector	Invitrogen
GW 4	pENTR3C	Entry vector	ORI (E.coli)		Kanamycin, ccdB gene	carries RBS site	Invitrogen
GW 25	pDM7 C-His	Bacterial expression vector	ORI (E.coli), T7 promotor, lac repressor	C-His	Ampicillin, chloramphenic ol, ccdB gene	PCR of gateway conversion cassette of pDM1 with MF110/MF111 cut with EcoRV/Nsi and cloned into pDM1 cut with NdeI, then blunt end with T4Pol then cut with NsiI	Max Felle, A. Neu

| GW 39 | pDFB6 C-Flag | Viral destination vector for Bac to Bac | ORI (E.coli), polyhydrin promotor | C-Flag | Ampicillin, chloramphenicol, ccdB gene, gentamicin | Gateway cassette amplification on pDM1 with MF103/MF104, cut KpnI/SacI, cloned into pFASTBAC1 | Max Felle, A. Neu |

E.1.10 Bacteria and cells

Sf21 (*Spodoptera frugiperda*) insect cells were used for Baculovirus-directed protein expression. The following bacterial strains were available as chemical competent cells in the institute and stored at -80°C.

Table 6 Bacterial strains – plasmid propagation

strain	description	resistance	genotype
DB3.1	The gyrA462 enables ccdB containing plasmid propagation.	streptomycin	F- gyrA462 endA1 glnV44 Δ(sr1-recA) mcrB mrr hsdS20(rB-, mB-) ara14 galK2 lacY1 proA2 rpsL20(Smr) xyl5 Δleu mtl1
DH5alpha	general DNA plasmid propagation	none	F- φ80lacZΔM15 Δ(lacZYA-argF) U169 endA1 recA1 hsdR17 (rk-, mk+) supE44 thi-1 gyrA96 relA1 phoA
DH10BAC	E. coli strain that carries the baculoviral shuttle vector bMON14272 with a low-copy number mini-F replicon with a kanamycin resitance marker and Tn7 transposon attachment sites within the LacZa peptide. The helper plasmid pMON7124 encodes for the transposase and confers resistance to tetracycline.	tetracycline, kanamycin	Bac-to-Bac Invitrogen
DH10EMBacYFP	*E. coli strain that carries a modified baculoviral shuttle vector bMON1427 having the v-cath* and *chiA* genes replaced by an ampicillin marker and *LoxP* sites. The EYFP gene under the control of the polyhydrin promotor was inserted via Cre/lox recombination (Modified Dh10MultiBac bacmid)	tetracycline, kanamycin, ampicillin	(Berger et al. 2004)
TOP10	general DNA plasmid propagation	streptomycin	F- mcrA Δ(mrr-hsdRMS-mcrBC) φ80lacZΔM15 ΔlacX74 nupG recA1 araD139 Δ(ara-leu)7697 galE15 galK16 rpsL(StrR) endA1 λ-
XL1 Blue	F´episome, general DNA plasmid propagation, blue/ white screening	tetracycline	recA1 endA1 gyrA96 thi-1 hsdR17 supE44 relA1 lac [F'proAB lacIqZDM15 Tn10 (Tetr)]

Table 7 Bacterial expression strains

BL21 (DE3)			F⁻ompT *gal hsdS$_B$ (r$_B$⁻m$_B$⁻) dcm* lon λDE3
BL21 (DE3) pLysS	low supression of T7-induced background expression	chloramphenicol	F⁻ompT *gal hsdS$_B$ (r$_B$⁻m$_B$⁻) dcm* lon λDE3 pLysS (Cam^R)
Rosetta 2 (DE3) pLysS	BL21 derivative encodes rare eucaryotic codons	chloramphenicol	F⁻*ompT hsdS$_B$* (r$_B$⁻m$_B$⁻) *gal dcm* (DE3) pLysS*RARE2* (Cam^R)
K12 TB1	NEB		F– ara Δ(lac-proAB) [φ80dlac Δ(lacZ)M15]

E.1.11 Mammalian cell lines

List of mammalian cell lines that were cultured in the course of this study.

Table 8 Mammalian cell lines

name	description	source	growth conditions	remarks
Hela S3	Human cervix carcinoma	DSZM No: ACC 161; from Becker institute	37°C, 5% CO2; RPMI 1640 + glutamax, 10% FBS; cells that are adjusted to growth in solution, but are also able to grow as adherent cells	cell line is a subclone of its parent Hela (DSM ACC 57) derived in 1955; human flat-moded hypotriploid karyotype with 32% polyploidy; epithelial-like cells growing in monolayers, in principal adjusted to growht in solution; 25-30h doubling time
HEK 293 T	Human embryonal kidney	DSZM No: ACC 305; A. Nemeth	37°C, 5% CO2; D-MEM + glutamax, 10% FBS	human near-triploid karyotype with 6% polyploidy; adherent fibroblastoid cells growing as monolayer; 25-30h doubling time
HCT-116	human colon carcinoma	DSZM No: ACC 581; from A. Nemeth	37°C, 5% CO2; McCoy's 5A + 10% FBS + 2 mM L-glutamine (alternatively D-MEM + glutamax, 10% FBS, adjustment within 3 passages)	human near-diploid karyotype with 3% polyploidy; epithelial-like small cells growing as monolayer; 25-30h doubling time; Dnmt3b expression according to (Rhee et al. 2002).
LS174 TR	human colorectal adenocarcinoma; LS174T + TET repressor	(LS174T: ATCC No: CI-188) provided by Madelon Maurice, ;(Van De Wetering et al. 2002);(Kessler et al. 2007).	37°C, 5% CO2; RPMI1640 + 25mM Hepes + glutamx, 10% FBS; 10µg/ml blasticidin	human diploid; 45,X; one X chromosome missing; no other chromosomal aberrations; adherent growth in cell patches; doubling time < 24h. A TET-repressor (TR) was stably integrated in the LS174T cell line confering blasticidin resistance.
LS88	human colorectal adenocarcinoma; LS174TR + shRNA against USP7	provided by Madelon Maurice; (Meulmeester et al. 2005); Kessler, 2007 #265}.	37°C, 5% CO2; RPMI1640 + 25mM Hepes + glutamx, 10% FBS; 10µg/ml blasticidin, Zeocin 500µg/ml	LS174TR cell line + pTER-USP7-1 plasmid carrying a shRNA for USP7 (Zeocin 500µg/ml); k.d of USP7 upon doxycycline treatment (1µg/ml) within 48-72hours down to 25%
LS89	human colorectal adenocarcinoma; pTER-USP7-N-myc plasmid carrying a N-myc-USP7	provided by Madelon Maurice; (Meulmeester et al. 2005); Kessler, 2007 #265}.	37°C, 5% CO2; RPMI1640 + 25mM Hepes + glutamx, 10% FBS; 10µg/ml blasticidin, Zeocin 500µg/ml	LS174TR cell line + pTER-USP7-N-myc plasmid carrying a N-myc-USP7 (Zeocin 500µg/ml); overexpression of N-myc USP7 upon doxycycline treatment (1µg/ml) within 24-48 up to 300-400%
LS126	human colorectal adenocarcinoma; pTER-USP7-3 plasmid carrying a shRNA for USP7	provided by Madelon Maurice; (Meulmeester et al. 2005); Kessler, 2007 #265}.	37°C, 5% CO2; RPMI1640 + 25mM Hepes + glutamx, 10% FBS; 10µg/ml blasticidin, Zeocin 500µg/ml	LS174TR cell line +pTER-USP7-3 plasmid carrying a shRNA for USP7 (Zeocin 500µg/ml); k.d of USP7 upon doxycycline treatment (1µg/ml) within 48-72hours down to 25%; grow more slowly than LS88 and LS89.
MCF-7	human breast adenocarcinoma	DSZM No: ACC 115; from Dr. Michael Nevels; Universitätsklinikum R.	37°C, 5% CO2; D-MEM + glutamax, 10% FBS (alternatively RPMI 1640 + glutamax, 10% FBS)	human hypotetraploid karyotype with 8% polyploidy; epithelial-like cells growing as monolayers; 50-70h doubling time, Dnmt3a, Dnmt3b expression according to (Roll et al. 2008).

Molt-4	human T cell leukemia	DSZM No: ACC 362; from Becker institute	37°C, 5% CO2; RPMI 1640 + glutamax, 15% FBS	human flat-moded hypertetraploid karyotypey; round cells growing in suspension, singly or in cluster; 40h doubling time, maximal denisty at 1.3 x 10^6 cells/ml
NCCIT	Human teratocarcinoma/ embryonic carcinoma cell line	PD Dr. Stefan Schweyer; Universität Göttingen	37°C, 5% CO2; RPMI 1640+ 25mM Hepes + glutamax, 10% FBS	Epithelial-like cells growing as monolayers with patch like structure; 24h doubling time, Dnmt3a, Dnmt3a2, Dnmt3b expression according to (Chen 2002).

E.1.12 Baculoviruses for S21 cells

List of baculoviruses used for protein expression in Sf21 cells. Baculovirus containing supernatants were stored at 4°C protected from light.

Table 9 Baculoviruses for S21 infection

Virus	source	Passage	Volume (ml)	remark
hDnmt3a N-6x-His	M. Felle; baculodirect Kit, P5	P6	50	Used for protein expression
hDnmt3b2 N-6x-His	M. Felle; bac-to-bac Invitrogen, P2	P3	50	Protein expression: 100µl/1x10^7cells; 60h infection
hDnmt3L C-Flag	M. Felle; bac-to-bac DH10EMBacYFP, P1	P2	100	Two positive clones: #6, #7; 200µl/1x10^7 cells, 48h infection
hDnmt1 N-6x His	DNMT1 (Karo) 16.08.06			20µl/15cm plae (1,2x10^7 cells)
hSnf2h N-Flag	Low MOI infection of P2	P3	50ml	100-150µl/1x10^7 cells; 60 hours infection
mTIP5 N-myc	M. Felle; bac-to-bac Invitrogen, P3	P3	50	NoRC: hSnf2H P3 25µl. TIP5 125µl on 1x10^7cells, 72 hours infection
hUSP7/ HAUSP	M. Felle; bac-to-bac DH10EMBacYFP,	P3	200	Two low MOI infections: #15, #100. protein expression with 100µl/1x10^7cells,
hUSP7/ HAUSP C223S (Canning et al 2004)	Infection on 15cm plate with 1,2x^7cells	P3	30	Protein expression with 400µl/1x10^7 cells, 72 hours infection

E.2 Methods

E.2.1 Escherichia coli (E. coli)

Growth of *E. coli* in liquid culture, cryo preservation and transformation of chemical- and electro-competent cells, prepared at the department, were done according to standard methods (Sambrook and Russell 2001, Molecular cloning).

E.2.2 Working with DNA

E.2.2.1 Standard procedures

In general, amplification of plasmid DNA in bacteria, purification, concentration determination, restriction enzyme digestion, ligation of DNA fragments, analysis of DNA on agarose and polyacrylamide gels, and amplification of the DNA by the polymerase chain reaction (PCR) were performed according to the standard protocols (Sambrook and Russell 2001, Molecular cloning). In addition, plasmid DNA was prepared with plasmid purification kits (Invitrogen) for different amounts of DNA. Isolation of DNA fragments from agarose gels was performed using the Qiagen Gel Extraction kit.

E.2.2.2 DNA precipitation methods

Ammonium-acetate and sodium-chloride precipitation was done as described (Sambrook and Russell 2001, Molecular cloning).

PEG8000 precipitation

The use of of polyethylenglycol 8000 at different concentrations allows the selective removal of smaller DNA fragments (Paithankar and Prasad 1991).
DNA fragments smaller than 200bp do not precipitate when using PEG8000 at 10% and MgCl$_2$ at 10mM final concentration. Depending on the volume of the DNA solution, fill up with TE-buffer. Add ½ volume of PEG solution (30% PEG8000, 30mM MgCl$_2$), vortex well and incubate 10-30min on ice (more efficient than at room temperature). Precipitates, although almost not visible, were pelleted (22°C, 13000g, 15-30min), washed with 70% ethanol, air-dried and dissolved in an appropriate volume of either MilliQ or TE-buffer.

E.2.2.3 Polyacrylamide and agarose gel electrophoresis

Agarose gel electrophoresis was generally performed with gels containing 0,8 -1,2% agarose in 1X TBE buffer, 1:10000 SYBR Safe (Invitrogen), in 1x TBE running buffer at a constant voltage of 100-120V.
In contrast to agarose gel electrophoresis, DNA was separated by polyacrylamide gel electrophoresis (PAGE) in 0.4 X TBE at 4°C at 100V. In order to remove unpolymerized acrylamide the gel was prerun for 1 hour at 80V. For visualization the gel was stained after

the gel run in 0,4x TBE containing ethidiumbromide (0,5mg/ml) for 15min and washed twice with water for 10min each.

E.2.2.4   DNA methylation with M. SssI

DNA was methylated using M. SssI methylase (NEB) according to the manufactor's instructions with some minor modifications. Briefly, 1µg of DNA was incubated with 4U enzyme and 1000µM SAM (Sigma A7007) for 2h at 37°C. For larger DNA amounts, the incubation time was prolonged. After the reaction had completed, the methylase was heat inactivated at 65°C for 20min.

E.2.2.5   Colony PCR

A pipet tip was dipped into a bacterial colony on an agar plate and the adhering cells were resuspended in 25µl water in a 0,2ml PCR tube and subsequently gridded on fresh LB plates containing the necessary antibiotics. All tubes were placed in the PCR cycler and cells lysed by heating to 100°C for 10min. Then, 25µl of colony PCR master mix were added to each tube in the PCR cycler, and the thermocycler program for colony PCR was started. Afterwards, the PCR reactions were analyzed on an agarose gel for presence of the amplicon.

50 µl	1 x (µl)
Primer for 100µM	0,5
Primer rev 100µM	0,5
dNTP´s 10 mM	1
Taq-Puffer 10x	5
Taq-Polym.	1
H2O + Kolonie	25
H2O	17
Total volume	**50**

PCR-Programm 35 Cycles

2 min 94°C // 40 sec 94°C/ 40 sec 55-58°C / 40 sec 72°C// 10 min 72°C

E.2.3   Protein analysis: standard procedures

Protein analysis was performed according to the standard protocols (Sambrook and Russell 2001, Molecular cloning). Generally, proteins were kept on ice (4°C), in the presence of protease inhibitors (either complete® (Roche), or a mix of Leupeptin, Pepstatin, Aprotinin (all 1 µg/ml), PMSF (0.2 to 1 mM)) and reducing agents (DTT 1mM, or ß- mercaptoethanol 5mM).

E.2.3.1   SDS-polyacrylamide gel electrophoresis (SDS-PAGE)

Resolving and stacking gels were prepared according to standard protocols using ready-to-use polyacrylamide solutions from Roth (Rotigel, 30%, 49:1 (for buffers see also E.1.2). For electrophoresis, protein samples were mixed with either SDS-PAGE sample buffer or 1/3

volume HU buffer, heat-denatured for 5min at 95°C or 10min at 65°C respectively and directly loaded onto the gel. Proteins were separated at 50mA until the dye front had reached the end of the gel. Following electrophoresis, proteins were stained with either Coomassie Blue, silver or subjected to Western blotting.

E.2.3.2 Silver staining of protein gels

The staining of protein gels with silver nitrate solution was carried out according to the protocol of Blum (Blum et al. 1987).

E.2.3.3 Semi dry Western Blot and immuno-dectection

Western Blot was performed as described (Sambrook and Russell 2001, Molecular Cloning) with the Towbin transfer buffer (192mM glycine, 25mM Tris, 20% methanol, 0.05% SDS). Blocking and antibody incubations were done in blocking solution (1x PBS, containing 5% dried milk and 0.1% Tween-20) whereas washing was performed in 1x PBST.

E.2.3.4 TCA precipitation of protein samples

Samples with low protein content can be TCA precipitated following resuspension in a smaller volume of loading dye. In general 10% of 100% TCA solution and 1µl of 2% deoxycholate solution are added to the protein sample. After vigorous vortexing, proteins are precipitated by centrifugation (13000g, 30min, 4°C), washed once with ice-cold 100% acetone and resuspended in 1/10th of the original volume in 2x Lämmli dye.

E.2.3.5 Acidic extraction of histiones

The following protocol was adapted from a protocol from R. Eskeland for the extraction of histones from S2 cells.

Mammalian cells (HEK293, LS174 and derivates, E.1.11) (stored in small aliquots of $2x10^7$ cells at -80°C) were resuspended in 1ml 1xPBS supplemented with protease inhibitors. Triton-X-100 was added to a final concentration of 0.3% following incubation for 10min at 4°C. NEM was added to 10mM final concentration for cells that were intended for ubiquitin analysis. After centrifugation (10min, 3500rpm, 4°C) the nuclear pellet was resuspended in 200µl ice-cold 0.4M HCl and incubated on a rotating device at 4°C overnight.

After centrifugation (20min, 13000g, 4°C) the supernatant was saved on ice, the nuclear pellet once more extracted by adding ½ volume of 0.4M HCl and incubated for 1h at 4°C. After centrifugation the supernatants were combined and dialyzed against three changes of 1l 100mM acetic acid for 1h each (MW cut off: 6-8kDa). The extracted histones were snap-frozen in liquid nitrogen, lyophilized overnight and dissolved in roughly 200µl of milliq water. The concentration was determined measuring the OD at 230nm (epsilon: 4.3 Abs. units/mg histone per 1ml) yielding roughly 200µl with 5-20mg/ml. Histones were stored at -80°C in small aliquots.

E.2.3.6   Size exclusion chromatography

Size exclusion chromatography (SEC), also referred to as gelfiltration chromatography, is a technique for the separation of proteins and polymers based on their molecular weight or more exact on their hydrodynamic radius given by their shape.

SEC was used for the analysis of higher molecular weight complexes from nuclear extracts from human placenta and Hela cells as well as for Dnmt1 dimerization studies.

For gelfiltration runs, superose6 or superdex200 gelfiltration columns (GE Healthcare) were washed with two column volumes (CV) water and equilibrated with running buffer for at least two CVs. If not stated differently, samples were centrifuged for 30min at 13.000g prior to loading with a maximum volume of 500µl. Separation was performed in SEC buffer (20mM Tris pH7.5, 150mM NaCl, 1mM EDTA, 1mM DTT) with a flow rate of 0.5ml/min and 500µl fractions taken.

Gelfiltration columns were calibrated with protein standards that meet the requirement of being spherical and inert.

E.2.4   GATEWAY technology

Although many different well evaluated expression systems exist, the expression of one's personal protein-of-interest (POI) still remains an elusive and laborious process based on trial and error.

In order to have a system that meets the requirement to rapidly monitor protein expression either constitutive or inducible in different organisms (E. coli, insect cells, mammalian cells), with different tags, different combination and location of tags (N- or C- terminal), a large library of expression vectors (destination vectors) using the GATEWAY technology from Invitrogen was acquired (E.1.9).

E.2.4.1   GATEWAY - vectors

Three different GATEWAY adapted vectors are available.

GATEWAY vector	Characteristics
Donor vector (pDONR)	Contains *att*P sites. Used to clone *att*B-flanked PCR products and genes of interest to generate entry clones
Entry vector (pENTR)	Contains *att*L sites. Used to clone PCR products or restriction fragments that do not contain *att* sites to generate entry clones
Destination vector (pDEST)	Contains *att*R sites. Recombines with the entry clone in an LR reaction to generate an expression clone. It contains elements necessary to express the gene of interest in the appropriate system (*i.e. E. coli*, mammalian, yeast, insect)

To enable recombinational cloning and efficient selection of entry or expression clones, most GATEWAY vectors contain two att sites flanking a cassette containing:

The ccdB gene (see below) for negative selection (present in donor, destination, entry vectors) and the chloramphenicol resistance gene (CmR) for counterselection (present in donor and destination vectors).

After a BP or LR recombination reaction (refer to the Invirogen manual for details), this cassette is replaced by the gene-of-interest (GOI) to generate the entry clones and expression clones, respectively

The presence of the ccdB gene allows negative selection of the donor, destination and some entry vectors in E. coli following recombination and transformation. The CcdB protein interferes with E. coli DNA gyrase, thereby inhibiting growth of most E. coli strains (e.g. DH5α, TOP10, but not XL1 blue). When recombination occurs, the ccdB gene is replaced by the GOI. Cells that take up unreacted vectors carrying the ccdB gene or by-product molecules retaining the ccdB gene will fail to grow. This allows high-efficiency recovery of the desired clones.

For propagation of ccdB gene containing vectors (pENTR3C, all donor and destination vectors) the DB3.1 E. coli strain needs to be used. It contains a gyrase mutation (gyrA462) that renders it resistant to the CcdB effects (E.1.10).

E.2.4.2 Creation of an Entry clone

There are three ways to create entry clones that contain your GOI.

For all three methods it is necessary to consider later applications like the organism of protein expression such as E. coli, insect cells and mammalian cells with their specific translational control elements (Shine Dalgarno, Kozak sequence), N- or C-terminal tags, as well as cleavage site for unique proteases (TEV, enterokinase). Especially the introduction of a stop codon needs to be taken into account.

The following three methods were applied to generate ENTRY clones.

A PCR product or a restriction enzyme fragment was cloned into a pENTR-vector to replace the ccdB gene. In our laboratory the pENTR3C vector containing a Shine Dalgarno and Kozak sequence was available.

A PCR-product with a specific blunt sequence overhang was directly cloned in pENTR TOPO directional vector using the TOPO-cloning technique from Invitrogen. This method worked quite well with 2-3 clones out of five clones being positive.

Generation of a PCR product containing attB sites and subsequent BP recombinase reaction with a pDONR-vector yielded efficiently positive ENTRY-clones.

E.2.4.3 Creation of a Destination clone

In order to create an expression clone a LR-clonase reaction (LR Clonase II mix) between a pENTR-GOI vector (attL sites, kanamycin resistance gene) and a pDEST vector (attR sites, ampicillin resitance gene, ccdB gene, chloramphenicol marker) has to be performed.

The reaction mixture is then transformed into DH5alpha or TOP10 competent cells and plated onto LB/Amp plates. Only the bacteria containing a pDEST-GOI plasmid are able to

grow, since the ccdB gene was replaced. Remaining entry vectors do not confer ampicillin resistance.

E.2.5 Sf21 insect cells and baculovirus protein expression system

E.2.5.1 General

Baculoviruses are a group of large double-stranded DNA viruses infecting insects. They feature a narrow host range with each type of baculovirus being virulent only to a specific insect species, while not infecting other insects, plants or mammals. AcNPV, Autographa californica Nuclear Polyhedrosis Virus, is a well-studied type that is, together with Sf (*Spodoptera frugiperda*) ovary tissue culture, a useful tool for recombinant protein expression.

During the baculovirus life cycle, two different forms of virus are produced by the infected host cell: extracellular virus particles bud during the early stage of infection (release 24 hours post infection) and spread infection to other organs of the insect. During the late stage of infection, occluded virus particles form in the nucleus of the host cell. Occluded virus consists of many nucleocapsids enveloped by a matrix mainly formed polyhedrin, a structural protein expressed at very high abundance. The polyhedrin matrix allows the virus to last in the environment after the death of the host. After ingestion of occluded virus, virions are released in the mid-gut of the next host and enter adjacent cells by endocytosis. *In vitro*, polyhedrin is not necessary for virus replication and can be deleted or replaced. As the polyhedrin promoter is the strongest promoter known at present, it allows for very high levels of expression of the heterologous protein placed under its control. In addition, the baculovirus genome and capsid structure tolerate insertions of sequence well so that large coding sequences may be introduced (Berger et al. 2004; Fitzgerald et al. 2006). Baculovirus expression systems are very versatile tools for protein expression as they allow high-level expression of large proteins providing also signal peptide cleavage, intron splicing, nuclear transport, phosphorylation, glycosylation and acetylation, the lack of which often limits the use of bacterial expression systems.

E.2.5.2 Growth and maintenance of Sf21 cells

Sf21 cells are cultivated in Sf-900 II medium (Invitrogen) supplemented with 63mg/l penicillin, 50mg/l streptomycin and 10% fetal bovine serum (Invitrogen). Sf21 cells were grown in suspension in either spinner bottles (75rpm) or Erlenmeyer flasks (approximately 100rpm) at 27°C. For a continuous and stable growth behavior, which is crucial for best and reproducible protein expression, Sf21 cells were kept in logarithmic growth, i.e. at cell densities between $5x10^5$ and $2x10^6$ cells/ml.

Freezing of Sf21 cells and thawing of cells was done according to the 'Insect' manual (Invitrogen).

E.2.5.3   Construction of recombinant baculoviruses

During the course of this study baculoviruses were created using three different systems:

BaculoDirect Baculovirus Expression Kit (Invitrogen)

The BaculoDirect System (Invitrogen) takes advantage of the *in vitro* GATEWAY LR reaction to transfer your GOI into the BaculoDirect linear DNA, thereby replacing the Herpes Simplex Virus type 1 thymidine kinase (HSV1 tk) gene and lacZ gene.
This reaction is catalyzed by LR Clonase II Enzyme Mix for BaculoDirect Kits.

The baculodirect Kit was used for the following proteins

Protein name	Vector	strategy
Dnmt3a human	pENTR3C -Dnmt3a	BamHI/EcoRI fragment of pRSETa Dnmt3a is ligated into pENTR3C cut with BamHI/EcoRI
Dnmt3b2 human	pENTR3C -Dnmt3b2	BamHI/EcoRI fragment of pRSETa Dnmt3b2 is ligated into pENTR3C cut with BamHI/EcoRI
Dnmt1 mouse	pENTR3C mDnmt1 full length	KpnI/NotI fragment of pet11 N-HisII mDnmt1 full length ligated into pENTR3c vector cut with the respective enzymes
Dnmt1 d553-578 mouse	pENTR3C mDnmt1 full length delta 553-578	KpnI/NotI fragment of pet11 N-HisII mDnmt1 full lengthdelta553-578 ligated into pENTR3c vector cut with the respective enzymes

The baculodirect Kit procedure was only successful for Dnmt3a which resulted in a N-6x His tagged Dnmt3a full-length recombinant baculovirus. Therefore the Baculodirect Expression Kit was discarded and not further applied.

Bac-toBac system (Invitrogen)

The Bac-to-Bac system was used to obtain fast and efficient recombinant baculoviruses. Briefly, the cDNA was cloned into a suitable pFastBac vector or transferred from the GATEWAY pENTR-vector into an appropriate pDEST vector using the LR reaction.
The pFastBac or pFastBac based pDEST vectors (E.1.9) contain the polyhedrin promoter, the GOI and a gentamycin resistance marker flanked by transposition elements (tn7). The pFastBac-GOI plasmid was transformed into E. coli DH10bac competent cells (E.1.10), which contained the bacmid DNA (tetracycline resistance marker) and a helper-plasmid (encoding a transposase, kanamycin resistance marker). Triple antibiotic and blue-white selection resulted in the selection of the recombinant bacmid DNA (transposition of the GOI + gentamycin into the bacmid DNA destroying the lacZ gene). The presence of the desired cDNA in the high molecular weight bacmid DNA was verified by PCR (with GOI and bacmid primer). The recombinant bacmid DNA was transfected into Sf21 cells ($9x10^5$ cells in one well of a 6-well plate) with Cellfectin (Invitrogen) to produce a first viral stock. This virus stock was amplified and used for protein expression (see below).

The baculoviruses for the following proteins were successfully generated using the bac-to-bac system.

Protein name	Vector	strategy
Dnmt3b2 human	pDEST10 -Dnmt3b2	LR reaction of pENTR3c- Dnmt3b2 with pDEST10 creating an N- 6x His Dnmt3b2.
mTIP5	pFastbac- N-myc mTIP5 (R. Strohner)	

Bac-to-bac/ Multibac system (Imré Berger)

The Bac-to-bac system was further improved to give rise to the possibility of expressing multiple proteins-of-interest from one bacmid (Berger et al. 2004; Fitzgerald et al. 2006). The system is based on two features:

Two different plasmids are available that either integrate into the bacmid DNA via tn7 transposition or via the Cre/lox system. For each plasmid exists a *multiplication module* that allows up to four genes to be separately cloned and expressed.

In our laboratory we have acquired the E. coli strain DH10EMBacYFP (E.1.10) (Berger et al. 2004) in which the bacmid DNA was modified in a way that the v-cath and chiA genes had been replaced by an ampicillin marker and LoxP sites. The v-cath gene encodes for a cathepsin L-like proteinase and the chiA for a chitinase that acts as a chaperone for proV-CATH. Thus the infected cells are less prone to cell lysis during infection and to proteolytic degradation, which results in a higher yield of full-length recombinant protein. The EYFP gene under the control of the polyhydrin promotor was inserted via Cre/lox recombination and allows the monitoring of protein expression via fluorescence measurement during the course of infection.

The baculoviruses for the following proteins were successfully generated using the bac-to-bac- "Berger" system.

Protein name	Vector	strategy
hDnmt3L	pDFB6-C-Flag hDnmt3L	LR reaction of pDONR hDnmt3L no stopp with pDFB6 C-flag creating an C-Flag hDnmt3L
hUSP7/ HAUSP	pDEST10 hUSP7	LR reaction of pDONR hUSP7 stopp with pDEST10 creating an N- 6x His TEV hUSP7

This is the system of choice to quickly generate suitable baculoviruses.

E.2.5.4   Transformation of DH10EMBacYFP cells

Chemically competent DH10EMBacYFP E. coli cells (prepared by E. Silberhorn; 100µl) were transformed with 60ng of pFastbac-GOI /pDEST-GOI plasmid. Selection by means of blue/white selection was done as described in the 'bac-to-bac' manual (Invitrogen).

E.2.5.5   Isolating recombinant bacmid DNA

After having transformed your pFastBac construct into DH10Bac or DH10EMBacYFP E.coli cells and performed the transposition reaction, recombinant bacmid DNA from positive white transformants was purified according the 'bac-to-bab' manual (Invitrogen).
Purified bacmid DNA is suitable for use in PCR analysis or transfection into Sf21 insect cells.

E.2.5.6   Transfection of Sf21 cells

The bacmid DNA preparations are transfected into Sf21 cells using the Cellfectin reagent (Invitrogen). For each protein-of-interest two bacmid DNA clones with two wells transfected each are used.
The transfection procedure was done according to the 'bac-to-bab' manual (Invitrogen).

E.2.5.7   Low MOI baculovirus amplification

Amplification of baculovirus is undertaken to preserve the virus stock and to gain a higher titer of virus of the initial virus stock that can be used for protein expression.
MOI (multiplicity of infection) is defined as the number of baculoviruses/ Sf21 cell. In order not to accumulate defective virus particles, that eventually would lower protein expression, baculovirus amplification with a MOI of 0.1or less is the method of choice.
Low MOI infection is performed in spinner flasks with 50-100ml culture volume and at a constant cell density of 1×10^6 cells/ml (always dilute back to this cell number). Once infected, Sf21 cells have to at least double once during the first 24 hours post-infection (e.g. 10% of the cells were infected, whereas the other 90% doubled). With this prerequisite growth arrest is usually observed another 24 hours later. If the baculovirus titer is lower it might take some days (passages) until growth arrest is reached (multiple rounds of virus amplification took place). Budded virus is released starting from 24 hours after infection.
As a rule of thumb, harvest the viral supernatant 48 hours after the calculated growth arrest.

E.2.5.8   Test expression of recombinant proteins in Sf1 cells

Once the baculovirus is amplified, the bacualoviral titer for large-scale high MOI protein expression needs be determined.
In a 6-well plate 1×10^6 cells are seeded per well in 2ml of culture medium. For the amount of virus added per well, assume a viral titer between 1×10^7 pfu/ml and 5×10^8 pfu/ml and a desired high MOI of 3 for optimal protein expression.
Add the estimated amount of virus (e.g. mock infection, 100, 40, 20, 10, 5 µl of virus) and evenly distribute the virus by putting the plate on a horizontal shaking platform for 1 hour.
Seal the 6-well plate with parafilm and incubate for 48 -72 hours at 27°C recording daily growth behavior and infection process which allows a rough titer determination.

Cells are harvested by scrapping cells off the plates, washing once with ice-cold PBS and freezing of the pellet in liquid nitrogen. Presence of the recombinant protein and functionality of the affinity tag were analyzed in a small-scale purification.

E.2.5.9 High MOI protein expression in Sf21 cells

Protein expression with baculovirus infection is performed with a MOI of 2-3 so that on average 2-3 baculoviruses infect one Sf21 cell.

Cells are grown in suspension in either spinner flasks or Erlenmeyer flasks (200-400ml) and are infected at a cell density of $1x10^6$ cells/ml with the respective amount of recombinant baculovirus (as determined before with test infections and/or fluorescence measurement). After 48 -72 hours cells are harvested (@ 5 -10min, 500g), snap frozen in liquid nitrogen and stored at -80°C until use.

E.2.6 Mammalian Tissue culture

E.2.6.1 Maintenance

Mammalian cells in culture were propagated in their recommended medium (E.1.11), containing 10% FCS and penicillin/streptomycin. All media were warmed to room temperature before used, but stored at 4°C. The medium of the cultures was changed every 2-3 days depending of the confluency of the cells. The cells were split at an estimated confluency of 70%. For splitting, trypsin/EDTA solution was added to the cells (3ml per P15 dish) and the dish incubated for 3-4min at 37°C. . The reaction was stopped by adding culture medium at three time the volume as EDTA/Trypsin. After determination of cell density, an appropriate volume of cells was transferred to a new flask and filled with medium to the final volume. Cells were incubated in a humidified incubator reserved for mammalian tissue culture at 37°C and 5% CO_2.

E.2.6.2 Harvesting cells

For cells to be used in experiments instead of further propagation, no sterility precautions were taken. Medium was removed and 1ml 1x PBS added (for less FCS contaminations, cells were once washed with PBS). Cells were removed from the flask surface using a cell scraper. The cell suspension was then centrifuged for 3min at 4000 rpm. After removing the supernatant, the cell pellet was snap frozen in liquid nitrogen and stored at -80°C.

E.2.6.3 Preparing cleared mammalian whole cell extracts (WCE)

All solutions were precooled on ice and all work was performed at 4°C. Cell pellets, either freshly prepared or frozen and thawed on ice, were resuspended in lysis buffer. For P15 plates with cells at 70% confluency, 150µl lysis buffer containing protease inhibitors were

used. The cell suspension was then incubated on ice for 30min, while vigorously vortexing every 10min. Afterwards, it was centrifuged for 30min at 13000 rpm at 4 °C on a tabletop centrifuge. The supernatant was saved and its protein concentration determined using a Bradford protein assay. The protein concentration was usually between 10 and 20mg/ml.

Cell line	Lysis buffer
Hela, HEK 293, LS174T	20mM Tris pH 7.5, 100mM NaCl, 0.1mM EDTA, 0.5% NP40
MCF7, NCCIT, HCT-116	50mM Tris pH 7.5, 150mM NaCl, 0.1mM EDTA, 0.1%NP40, 0.3% Triton-X100

E.2.6.4   Transient transfection of mammalian cells

Linear polyethylenimine (PEI, MW 25,000) with secondary amines was used for the transfection of plasmid DNA into HEK293 and HeLa cells.
PEI is prepared as a 1mg/ml solution in water adjusted to pH 7,4 and stored at -20°C.
The plasmid DNA (roughly 20-30µg/ 4-5x10^6 cells on P15) is diluted in 1/10th of culture volume in serum free medium. PEI is thawed and vortexed vigorously for 10 seconds prior to addition to the DNA. 3µl of the PEI solution/1µg DNA is added to the DNA solution, mixed for 10 seconds and incubated for 20min at room temperature to allow for complex formation.
While slowly moving the culture dish the DNA/lipid mixture is added drop wise to the cells cultured in complete medium. PEI does not have to be withdrawn from the medium.

E.2.6.5   Purification of EGFP fusion proteins from mammalian cells

The following proteins were expressed in HEK293 cells (E.1.11) as C-terminal fusion proteins with EGFP (enhanced green fluorescent protein) after transient transfection of the respective plasmids (E.1.8) carrying the gene-of-interest with an N-terminal EGFP
HEK293 T cells were maintained as described (E.2.6.1) and transient transfection was carried out according to the protocol mentioned above (E.2.6.4) with the subsequent specifications.
For each construct four P15 plates with HEK293 T cells at roughly 70% confluence (1,2-1,4x10^7 cells) were transfected with 30µg of plasmid DNA/plate. Transfection efficiency reached approximately 30% after 72 hours as estimated from microscope visualization (Zeiss, Axiovert200). Cells were harvested (E.2.6.2) and cell lysates prepared (E.2.6.3) in **lysis buffer** (20mM Tris pH 7.5, 100mM NaCl, 0.1mM EDTA, 0.5% NP40 supplemented with protease inhibitors).
15µl of GFP-binding protein coupled to sepharose (referred to as GFP binder; Rothbauer et. Al 2008) equilibrated with **wash buffer** (20mM Tris/HCl, pH 7,5, 150mM NaCl, 0.5mM EDTA) was incubated with WCE from one P15 plate diluted 1:2 with wash buffer for 2 hours at 4°C on a rotating device. Immunocomplexes were pulled down by centrifugation (@2500rpm, 4°C, 2min) and the supernatant collected (referred to as flowthrough).

Beads were washed three times with EX-300 +0.05% NP40 and either boiled in SDS-PAGE sample buffer for subsequent SDS-PAGE and Western Blot analysis or resuspended in 60µl EX-100 buffer supplemented with 20% glycerol and 0.05% NP40 and stored at -80°C for functional *in vitro* assays.

E.2.6.6   Knockdown and overexpression of target proteins in mammalian cells

For USP7 knockdown and overexpression studies, cell lines based on the colorectal adenocarcinoma cell line LS174T, carrying plasmids with either shRNA (LS88, LS126) or N-myc-USP7 (LS89) under the control of a tetracycline/doxycycline inducible promoter were kindly provided by M. Maurice (E.1.11) (Van De Wetering et al. 2003; Meulmeester et al. 2005; Kessler et al. 2007).

For doxycycline treatment, cells were seeded on a 10cm tissue culture plate with a cell number giving rise to 50-60% confluency on the day of harvest. Cells were grown in RPMI1640/Hepes (GIBCO) supplemented with blasticidin (10µg/ml), Zeocin (200µg/ml; normally 500µg/ml) and TET-FBS (clonetech #631106; special approved FBS for tetracycline inducible systems). Doxycycline (1mg/ml in water; store at -20°C in the dark) induction was performed with the addition of doxycycline to a final concentration of 1µg/ml (1:1000).

Cell harvest and preparation of WCE were done as described (E.2.6.2, E.2.6.3) but in the presence of 10mM NEM.

E.2.6.7   Purification of ubiquitinylated proteins with dsk2p

WCE were prepared in 1xPBS+0.3% Triton-X-100 supplemented with 10mM NEM – an inhibitor of deubiquitinating enzymes.

The residual pellet was used for acidic extraction of histones (E.2.3.5).

50µl of GST or GST-dsk2p (ubiquitin binding protein, E.2.8.6) were incubated with 3mg of WCE in 1ml MobiCol columns at 4°C overnight. After centrifugation the flowthrough was collected and the beads washed 3x times with 500µl lysis buffer and 3x with EX-300+0.05%NP40 with 5min incubation steps in-between.

Bound proteins were eluted together with GST or GST-dsk2p from the glutathione sepharose with 50µl elution buffer (50mM Tris pH 8.0, 150mM NaCl, 10mM reduced glutathione) for 1h at 16°C shaking at 1300rpm. Optional a second elution can be performed. Residual beads were washed twice with lysis buffer and resuspended in 50µl HU buffer.

Samples were analyzed by Western Blot following immuno-detection with antibodies directed against the proteins of interest.

E.2.7   Purification of recombinant proteins from Sf21 cells

Figure 55 shows a combined result of the most commonly purified proteins during this thesis. Expression and purification was optimized for each protein as described in the following sections.
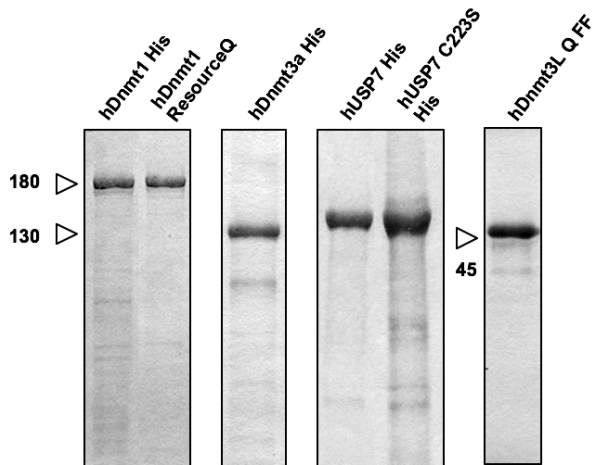
Figure 55 Purified recombinant proteins: hDnmt1, hDnmt3a, hUSP7, hDnmt3L

The indicated proteins were expressed in S21 cells using the baculovirus system, purified and analyzed by SDS- PAGE. Proteins were visualized by Coomassie Blue staining. Relative protein sizes are indicated (kDA).

E.2.7.1 Preparing Sf21 cleared cell lysate

After optimizing protein expression and initial test purifications, a typical large-scale expression started from $2{,}0\text{-}2{,}5\times10^8$ insect cells. Purification was performed in the cold room and samples were always kept on ice. Protease inhibitors PMSF (1mM), Leupeptin (1-10µg/ml), Aprotinin, Pepstatin (1µg/ml) were added to buffers prior to use.

Sf21 cell pellets were resuspended in 10ml lysis buffer corresponding to the affinity tag with which the protein of interest was to be purified.

The cell suspension was snap frozen in liquid nitrogen and thawed in cold water. The freeze-thaw procedure was repeated twice and the suspension subsequently treated with five strokes of A-type pestle (loose) and five strokes of B-type pestle (tight) in a dounce homogenizer. Cells were further lysed by sonification with a Branson Sonifier 250D (large tip; 3x for 30s at 50% amplitude and 50% duty cycle with a cooling period 30s of in between). The lysate was cleared by centrifugation (@ 30min, 20000g, 4 °C) and subsequently used for protein purification.

E.2.7.2 Purification of His-tagged hDnmt1 (two steps)

Recombinant histidine-tagged hDnmt1 from Sf21 cells was purified in two steps, by Ni-NTA agarose (Qiagen) purification followed by conventional chromatography (ResourceQ, GE Healthcare). Ni-NTA purification was done as described (Yokochi and Robertson 2002).

Elution fractions were either directly dialyzed against two changes of 1 liter of dialysis buffer (Ex200-buffer, 2mM ß-mercaptoethanol) or applied onto a Hi Trap Desalting column (GE Healthcare) for further purification on an anion exchange matrix (ResourceQ).

Anion exchange chromatography (Resource Q 6ml, GE Healthcare)

The eluate of the desalting column (20mM Hepes, pH 7.9; 50mM NaCl, 1mM EDTA; 1.5 mMMgCl$_2$; 10% Glycerol; 1mM DTT) was loaded onto ResouceQ column equilibrated with desalting buffer (DB50) and eluted with a linear gradient from 50-600mM NaCl. Peak fractions (1ml) of Dnmt1 (250-300mM NaCl) were pooled, supplied with fresh protease inhibitors, b-mercaptoethanol, and snap frozen in liquid nitrogen and stored at -80°C.

Heparin chromatography

Dnmt1 was once further purified for analytical ultracentrifugation analyis.

Briefly, the Dnmt1 eluate of the ResourceQ column (aproximatedly 250-300mM NaCl) was applied onto a Heparin HP 1ml column (GE Healthcare) equilibrated DB250 (20mM Hepes, pH 7.9; 250mM NaCl, 1mM EDTA; 1.5mM $MgCl_2$; 10% Glycerol; 1mM DTT), step eluted with DB600 buffer and finally transferred into DB100 using a desalting column.

E.2.7.3   Purification of His-tagged hDnmt3a

Histidine-tagged hDnmt3a was expressed in Sf21 cells and purified via Ni-NTA agarose (Qiagen) as described by Robertson (Yokochi and Robertson 2002).

E.2.7.4   Purification of His-tagged hDnmt3b2

Although the hDnmt3b2 baculovirus established gave good results in preliminary infection experiments, the purification of histidine tagged Dnmt3b2 from Sf21 cells did neither work very well with the protocol for hDmt3a purification from Sf21 cells nor with the hDnmt3b2 purification protocol from bacteria.

Therefore the purification procedure was not further optimized.

E.2.7.5   Purification of His-tagged USP7

The purification of histidine-tagged USP7/USP7 C223S from Sf21 cells was done as described previously (Canning et al. 2004).

E.2.7.6   Purification of hDnmt3L (two steps)

The purification of Flag-tagged Dnmt3L was done as described for Flagged-tagged hSnf2H by R. Srohner (Strohner et al. 2004b).

Although hDnmt3L was purified via Flag-tag to high purity, DNA and histones were associated with the preparation.

Dnmt3L eluted from Flag-M2 agarose (Sigma) in EX-300/ 0.05% NP40 buffer was diluted with EX-0/ 0.05% NP40 buffer to 150mM KCl concentration and loaded on a Q FF column (1ml, GE Healthcare) equilibrated with loading buffer. hDnmt3L was eluted applying a linear gradient from 150-600mM KCl in EX-buffer/ 0.05% NP40 over 10 column volumes. Peak fractions (250-300mM KCl) were pooled, snap frozen in small aliquots and stored at -80°C.

E.2.8   Expression and purification of recombinant proteins from E. coli

Figure 56 shows a combined result of the proteins purified from E. coli during this thesis. Expression and purification was optimized for each protein as described in the following sections.
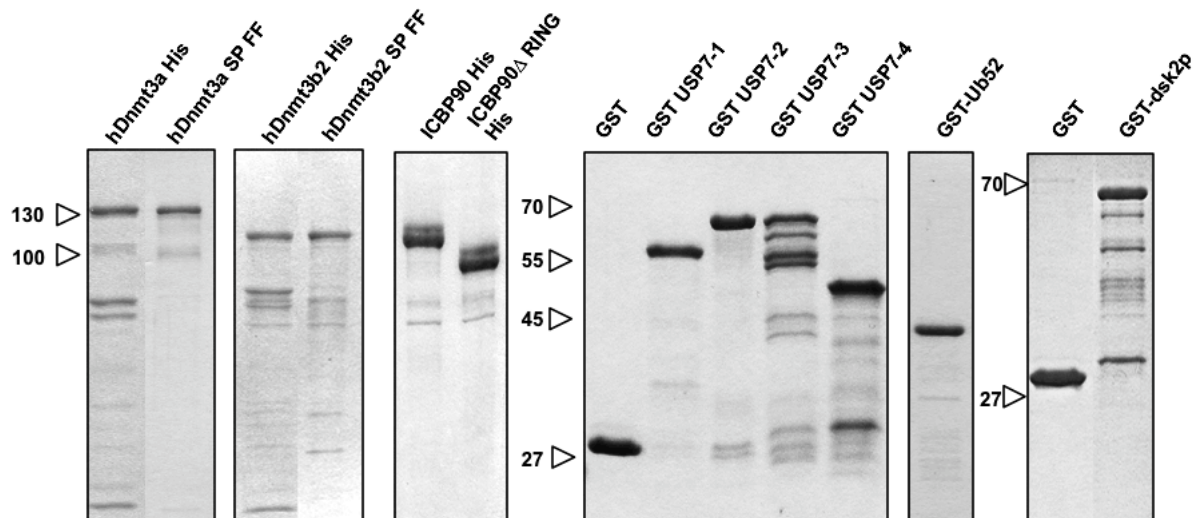
Figure 56 Recombinant proteins from E. coli: Dnmt3a, Dnmt3b2, ICBP90, ICBP90ΔRING, GST-USP7 domains I-IV, GST-Ub52, GST, GST-dsk2p

The indicated proteins were expressed in *E. coli* cells, purified and analyzed by SDS- PAGE. Proteins were visualized by Coomassie Blue staining. Relative protein sizes are indicated (kDA).

E.2.8.1   Preparation of a cleared bacterial cell lysate

Induced bacteria (prepared as described in each individual section) were harvested by centrifugation at 9000 rpm (A.6.9 rotor, centricon) for 15 min and 4°C. The supernatant was discarded, the pellet washed once with 1x PBS and subsequently stored at -80°C until use.

On the day of purification, 10ml of lysis buffer supplemented with protease inhibitors per 1g of bacterial pellet was added to the frozen cells, thawed in cold water and transferred to ice. Lysozyme was added (1mg/1ml lysate) following incubation on a rotating device for 30min at 4°C. Cells were further opened by treatment with five strokes of a B-type pestle (tight) in a dounce homognizer. The suspension (usually viscous at this point) was then cooled using a freezing mixture and sonified using a Branson digital sonifier 250D (big tip) 5 times for 30 seconds at 50% amplitude and 50% duty cycle with 30 seconds pause in between. Afterwards, the insoluble fraction was removed by centrifugation for 30min at 20000g and 4°C. The resulting supernatant was then used for further purification.

E.2.8.2   Purification of His-tagged Dnmt3a and Dnmt3b2 (1-2 steps)

The expression and purification of N-Flag-C-His Dnmt3a/3b2 was initially adapted from A. Jeltsch (Gowher and Jeltsch 2001) and modified.

Expression

Bl21 cells were transformed with the respective plasmids (pETM Dnmt3a/Dnmt3b2, E.1.8). An overnight culture was inoculated and grown at 37°C at 180 rpm overnight in SOB/Amp (100µg/ml) medium.

MATERIALS AND METHODS

Expression culture (usually 5 liter culture volume total, with 1 liter culture volume in 2 liter Erlenmeyer flask) was inoculated with an OD_{600} of 0.1 and grown at 30°C up to an OD_{600} of 0.5-0.6. Culture flasks were cooled down on ice for five minutes and protein expression was induced with 1mM IPTG for 3h at 24°C (cells usually grew up to OD_{600} 1.1-1.2). Cells were harvested (@, 15min, 9000rpm, A6.9), washed once with ice-cold 1xPBS (@ 10min, 4500rpm, 4°C), snap frozen in 1 liter culture pellet (50ml falcon tube) and stored at -80°C until use.

Before and after induction an aliquot (usually 1ml) of the culture was removed and centrifuged (1min, 13000g). The bacterial cell pellet was resupended in 15µl HU buffer/0.1 OD_{600}, boiled for 10min at 65°C, sonified (Branson sonifier, 3x bursts, output 20%) and loaded onto a SDS-PAGE of adequate percentage to check for recombinant protein expression.

Ni-NTA agarose purification

Purification was performed in the cold room and samples were always kept on ice. Protease inhibitors PMSF (1mM), Leupeptin (1-10µg/ml), Aprotinin, Pepstatin (1µg/ml) and ß mercaptoethanol (5mM) were added to buffers prior to use.

Lysis buffer: 20mM NaP, pH 7.4; 500mM NaCl; 0.1% NP-40; 5mM imidazole
Wash buffer1: 20mM NaP, pH 7.4; 500mM NaCl; 0.1% NP-40; 20mM imidazole
Wash buffer2: 20mM NaP, pH 7.4; 500mM NaCl; 0.1% NP-40; 40mM imidazole
Elution buffer: 20mM NaP, pH 7.4; 500mM NaCl; 1mM EDTA, 0.1% NP-40; 250mM imidazole, 10% glycerole

Bacterial cell lysate was prepared as described above (E.2.8.1).
Ni-NTA agarose beads (Qiagen) (500µl solid beads/ 1g cell pellet) equilibrated in batch with lysis buffer and incubated with the hDnmt3a/3b2 load on an overhead shaker for 1-1.5 hours at 4°C. After centrifugation (3min, 1000rpm, 4°C) the resin was washed once with lysis buffer, twice with wash buffer1 and twice with wash buffer2. All washing steps are performed with 10ml/g cell pellet and five minutes incubation a rotating device. The Ni-NTA agarose was transferred into a 2ml reaction cup (max. 1ml agarose beads) and bound proteins were batch - eluted from the beads with the addition of elution buffer (4x times bead volume) with 10 min incubations in between the elution steps.

Elution fractions were combined and directly dialyzed against two changes of 1 liter of dialysis buffer1 (EX-100-buffer, 0.05% Np40, 5mM ß-mercaptoethanol) or dialysis buffer2 (EX-500 buffer, 0.05% Np40, 5mM ß-mercaptoethanol).

When performing a dialysis in lower salt concentrations (50-250mM NaCl) Dnmt3a and Dnmt3b2 form precipitates (roughly 40-50% and 80% of protein content respectively), which can be removed by centrifugation (@30min, 13000g, 4°C), whereas 500-1000mM salt seems to stabilize misfolded Dnmt3a/b2.

This effect is reflected by the higher specific activity of EX100 versus EX500 hDnmt3a/3b2 preparations. The overall yield of recombinant protein is very low, especially for Dnmt3b2.

Out of six liter culture (almost 20g cell pellet) the overall yield for Dnmt3a and Dnmt3b2 were 1,3mg and 160µg respectively.

In low salt buffer (EX-100) Dnmt3a was usually soluble at a concentration of 100ng/µl, whereas Dnmt3b2 only at 20-25ng/µl. Under high salt conditions (500-1000mM KCl) protein concentrations up to 1µg/µl were possible.

SP FF chromatography

Both Dnmt3a and Dnmt3b2 bind to a cation exchange matrix (SP FF, GE Healthcare) under physiological pH conditions. Imidazole containing elution buffer was replaced either by dialysis or desalting column with SP-200 buffer (200mM NaCl, 20mM Tris, 7.5, 2mM $MgCl_2$, 1mM EDTA, 10% glycerol, 1mM DTT).

Precipitated material was removed by centrifugation (30min, 4°C, 13,000g) and filtration (0,45µm). The sample was loaded onto the SP FF column, washed with SP-300 buffer and step eluted with SP-500 buffer. Peak fractions were combined, either directly or after dialyosis snap frozen in small aliquots in liquid nitrogen and stored at -80°C.

During this dialysis step, Dnmt3b2 precipitates formed.

E.2.8.3   Purification of His-tagged ICBP90 and ICBP90∆RING

Bl21 cells were transformed with the respective plasmids (pDM7 C-His ICBP90, pDM7 C-His ICBP90∆RING, E.1.8).

Expression of recombinant proteins was done as described for Dnmt3a/b2 (E.2.8.2). The Ni-NTA purification was performed previously for USP7 (E.2.7.5).

ICBP90 and ICB90∆RING were very well expressed in Bl21 cells and could be well purified. 2 liter of culture yielded approximately 9mg of recombinant protein.

E.2.8.4   Purification of GST-tagged USP7 domains

The plasmids pGEX USP7-2 (aa 212-561), USP7-3 (aa561-916), USP7-4 (aa913-1102) (E.1.8) were kindly provided by B. Härtl/H. Götze (unpublished; Prof. Dr. Dobner, Heinrich Pette Institut, Molekulare Virilogie, Hamburg) and pGEX 4T1 USP7 TRAF domain (aa1-215) were transformed into Bl21 cells.

Expression

Expression culture (200ml) was inoculated in SOB/Ampicillin medium (100µg/ml) with an OD_{600} of 0.1 and grown at 37°C up to an OD_{600} of 0.5-0.6. Protein expression was induced with 1mM IPTG for 3,5h at 37°C (cells usually grew up to an OD_{600} of 1.3).

Purification via Glutathione sepharose

Purification was performed in the cold room and samples were always kept on ice. Protease inhibitors PMSF (1mM), Leupeptin (10µg/ml), Aprotinin, Pepstatin (1µg/ml) were added to buffers prior to use.

Cells were harvested and bacterial cell lysate from 200ml culture was prepared as described above (E.2.8.1) in lysis buffer (20mM Tris pH 7.5, 100mM NaCl, 1mM EDTA, 0.1% NP40). Glutathione sepharose (2ml 50% slurry, GE Healthcare) was equilibrated in batch with lysis buffer and incubated with the GST-USP7 constructs load on an overhead shaker for 1 hour at 4°C. After centrifugation (5min, 200g, 4°C) the beads were washed three times for five minutes each with 50ml lysis buffer. The resin was transferred into 2ml reaction tubes (1ml beads max.) equilibrated three times with EX-300 buffer (with 20% glycerol, no NP40). A 50% slurry soltion was prepared and 100µl aliquots were snap frozen in liquid nitrogen and stored at -80°C.

E.2.8.5 Purification of GST-tagged Ub52

The plasmid pGEX-Ub52 (E.1.8) was kindly provided by R. D. Everett (Canning et al. 2004) and transformed into Bl21 cells. Expression and purification was done as previously described.

E.2.8.6 Purification of GST and GST-dsk2p ubiquitin binding protein

The plasmids for GST and GST-dsk2p expression (E.1.8) were kindly provided R. Steinbauer (Anindya et al. 2007) and transformed into Bl21 cells. Expression and purification was done as described for the GST-USP7 domains (E.2.8.4).

E.2.8.7 Purification of MBP-hTS (Two steps)

The "targeting domain" (TS) of hDnmt1 is purified as a C-terminal fusion protein to maltose binding protein (MBP). The MBP moiety is cleaved with TEV-protease and separated through an anion exchange chromatography step.
The plasmid pMal c2x TEV hTS C-Flag (aa 316-601) (E.1.8) was transformed into K12TB1 E. coli cells and expression carried out as described for GST-USP7 domains (E.2.8.4).

Purification via Amylose resin (NEB)

Purification was done as decribed in the manula for purification of MBP-fusion proteins (NEB).

TEV protease cleavage

TEV protease is expressed and provided by the department (U. Stöckl). The molar ratio, incubation time and temperature for optimal cleavage were titrated in a preliminary experiment. For the given TEV protease batch (2.5mg/ml) the following conditions were determined: a molar ratio MBP-hTS/ TEV: 1:30 (protein conc: 1:100), incubation at 16°C overnight.

Q FF chromatography

The TEV eluate was loaded on a Q FF column (GE Healthcare) (20mM Tris pH 7.5, 2mM MgCl$_2$, 1mMEDTA, 10% glycerol, 1mM DTT). Under these conditions MBP and TEV protease do not bind to the matrix. hTS could be step eluted from the Q FF column with column buffer +400mM NaCl. The peak fractions were pooled, shock frozen in liquid nitrogen and stored at -80°C
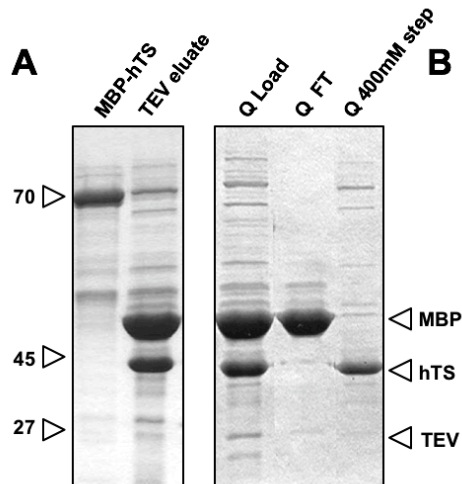
Figure 57 MBP-hTS purification

Potein analysis of MBP-hTS purification on 12% SDS-PAGE and Coomassie blue staining A.) Purified MBP-hTS and hTS and MBP after TEV cleavage. B.) hTS is separated from MBP and TEV with Q FF chromatography.

E.2.9   Preparation of nuclear extracts

E.2.9.1   Nuclear extracts from human placenta

The following protocol for the preparation of a nuclear extract from human placenta was established on a protocol provided by Dr. J. Griesenbeck and on published data for Dnmt1 preparations from human placenta (Wang et al. 1984; Pfeifer et al. 1985; Gorski et al. 1986; Yoo et al. 1987).

Purification was performed in the cold room and samples were always kept on ice. Protease inhibitors PMSF (1mM), Leupeptin (10µg/ml), Aprotinin, Pepstatin (1µg/ml) were added to buffers prior to use. (Since Leupeptin, Aprotinin and Pepstatin are very expensive, they were used only for buffer volumes > 100ml)

Fresh human placenta was received directly after birth and placed into ice-cold **wash buffer** 1x PBS supplemented with 1mM DTT and 1mM PMSF.

Human placenta is extensively rinsed three times with **wash buffer** to wash away blood. Fibrous membrane, fat and connective tissue are removed and remaining soft tissue is cut into small pieces (approximately 1-2cm^3, referred to as nuggets) that are directly shock frozen in liquid nitrogen and stored at -80°C until use.

Nuclei preparation

Approximately 1l of **buffer A (**20mM Hepes pH 7.6, 2mM EDTA, 1mM EGTA, 15mM KCl, 10% glycerol, 0.01% NP-40, 0.2mM spermidine, 0.5mM spermine, 1mM DTT) is added to 300g of placenta nuggets in a plastic bag. Nuggets are pre-thawed under running water to

facilitate homogenization and subsequently homogenized three times in a Waring Blender for 20sec each at full speed.

The homogenate is successively filtered through metal gauze of two different pore sizes (1500μm and 500μm respectively; (Uchida et al. 1993)) and centrifuged (@10min, 1300g, 4°C)

The pellet is resuspended in 100ml **buffer A**, filtered through metal gauze of two different pore sizes (200μm and 75μm respectively) and centrifuged. Again the pellet is resuspended in 100ml **buffer A** (supplemented with leupeptin, aprotinin, peptstatin) using a donce homogenizer (loose pestle) and filtered through three layers of Miracloth to remove fat).

The filtrate is centrifuged (@ 5min, 4500rpm, 4°C, 50ml falcon tube) and roughly 25ml NPV (nuclear packed volume) of crude nuclei are recovered (white color, fat containing).

The quality of prepared nuclei can be checked visually performing a DAPI stain.

A tip of a small spatula of nuclei are resuspended in 1x PBS, DAPI (stock 40μg/μl, stored in the dark) is added to a 1:100 dilution and incubated on ice for 3min. Nuclei are washed 3x times with 1x PBS (@2min, 2000rpm, 4°C) and resuspended in 200μl 1x PBS. A small drop is put on a microscope slide and covered with a glass slip. Visualization is performed with confocal microscope (Zeiss, Axiovert200).
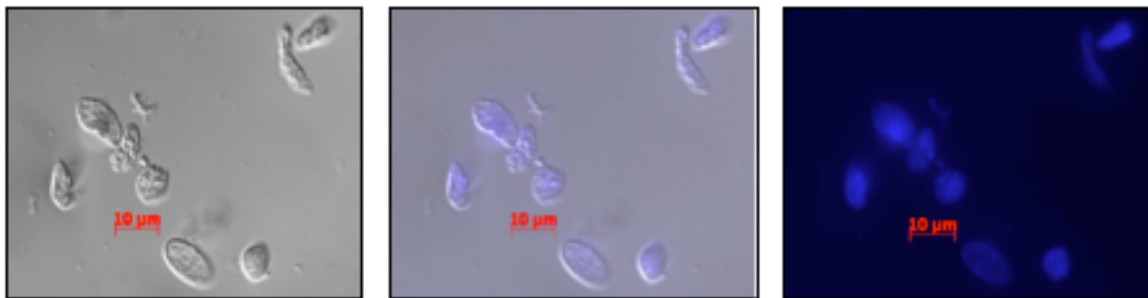
Figure 58 Nuclei from human placenta

Nuclei prepared from human placenta are DAPI stained. Size bar is indicated in red.

Nuclear extraction

0,9 volumes of **buffer C (**20mM Hepes pH 7.9, 20% glycerol, 420mM NaCl, 1.5mM $MgCl_2$, 0.2mM EDTA, 1mM DTT) are added to the nuclear pellet followed by douncing 3-5 times with a loose pestle (L-type) and 3 times with a tight pestle (S-type). The solution is transferred into Beckman Ti45 centrifugation tubes and while stirring, 5M NaCl is slowly added drop wise to raise the salt concentration by 100mM to approximately 300mM. The nuclear extract is incubated on a rotating device with 3-5x vortexing for 30-45 minutes and subsequently centrifuged (Beckman ultracentrifuge, 4°C, 120,000g, 90min)

Fat on top of the supernatant (referred to as nuclear extract) is removed with kimwipe and chromatin on the bottom of the tube is avoided as much as possible.

The nuclear extract is saturated with ammonium sulfate to 60-65% (0.33g AS/ml extract) over a period of 15min followed by a 30min incubation time.

After centrifugation (@30000g, 4°C, Kontron A8.24, 30min) the pellet (rather slimy) is properly resuspended with Dounce homogenizer in 3.5ml **buffer D50 (**20mM Hepes pH 7.9, 20% glycerol, 50mM NaCl, 2mM $MgCl_2$, 1mM EDTA, 1mM DTT with all protease inhibitors). Dialysis is performed twice for 2h against 2l of **buffer D50** (do not dialyze overnight) and centrifuged (30min, 13000g, 4°C). The resulting nuclear extract (referred to as NucD60) with approximately 4ml and an average yield of 20mg/ml was stored in aliquots at -80°C.

E.2.9.2 Nuclear extracts from HelaS3 cells

The protocol for the preparation of nuclear extracts from Hela cells was done as described by F. Pugh (Pugh 1995).

HelaS3 cells (E.1.11) were grown in spinner flasks in RPMI 1640 supplemented with glutamax, 10% FBS and penicillin/streptomycin at 37°C, 5% CO_2. Cells of a 10 liter culture were harvested with a cell density of approximately $1x10^6$ cells/ml (@ 15min, 4°C 4650g). The quality of the prepared nuclei was checked visually with DAPI stain (see nuclei preparation from placenta, E.2.9.1).
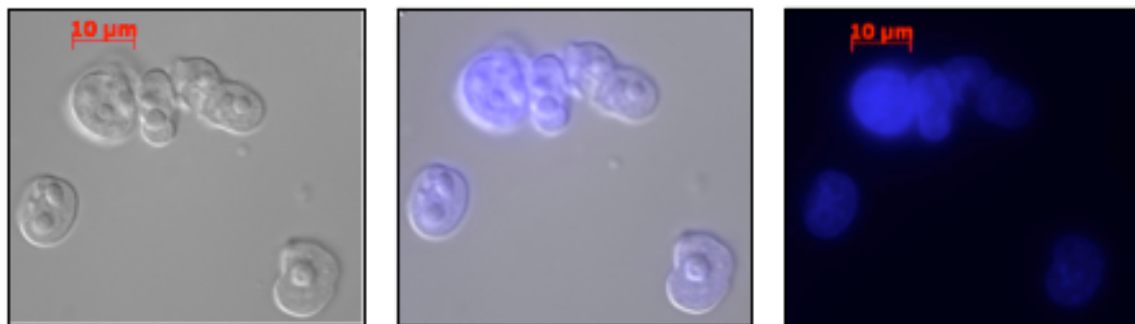
Figure 59 Nuclei prepared from HelaS3 cells

Nuclei prepared from human placenta are DAPI stained. Size bar is indicated in red.

E.2.9.3 MNase prepared nuclear extracts from HelaS3 cells

In order to prepare a nuclear extract that is also enriched in protein associated with chromatin, HelaS3 nuclei (prepared as described above) were enzymatically treated with MNase (Micrococcal nuclease) and mechanically treated with a Dounce homogenizer to solubilise nuclear proteins normally tightly bound to nucleosomes.

The following protocol was modified according to G. Längst (Langst et al. 1997).

The nuclear pellet (10ml) is washed twice with **buffer A** (15mM Hepes pH 7.6, 15mM NaCl, 60mM KCl, 2mM $MgCl_2$ suplemented with 1mM PMSF, 10µg/ml leupeptin, 1µg/ml aprotinin and pepstatin.). After centrifugation (5min, 1000g, 4°C) the nuclear pellet is resuspended in 2 nuclear packed volumes final (add 1 NPV) in buffer A, $CaCl_2$ is added to a final concentration of 1mM, followed by incubation in a water bath until the temperature of the nuclei solution reaches 25°C. A 100µl aliquot for later DNA analysis is removed.

After addition of 3000U MNase/ml NPV (Sigma, N5386, 3U/µl of NPV), the nuclei solution is incubated for 20min at 25°C on a rotating device. The MNase reaction is stopped with the addition of ¼ volume of 4x Stop solution (20mM EDTA, 20mM Hepes pH 7.6). A 100µl aliquot is withdrawn for DNA analysis.

The nuclei are dounced with 20-40 strokes in a Dounce homogenizer (S=B-type pestle) and subsequently centrifuged (@ 30min, 13000g, 4°C). Fat and fluffy stuff floating on top are avoided.

DNA analysis

The 100µl aliquots are dounced 30x and centrifuged (@13000g, 30min). 300µl of 4x stop buffer and 100µl of 4% SDS are added. RNAse digest (50µg) is performed for 1 hour at 37°C and proteinaseK digest (50µg) for 1h at 55°C. DNA is precipitated and analyzed on 1.5% agarose gel.

E.2.10 Chromatin – assembly and analysis of arrays

Figure 60 shows the results of a typical MNase digest analysis of DREX assembled DNA and a DNA nucleosome assembly using the salt gradient dialysis method. The amount of DNA, DREX extract, MNase und nucleosomes had to be optimized for each experiment as described in the following sections
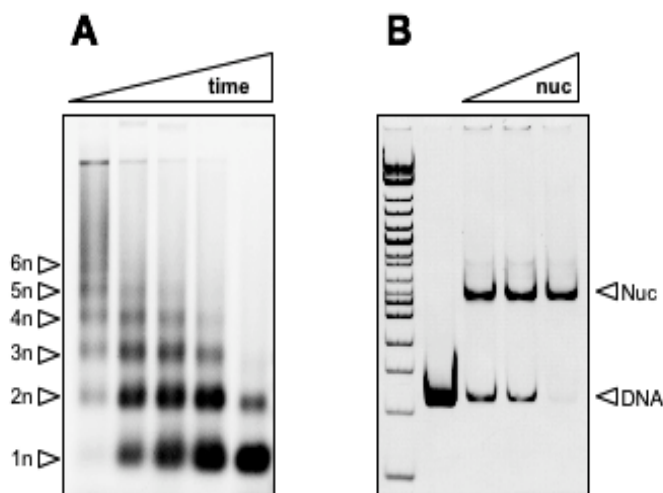
Figure 60 MNase digest and chromatin salt assembly

(**A.**) Micrococcal nuclease (MNase) analysis of chromatin assembled with *Drosophila* embryo extracts (DREX). DREX assembled plasmid DNA was digested with increasing time (15, 30, 60, 90, 120 seconds) with MNase. The regular fragment ladder indicative of the nucleosomal array is shown (1n-6n). **B**) Reconstitution of chromatin arrays using gradient salt dialysis. Different ratios (1.3; 1.5; 1.7:1) of histone to DNA (77WID) were used in salt assembly and tested for nucleosome occupancy. On a 5% PAA gel in 0.4X TBE. Nucleosomes and DNA were visualized by agarose gel electrophoresis and ethidium bromide staining.

E.2.10.1   Chromatin assembly using the Drosophila embryo extract (DREX)

Drosophila embryo extract (DREX; provided in the lab) assembly was performed as described (Becker and Wu 1992). A standard assembly reaction contained 900ng of circular DNA, 12µl McNAP (30mM $MgCl_2$, 10mM DTT, 30mM ATP, 300mM creatine phosphate, 10µg/ml creatine phosphate kinase (diluted in 100mM imidazole)) and varying amounts of

Drosophila embryo extract (20-70µl, depending on extract). The volume was increased with EX-100 to a final volume of 120µl. Chromatin assemblies were performed in 0.5ml PCR tubes in a Perkin Elmer PCR machine for 6 hours at 26°C. The quality of the assembled chromatin was analyzed by MNase digestion.

E.2.10.2   Chromatin assembly using the salt gradient dialysis technique

Chromatin assembly of DNA fragments with histone octamers from drosophila using the salt dialysis technique were routinely performed by our technician R. Gröbner-Ferreira.
Nucleosomes were assembled from DNA and histones by the salt gradient dialysis technique according to Rhodes (Rhodes and Laskey 1989).

E.2.10.3   Chromatin analysis by Micrococcal Nuclease (MNase) digestion

Micrococcal nuclease (MNase; Sigma N5386) cleaves DNA preferentially in the linker region between individual nucleosomes. Partial MNase digestion generates a regular DNA fragment ladder, thereby allowing qualitative analysis of the obtained grade of chromatin assembly. Typically, 900ng of chromatin was partially digested with MNase (MNase concentration has to be optimized for each assembly method) for 30, 60, and 120 sec in EX-100 buffer supplemented with 3mM of 3mM $CaCl_2$ at 20°C. In order to have reproducible results the MNase-mix (180µl) and DNA samples (120µl) were separately incubated for 5min at 20°C. The reaction was stopped by the addition of 0.2 volumes of stop solution (4% SDS, 100 mM EDTA). Prior to deproteinization, DREX assembled chromatin was incubated with RNase (1µg) for 1 hour at 37°C. All reactions were supplemented with proteinase K (10µg/ reaction) and glycogen (10µg) and deproteinized for at least 1 hour at 45°C or overnight at room temperature. The DNA was purified by ethanol precipitation (0.5 vol 7,5M NH_4Ac and 2.5 vol 100% ethanol were added, incubated for 30min on ice, centrifuged for 30min at 13000g and washed once with 70% ethanol), air dried, dissolved in 10µl loading buffer and analysed on 1.3% agarose gels (stained afterwards with ethidium bromide).

E.2.10.4   DNA fragments

DNA fragments assembled by salt dialysis were PCR amplified on purified restriction fragments from the SLONING DNA provided by A. Schrader. The SLONING DNA consists of three repeats of the nucleosome positioning sequence 601 ((Thåström et al. 2004a); referred to as WID, 147bp) flanked by a partial rDNA promoter sequence (approximately 70bp) on the left and a partial HSP7 promoter sequence (approximately 70bp) on the right. By using different combinations of restriction enzymes, symmetrical and asymmetrical DNA overhangs of variable length, relative to the WID sequence, can be generated. The DNA fragments were amplified by PCR and purified DNA fragments (E.2.2.2) were subsequently used for nucleosome assembly reactions.
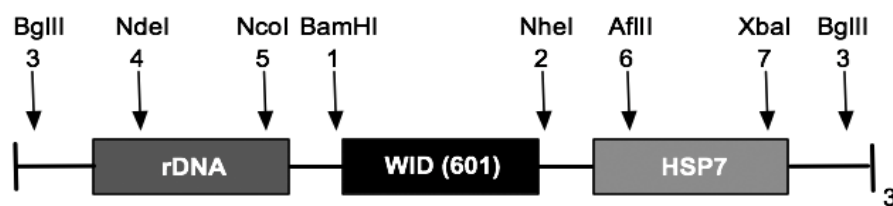
Figure 61 SLONING DNA

A section of the SLONING DNA is shown with the position of the flanking sequences with the indicated restriction enzymes.

Template	Primer_fw	Primer_rev	DNA template (PCR)	Annealing Tm
15WID	AP16	AP8	NcoI/NheI	58°C
15WID15	AP16	AP17	NcoI/AflII	58°C
22WID22	AP3	AP13	NcoI/AflII	58°C
40WID40	AP5	AP14	NdeI/XbaI	55°C
60WID	AP11	AP8	BglII/NheI	55°C
60WID60	AP11	AP12	BglII	55°C
77WID77	AP1	AP15	BglII	58°C
22WID	AP3	AP8	NcoI/NheI	57°C
40WID	AP5	AP8	NdeI/NheI	57°C
77WID	AP1	AP8	BglI/NheI	57°C
WID	AP7	AP8	BamHI/NheI	57°C

E.2.10.5   EMSA (electromobility shift assay)

The ability of proteins such as transcription factors or DNA binding proteins to bind to DNA or nucleosomes can be assessed according to the running behavior in an agarose or polyacrylamide gel system (E.2.2.3). If binding to DNA or nucleosomes occurs, the mobility is impaired resulting in either a slower migration velocity or a complete loss of migration, i.e the protein-DNA/ nucleosome complex cannot enter the gel and is retained in the pocket.
EMSAs for Dnmt3a/b were performed in 20µl reaction volume in 20mM Tris pH 7.6, 30mM KCl, 5mM EDTA, 1mM DTT, 5µM SAM, 20% glycerol. Dnmt3a/b was incubated with DNA or nucleosome for 15min at 26°C to allow for complex formation. After incubation the samples were put on ice loaded on either a 1.5% agarose gel or a 5%-15% polyacrylamide gel in 0,4X TBE (E.2.2.3) and run at 4°C.

E.2.10.6   Separation of chromatin applying sucrose gradient

Nucleosomal templates of different size can be separated on a sucrose gradient. The puc18:12x601 plasmid was digested with AvaI yielding 12x601 fragments (approximately 200bp, 601 sequence centered) and the puc18 backbone (approximately 2500bp). Restriction fragments and plasmid DNA was subsequently assembled into nucleosomes with *Drosophila* histones by the method of salt dialysis (E.2.10.2). 2.5µg of mono-nucleosomes and 2.5µg of nucleosomal plasmid were loaded on 10-45% sucrose gradient in EX-50 buffer

without glycerole and separated by centrifugation (18h, 30,000rpm, SW40, no brake). 400µl of the 600µl fractions collected were ethanol precipitated overnight with ammoniumacetate (E.2.2.2) and loaded onto a 1.3% agarose gel.

Analysis of Dnmt3L with chromatin/DNA was performed as described in the following:

10µg Dnmt3L, 5µg chromatin or DNA, 200µg/µl BSA (and PGA 2mg/ml) were dialyzed in 100µl against EX-100 buffer (w/o glycerole) for 1.5 hours prior to loading. For Western Blot analysis, 20µl of each fraction was supplemented with Lämmli dye and loaded onto a 12% SDS PAGE. The sucrose gradient and DNA analysis were performed by our technician R. Gröbner-Ferreira.

E.2.11 Activity assays

E.2.11.1 *In vitro* DNA methyltransferase assay for Dnmt3a/b

The enzymatic activity of Dnmt3a and Dnmt3b can be monitored in a radioactive *in vitro* assay, in which the transfer of the [3H]- labelled methyl-group from S'adenosyl-methionine (GE Healthcare, TRK581-250UCi, 9.25MBeq with 1.0mCi/ml 63.0Ci/mmol) to the C-5 position of cytosine in a CpG dependent context is catalyzed.

In a reaction volume of 50µl, Dnmt3a and Dnmt3b2 were typically used at a concentration of 100nM, linear or circular DNA (CpG sites) at 500nM, oligonucleotides (CpG sites) at 5µM, BSA at 0.2µg/µl and [3H]-SAM at 480nM (1.5µl) in DNA methyltransferase buffer (20mM Hepes, pH 7.6, 1mM EDTA, 1mM DTT).

The following templates were used:

Oligonucleotides:

Nonmethylated (nm) and (m) methylated primers were diluted to a final concentration of 100 pmol/µl. Nm-forward and nm-reverse oligos were mixed in a reaction tube to yield non-methylated, nm-forward and m-reverse oligos to yield hemimethylated substrates respectively. The reactions were heated to 95°C in a thermomixer for 10min, then the heating was switched off, and the reaction was allowed to cool to room temperature.

air_met_up	TGC GGA Atx GTC TAA xGx GTG GAA TxG TCC CCT TG
air_up	TGCGGAATCGTCTAACGCGTGGAATCGTCCCCTTG
air_do	CAAGGGGACGATTCCACGCGTTAGACGATTCCGCA

x denotes methylated cytosine

DNA:

Plasmid/ PCR	length (nt)	CpG sites
pRSETB Dnmt1 BamHI	3967	227
BN601 MF79/80 PCR	342	27
BN601 MF124/125 PCR	147	15

PCR fragments were generated with the indicated primer pairs on pGA4 BN-601-m1 (#56).

Procedure:

Mix Buffer, BSA, Dnmt3a/b and water

Add [3H]- labeled SAM (see above) and incubate for 5min at 37°C

Withdraw "0" timepoint; "no DNA" sample (background reference), stop with the addition of 10µl of 10mM non-labeled SAM and put on ice

add respective DNA template

incubate at 37°C for 20-60min.

at the desired time points add 10µl 10mM unlabeled SAM (this stops further incorporation of radioactive SAM)

spot the whole reaction onto DE81 filter (2,5cm diameter; Whatman) and put directly into a 0.2M ammonium carbonate solution

3x10min wash with a 0.2M ammonium carbonate solution

1x H_2O wash

1x 100% EtOH wash

dry filter in 37°C incubator for 30min

put dried filter into Mini-Poly-Q Vial

add 5ml Ultima Gold LSC-Cocktail per vial

measure each sample for 1min in Scintillation counter

E.2.11.2   *In vitro* DNA methyltransferase assay for Dnmt1

Dnmt1 – the maintenance DNA methyltransferase – preferentially methylates hemi-methylated (hm) DNA (Pradhan et al. 1999). Dnmt1's enzymatic activity is measured in a radioactive DNA methyltransferase assay, as described for the de novo methyltransferases Dnmt3a and Dnmt3b2 with the following exceptions.

Dnmt1 is used at a concentration of 60nM, [3H]-SAM at 320nM (1.0µl) in Dnmt1 reaction buffer (10mM Tris pH 7.6, 100mM KCl, 1mM EDTA, 1mM DTT.

E.2.11.3   *In vitro* ubiquitinylation assay

Components:

E1 activating enzyme (Biomol, UW9410; 320ng/µl; MW 119kDA; His tagged recombinant protein; 20mM Tris pH 7.5, 0.5mM DTT)

E2 conjugating enzyme UBCH5c (BioMol, UW9070, 1mg/lml, MW 17kDA, His tagged recombinant protein; in 20mM Tris pH 7.5, 0.5mM DTT)

ICBP90 and **ICBP90ΔRING** (own preparation E.2.8.3, C-terminal His tag)

Ubiquitin from bovine erythorcytes (Sigma U- 6253, 2mg/ml, in water)

Flag tagged ubiquitin (Boston Biochem, U-120; 5mg/ml; N-terminal flag tagged human recombinant ubiquitin, in water)

Methylated ubiquitin (Boston Biochem, U-502, 5mg/ml; human recombinant ubiquitin with methylated lysines that only allows fro monoubiqutinylation; in water)

1x reaction buffer (50mM Tris pH 7.5, 50mM NaCl, 5mM MgCl$_2$, 0.05% NP40, 1mM DTT, 5mM ATP; prepared as 5x reaction buffer; ATP stored in small aliquots and DTT are add prior to use)

Standard ubiquitinylation reactions (10µl) contained 100ng E1 activating enzyme, 300ng E2 conjugating enzyme, 1µg ubiquitin/ methyl- ubiquitin or 100ng flag tagged ubiquitin and 250-500ng ICBP90 or ICBP90ΔRING in 1x reaction buffer. The reaction was usually carried out in duplicate, incubated for 2 hours at 37°C and stopped with the addition of HU-buffer (E.1.2) and boiled for 10min at 65°C. Samples were resolved by SDS-PAGE (E.2.3.1) and ubiquitination reaction was analyzed by Western Blot (E.2.3.3) using antibodies directed either against ICBP90 (Hopfner et al. 2000; Hopfner et al. 2001), His tag or flag tag.

E.2.11.4   *In vitro* USP7 activity assay

USP7's potential activity as an ubiquitin specific protease was tested with an ubiquitin specific cleavage assay on an ubiquitin like substrate fused to GST (GST-Ub52, E.2.8.5) (Baker and Board 1991) as essentially established in the laboratory of R. D. Everett (Canning et al. 2004).

E.2.11.5   Coupled ATPase activity assay

The ATPase activites of the DREX and mouse transcription extracts were measured using an enzyme coupled assay, adapted from Lindsley (Lindsley 2001). ATP that is consumed in chromatin remodeling reactions is continuously regenerated while NADH is oxidized to NAD$^+$ (Figure 62). The decline of NADH is monitored at a wavelength of 355nm in a GeniosPRO plate reader (GeniosPRO; XFLUOR4GENIOSPRO Version: V 4.64) in a 96 well format, and 20sec intervals at 29°C.
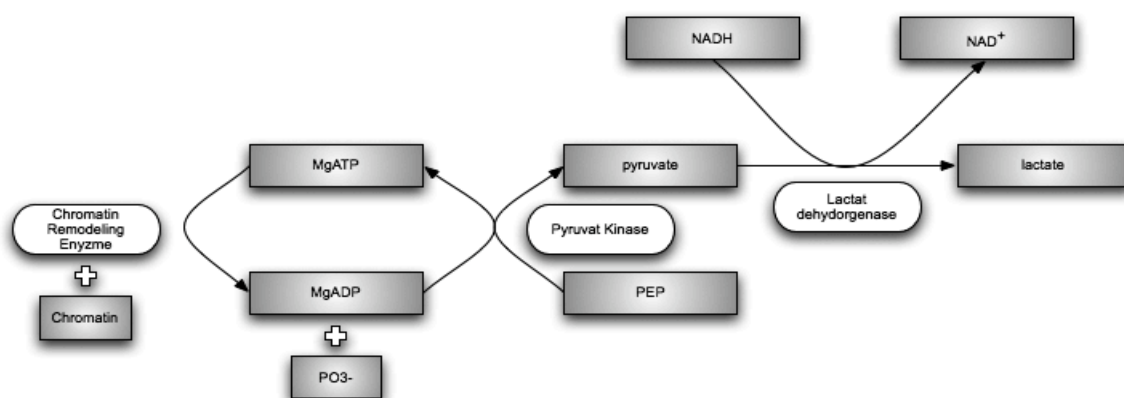
Figure 62 Coupled ATPase activity assay
Overview of coupled ATPase activity assay (Lindsley 2001) that indirectly couples the regeneration of ADP + phosphoric acid to ATP with the consumption of NADH to NAD$^+$.

The ATPase activity of 5µl of the mouse TX extract and 0.5µl of the DREX extract was followed in a 100µl reaction mixture containing 50mM Tris, pH 7.6, 5mM MgCl2, 150mM KAc, 6mM phophoenolpyruvate, 0.3mM NADH, 15U pyruvate kinase, 20U lactate

dehydrogenase and 2µg of DNA. The inhibitor Phophokanymycin (Muthuswami et al. 2000) and its Mock-inhibitor Kanamycin were added to 0.5mM final concentration. The ATPase reaction was started with the addition of 0.3mM ATP. All measurements were performed in triplicates.

E.2.12 Working with antibodies

E.2.12.1   Immunoprecipitation

The high affinity of an antibody for its antigen is used in immunoprecipitation to precipitate a target protein out of a complex mixture by binding it with a specific antibody that is immobilized on a solid phase, usually proteinA/G sepharose. Interaction partners of the target protein, such as proteins, DNA or RNA, can be co-purified by this method and identified or confirmed in subsequent experiments.

All steps were carried out on ice or at 4°C and buffers supplemented with protease inhibitors PMSF (1mM), Leupeptin (1-10µg/ml), Aprotinin, Pepstatin (1µg/ml) prior to use. If not stated differently, the following **IP buffer** was used for IP experiments:

50mM Tris pH 7.5, 150mM NaCl, 0.1mM EDTA, 0.05% NP-40.

Per IP experiment, 100µl of proteinG bead slurry were washed three times with 850µl IP buffer by resuspending, centrifuging shortly in a tabletop centrifuge and removing the supernatant.

In order to verify that the binding of one's protein-of-interest (POI) is not due to unspecific interaction with the bead matrix, half of the equilibrated proteinG beads were added to the protein mixture to be analyzed (recombinant proteins, WCE, nuclear extract). 10x IP buffer was added to obtain a final concentration of 1x. The suspension was incubated on the rotating wheel at 4°C for 2 hours. As an additional control, commercially available immunoglobulins (IgG) isolated from the same species of the target specific antibody, can be added (2.5-5µg). The precleared sample/ lysate was stored at 4°C until further usage and the proteinG beads referred to as either "preclearing beads" or "IgG control".

The second half of the washed proteinG beads was charged with antibodies from tissue culture supernatant (TCS). 25µl of solid beads were incubated with 400µl TSC for 2h at 4°C on the rotating wheel. Afterwards, the beads were washed twice with 1000µl IP buffer added to the previously prepared precleared sample/lysate and incubated at 4°C for 14h on the rotating wheel. The beads were then washed three times with 1000µl IP buffer and resuspended in 50µl HU buffer after removal of the supernatant. The suspension was heated to 65°C for 10 min and subjected to SDS PAGE analysis.

E.2.12.2   Cross–linking of antibodies to proteinA/G sepharose

Dimethyl pimelimidate dihydrochloride (Sigma D8388, DMP) is a homobifunctional cross-linking reagent that reacts with primary amines to form amidine bonds. Hence, antibodies can be covalently attached to proteinA/G sepharose not interfering with later gel analysis.

Components:

Sodium borate solution pH 9.0 (200mM sodium borate is soluble when heated to 60°C. pH is adjusted with HCl)

Dimethyl pimelimidate (stored at -20°C; prior to use incubate for 30min at 37°C; remove amount needed and to sample in 200mM sodium borate solution pH 9.0)

Ethanolamine solution (200mM, pH8.0; dilute stock solution with water and adjust pH with HCl)

Coupling of antibodies to proteinA/G sepharose beads

All steps are performed at 4°C. 1000µl of proteinA/G sepharose is equilibrated with 20 column volumes (CV) of 1x PBS and incubated with antibody (purified) or tissue culture supernatant (TCS) for 1 hour or over night. For optimal saturation of proteinA/G beads with antibodies the TCS should be titrated. In general 200-400µl of TCS (monoclonal antibodies) completely saturated 20µl solid proteinA/G beads. To warrant optimal binding 1/10th of 1.0M Tris buffer pH 8.0 is added to the TCS.

Beads are recovered by centrifugation (@ 3min, 200g, 4°C), following two washes with 10 CV of 100mM Tris pH 8.0 and three washes with 10CV of 10mM Tris pH 8.0 with 5min incubations in between.

Cross linking of antibodies

All steps are performed at room temperature.

ProteinA/G sepharose coupled with antibody is equilibrated three times with 20 CV of sodium borate solution for 10min each on a rotating device (@3min, 200g). Beads are resuspended in 10 CV of sodium borate solution. After addition of 50mg of dimethyl pimelimidate (20mM final) beads are incubated for 30min on a rotating device. This step is further repeated twice.

The cross-linking reaction is stopped by washing the beads once with 10-20CV of ethanolamine followed by incubation for 2 hours.

The following steps are carried out at 4°C.

Beads are washed twice with 10CV with 1x PBS and not cross-linked antibodies eluted with 100mM glycine pH 3.0. First they are washed once with 100mM glycine pH 3.0 (10 CV; @3min, 200g, 4°C) and then incubated for 5min in the same buffer. Beads should not be incubated longer since this might affect the stability of the antibody.

Finally antibody coupled proteinA/G sepharose is washed three times with 10 CV of 1x PBS, resuspended in 1 CV of 1x PBS supplemented with 0.02% sodium azide and stored at 4°C.

E.2.12.3   Limited proteolysis for domain mapping

The domain structure of a protein can be elucidated using limited proteolysis. In this method, a protease with recognition sites distributed all over the protein to be analyzed is incubated with the protein at a protease concentration and reaction time that will only lead to partial proteolysis. V8 protease (Sigma P6181; 0.1mg/ml in water) is a serine endoprotease from

the *Staphylococcus aureus* strain V8 that exhibits a high specificity for peptide bonds on the carboxy terminal side of aspartic and glutamic acid residues.

For V8 limited proteolysis, a molar ratio of substrate to protease of 200:1 was used in 100mM Tris pH 7.8, 0.2% SDS. One reaction was set up and preincubated without protease for 15min at 37°C. After addition of V8 protease, samples (60µg of protein) were withdrawn at the desired time points (i.e. after 0, 5, 10, 15, 30, 45, 60, 90, and 120min), mixed with Laemmli buffer and immediately at 95°C for 10min to fully inactivate V8 protease.

1/3rd of the reaction was subjected to SDS-PAGE (15% SDS gel) and Coomassie Blue staining to confirm the success of proteolysis. For subsequent Western blotting, 1/10th of the reaction was applied.

E.2.13 Bisulfite conversion and analysis of CpG site methylation

The methylation status of a DNA sequence can best be determined using sodium bisulfite treatment. Incubation of the target DNA with sodium bisulfite results in conversion of unmethylated cytosine residues into uracil, leaving the methylated cytosine unchanged. Therefore, bisulfite treatment gives rise to different DNA sequences for methylated and unmethylated DNA.

E.2.13.1 DNA template for bisulfite conversion

For DNA methylation studies, a DNA fragment from the pGA BNA-601-m1 vector (E.1.8) carrying a modified 601 nucleosome positioning sequence ((Thåström et al. 2004b), modified according to G. Längst) and flanking regions was PCR amplified with oligonucleotides MF79/80 (E.1.7) yielding a 342bp DNA fragment with 27 CpG sites.

PCR reaction was performed as described (E.2.10.4) and PCR fragments PEG precipitated (E.2.2.2). Nucleosomal template was prepared with drosophila histones by salt dialysis (E.2.10.2) with a histone to DNA ratio that would yield exclusively nucleosomal DNA. As competitor DNA the CpG less vector pCpGL-basic was used (E.1.8).

E.2.13.2 DNA methylation reaction

The DNA methylation reaction with Dnmt3a/b was carried out in a reaction volume of 40µl in DNA methyltransferase buffer (20mM Hepes, pH 7.6, 1mM EDTA, 1mM DTT). Dnmt3a and Dnmt3b2 were used at a concentration of 600nM and 200nM, DNA or nuclesomal DNA (CpG sites) for Dnmt3a and Dnmt3b2 at 600nM and 100nM respectively, BSA at 0.2µg/µl and SAM (Sigma A7007, 10mM) at 250µM.

The reaction was mixed well and incubated for 1 hour at 37°C. Another 250µM SAM was added following incubation for 1-1,5 hours. This step was repeated twice. The reaction was heat-inactivated at 65°C for 20min. 40µl of the reaction were directly subjected to bisulfite conversion.

E.2.13.3   Bisulfite conversion with Epitect Kit (Qiagen)

40µl of the DNA methylation reaction was processed with the Epitect bisulfite conversion kit (Qiagen) with the following exceptions. The last 60°C incubation step was prolonged from 2h 55min to 6 hours. After DNA workup, the two DNA eluates were combined following PCR amplification of bisulfite converted DNA.

E.2.13.4   PCR amplification of bisulfite converted DNA

After bisulfite treatment of DNA, the upper and lower strand are no longer complementary to one another and thus can be individually analyzed.

The upper (+) and the lower strand (-) were PCR amplified with primer pairs MF81/82 and MF112/113 respectively. The PCR reaction was performed as described for colony PCR (E.2.2.5) except that 8µl of the bisulfite converted DNA were used as template, the annealing temperature was at 56°C and 40 amplification cycles were applied.

E.2.13.5   TA-Cloning of PCR fragments and sequencing

PCR fragments (3µl) were cloned into the pGEM-T-EASY vector (Promega) according to the manufacturer's instructions.

E.2.13.6   Analysis of bisulfite converted DNA

Analysis of bisulfite converted DNA was done with BiQ ANALYZER software (http://biq-analyzer.bioinf.mpi-inf.mpg.de/) that had been provided by C. Bock (Bock et al. 2005).

Sequencing files in txt or fasta format are uploaded into the program following a ClustalW alignment against the non-bisulfite treated DNA of the same strand. The program guides through multiple steps of quality assurance, checking for right orientation, sufficient bisulfite conversion rate (90% is the default cut-off) and identical sequences. Each step can be corrected manually, giving the possibility to account for CpA and CpT methylation that is normally evaluated as incomplete bisulfite conversion by the program. The results are presented in a single HTML documentation file. The raw data is presented as both, "derived methylation data" in which the CpG site number with the corresponding methylation status is given (1= meC; 0= C, X= non CpG or ambiguous position) and as "results in machine readable format" in which the position of the CpG site (distance between CpG and CpG = number of bp+2) and the respective methylation status is shown. Both data can be copied and pasted as unicode format into an Exel spreadsheet and subsequent statistical analysis be performed.

E.2.14 MALDI – Matrix Assisted Laser Desorption Ionization

E.2.14.1   Sample preparation for protein identification by MALDI-MS analysis

Proteins to be identified were separated via gel electrophoresis and subsequently sent to MALDI-MS identification either to the Zentrallabor für Proteinanalytik, LMU München, or to the Prof. Dr. R. Deutzmann, University of Regensburg. There, proteins were subjected to tryptic digestion and analyzed via MALDI-MS.

20µl of previously prepared SDS gel electrophoresis samples were loaded on 4 -12% NuPage gradient gels and run in MOPS running buffer containing antioxidants for 1.5 hours at 200V and 50mA. The gel was stained with Simple Stain (Invitrogen) according to instructions given and protein bands unique for "specific" beads cut out and sent for MALDI analysis.

E.2.14.2   MALDI analysis following immunoprecipitation

For MALDI analysis Dnmt1 was immunoprecipitated with 50µl proteinG sepharose cross-linked with anti Dnmt1 antibody 2C1 (E.2.12.2) from 9mg placenta nuclear extract (E.2.9.1), 4,5mg Hela S3 nuclear extract (E.2.9.2) and 2mg MNase released Hela S3 nuclear extract E.2.9.3). Prior to immunoprecipitation the extracts were precleared with 50µl proteiG sepharose for 2 hours at 4°C. Immunoprecipitation was carried out in 1x PBS supplemented with protease inhibitors for 2h at 4°C. Beads were washed 3 times with 1x PBS with 10min incubation in-between following addition of 40µl HU buffer and boiling 10min at 65°C. Proteins bands of interest were treated as described above.

E.2.14.3   MALDI analysis using iTRAQ labeling

Immunoprecipitation was performed as described (E.2.14.2) and bound proteins were eluted from the 'beads' with 100µl 100mM glycine pH 3.0 (5min incubation) by acidic denaturation. The samples were neutralized with 1/th volume of 500mM Tris pH 8.0, 1.5M NaCl and methanol/chloroform precipitation of proteins performed as described in the following:

Methanol/-Chloroform precipitation

Up to 200µl of protein sample can be processed in a 2ml reaction tube.

400µl of methanol is added to 100µl of protein sample and mixed well by vortexing. Additional 100µl of chloroform are added and once again mixed. For phase separation 300µl of water are added to the sample and mixed vigorously. After incubation on ice for 5min, the sample is centrifuged (5min, 4°C, 130000g) following removal of the upper phase while keeping the interphase with precipitated proteins. 300µl of methanol is added and again incubated on ice for 5min following centrifugation. The supernatant is removed, the protein pellet dried in a vacuum pump and stored until use at -20°C.

iTRAQ labeling

Lyophilized protein samples were resuspended in 20 µl dissolution buffer and reduced with 5mM Tris-(2-carboxyethyl) phosphine at 60°C for 1 h. Cysteins were blocked with 10mM methyl methanethiosulfonate (MMTS) at room temperature for 10 min as described previously (Ross et al. 2004; Chen and Andrews 2009). After tryptic digestion (3µg pure trypsin) for 20 h at 37°C, 70 µl ethanol was added to the needed vials of iTRAQ™ reagents. Tryptic peptides of the 'specific' and 'control' immunoprecipitations were incubated with different combinations of the four iTRAQ™ reagents for 2h at room temperature. The two labeling reactions were combined and lyophilized.

Separation of peptides by liquid chromatography (LC):

The combined differently labeled peptides were dissolved in 40ul 0.1% TFA for 2h at ambient temperature following centrifugation (@10min, 13,000g). The supernatant was recovered, 10ul loaded on a C18-Pep-Mep reversed phase column (75um i.D. x 15cm) and peptides separated with the nano-flow HPLC-system (Dionex) applying a linear gradient of 5% to 95% of buffer B (80% acetone-nitril, 0.05% TFA) for 135 min. Fractions were collected every 20s for 127min, automatically mixed with 5 volumes of CHCA-matrix (2mg/ml in 70% aceton-nitrile, 0.1% TFA) and spotted on a MALDI-target by the probot-system (Dionex).

MALDI-MS/MS Analysis:

Spotted fractions were analyzed with a MALDI-TOF/TOF-system of the 4700 series (Applied Biosystems). The Cal 4700 standard peptide mixture was used routinely for calibration. For ionization the laser intensity was adjusted from sample to sample and usually 1000 shots in MS-mode and 2500 shots in MSMS-Mode were applied. The MS spectrum was recorded and subsequently the six most intense peaks per spot were further fragmented yielding the respective MSMS spectra. In order to avoid peptides derived from IgG-molecules or trypsin, prominent peptide-masses of these molecules were placed on an eclusion list.

Database-search and data-evaluation:

The measured m/z ratios were assigned to the peptide and the respective protein by MASCOT database search in the human database. Only non-redundant peptides with a C.I. > 95% were included in the analysis. The peak area for the iTRAQ reporter ions were interpreted, corrected by the GPS-Explorer software and the raw dataset exported to Microsoft Excel. The average of all peptides of a given protein were calculated and outliers were deleted by manual evaluation. The ratios of the iTRAQ reporter-ion derived from the 'specific' IP over iTRAQ reporter-ions derived from 'control' IP were established.

E.2.15 CHIP- chromatin immunoprecipiation

Chromatin immunoprecipitation (CHIP) is a widely applied technique to show localization of factors on DNA at certain genomic loci. Proteins are formaldehyde cross-linked either directly to the DNA or via interaction partners. After solubilization and fractionation of the chromatin

POI's can be immunoprecipitated via a target specific antibody together with the associated chromatin. After protein digest and reversal of the formaldehyde cross-link the co-immunoprecipitated DNA can be purified. In the case of known targets the DNA can be directly analyzed in qPCR or if no target gene is known, be amplified for Micro-Array analysis which is referred to as CHIP-on-CHIP.

The following protocols for CHIP were adapted from protocols kindly provided by Dr. A. Rascle and Dr. A. Németh.

E.2.15.1   CHIP buffers, chemicals and enzymes

If not stated differently, all solution were prepared with milliQ water and filtered through a 0,22µm filter. In addition, SDS(+), Triton and IP buffer were supplemented with protease inhibitors (10ug/ml Aprotinin, 10ug/ml Leupeptin, 0.5mM PMSF) prior to use.

Filter tips and 1,5ml reaction cups were from Sarstedt (Biosphere, DNAse and RNAse free). If not stated differently all solutions were filtered (0,022µm) and stored at room temperature.

SDS(+) Buffer *:		
	100mM NaCl 5M:	5ml
	50mM Tris pH 8.0	1M: 12.5ml
	5mM EDTA 0.5M:	2.5ml
	0.5% SDS 20%:	6.25ml
	250ml	

SDS(-) Buffer *:   Same as SDS(+) without SDS – used on cells not FA cross-linked when testing antibodies: cell pellet is resuspended in SDS(-) Buffer first, then SDS is added to a final concentration of 0.5%.

Triton Dilution Buffer *:		
	100mM NaCl 5M:	5ml
	100mM Tris pH 8.0	1M: 25ml
	5mM EDTA 0.5M:	2.5ml
	5% Triton X-100	20%:
	62.5ml	
	250ml	

IP Buffer *:   1 volume SDS(+) Buffer + 0.5 volume Triton
Dilution Buffer

Add protease inhibitors prior to use

Eltuion Buffer :   1% SDS, 0.1M NaHCO$_3$ (always prepare fresh from stock components; 20% SDS, 1M NaHCO$_3$)

150mM Wash Buffer :		
	150mM NaCl 5M:	15ml
	20mM Tris pH 8.0	1M: 10ml
	5mM EDTA 0.5M:	5ml

		1% Triton X-100	20%:	25ml
		0.2% SDS 20%:		5ml
		500ml		

500mM Wash Buffer :		500mM NaCl 5M:		50ml
		20mM Tris pH 8.0		1M: 10ml
		5mM EDTA 0.5M:		5ml
		1% Triton X-100	20%:	25ml
		0.2% SDS 20%:		5ml
		500ml		

LiCl Wash Buffer :		0.5% (w/v) Deoxycholic acid	10%:	25ml
		1mM EDTA 0.5M:		1ml
		250mM LiCl 2M:		62.5ml
		0.5% (v/v) NP-40	10%:	25ml
		10mM Tris pH 8.0		1M: 5ml
		500ml		

TE Buffer:	10mM Tris, pH 8.0
	1mM EDTA
	50ml

Glycogen (Roche #901-393; 20mg/ml; -20˚C)

Proteinase K (SIGMA P-6556; 20mg/ml stock in H2O; -20˚C)

RNAseA (Invitrogen, 20mg/ml, from Mini-prep kits, stored at room temperature)

ProteinG sepharose (GE Healthcare, from E. Kremmer):

ProteinG sepharose stored in 20% ethanol at 4°C is washed twice with 1x PBS and three times with IP buffer). Usually 300 to 400µl proteinG beads are resuspended in 1000µl IP buffer supplemented with 500µg/ml BSA (Fatty Acid free SIGMA A-7511; 25mg/ml stock in H2O) and 500µg/ml Salmon Sperm DNA (Gibco 15632-011) and incubated on wheel for a few hours and stored at 4˚C.

E.2.15.2 CHIP antibodies

The following antibodies were used for chromatin immunoprecipitation.

Table 10 Antibodies for chromatin immunoprecipitation

antibody	source	species	amount
anti Dnmt1 2G3-1, 2E8-1, 2C1, 2C12	E. Kremmer, Helmoltz Gesellschaft	rat monoclonal, TCS	1:1:1:1 mixture, 1300µl/60µl slurry proteinG sepharose as titrated
anti H3	abcam ab 1791	rabbit polyclonal	5µg
anti HAUSP/ USP7	Bethyl laboratories	rabbit polyclonal	10µg

anti ICBP90/NP95	BD Transduction laboratories 612264	mouse monoclonal, IgG2a	5µg
anti ICBP90	C.Bonner, references (Hopfner et al. 2000),(Hopfner et al. 2001)	mouse monoclonal	5µg
anti Sp1	Upstate 07-645	rabbit polyclonal	10µg
Anti RNAPII CTD 8WG16 (non-Ph-CTD)	D. Eick; (Thompson et al. 1989; Xie et al. 2006)	mouse monolconal, TCS	1000µl / 60µl slurry protein G sepharose, as titrated
IgG rat normal	sc-2026	rat polyclonal	4µg
IgG rabbit normal	sc-2027	rabbit polyclonal	4µg

E.2.15.3   Formaldehyde cross-link of mammalian cells

Mammalian cells of interest (E.1.11) were grown in their respective medium on 15cm tissue culture plates to a confluency of 60-80%. Prior to fixation, cells from o 15cm plate were detached with Trypsin/EDTA treatment and the cell number determined.

The other culture dishes were subsequently subjected to the formaldehyde cross-link procedure. Tissue culture plates were put on a shaking platform and fixation started with the addition of formaldehyde solution (SIGMA F1635) to a final concentration of 1% (550µl of 37% solution to 20ml medium). Fixation was carried out for 10-20min at room temperature and stopped with the addition of 800µl 3.25M glycine (125mM final concentration) following 5min incubation. Cells were then washed twice with 10ml ice-cold 1xPBS, harvested, adjusted to $2x10^7$cells/ml with 1xPBS and 1ml aliquots snap frozen in liquid nitrogen and stored at -80°C.

E.2.15.4   Cell lysis and chromatin isolation

Cell pellets of $2x10^7$ cells were properly resuspended in 1ml SDS(+) buffer (including protease inhibitors). Samples were cooled on ice.

Sonication was performed with 7 cycles of 20 bursts (50% output control, 20% intensity output (position 3)) with 30sec cooling in-between.

After sonication, ½ volume of Triton Dilution buffer was added and the sample stored on ice until all cell pellets had been worked up. Cell debris was removed by centrifugation (5min, 16000g, 4°C) and the supernatant used for subsequent immnoprecipitations.

E.2.15.5   Chromatin Immunoprecipitation

The efficiency of the immunoprecipitation reaction depends on multiple factors: the amount of one's protein of interest (POI) in the cell, the quality of the specific antibody in immunoprecipitation, buffer conditions and the amount of antibody used per IP reaction. For optimal results these parameters should be verified in pilot experiments.

Initially, the immunoprecipitation setup was used for $3.3x10^6$ cells, but was then applied on $2x10^7$ cells.

Preclearing of the whole cell lysate (E.2.15.4) was performed with 60µl slurry of preblocked proteinG sepharose/2x10^7 cells (E.2.15.1) for 1h at 4°C. After centrifugation (5min, 500g, 4°C) the supernatant, which was then referred to as Input lysate, was used for specific immunoprecipitation. 2x 50µl were kept for the Input (total) control and stored on ice until the DNA workup (see below). The precleared lysate, although not recommended, can be frozen on dry ice an stored up to several weeks at -80°C.

Immunoprecipitation was carried out with 1.35ml lysate/IP corresponding to approximately 2x10^7 cells/IP (27x of input). The primary antibody was added following incubation for 1.5h. 60µl slurry of preblocked proteinG sepharose was dispensed per IP using a cut tip and subsequently incubated for another 2.5h. A no antibody control (IgG or protein A alone) was included.

When working with an antibody tissue culture supernatant (TCS) the preblocked proteinG sepharose was incubated for at least 2 hours with an adequate amount of TCS with 10% IP buffer and afterwards washed twice with IP buffer. The input lysate was then directly incubated with the antibody coupled proteinG beads.

The Immuno-complexes bound to proteinG sepharose were washed with volumes of 1ml according to the procedure outlined below to remove unspecific protein and DNA interactions. Washing steps were carried out at 4°C.

2x IP Buffer - short

2x 150mM NaCl Wash Buffer -short

2x 500mM NaCl Wash Buffer – 5min on wheel

4°C

2x LiCl Wash Buffer – 5min on wheel 4°C

2x TE – short (buffer and washing at RT)

Elution of chromatin immuno-complexes from proteinG sepharose was performed in two steps at 37°C for 15min at 800rpm. The first elution was done with 230µl of elution buffer and the second elution with 200µl elution buffer. 200µl were withdrawn after each step, combined and transferred into a 500µl PCR reaction cup for the DNA work-up (see below)

The input DNA was filled up to 400µl with elution buffer and treated in parallel with the IP samples.

E.2.15.6   Reverse cross-link and purification of DNA

2µl of RNAse (20mg/ml) were added to Input, IP, DNA and pellet samples and incubated for 2 hours at 37°C. 5µl of proteinaseK (20mg/ml) were added following incubation for 4 hours at 42°C. Reversal of cross-link was performed at 65°C for 8 hours. For convenience these steps were carried our overnight in the Perkin Elmer PCR machine.

DNA purification was done as described in the following:

400µl sample together with 50µl water and 100µl 2M LiCl are transferred into a 1.5 ml reaction cup. 500µl of Phenol/Chloroform/Isoamylalcohol (25/24/1, pH 8.0, Roth) are added

and the mixture is vortexed for 1min. After centrifugation (5min, 13000g, RT) 500µl of the upper aqueous phase are transferred into a new reaction cup, 2µl glycogen (20mg/ml) and 1ml ethanol are added. Ethanol precipitation is performed for 1h at -20°C, following centrifugation (30min, 13000g, 4°C) and washing with 1ml of 70% ethanol. The white pellet is dried for 30min at 37°C and dissolved in 40µl of TE buffer.

The DNA is diluted to 200µl with milliQ water and stored at-20°C.

4µl are used for each qPCR reaction.

E.2.16 Quantitative REAL-TIME PCR (qPCR)

E.2.16.1 qPCR - principles and theory

In general, the polymerase chain reaction (PCR) is a method to amplify a DNA segment of choice *in vitro* with appropriate oligonucleotides. A target double-stranded (ds) DNA is incubated with a heat resistant DNA polymerase (Taq, isolated form the bacteria *Thermus aquaticus*) desoxynucleotides and a vast surplus of oligonucleotides complementary to the sense and anti-sense strand of the region on interest to be amplified. During the course of multiple rounds of denaturation, primer annealing and DNA polymerization the target DNA fragment bordered by the specific primers is amplified.

With every cycle of new synthesis and denaturation the amount of the target DNA segment is doubled. Thus, the PCR reaction leads to an exponential amplification, since the newly synthesized DNA provide for an additional template.

Quantitative REAL-TIME PCR (in the following referred to as qPCR) is a very sensitive method that not only detects extremely low amounts of synthesized dsDNA, but also allows to record the kinetic course of the reaction and thus to determine the amount of DNA at the onset of the reaction.

The initial amplification reaction is described as follows:

$$Z_{(n)} = Z_{(0)} * A_v{}^n$$

where Z(*n*) is the amount of target DNA after amplification with the cycle number *n*. Z(*0*) is the initial amount of DNA at the beginning of the reaction. The basis of the exponential function, is referred to as amplification value A_v with a maximum value of 2 if the reaction runs with reaction efficiency *E* of 1.0 thus 100%. From the formula above, it is evident that little variations in the reaction's efficiency lead to drastic differences in the amount of product. The efficiency of the reaction is primarily dependent on the optimization of the PCR reaction and can vary substantially according to reaction conditions and the quality of the oligonucleotides.
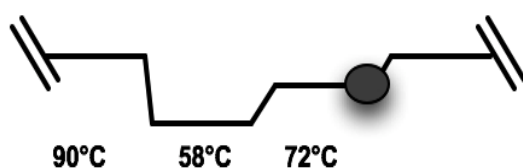
Figure 63 Sheme of a typical qPCR cycle

Shematic view of a typical qPCR cycle comprising a 90°C denaturation step, an annealing step (indicated annealing temparature of 58°C) and an elongation step at 72°C. At the end of the elongation step the fluorescence signal (grey bubble), which is directly proportional to the amount of dsDNA in the reaction tube, is recorded.

At the end of the reaction, when the activity of the *Taq* polymerase decreases and PCR components become limiting, the amount of product reaches a constant value – the plateau of the reaction. The kinetic of the reaction is determined through the change in the intensity of the fluorescence signal which is recorded at the end of each elongation cycle.

In our laboratory the detection of dsDNA is performed with the SYBR Green reagent (Roche), that after intercalation into ds DNA excerts characteristic excitation and emission spectra at 509 and 526nm respectively. The measured fluorescence signal is directly proportional to the amount of dsDNA in the reaction tube. Hence, a clear disadvantage of this method is that also potential primer dimers or unspecific reaction products contribute to the fluorescence signal and thus taint the quantitative analysis. A melt curve analysis provided by the qPCR cycler (Corbett Reseach, RG300), verifies the purity of the reaction product.
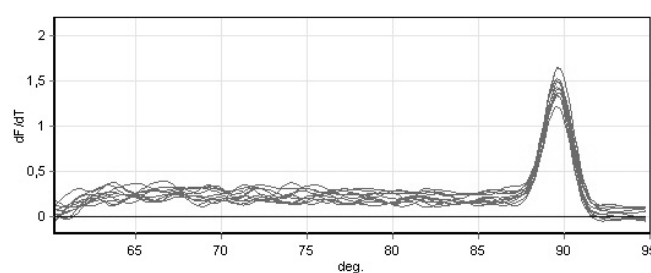
Figure 64 qPCR - melt curve analysis

Melt curve analysis at the end of a qPCR run. The temperature is raised in 0.5°C increments from 60°C to 95°C and the fluorescence signal is recorded. As can be seen in the diagram only one specific product was amplified.

E.2.16.2   Absolute, relative and comparative quantitation

The basis of quantitation is the *ct*-value (cycle threshold) that is defined as the intersection between an amplification curve and a threshold line. The threshold must be set in the linear phase of the amplification plot – where the logarithm of the fluorescence signal is plotted against the cycle number (Figure 65).

Absolute quantitation

Absolute quantitation is only possible if a standard curve of one's target DNA with one specific primer set is generated. Therefore a dilution series of known concentration is amplified and the respective *ct*-values of the DNA samples are plotted against the logarithm of the respective concentration. When analyzing an unknown sample with the same primer pair, the concentration can be read out from the standard curve with the determined *ct*-value.

Relative quantitation

Very often a relative increase or decrease in comparison to a defined sample is of interest. For example in CHIP analysis the ratio of a certain target DNA immunoprecipitated with a specific antibody versus the IgG control is the readout of enrichment. In this case the same primer pair with the same amplification efficiency (E.2.16.3) is used for both samples. Thus, either assuming an amplification value of 2.0 or having determined the exact primer efficiency for the specific primer pair, one can calculate a relative concentration for both samples with the following formula:

$$C_r = A_v^{-ct}$$

where C_r is the relative concentration, A_v the amplification value and ct the cycle threshold value. The ratio of the calculated concentrations gives the degree of enrichment.

Comparative quantitation

The comparative analysis mode of the RotorGene software calculates in principle a relative concentration of all samples analyzed as described above. But instead of assuming an optimal amplification value, the software determines from the exponential phase of each qPCR reaction a respective amplification value that is set as basis for the formula above. For optimal primer pairs the amplification value is virtually the same for high and low DNA concentrations (see primer efficiency) and thus allows the same calculations as mentioned above. Interestingly, the amplification values were always 10-15% lower than the amplification values determined manually (E.2.16.3). Of course, this can have a profound effect on the data, for my example in CHIP analysis it could lead to a less significant enrichment of a certain target DNA versus IgG control.
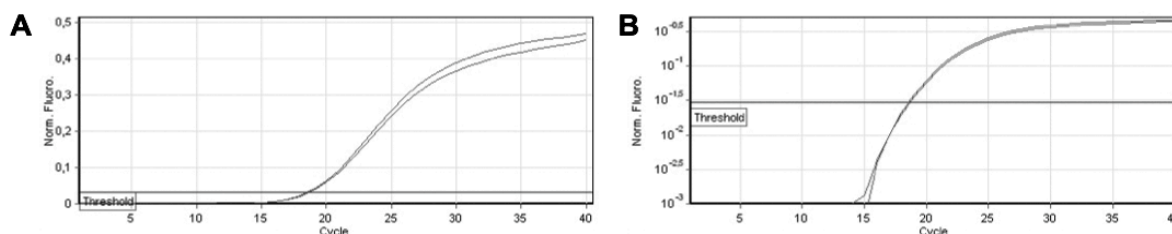
Figure 65 Exponential and logarithmic amplification curve

A.) Exponential amplification curve of a sample in duplicate. The norm –fluorescence is blotted against the cycle number. The threshold line is indicated. B.) Logarithmic plot of the amplification curve (A). The threshold line was placed in the linear phase of the reaction - assuming an optimal qPCR condition.

E.2.16.3 Primer efficiency

For optimal and reliable results it is crucial that the PCR reaction works equally well for samples with a high and a low DNA content. Also for comparison of different genomic loci it is indispensible that the amplification efficiency E of a PCR reaction using SYBR Green lies at least between 90% and 110% better between 95% and 105%.

In order to determine the amplification efficiency of a given primer pair, five 1:5 dilutions of target DNA (sonified HCT-116 genomic DNA, E.2.16.7) were prepared and a standard curve as described under absolute quantitation was generated.

From the linear slope of the graph (calculated by the RotorGene software) the amplification value Av and the reaction efficiency E are calculated according to the following formulas:

$$A_v = 10^{(-1/m)}$$

$$E(\%) = \left(\frac{A_v}{2}\right) * 100$$

where m is the slope of the standard curve.
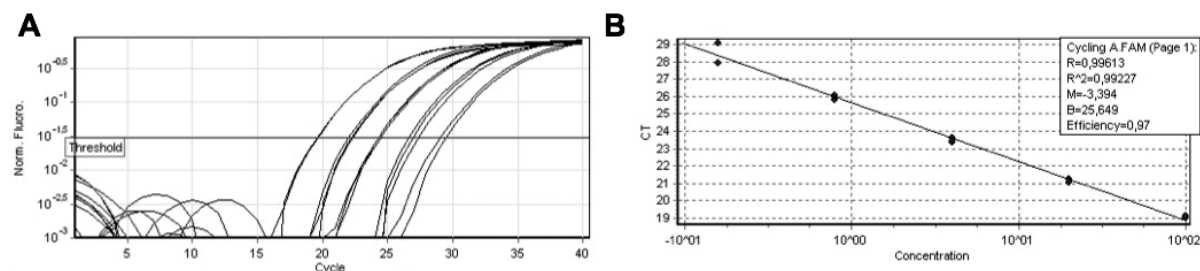
Figure 66 DNA dilution series and standard curve analysis

A.) Amplification curves of five samples in triplicate in 1:5 dilution steps plotted in logarithmic scale. B.) Standard curve as given by the RotorGene Software. The *ct* values are plotted against the logarithm of the concentration. The slope M and the efficiency E is given in graph as well as R^2 which is a statistical parameter indicating the correlation of two values. A R^2 value >0.99 provides good confidence in correlating two values.

Table 11 Amplification value and primer efficiency

Gene	primer pair	Amplification value A_v	Efficiency E (%)
HoxA7	MC15/16	2,088	104,40%
HoxA7	MC17/18	2,108	105,40%
HoxA7	MC113/114	2,004	100,20%
HoxA7	MC117/118	1,924	96,10%
HoxA7	MC121/122	1,995	99,80%
WNT1	MC23/24	1,82	91,40%
WNT1	MC135/136	2,014	100,70%
WNT1	MC99/100	2,05	102,60%
WNT1	MC127/128	1,936	96,80%
WNT1	MC129/130	2,12	106,00%
IGFBP3	MC39/40	2,01	100,50%
IGFBP3	MC41/42	2,009	100,40%
IGFBP3	MC107/108	2,033	101,70%
IGFBP3	MC109/110	1,979	98,90%
POLR2A	MC101/102	1,994	99,70%

E.2.16.4   qPCR reaction setup

qPCR reaction setup:

	µl/ reaction
master mix (MM)	9.67
HotStar Taq Qiagen 5u/ul	0.08
[1:400 000] SG stock (SYBR Green)	0.25
primer 1 [10uM]	0.40
primer 2 [10uM]	0.40
water	5.2
total	16.0

Master-Mix (MM)

	µl/ reaction
Qiagen 10xPCR buffer	2.0
MgCl2 Qiagen 25mM	0.8
25mM dNTPs	0.16
Water	6.71
total	9.67

4µl of DNA-sample are added to each qPCR reaction (total volume 20µl). In the total reaction MgCl$_2$, oligonucleotides and dNTP's are at a final concentration of 2.5mM, 0.2µM and 200µM respectively. The SYBR Green concentration for optimal detection had been titrated empirically. The qPCR reaction was performed in the RotorGene RG300 machine from Corbett Research. SYBR Green was excited in the FAM/SYBR channel at 470nm and the fluorescence detected at 510nm.

A three – step PCR program was used:

cycle step	temperature	time	number of cycles
initial denaturation	95	15min	1
denaturation	95	15sec	40
annealing	58	20sec	
extension	72	30sec	
Melt curve	60-95	0.5°C/5sec	

E.2.16.5   qPCR oligonucleotides and gene targets

qPCR primer were designed using the freely available *perlprimer* software (http://perlprimer.sourceforge.net/, (Marshall 2004)) with the following modulation.

The primer annealing temperature Tm was set to 65-68°C with a temperature difference of 1-2°C. The amplicon length was chosen between 50 and 150bp. The primer length was set to 20-28 nucleotides. The primer pairs with the lowest ∆G- value for full dimers and if possible with a C or G at their 3'end were chosen.

Binding of oligonucleotides to unique genomic loci was verified using the *UCSC Genome Browser* which was also chosen for the retrieval of genomic sequences.

Table 12 qPCR primers for CHIP analyis

Name	Target gene	Sequence
MC15	HoxA7	TGAGGTCGGGTTTATGGTGTG
MC16	HoxA7	AACCCTTCCCCTAAACGCC
MC17	HoxA7	CCTGGACCCTCTGAAAGTGATG
MC18	HoxA7	CACCATAAACCCGACCTCACA
MC23	WNT1	CCAGGGTTGTTAAAGCCAGACT
MC24	WNT1	CAGTTGCGGCGACTTTGG
MC39	IGFBP3	GGCTCCCTGAGACCCAAATG
MC40	IGFBP3	CGCTCCGCATTCGTGTGTA

MC41	IGFBP3	CACTCCACCCCCACAAACTC
MC42	IGFBP3	CTTCGGTGACCAACAGAGGAC
MC99	WNT1	GTCCTCCTAAGTCCCTTCCTATTCTC
MC100	WNT1	CCCAACCTCATTTCCACATCATCAC
MC101	POLR2A	TTTGCTGAAGATGAAACCGTTGTCC
MC102	POLR2A	CTTTAATCCCACCGCCTCTCCT
MC107	IGFBP3	GGAGACAAGGTATGTGGGCTGTG
MC108	IGFBP3	CAGCACTGATGGAAGGATGAACTC
MC109	IGFBP3	TCAGAGACTCGAGCACAGCA
MC110	IGFBP3	CAACACAGCCGCCTAAGTCAC
MC113	HoxA7	CTGCCCTGAGAATGTGCTGAG
MC114	HoxA7	GTGCCAAGCCAGAGAAGGAG
MC117	HoxA7	TTTATGAGTTGTTCGGCCCTTCCA
MC118	HoxA7	GTTCATGTTCACGGTTCTCATCCAC
MC121	HoxA7	ATTTGAGCCTCTTGCCCTTCC
MC122	HoxA7	CTCCGCCAATCTCAGCAGTC
MC127	WNT1	TCTCTTCCCACCTCTGCTTGAC
MC128	WNT1	CCTTTATCCCTTATGAGTTTCTTCCCAC
MC129	WNT1	TGCCATGTGACGAAGAAAGAGCC
MC130	WNT1	AAGTTGCTGGGAGGTGGGAG
MC135	WNT1	GGATTTCCCTGACCACAGCC
MC136	WNT1	GAGATGCTTAACCGCCCAGGA

Table 13 Genes of interest in CHIP analysis

Gene	Region	Primer pair	comment
HoxA7	chr7:27,164,029-27,164,237	MC15/16	Dnmt1 CHIP, Region E, (Wu et al. 2008)
HoxA7	chr7:27,164,029-27,164,237	MC17/18	
WNT1	chr12:47,658,373-47,658,671	MC23/24	Dnmt1 CHIP, (Viré et al. 2005)
IGFBP3	chr7:45,927,409-45,927,917	MC39/40	MSP analysis by R. Kappler
IGFBP3	chr7:45,927,409-45,927,917	MC41/42	
POLR2A	chr17:7,323,162-7,363,161	MC101/102	Serves as a reference gene

E.2.16.6   qPCR evaluation of CHIP samples

DNA from CHIP samples was purified as described in E.2.15.6 and 4µl taken per qPCR reaction. All samples were analyzed in triplicate. For the primer pairs of the genomic regions of interest the primer efficiency was determined (E.2.16.3) and each sample analyzed as described for relative quantitation (E.2.16.2). In order to provide for statistical analysis of the qPCR reaction, each "specific" CHIP sample was divided by all three IgG control reactions yielding 9 "specific" CHIP sample/ IgG ratios. From these data average value and standard deviation was calculated. For good qPCR samples the deviation from the average ct – value of the triplicate reaction was usually < 0.3, for low DNA content < 0.5. Due to the fact that the

DNA content of IgG control samples was at the edge of the detection limit, outliers with deviations > 0.5 were dismissed from the evaluation.

For the evaluation of three biological replicas, an average value and the respective standard deviation were derived from all ratios determined. This includes also results from two different primer pairs specific for the same region of interest, as given for example by MC15/16 and MC17/18 for the HoxA7 locus, as long as primer efficiencies are almost equal (average +/- 5%).

In publications it is often found that the specific enrichment of a DNA sample versus IgG control is plotted as percentage of the Input sample. Typical CHIP efficiencies for abundant DNA binding proteins and good antibodies are in the range of 1-10% of the Input sample. For histone H3 (RB gene promoter, HoxA7) and RNA PolymeraseII (POLR2A locus) efficiencies of 5%-7% and 9% respectively could be observed.

The enrichment of the POI's Dnmt1, ICBP90 and USP7 was reproducible in the range of 0.05% - 0.1% with $2x10^7$ cells/ IP reaction. Initially the amount of antibody necessary for almost full depletion of the target protein from a WCE of a given cell number was titrated for all proteins under investigation. This was done during the establishment of the CHIP procedure for whole cell extracts of $3.3x10^6$ cells from the LS174T cell line. When changing to the HCT-116 cell line, the amount of cells used/ IP reaction was raised to $2x10^7$ cells (factor of 6) but the amount of antibody only increased by a factor of 2. This could in part account for the low CHIP efficiency. Therefore in the evaluation the specific enrichment was not plotted as percentage of the Input.

E.2.16.7   Isolation of genomic DNA for qPCR analysis

In order to validate oligonucleotides designed for the amplification of target regions of interest in qPCR, genomic DNA from the cell lines of interest was isolated.

Cell lines of choice were grown on 15cm plates to confluency (usually 2-4 15cm plates). The medium was withdrawn and 6ml of lysis buffer (50mM Tris, pH 8.0, 20mM EDTA, 1% SDS) added. Cells were lysed immediately and RNAseA digest performed with 25µl (20mg/ml) for 2h at 37°C.

After addition of 25µl of ProteinaseK (10mg/ml, Sigma) tissue culture plates were incubated at 37°C overnight. The highly viscous solution was vortexed for 5-10min and 3-5 bursts of sonication applied in order to shear the genomic DNA. The DNA was precipitated with the addition of 0.5V of 7.5 ammoniumacetate and 2V of 100% ice-cold ethanol following centrifugation (30min, 4°C, 20,000g). After washing with 70% ethanol the DNA was dried (but avoid complete drying) and dissolved in 2-4ml of warmed milliQ water. Complete dissolving was achieved through incubation at 45°C in a thermo shaker.

If the DNA solution was still viscous, 2-3 bursts with the Branson Digital Sonifier (10-20% output, 2sec bursts) were applied. Approximately, 700-900µg of genomic DNA with an average size of 10-20kb were recovered from one 15 cm tissue culture plate.

Typically, 20ng of isolated DNA was used per qPCR reaction. For the determination of the primer efficiency in qPCR, genomic DNA was further sheared to 500 to 1000bp.

F REFERENCES

Aapola, U., Liiv, I., and Peterson, P. 2002. Imprinting regulator DNMT3L is a transcriptional repressor associated with histone deacetylase activity. *Nucleic Acids Res* **30**(16): 3602-3608.

Aapola, U., Scott, H.S., Ollila, J., Vihinen, M., Heino, M., Shintani, A., Kawasaki, K., Minoshima, S., Krohn, K., Antonarakis, S.E. et al. 2000. Isolation and initial characterization of a novel zinc finger gene, DNMT3L, on 21q22.3, related to the cytosine-5-methyltransferase 3 gene family. *Genomics* **65**(3): 293-298.

Achour, M., Jacq, X., Rondé, P., Alhosin, M., Charlot, C., Chataigneau, T., Jeanblanc, M., Macaluso, M., Giordano, A., Hughes, A.D. et al. 2007. The interaction of the SRA domain of ICBP90 with a novel domain of DNMT1 is involved in the regulation of VEGF gene expression. *Oncogene*.

Agalioti, T., Chen, G., and Thanos, D. 2002. Deciphering the transcriptional histone acetylation code for a human gene. *Cell* **111**(3): 381-392.

Aguirre-Arteta, A.M., Grunewald, I., Cardoso, M.C., and Leonhardt, H. 2000. Expression of an alternative Dnmt1 isoform during muscle differentiation. *Cell Growth Differ* **11**(10): 551-559.

Ahn, S.H., Kim, M., and Buratowski, S. 2004. Phosphorylation of serine 2 within the RNA polymerase II C-terminal domain couples transcription and 3' end processing. *Mol Cell* **13**(1): 67-76.

Amerik, A.Y. and Hochstrasser, M. 2004. Mechanism and function of deubiquitinating enzymes. *Biochim Biophys Acta* **1695**(1-3): 189-207.

Anindya, R., Aygun, O., and Svejstrup, J. 2007. Damage-Induced Ubiquitylation of Human RNA Polymerase II by the Ubiquitin Ligase Nedd4, but Not Cockayne Syndrome Proteins or BRCA1. *Mol Cell* **28**(3): 386-397.

Aoki, A., Suetake, I., Miyagawa, J., Fujio, T., Chijiwa, T., Sasaki, H., and Tajima, S. 2001. Enzymatic properties of de novo-type mouse DNA (cytosine-5) methyltransferases. *Nucleic Acids Res* **29**(17): 3506-3512.

Arima, Y., Hirota, T., Bronner, C., Mousli, M., Fujiwara, T., Niwa, S., Ishikawa, H., and Saya, H. 2004. Down-regulation of nuclear protein ICBP90 by p53/p21Cip1/WAF1-dependent DNA-damage checkpoint signals contributes to cell cycle arrest at G1/S transition. *Genes Cells* **9**(2): 131-142.

Arita, K., Ariyoshi, M., Tochio, H., Nakamura, Y., and Shirakawa, M. 2008. Recognition of hemi-methylated DNA by the SRA protein UHRF1 by a base-flipping mechanism. *Nature*: 5.

Avvakumov, G., Walker, J., Xue, S., Li, Y., Duan, S., Bronner, C., Arrowsmith, C., and Dhe-Paganon, S. 2008. Structural basis for recognition of hemi-methylated DNA by the SRA domain of human UHRF1. *Nature*: 5.

Baarends, W.M., Hoogerbrugge, J.W., Roest, H.P., Ooms, M., Vreeburg, J., Hoeijmakers, J.H., and Grootegoed, J.A. 1999. Histone ubiquitination and chromatin remodeling in mouse spermatogenesis. *Dev Biol* **207**(2): 322-333.

Baarends, W.M., Wassenaar, E., van der Laan, R., Hoogerbrugge, J., Sleddens-Linkels, E., Hoeijmakers, J.H., de Boer, P., and Grootegoed, J.A. 2005. Silencing of unpaired chromatin and histone H2A ubiquitination in mammalian meiosis. *Mol Cell Biol* **25**(3): 1041-1053.

Bachman, K. 2001. Dnmt3a and Dnmt3b Are Transcriptional Repressors That Exhibit Unique Localization Properties to Heterochromatin. *Journal of Biological Chemistry* **276**(34): 32282-32287.

Bacolla, A., Pradhan, S., Roberts, R.J., and Wells, R.D. 1999. Recombinant human DNA (cytosine-5) methyltransferase. II. Steady-state kinetics reveal allosteric activation by methylated dna. *J Biol Chem* **274**(46): 33011-33019.

Baker, R.T. and Board, P.G. 1991. The human ubiquitin-52 amino acid fusion protein gene shares several structural features with mammalian ribosomal protein genes. *Nucleic Acids Res* **19**(5): 1035-1040.

Bannister, A.J., Zegerman, P., Partridge, J.F., Miska, E.A., Thomas, J.O., Allshire, R.C., and Kouzarides, T. 2001. Selective recognition of methylated lysine 9 on histone H3 by the HP1 chromo domain. *Nature* **410**(6824): 120-124.

Bartee, L. and Bender, J. 2001. Two Arabidopsis methylation-deficiency mutations confer only partial effects on a methylated endogenous gene family. *Nucleic Acids Res* **29**(10): 2127-2134.

Bartolomei, M.S., Zemel, S., and Tilghman, S.M. 1991. Parental imprinting of the mouse H19 gene. *Nature* **351**(6322): 153-155.

Baumbusch, L.O., Thorstensen, T., Krauss, V., Fischer, A., Naumann, K., Assalkhou, R., Schulz, I., Reuter, G., and Aalen, R.B. 2001. The Arabidopsis thaliana genome contains at least 29 active genes encoding SET domain proteins that can be assigned to four evolutionarily conserved classes. *Nucleic Acids Res* **29**(21): 4319-4333.

Becker, P.B. and Hörz, W. 2002. ATP-dependent nucleosome remodeling. *Annu Rev Biochem* **71**: 247-273.

Becker, P.B. and Wu, C. 1992. Cell-free system for assembly of transcriptionally repressed chromatin from Drosophila embryos. *Mol Cell Biol* **12**(5): 2241-2249.

Beisel, C., Imhof, A., Greene, J., Kremmer, E., and Sauer, F. 2002. Histone methylation by the Drosophila epigenetic transcriptional regulator Ash1. *Nature* **419**(6909): 857-862.

Benetti, R., García-Cao, M., and Blasco, M.A. 2007. Telomere length regulates the epigenetic status of mammalian telomeres and subtelomeres. *Nat Genet* **39**(2): 243-250.

Berger, I., Fitzgerald, D.J., and Richmond, T.J. 2004. Baculovirus expression system for heterologous multiprotein complexes. *Nat Biotechnol* **22**(12): 1583-1587.

Bernstein, B.E., Mikkelsen, T.S., Xie, X., Kamal, M., Huebert, D.J., Cuff, J., Fry, B., Meissner, A., Wernig, M., Plath, K. et al. 2006. A bivalent chromatin structure marks key developmental genes in embryonic stem cells. *Cell* **125**(2): 315-326.

Bernstein, E. and Hake, S.B. 2006. The nucleosome: a little variation goes a long way. *Biochem Cell Biol* **84**(4): 505-517.

Bestor, T.H. 1988. Cloning of a mammalian DNA methyltransferase. *Gene* **74**(1): 9-12.

-. 2000. The DNA methyltransferases of mammals. *Hum Mol Genet* **9**(16): 2395-2402.

Bestor, T.H. and Ingram, V.M. 1983. Two DNA methyltransferases from murine erythroleukemia cells: purification, sequence specificity, and mode of interaction with DNA. *Proc Natl Acad Sci USA* **80**(18): 5559-5563.

Bienz, M. 2005. The PHD finger, a nuclear protein-interaction domain. *Trends Biochem Sci* **31**(1): 35-40.

Bird, A. 2002. DNA methylation patterns and epigenetic memory. *Genes Dev* **16**(1): 6-21.

Bird, A., Taggart, M., Frommer, M., Miller, O.J., and Macleod, D. 1985. A fraction of the mouse genome that is derived from islands of nonmethylated, CpG-rich DNA. *Cell* **40**(1): 91-99.

Bird, A.P. and Southern, E.M. 1978. Use of restriction enzymes to study eukaryotic DNA methylation: I. The methylation pattern in ribosomal DNA from Xenopus laevis. *J Mol Biol* **118**(1): 27-47.

Bonapace, I.M., Latella, L., Papait, R., Nicassio, F., Sacco, A., Muto, M., Crescenzi, M., and Di Fiore, P.P. 2002. Np95 is regulated by E1A during mitotic reactivation of terminally differentiated cells and is essential for S phase entry. *J Cell Biol* **157**(6): 909-914.

Bonfils, C., Beaulieu, N., Chan, E., Cotton-Montpetit, J., and MacLeod, A.R. 2001. Characterization of the human DNA methyltransferase splice variant Dnmt1b. *J Biol Chem* **275**(15): 10754-10760.

REFERENCES

Boritzki, T.J., Jackson, R.C., Morris, H.P., and Weber, G. 1981. Guanosine-5'-phosphate synthetase and guanosine-5'-phosphate kinase in rat hepatomas and kidney tumors. *Biochim Biophys Acta* **658**(1): 102-110.

Bostick, M., Kim, J.K., Estève, P.O., Clark, A., Pradhan, S., and Jacobsen, S.E. 2007. UHRF1 Plays a Role in Maintaining DNA Methylation in Mammalian Cells. *Science*.

Bourc'his, D. and Bestor, T.H. 2004. Meiotic catastrophe and retrotransposon reactivation in male germ cells lacking Dnmt3L. *Nature* **431**(7004): 96-99.

Bourc'his, D., Xu, G.L., Lin, C.S., Bollman, B., and Bestor, T.H. 2001. Dnmt3L and the establishment of maternal genomic imprints. *Science* **294**(5551): 2536-2539.

Boutell, C., Canning, M., Orr, A., and Everett, R.D. 2005. Reciprocal activities between herpes simplex virus type 1 regulatory protein ICP0, a ubiquitin E3 ligase, and ubiquitin-specific protease USP7. *J Virol* **79**(19): 12342-12354.

Brehm, A., Längst, G., Kehle, J., Clapier, C.R., Imhof, A., Eberharter, A., Muller, J., and Becker, P.B. 2000. dMi-2 and ISWI chromatin remodelling factors have distinct nucleosome binding and mobilization properties. *Embo J* **19**(16): 4332-4341.

Brinkman, A.B., Roelofsen, T., Pennings, S.W., Martens, J.H., Jenuwein, T., and Stunnenberg, H.G. 2006. Histone modification patterns associated with the human X chromosome. *EMBO Rep* **7**(6): 628-634.

Bronner, C., Achour, M., Arima, Y., Chataigneau, T., Saya, H., and Schinikerth, V. 2007. The UHRF family: Oncogenes that are drugable targets for cancer therapy in the near future? *Pharmacol Ther* **115**(3): 419-434.

Bronner, C., Hopfner, R., and Mousli, M. 2002. Transcriptional regulation of the human topoisomerase IIalpha gene. *Anticancer Res* **22**(2A): 605-612.

Brownell, J.E., Zhou, J., Ranalli, T., Kobayashi, R., Edmondson, D.G., Roth, S.Y., and Allis, C.D. 1996. Tetrahymena histone acetyltransferase A: a homolog to yeast Gcn5p linking histone acetylation to gene activation. *Cell* **84**(6): 843-851.

Canning, M., Boutell, C., Parkinson, J., and Everett, R.D. 2004. A RING finger ubiquitin ligase is protected from autocatalyzed ubiquitination and degradation by binding to ubiquitin-specific protease USP7. *J Biol Chem* **279**(37): 38160-38168.

Cao, R., Tsukada, Y., and Zhang, Y. 2005. Role of Bmi-1 and Ring1A in H2A ubiquitylation and Hox gene silencing. *Mol Cell* **20**(6): 845-854.

Chang, Y.S., Wang, L., Suh, Y.A., Mao, L., Karpen, S.J., Khuri, F.R., Hong, W.K., and Lee, H.Y. 2004. Mechanisms underlying lack of insulin-like growth factor-binding protein-3 expression in non-small-cell lung cancer. *Oncogene* **23**(39): 6569-6580.

Chedin, F., Lieber, M.R., and Hsieh, C.L. 2002. The DNA methyltransferase-like protein DNMT3L stimulates de novo methylation by Dnmt3a. *Proc Natl Acad Sci USA* **99**(26): 16916-16921.

Chen, C., Seth, A.K., and Aplin, A.E. 2006. Genetic and expression aberrations of E3 ubiquitin ligases in human breast cancer. *Mol Cancer Res* **4**(10): 695-707.

Chen, T. 2002. A Novel Dnmt3a Isoform Produced from an Alternative Promoter Localizes to Euchromatin and Its Expression Correlates with Active de Novo Methylation. *Journal of Biological Chemistry* **277**(41): 38746-38754.

Chen, T., Tsujimoto, N., and Li, E. 2004. The PWWP domain of Dnmt3a and Dnmt3b is required for directing DNA methylation to the major satellite repeats at pericentric heterochromatin. *Mol Cell Biol* **24**(20): 9048-9058.

Chen, T., Ueda, Y., Xie, S., and Li, E. 2002. A novel Dnmt3a isoform produced from an alternative promoter localizes to euchromatin and its expression correlates with active de novo methylation. *J Biol Chem* **277**(41): 38746-38754.

Chen, X. and Andrews, P.C. 2009. Quantitative proteomics analysis of pancreatic zymogen granule membrane proteins. *Methods Mol Biol* **528**: 327-338.

Cheng, X., Kumar, S., Posfai, J., Pflugrath, J.W., and Roberts, R.J. 1993. Crystal structure of the HhaI DNA methyltransferase complexed with S-adenosyl-L-methionine. *Cell* **74**(2): 299-307.

Chuang, L.S., Ian, H.I., Koh, T.W., Ng, H.H., Xu, G., and Li, B.F. 1997. Human DNA-(cytosine-5) methyltransferase-PCNA complex as a target for p21WAF1. *Science* **277**(5334): 1996-2000.

Ciechanover, A., Elias, S., Heller, H., Ferber, S., and Hershko, A. 1980. Characterization of the heat-stable polypeptide of the ATP-dependent proteolytic system from reticulocytes. *J Biol Chem* **255**(16): 7525-7528.

Citterio, E., Papait, R., Nicassio, F., Vecchi, M., Gomiero, P., Mantovani, R., Di Fiore, P.P., and Bonapace, I.M. 2004. Np95 is a histone-binding protein endowed with ubiquitin ligase activity. *Mol Cell Biol* **24**(6): 2526-2535.

Clague, M.J. and Urbé, S. 2006. Endocytosis: the DUB version. *Trends Cell Biol* **16**(11): 551-559.

Clapier, C.R. and Cairns, B.R. 2009. The Biology of Chromatin Remodeling Complexes. *Annu Rev Biochem*.

Cooper, D.N., Taggart, M.H., and Bird, A.P. 1983. Unmethylated domains in vertebrate DNA. *Nucleic Acids Res* **11**(3): 647-658.

Cremer, T., Küpper, K., Dietzel, S., and Fakan, S. 2004. Higher order chromatin architecture in the cell nucleus: on the way from structure to function. *Biol Cell* **96**(8): 555-567.

Cross, S.H., Charlton, J.A., Nan, X., and Bird, A.P. 1994. Purification of CpG islands using a methylated DNA binding column. *Nat Genet* **6**(3): 236-244.

Culhane, J.C. and Cole, P.A. 2007. LSD1 and the chemistry of histone demethylation. *Current opinion in chemical biology* **11**(5): 561-568.

Cummins, J.M., Rago, C., Kohli, M., Kinzler, K.W., Lengauer, C., and Vogelstein, B. 2004. Tumour suppression: disruption of HAUSP gene stabilizes p53. *Nature* **428**(6982): 1 p following 486.

Cummins, J.M. and Vogelstein, B. 2004. HAUSP is required for p53 destabilization. *Cell Cycle* **3**(6): 689-692.

Czermin, B., Schotta, G., Hülsmann, B.B., Brehm, A., Becker, P.B., Reuter, G., and Imhof, A. 2001. Physical and functional association of SU(VAR)3-9 and HDAC1 in Drosophila. *EMBO Rep* **2**(10): 915-919.

Daniel, J.A., Torok, M.S., Sun, Z.W., Schieltz, D., Allis, C.D., Yates, J.R., and Grant, P.A. 2004. Deubiquitination of histone H2B by a yeast acetyltransferase complex regulates transcription. *J Biol Chem* **279**(3): 1867-1871.

Datta, J., Majumder, S., Bai, S., Ghoshal, K., Kutay, H., Smith, D.S., Crabb, J.W., and Jacob, S.T. 2005. Physical and functional interaction of DNA methyltransferase 3A with Mbd3 and Brg1 in mouse lymphosarcoma cells. *Cancer Res* **65**(23): 10891-10900.

David, G., Grandinetti, K.B., Finnerty, P.M., Simpson, N., Chu, G.C., and Depinho, R.A. 2008. Specific requirement of the chromatin modifier mSin3B in cell cycle exit and cellular differentiation. *Proc Natl Acad Sci USA* **105**(11): 4168-4172.

de Napoles, M., Mermoud, J.E., Wakao, R., Tang, Y.A., Endoh, M., Appanah, R., Nesterova, T.B., Silva, J., Otte, A.P., Vidal, M. et al. 2004. Polycomb group proteins Ring1A/B link ubiquitylation of histone H2A to heritable gene silencing and X inactivation. *Dev Cell* **7**(5): 663-676.

DeChiara, T.M., Robertson, E.J., and Efstratiadis, A. 1991. Parental imprinting of the mouse insulin-like growth factor II gene. *Cell* **64**(4): 849-859.

Dellino, G.I., Schwartz, Y.B., Farkas, G., McCabe, D., Elgin, S.C., and Pirrotta, V. 2004. Polycomb silencing blocks transcription initiation. *Mol Cell* **13**(6): 887-893.

Dennis, K., Fan, T., Geiman, T., Yan, Q., and Muegge, K. 2001. Lsh, a member of the SNF2 family, is required for genome-wide

REFERENCES

methylation. *Genes Dev* **15**(22): 2940-2944.

Deplus, R., Brenner, C., Burgers, W.A., Putmans, P., Kouzarides, T., de Launoit, Y., and Fuks, F. 2002. Dnmt3L is a transcriptional repressor that recruits histone deacetylase. *Nucleic Acids Res* **30**(17): 3831-3838.

Di Croce, L., Raker, V.A., Corsaro, M., Fazi, F., Fanelli, M., Faretta, M., Fuks, F., Lo Coco, F., Kouzarides, T., Nervi, C. et al. 2002. Methyltransferase recruitment and DNA hypermethylation of target promoters by an oncogenic transcription factor. *Science* **295**(5557): 1079-1082.

Ding, F. and Chaillet, J.R. 2002. In vivo stabilization of the Dnmt1 (cytosine-5)- methyltransferase protein. *Proc Natl Acad Sci USA* **99**(23): 14861-14866.

Dong, K.B., Maksakova, I.A., Mohn, F., Leung, D., Appanah, R., Lee, S., Yang, H.W., Lam, L.L., Mager, D.L., Schübeler, D. et al. 2008. DNA methylation in ES cells requires the lysine methyltransferase G9a but not its catalytic activity. *EMBO J* **27**(20): 2691-2701.

Dorigo, B., Schalch, T., Kulangara, A., Duda, S., Schroeder, R.R., and Richmond, T.J. 2004. Nucleosome arrays reveal the two-start organization of the chromatin fiber. *Science* **306**(5701): 1571-1573.

Dupré, S., Volland, C., and Haguenauer-Tsapis, R. 2001. Membrane transport: ubiquitylation in endosomal sorting. *Curr Biol* **11**(22): R932-934.

Egger, G., Jeong, S., Escobar, S.G., Cortez, C.C., Li, T.W., Saito, Y., Yoo, C.B., Jones, P.A., and Liang, G. 2006. Identification of DNMT1 (DNA methyltransferase 1) hypomorphs in somatic knockouts suggests an essential role for DNMT1 in cell survival. *Proc Natl Acad Sci USA* **103**(38): 14080-14085.

Ehrlich, M., Sanchez, C., Shao, C., Nishiyama, R., Kehrl, J., Kuick, R., Kubota, T., and Hanash, S.M. 2008. ICF, an immunodeficiency syndrome: DNA methyltransferase 3B involvement, chromosome anomalies, and gene dysregulation. *Autoimmunity* **41**(4): 253-271.

Eisen, J.A., Sweder, K.S., and Hanawalt, P.C. 1995. Evolution of the SNF2 family of proteins: subfamilies with distinct sequences and functions. *Nucleic Acids Res* **23**(14): 2715-2723.

Emre, N.C., Ingvarsdottir, K., Wyce, A., Wood, A., Krogan, N.J., Henry, K.W., Li, K., Marmorstein, R., Greenblatt, J.F., Shilatifard, A. et al. 2005. Maintenance of low histone ubiquitylation by Ubp10 correlates with telomere-proximal Sir2 association and gene silencing. *Mol Cell* **17**(4): 585-594.

Espada, J., Ballestar, E., Santoro, R., Fraga, M., Villar-Garea, A., Nemeth, A., Lopez-Serra, L., Ropero, S., Aranda, A., Orozco, H. et al. 2007. Epigenetic disruption of ribosomal RNA genes and nucleolar architecture in DNA methyltransferase 1 (Dnmt1) deficient cells. *Nucleic Acids Res* **35**(7): 2191-2198.

Espinosa, J.M. 2008. Histone H2B ubiquitination: the cancer connection. *Genes Dev* **22**(20): 2743-2749.

Esteve, P., Chin, H., Smallwood, A., Feehery, G., Gangisetty, O., Karpf, A., Carey, M., and Pradhan, S. 2006. Direct interaction between DNMT1 and G9a coordinates DNA and histone methylation during replication. *Genes Dev* **20**(22): 3089-3103.

Everett, R.D., Meredith, M., Orr, A., Cross, A., Kathoria, M., and Parkinson, J. 1997. A novel ubiquitin-specific protease is dynamically associated with the PML nuclear domain and binds to a herpesvirus regulatory protein. *EMBO J* **16**(7): 1519-1530.

Fan, T., Hagan, J.P., Kozlov, S.V., Stewart, C.L., and Muegge, K. 2005. Lsh controls silencing of the imprinted Cdkn1c gene. *Development* **132**(4): 635-644.

Fatemi, M., Fatemi, M.e.a., Hermann, A., Pradhan, S., and Jeltsch, A. 2001a. The activity of the murine DNA methyltransferase Dnmt1 is controlled by interaction of the catalytic domain with the N-terminal part of the enzyme leading to an allosteric activation of the enzyme after binding to methylated DNA. *J Mol Biol* **309**(5): 1189-1199.

Fatemi, M.e.a., Fatemi, M., Hermann, A., Pradhan, S., and Jeltsch, A. 2001b. The activity of the murine DNA methyltransferase Dnmt1 is controlled by interaction of the catalytic domain with the N-terminal part of the enzyme leading to an allosteric activation of the enzyme after binding to methylated DNA. *J Mol Biol* **309**(5): 1189-1199.

Feinberg, A.P. 2004. The epigenetics of cancer etiology. *Semin Cancer Biol* **14**(6): 427-432.

Fellinger, K., Rothbauer, U., Felle, M., Längst, G., and Leonhardt, H. 2009. Dimerization of DNA methyltransferase 1 is mediated by its regulatory domain. *J Cell Biochem* **106**(4): 521-528.

Felsenfeld, G., Burgess-Beusse, B., Farrell, C., Gaszner, M., Ghirlando, R., Huang, S., Jin, C., Litt, M., Magdinier, F., Mutskov, V. et al. 2004. Chromatin boundaries and chromatin domains. *Cold Spring Harb Symp Quant Biol* **69**: 245-250.

Felsenfeld, G. and Groudine, M. 2003. Controlling the double helix. *Nature* **421**(6921): 448-453.

Fernández-Montalván, A., Bouwmeester, T., Joberty, G., Mader, R., Mahnke, M., Pierrat, B., Schlaeppi, J.M., Worpenberg, S., and Gerhartz, B. 2007. Biochemical characterization of USP7 reveals post-translational modification sites and structural requirements for substrate processing and subcellular localization. *FEBS J* **274**(16): 4256-4270.

Fischle, W. 2008. Talk is cheap--cross-talk in establishment, maintenance, and readout of chromatin modifications. *Genes Dev* **22**(24): 3375-3382.

Fischle, W., Tseng, B.S., Dormann, H.L., Ueberheide, B.M., Garcia, B.A., Shabanowitz, J., Hunt, D.F., Funabiki, H., and Allis, C.D. 2005. Regulation of HP1-chromatin binding by histone H3 methylation and phosphorylation. *Nature* **438**(7071): 1116-1122.

Fischle, W., Wang, Y., and Allis, C.D. 2003a. Histone and chromatin cross-talk. *Curr Opin Cell Biol* **15**(2): 172-183.

Fischle, W., Wang, Y., Jacobs, S.A., Kim, Y., Allis, C.D., and Khorasanizadeh, S. 2003b. Molecular basis for the discrimination of repressive methyl-lysine marks in histone H3 by Polycomb and HP1 chromodomains. *Genes Dev* **17**(15): 1870-1881.

Fitzgerald, D.J., Berger, P., Schaffitzel, C., Yamada, K., Richmond, T.J., and Berger, I. 2006. Protein complex expression by using multigene baculoviral vectors. *Nat Methods* **3**(12): 1021-1032.

Flaus, A., Martin, D.M., Barton, G.J., and Owen-Hughes, T. 2006a. Identification of multiple distinct Snf2 subfamilies with conserved structural motifs. *Nucleic Acids Res* **34**(10): 2887-2905.

-. 2006b. Identification of multiple distinct Snf2 subfamilies with conserved structural motifs. *Nucleic Acids Res* **34**(10): 2887-2905.

Fleming, A.B., Kao, C.F., Hillyer, C., Pikaart, M., and Osley, M.A. 2008. H2B ubiquitylation plays a role in nucleosome dynamics during transcription elongation. *Mol Cell* **31**(1): 57-66.

Fujimori, A., Matsuda, Y., Takemoto, Y., Hashimoto, Y., Kubo, E., Araki, R., Fukumura, R., Mita, K., Tatsumi, K., and Muto, M. 1998. Cloning and mapping of Np95 gene which encodes a novel nuclear protein associated with cell proliferation. *Mamm Genome* **9**(12): 1032-1035.

Fuks, F., Burgers, W.A., Brehm, A., Hughes-Davies, L., and Kouzarides, T. 2000. DNA methyltransferase Dnmt1 associates with histone deacetylase activity. *Nat Genet* **24**(1): 88-91.

Fuks, F., Burgers, W.A., Godin, N., Kasai, M., and Kouzarides, T. 2001. Dnmt3a binds deacetylases and is recruited by a sequence-specific repressor to silence transcription. *Embo J* **20**(10): 2536-2544.

REFERENCES

Fuks, F., Hurd, P.J., Deplus, R., and Kouzarides, T. 2003. The DNA methyltransferases associate with HP1 and the SUV39H1 histone methyltransferase. *Nucleic Acids Res* **31**(9): 2305-2312.

Gardner, R.G., Nelson, Z.W., and Gottschling, D.E. 2005. Ubp10/Dot4p regulates the persistence of ubiquitinated histone H2B: distinct roles in telomeric silencing and general chromatin. *Mol Cell Biol* **25**(14): 6123-6139.

Ge, Y.Z., Pu, M.T., Gowher, H., Wu, H.P., Ding, J.P., Jeltsch, A., and Xu, G.L. 2004. Chromatin targeting of de novo DNA methyltransferases by the PWWP domain. *J Biol Chem* **279**(24): 25447-25454.

Geiman, T.M., Sankpal, U.T., Robertson, A.K., Chen, Y., Mazumdar, M., Heale, J.T., Schmiesing, J.A., Kim, W., Yokomori, K., Zhao, Y. et al. 2004a. Isolation and characterization of a novel DNA methyltransferase complex linking DNMT3B with components of the mitotic chromosome condensation machinery. *Nucleic Acids Res* **32**(9): 2716-2729.

Geiman, T.M., Sankpal, U.T., Robertson, A.K., Zhao, Y., Zhao, Y., and Robertson, K.D. 2004b. DNMT3B interacts with hSNF2H chromatin remodeling enzyme, HDACs 1 and 2, and components of the histone methylation system. *Biochem Biophys Res Commun* **318**(2): 544-555.

Gelato, K.A. and Fischle, W. 2008. Role of histone modifications in defining chromatin structure and function. *Biol Chem* **389**(4): 353-363.

Ghoshal, K., Datta, J., Majumder, S., Bai, S., Kutay, H., Motiwala, T., and Jacob, S.T. 2005. 5-Aza-deoxycytidine induces selective degradation of DNA methyltransferase 1 by a proteasomal pathway that requires the KEN box, bromo-adjacent homology domain, and nuclear localization signal. *Mol Cell Biol* **25**(11): 4727-4741.

Gibbons, R.J., McDowell, T.L., Raman, S., O'Rourke, D.M., Garrick, D., Ayyub, H., and Higgs, D.R. 2000. Mutations in ATRX, encoding a SWI/SNF-like protein, cause diverse changes in the pattern of DNA methylation. *Nat Genet* **24**(4): 368-371.

Glozak, M.A., Sengupta, N., Zhang, X., and Seto, E. 2005. Acetylation and deacetylation of non-histone proteins. *Gene* **363**: 15-23.

Golderer, G. and Gröbner, P. 1991. ADP-ribosylation of core histones and their acetylated subspecies. *Biochem J* **277 (Pt 3)**: 607-610.

Goldknopf, I.L. and Busch, H. 1975. Remarkable similarities of peptide fingerprints of histone 2A and nonhistone chromosomal protein A24. *Biochem Biophys Res Commun* **65**(3): 951-960.

Goldknopf, I.L., Sudhakar, S., Rosenbaum, F., and Busch, H. 1980. Timing of ubiquitin synthesis and conjugation into protein A24 during the HeLa cell cycle. *Biochem Biophys Res Commun* **95**(3): 1253-1260.

Goll, M.G., Kirpekar, F., Maggert, K.A., Yoder, J.A., Hsieh, C.L., Zhang, X., Golic, K.G., Jacobsen, S.E., and Bestor, T.H. 2006. Methylation of tRNAAsp by the DNA methyltransferase homolog Dnmt2. *Science* **311**(5759): 395-398.

Gonzalo, S., Jaco, I., Fraga, M.F., Chen, T., Li, E., Esteller, M., and Blasco, M.A. 2006. DNA methyltransferases control telomere length and telomere recombination in mammalian cells. *Nat Cell Biol* **8**(4): 416-424.

Gorski, K., Carneiro, M., and Schibler, U. 1986. Tissue-specific in vitro transcription from the mouse albumin promoter. *Cell* **47**(5): 767-776.

Gowher, H. and Jeltsch, A. 2001. Enzymatic properties of recombinant Dnmt3a DNA methyltransferase from mouse: the enzyme modifies DNA in a non-processive manner and also methylates non-CpG [correction of non-CpA] sites. *J Mol Biol* **309**(5): 1201-1208.

-. 2002. Molecular enzymology of the catalytic domains of the Dnmt3a and Dnmt3b DNA methyltransferases. *J Biol Chem* **277**(23): 20409-20414.

Gowher, H., Liebert, K., Hermann, A., Xu, G., and Jeltsch, A. 2005a. Mechanism of stimulation of catalytic activity of Dnmt3A and Dnmt3B DNA-(cytosine-C5)-methyltransferases by Dnmt3L. *J Biol Chem* **280**(14): 13341-13348.

Gowher, H., Stockdale, C.J., Goyal, R., Ferreira, H., Owen-Hughes, T., and Jeltsch, A. 2005b. De novo methylation of nucleosomal DNA by the mammalian Dnmt1 and Dnmt3A DNA methyltransferases. *Biochemistry* **44**(29): 9899-9904.

Grant, P.A., Duggan, L., Côté, J., Roberts, S.M., Brownell, J.E., Candau, R., Ohba, R., Owen-Hughes, T., Allis, C.D., Winston, F. et al. 1997. Yeast Gcn5 functions in two multisubunit complexes to acetylate nucleosomal histones: characterization of an Ada complex and the SAGA (Spt/Ada) complex. *Genes Dev* **11**(13): 1640-1650.

Grewal, S.I. and Elgin, S.C. 2002. Heterochromatin: new possibilities for the inheritance of structure. *Curr Opin Genet Dev* **12**(2): 178-187.

Hake, S.B., Xiao, A., and Allis, C.D. 2004. Linking the epigenetic 'language' of covalent histone modifications to cancer. *Br J Cancer* **90**(4): 761-769.

Hancock, R. and pm026. 2000. A new look at the nuclear matrix. *Chromosoma* **109**(4): 219-225.

Handa, V. and Jeltsch, A. 2005. Profound flanking sequence preference of Dnmt3a and Dnmt3b mammalian DNA methyltransferases shape the human epigenome. *J Mol Biol* **348**(5): 1103-1112.

Hartmann, W., Waha, A., Koch, A., Goodyer, C.G., Albrecht, S., von Schweinitz, D., and Pietsch, T. 2000. p57(KIP2) is not mutated in hepatoblastoma but shows increased transcriptional activity in a comparative analysis of the three imprinted genes p57(KIP2), IGF2, and H19. *Am J Pathol* **157**(4): 1393-1403.

Hashimoto, H., Horton, J., Zhang, X., Bostick, M., Jacobsen, S., and Cheng, X. 2008. The SRA domain of UHRF1 flips 5-methylcytosine out of the DNA helix. *Nature*: 5.

Hata, K., Okano, M., Lei, H., and Li, E. 2002. Dnmt3L cooperates with the Dnmt3 family of de novo DNA methyltransferases to establish maternal imprints in mice. *Development* **129**(8): 1983-1993.

Hata, K., Okano, M., Li, E., and Sasaki, H. 2007. Role of the Dnmt3 family in de novo methylation of imprinted and repetitive sequences during male germ cell development in the mouse. *Hum Mol Genet* **16**(19): 2272-2280.

Heir, R., Ablasou, C., Dumontier, E., Elliott, M., Fagotto-Kaufmann, C., and Bedford, F.K. 2006. The UBL domain of PLIC-1 regulates aggresome formation. *EMBO Rep* **7**(12): 1252-1258.

Henderson, A.S., Warburton, D., and Atwood, K.C. 1972. Location of ribosomal DNA in the human chromosome complement. *Proc Natl Acad Sci USA* **69**(11): 3394-3398.

Hendzel, M.J., Wei, Y., Mancini, M.A., Van Hooser, A., Ranalli, T., Brinkley, B.R., Bazett-Jones, D.P., and Allis, C.D. 1997. Mitosis-specific phosphorylation of histone H3 initiates primarily within pericentromeric heterochromatin during G2 and spreads in an ordered fashion coincident with mitotic chromosome condensation. *Chromosoma* **106**(6): 348-360.

Henry, K.W., Wyce, A., Lo, W.S., Duggan, L.J., Emre, N.C., Kao, C.F., Pillus, L., Shilatifard, A., Osley, M.A., and Berger, S.L. 2003. Transcriptional activation via sequential histone H2B ubiquitylation and deubiquitylation, mediated by SAGA-associated Ubp8. *Genes Dev* **17**(21): 2648-2663.

Herman, H., Lu, M., Anggraini, M., Sikora, A., Chang, Y., Yoon, B.J., and Soloway, P.D. 2003. Trans allele methylation and paramutation-like effects in mice. *Nat Genet* **34**(2): 199-202.

Hermann, A., Gowher, H., and Jeltsch, A. 2004a. Biochemistry and biology of mammalian DNA methyltransferases. *Cell Mol Life Sci* **61**(19-20): 2571-2587.

Hermann, A., Goyal, R., and Jeltsch, A. 2004b. The Dnmt1 DNA-(cytosine-C5)-methyltransferase methylates DNA processively

REFERENCES

with high preference for hemimethylated target sites. *J Biol Chem* **279**(46): 48350-48359.

Hershko, A., Heller, H., Elias, S., and Ciechanover, A. 1983. Components of ubiquitin-protein ligase system. Resolution, affinity purification, and role in protein breakdown. *J Biol Chem* **258**(13): 8206-8214.

Hicke, L. 2001. Protein regulation by monoubiquitin. *Nat Rev Mol Cell Biol* **2**(3): 195-201.

Hochstrasser, M. 2000. Evolution and function of ubiquitin-like protein-conjugation systems. *Nat Cell Biol* **2**(8): E153-157.

Holbert, M.A. and Marmorstein, R. 2005. Structure and activity of enzymes that remove histone modifications. *Curr Opin Struct Biol* **15**(6): 673-680.

Holowaty, M.N., Sheng, Y., Nguyen, T., Arrowsmith, C., and Frappier, L. 2003. Protein interaction domains of the ubiquitin-specific protease, USP7/HAUSP. *J Biol Chem* **278**(48): 47753-47761.

Hölzel, M., Rohrmoser, M., Orban, M., Hömig, C., Harasim, T., Malamoussi, A., Gruber-Eber, A., Heissmeyer, V., Bornkamm, G., and Eick, D. 2007. Rapid conditional knock-down-knock-in system for mammalian cells. *Nucleic Acids Res* **35**(3): e17.

Hong, S., Cho, Y.W., Yu, L.R., Yu, H., Veenstra, T.D., and Ge, K. 2007. Identification of JmjC domain-containing UTX and JMJD3 as histone H3 lysine 27 demethylases. *Proc Natl Acad Sci USA* **104**(47): 18439-18444.

Hopfner, R., Mousli, M., Garnier, J.M., Redon, R., du Manoir, S., Chatton, B., Ghyselinck, N., Oudet, P., and Bronner, C. 2001. Genomic structure and chromosomal mapping of the gene coding for ICBP90, a protein involved in the regulation of the topoisomerase IIalpha gene expression. *Gene* **266**(1-2): 15-23.

Hopfner, R., Mousli, M., Jeltsch, J.M., Voulgaris, A., Lutz, Y., Marin, C., Bellocq, J.P., Oudet, P., and Bronner, C. 2000. ICBP90, a novel human CCAAT binding protein, involved in the regulation of topoisomerase IIalpha expression. *Cancer Res* **60**(1): 121-128.

Horn, P.J. and Peterson, C.L. 2002. Molecular biology. Chromatin higher order folding--wrapping up transcription. *Science* **297**(5588): 1824-1827.

Hsu, D.W., Lin, M.J., Lee, T.L., Wen, S.C., Chen, X., and Shen, C.K. 1999. Two major forms of DNA (cytosine-5) methyltransferase in human somatic tissues. *Proc Natl Acad Sci USA* **96**(17): 9751-9756.

Hu, M., Li, P., Li, M., Li, W., Yao, T., Wu, J.W., Gu, W., Cohen, R.E., and Shi, Y. 2002. Crystal structure of a UBP-family deubiquitinating enzyme in isolation and in complex with ubiquitin aldehyde. *Cell* **111**(7): 1041-1054.

Huang, T.T. and D'Andrea, A.D. 2006. Regulation of DNA repair by ubiquitylation. *Nat Rev Mol Cell Biol* **7**(5): 323-334.

Hwang, W.W., Venkatasubrahmanyam, S., Ianculescu, A.G., Tong, A., Boone, C., and Madhani, H.D. 2003. A conserved RING finger protein required for histone H2B monoubiquitination and cell size control. *Mol Cell* **11**(1): 261-266.

Iida, T., Suetake, I., Tajima, S., Morioka, H., Ohta, S., Obuse, C., and Tsurimoto, T. 2002. PCNA clamp facilitates action of DNA cytosine methyltransferase 1 on hemimethylated DNA. *Genes Cells* **7**(10): 997-1007.

Iizuka, M. and Smith, M.M. 2003. Functional consequences of histone modifications. *Curr Opin Genet Dev* **13**(2): 154-160.

Jackson-Grusby, L., Beard, C., Possemato, R., Tudor, M., Fambrough, D., Csankovszki, G., Dausman, J., Lee, P., Wilson, C., Lander, E. et al. 2001. Loss of genomic methylation causes p53-dependent apoptosis and epigenetic deregulation. *Nat Genet* **27**(1): 31-39.

Jähner, D., Stuhlmann, H., Stewart, C.L., Harbers, K., Löhler, J., Simon, I., and Jaenisch, R. 1982. De novo methylation and expression of retroviral genomes during mouse embryogenesis. *Nature* **298**(5875): 623-628.

Jeanblanc, M., Mousli, M., Hopfner, R., Bathami, K., Martinet, N., Abbady, A.Q., Siffert, J.C., Mathieu, E., Muller, C.D., and Bronner, C. 2005. The retinoblastoma gene and its product are targeted by ICBP90: a key mechanism in the G1/S transition during the cell cycle. *Oncogene* **24**(49): 7337-7345.

Jeltsch, A. 2002. Beyond Watson and Crick: DNA methylation and molecular enzymology of DNA methyltransferases. *Chembiochem* **3**(4): 274-293.

Jenkins, Y., Markovtsov, V., Lang, W., Sharma, P., Pearsall, D., Warner, J., Franci, C., Huang, B., Huang, J., Yam, G.C. et al. 2005. Critical role of the ubiquitin ligase activity of UHRF1, a nuclear RING finger protein, in tumor cell growth. *Mol Biol Cell* **16**(12): 5621-5629.

Jenuwein, T. and Allis, C.D. 2001. Translating the histone code. *Science* **293**(5532): 1074-1080.

Jia, D., Jurkowska, R.Z., Zhang, X., Jeltsch, A., and Cheng, X. 2007. Structure of Dnmt3a bound to Dnmt3L suggests a model for de novo DNA methylation. *Nature*.

Joo, H.Y., Zhai, L., Yang, C., Nie, S., Erdjument-Bromage, H., Tempst, P., Chang, C., and Wang, H. 2007. Regulation of cell cycle progression and gene expression by H2A deubiquitination. *Nature* **449**(7165): 1068-1072.

Jurkowska, R., Anspach, N., Urbanke, C., Jia, D., Reinhardt, R., Nellen, W., Cheng, X., and Jeltsch, A. 2008. Formation of nucleoprotein filaments by mammalian DNA methyltransferase Dnmt3a in complex with regulator Dnmt3L. *Nucleic Acids Research*: 8.

Kaneda, M., Okano, M., Hata, K., Sado, T., Tsujimoto, N., Li, E., and Sasaki, H. 2004. Essential role for de novo DNA methyltransferase Dnmt3a in paternal and maternal imprinting. *Nature* **429**(6994): 900-903.

Kang, E.S., Park, C.W., and Chung, J.H. 2001. Dnmt3b, de novo DNA methyltransferase, interacts with SUMO-1 and Ubc9 through its N-terminal region and is subject to modification by SUMO-1. *Biochem Biophys Res Commun* **289**(4): 862-868.

Kao, C.F., Hillyer, C., Tsukuda, T., Henry, K., Berger, S., and Osley, M.A. 2004. Rad6 plays a role in transcriptional activation through ubiquitylation of histone H2B. *Genes Dev* **18**(2): 184-195.

Karagianni, P., Amazit, L., Qin, J., and Wong, J. 2008. ICBP90, a novel methyl K9 H3 binding protein linking protein ubiquitination with heterochromatin formation. *Mol Cell Biol* **28**(2): 705-717.

Kerscher, O., Felberbaum, R., and Hochstrasser, M. 2006. Modification of proteins by ubiquitin and ubiquitin-like proteins. *Annu Rev Cell Dev Biol* **22**: 159-180.

Kessler, B.M., Fortunati, E., Melis, M., Pals, C.E., Clevers, H., and Maurice, M.M. 2007. Proteome changes induced by knock-down of the deubiquitylating enzyme HAUSP/USP7. *J Proteome Res* **6**(11): 4163-4172.

Khorasanizadeh, S. 2004. The nucleosome: from genomic organization to genomic regulation. *Cell* **116**(2): 259-272.

Kim, G.D., Ni, J., Kelesoglu, N., Roberts, R.J., and Pradhan, S. 2002. Co-operation and communication between the human maintenance and de novo DNA (cytosine-5) methyltransferases. *Embo J* **21**(15): 4183-4195.

Kim, J., Hake, S.B., and Roeder, R.G. 2005. The human homolog of yeast BRE1 functions as a transcriptional coactivator through direct activator interactions. *Mol Cell* **20**(5): 759-770.

Kimura, H. and Shiota, K. 2003. Methyl-CpG-binding protein, MeCP2, is a target molecule for maintenance DNA methyltransferase, Dnmt1. *J Biol Chem* **278**(7): 4806-4812.

Kinyamu, H.K., Chen, J., and Archer, T.K. 2005. Linking the ubiquitin-proteasome pathway to chromatin remodeling/modification by nuclear receptors. *J Mol Endocrinol* **34**(2): 281-297.

Kladde, M.P., Xu, M., and Simpson, R.T. 1999. DNA methyltransferases as probes of chromatin structure in vivo. *Meth Enzymol* **304**: 431-447.

REFERENCES

Klug, M. and Rehli, M. 2006. Functional analysis of promoter CpG methylation using a CpG-free luciferase reporter vector. *Epigenetics : official journal of the DNA Methylation Society* **1**(3): 127-130.

Klymenko, T., Papp, B., Fischle, W., Köcher, T., Schelder, M., Fritsch, C., Wild, B., Wilm, M., and Müller, J. 2006. A Polycomb group protein complex with sequence-specific DNA-binding and selective methyl-lysine-binding activities. *Genes Dev* **20**(9): 1110-1122.

Kornberg, R.D. 1974. Chromatin structure: a repeating unit of histones and DNA. *Science* **184**(139): 868-871.

Kriaucionis, S. and Bird, A.P. 2003. DNA methylation and Rett syndrome. *Hum Mol Genet* **12 Spec No 2**: R221-227.

Kumar, S., Cheng, X., Klimasauskas, S., Mi, S., Posfai, J., Roberts, R.J., and Wilson, G.G. 1994. The DNA (cytosine-5) methyltransferases. *Nucleic Acids Res* **22**(1): 1-10.

Kuzmichev, A., Jenuwein, T., Tempst, P., and Reinberg, D. 2004. Different EZH2-containing complexes target methylation of histone H1 or nucleosomal histone H3. *Mol Cell* **14**(2): 183-193.

Lachner, M. and Jenuwein, T. 2002. The many faces of histone lysine methylation. *Curr Opin Cell Biol* **14**(3): 286-298.

Langst, G., Blank, T.A., Becker, P.B., and Grummt, I. 1997. RNA polymerase I transcription on nucleosomal templates: the transcription termination factor TTF-I induces chromatin remodeling and relieves transcriptional repression. *Embo J* **16**(4): 760-768.

Langst, G., Bonte, E.J., Corona, D.F., and Becker, P.B. 1999. Nucleosome movement by CHRAC and ISWI without disruption or trans-displacement of the histone octamer. *Cell* **97**(7): 843-852.

Lee, J.S., Shukla, A., Schneider, J., Swanson, S.K., Washburn, M.P., Florens, L., Bhaumik, S.R., and Shilatifard, A. 2007a. Histone crosstalk between H2B monoubiquitination and H3 methylation mediated by COMPASS. *Cell* **131**(6): 1084-1096.

Lee, M.G., Villa, R., Trojer, P., Norman, J., Yan, K.P., Reinberg, D., Di Croce, L., and Shiekhattar, R. 2007b. Demethylation of H3K27 regulates polycomb recruitment and H2A ubiquitination. *Science* **318**(5849): 447-450.

Lehnertz, B., Ueda, Y., Derijck, A.A., Braunschweig, U., Perez-Burgos, L., Kubicek, S., Chen, T., Li, E., Jenuwein, T., and Peters, A.H. 2003. Suv39h-mediated histone H3 lysine 9 methylation directs DNA methylation to major satellite repeats at pericentric heterochromatin. *Curr Biol* **13**(14): 1192-1200.

Lei, H., Oh, S.P., Okano, M., Jüttermann, R., Goss, K.A., Jaenisch, R., and Li, E. 1996. De novo DNA cytosine methyltransferase activities in mouse embryonic stem cells. *Development* **122**(10): 3195-3205.

Leonhardt, H., Page, A.W., Weier, H.U., and Bestor, T.H. 1992. A targeting sequence directs DNA methyltransferase to sites of DNA replication in mammalian nuclei. *Cell* **71**(5): 865-873.

LeRoy, G., Orphanides, G., Lane, W.S., and Reinberg, D. 1998. Requirement of RSF and FACT for transcription of chromatin templates in vitro. *Science* **282**(5395): 1900-1904.

Li, B., Zhou, J., Liu, P., Hu, J., Jin, H., Shimono, Y., Takahashi, M., and Xu, G. 2007a. Polycomb protein Cbx4 promotes SUMO modification of de novo DNA methyltransferase Dnmt3a. *Biochem J* **405**(2): 369-378.

Li, E. 2002a. Chromatin modification and epigenetic reprogramming in mammalian development. *Nat Rev Genet* **3**(9): 662-673.

-. 2002b. Chromatin modification and epigenetic reprogramming in mammalian development. *Nat Rev Genet* **3**(9): 662-673.

Li, E., Bestor, T.H., and Jaenisch, R. 1992. Targeted mutation of the DNA methyltransferase gene results in embryonic lethality. *Cell* **69**(6): 915-926.

Li, H., Rauch, T., Chen, Z.X., Szabó, P.E., Riggs, A.D., and Pfeifer, G.P. 2006. The histone methyltransferase SETDB1 and the DNA methyltransferase DNMT3A interact directly and localize to promoters silenced in cancer cells. *J Biol Chem* **281**(28): 19489-19500.

Li, J.Y., Pu, M.T., Hirasawa, R., Li, B.Z., Huang, Y.N., Zeng, R., Jing, N.H., Chen, T., Li, E., Sasaki, H. et al. 2007b. Synergistic function of DNA methyltransferases Dnmt3a and Dnmt3b in the methylation of Oct4 and Nanog. *Mol Cell Biol* **27**(24): 8748-8759.

Li, M., Chen, D., Shiloh, A., Luo, J., Nikolaev, A.Y., Qin, J., and Gu, W. 2002. Deubiquitination of p53 by HAUSP is an important pathway for p53 stabilization. *Nature* **416**(6881): 648-653.

Lin, I.G., Han, L., Taghva, A., O'Brien, L.E., and Hsieh, C.L. 2002. Murine de novo methyltransferase Dnmt3a demonstrates strand asymmetry and site preference in the methylation of DNA in vitro. *Mol Cell Biol* **22**(3): 704-723.

Lindsley, J.E. 2001. Use of a real-time, coupled assay to measure the ATPase activity of DNA topoisomerase II. *Methods Mol Biol* **95**: 57-64.

Ling, Y., Sankpal, U.T., Robertson, A.K., McNally, J.G., Karpova, T., and Robertson, K.D. 2004. Modification of de novo DNA methyltransferase 3a (Dnmt3a) by SUMO-1 modulates its interaction with histone deacetylases (HDACs) and its capacity to repress transcription. *Nucleic Acids Res* **32**(2): 598-610.

Lucifero, D., Mann, M.R., Bartolomei, M.S., and Trasler, J.M. 2004. Gene-specific timing and epigenetic memory in oocyte imprinting. *Hum Mol Genet* **13**(8): 839-849.

Luger, K. 2003. Structure and dynamic behavior of nucleosomes. *Curr Opin Genet Dev* **13**(2): 127-135.

-. 2006. Dynamic nucleosomes. *Chromosome Res* **14**(1): 5-16.

Luger, K., Mäder, A.W., Richmond, R.K., Sargent, D.F., and Richmond, T.J. 1997. Crystal structure of the nucleosome core particle at 2.8 A resolution. *Nature* **389**(6648): 251-260.

Luger, K. and Richmond, T.J. 1998. DNA binding within the nucleosome core. *Curr Opin Struct Biol* **8**(1): 33-40.

Luo, R.X., Postigo, A.A., and Dean, D.C. 1998. Rb interacts with histone deacetylase to repress transcription. *Cell* **92**(4): 463-473.

Lusser, A. and Kadonaga, J.T. 2003. Chromatin remodeling by ATP-dependent molecular machines. *Bioessays* **25**(12): 1192-1200.

Magnaghi-Jaulin, L., Groisman, R., Naguibneva, I., Robin, P., Lorain, S., Le Villain, J.P., Troalen, F., Trouche, D., and Harel-Bellan, A. 1998. Retinoblastoma protein represses transcription by recruiting a histone deacetylase. *Nature* **391**(6667): 601-605.

Marshall, O.J. 2004. PerlPrimer: cross-platform, graphical primer design for standard, bisulphite and real-time PCR. *Bioinformatics* **20**(15): 2471-2472.

Martin, C. and Zhang, Y. 2005. The diverse functions of histone lysine methylation. *Nat Rev Mol Cell Biol* **6**(11): 838-849.

McGinty, R.K., Kim, J., Chatterjee, C., Roeder, R.G., and Muir, T.W. 2008. Chemically ubiquitylated histone H2B stimulates hDot1L-mediated intranucleosomal methylation. *Nature* **453**(7196): 812-816.

McGrath, J. and Solter, D. 1984. Completion of mouse embryogenesis requires both the maternal and paternal genomes. *Cell* **37**(1): 179-183.

Mellor, J. 2006. It takes a PHD to read the histone code. *Cell* **126**(1): 22-24.

Mertineit, C., Yoder, J.A., Taketo, T., Laird, D.W., Trasler, J.M., and Bestor, T.H. 1998. Sex-specific exons control DNA methyltransferase in mammalian germ cells. *Development* **125**(5): 889-897.

Metzger, E., Wissmann, M., and Schüle, R. 2006. Histone demethylation and androgen-dependent transcription. *Curr Opin*

REFERENCES

Genet Dev **16**(5): 513-517.

Meulmeester, E., Maurice, M.M., Boutell, C., Teunisse, A.F., Ovaa, H., Abraham, T.E., Dirks, R.W., and Jochemsen, A.G. 2005. Loss of HAUSP-mediated deubiquitination contributes to DNA damage-induced destabilization of Hdmx and Hdm2. *Molecular Cell* **18**(5): 565-576.

Michael, D. and Oren, M. 2003. The p53-Mdm2 module and the ubiquitin system. *Semin Cancer Biol* **13**(1): 49-58.

Min, J., Zhang, Y., and Xu, R.M. 2003. Structural basis for specific binding of Polycomb chromodomain to histone H3 methylated at Lys 27. *Genes Dev* **17**(15): 1823-1828.

Minsky, N. and Oren, M. 2004. The RING domain of Mdm2 mediates histone ubiquitylation and transcriptional repression. *Mol Cell* **16**(4): 631-639.

Minsky, N., Shema, E., Field, Y., Schuster, M., Segal, E., and Oren, M. 2008. Monoubiquitinated H2B is associated with the transcribed region of highly expressed genes in human cells. *Nat Cell Biol* **10**(4): 483-488.

Miura, M., Watanabe, H., Sasaki, T., Tatsumi, K., and Muto, M. 2001. Dynamic changes in subnuclear NP95 location during the cell cycle and its spatial relationship with DNA replication foci. *Exp Cell Res* **263**(2): 202-208.

Mori, T. 2004. NIRF is a ubiquitin ligase that is capable of ubiquitinating PCNP, a PEST-containing nuclear protein. *FEBS Letters* **557**(1-3): 209-214.

Mousli, M., Hopfner, R., Abbady, A.Q., Monté, D., Jeanblanc, M., Oudet, P., Louis, B., and Bronner, C. 2003. ICBP90 belongs to a new family of proteins with an expression that is deregulated in cancer cells. *Br J Cancer* **89**(1): 120-127.

Mueller, R.D., Yasuda, H., Hatch, C.L., Bonner, W.M., and Bradbury, E.M. 1985. Identification of ubiquitinated histones 2A and 2B in Physarum polycephalum. Disappearance of these proteins at metaphase and reappearance at anaphase. *J Biol Chem* **260**(8): 5147-5153.

Mujtaba, S., Zeng, L., and Zhou, M.M. 2007. Structure and acetyl-lysine recognition of the bromodomain. *Oncogene* **26**(37): 5521-5527.

Müller, J., Hart, C.M., Francis, N.J., Vargas, M.L., Sengupta, A., Wild, B., Miller, E.L., O'Connor, M.B., Kingston, R.E., and Simon, J.A. 2002. Histone methyltransferase activity of a Drosophila Polycomb group repressor complex. *Cell* **111**(2): 197-208.

Muthuswami, R., Mesner, L.D., Wang, D., Hill, D.A., Imbalzano, A.N., and Hockensmith, J.W. 2000. Phosphoaminoglycosides inhibit SWI2/SNF2 family DNA-dependent molecular motor domains. *Biochemistry* **39**(15): 4358-4365.

Muto, M., Fujimori, A., Nenoi, M., Daino, K., Matsuda, Y., Kuroiwa, A., Kubo, E., Kanari, Y., Utsuno, M., Tsuji, H. et al. 2006. Isolation and Characterization of a Novel Human Radiosusceptibility Gene, NP95. *Radiat Res* **166**(5): 723-733.

Muto, M., Kanari, Y., Kubo, E., Takabe, T., Kurihara, T., Fujimori, A., and Tatsumi, K. 2002. Targeted disruption of Np95 gene renders murine embryonic stem cells hypersensitive to DNA damaging agents and DNA replication blocks. *J Biol Chem* **277**(37): 34549-34555.

Myant, K. and Stancheva, I. 2008. LSH Cooperates with DNA Methyltransferases To Repress Transcription. *Mol Cell Biol* **28**(1): 215-226.

Nakagawa, T., Kajitani, T., Togo, S., Masuko, N., Ohdan, H., Hishikawa, Y., Koji, T., Matsuyama, T., Ikura, T., Muramatsu, M. et al. 2008. Deubiquitylation of histone H2A activates transcriptional initiation via trans-histone cross-talk with H3K4 di- and trimethylation. *Genes Dev* **22**(1): 37-49.

Narlikar, G.J., Fan, H.Y., and Kingston, R.E. 2002. Cooperation between complexes that regulate chromatin structure and transcription. *Cell* **108**(4): 475-487.

Negishi, M., Saraya, A., Miyagi, S., Nagao, K., Inagaki, Y., Nishikawa, M., Tajima, S., Koseki, H., Tsuda, H., Takasaki, Y. et al. 2007. Bmi1 cooperates with Dnmt1-associated protein 1 in gene silencing. *Biochem Biophys Res Commun* **353**(4): 992-998.

Németh, A., Guibert, S., Tiwari, V., Ohlsson, R., and Längst, G. 2008. Epigenetic regulation of TTF-I-mediated promoter-terminator interactions of rRNA genes. *EMBO J* **27**(8): 1255-1265.

Ng, H.H., Zhang, Y., Hendrich, B., Johnson, C.A., Turner, B.M., Erdjument-Bromage, H., Tempst, P., Reinberg, D., and Bird, A.P. 1999. MBD2 is a transcriptional repressor belonging to the MeCP1 histone deacetylase complex. *Nat Genet* **23**(1): 58-61.

Nicassio, F., Corrado, N., Vissers, J.H., Areces, L.B., Bergink, S., Marteijn, J.A., Geverts, B., Houtsmuller, A.B., Vermeulen, W., Di Fiore, P.P. et al. 2007. Human USP3 is a chromatin modifier required for S phase progression and genome stability. *Curr Biol* **17**(22): 1972-1977.

Nicolas, E., Ait-Si-Ali, S., and Trouche, D. 2001. The histone deacetylase HDAC3 targets RbAp48 to the retinoblastoma protein. *Nucleic Acids Res* **29**(15): 3131-3136.

Nijman, S.M., Luna-Vargas, M.P., Velds, A., Brummelkamp, T.R., Dirac, A.M., Sixma, T.K., and Bernards, R. 2005. A genomic and functional inventory of deubiquitinating enzymes. *Cell* **123**(5): 773-786.

Ogawa, O., Eccles, M.R., Szeto, J., McNoe, L.A., Yun, K., Maw, M.A., Smith, P.J., and Reeve, A.E. 1993. Relaxation of insulin-like growth factor II gene imprinting implicated in Wilms' tumour. *Nature* **362**(6422): 749-751.

Oh, Y.M., Yoo, S.J., and Seol, J.H. 2007. Deubiquitination of Chfr, a checkpoint protein, by USP7/HAUSP regulates its stability and activity. *Biochem Biophys Res Commun* **357**(3): 615-619.

Okano, M., Bell, D.W., Haber, D.A., and Li, E. 1999. DNA methyltransferases Dnmt3a and Dnmt3b are essential for de novo methylation and mammalian development. *Cell* **99**(3): 247-257.

Okano, M., Xie, S., and Li, E. 1998. Cloning and characterization of a family of novel mammalian DNA (cytosine-5) methyltransferases. *Nat Genet* **19**(3): 219-220.

Okuwaki, M. and Verreault, A. 2003. Maintenance DNA methylation of nucleosome core particles. *J Biol Chem* **279**(4): 2904-2912.

-. 2004. Maintenance DNA methylation of nucleosome core particles. *J Biol Chem* **279**(4): 2904-2912.

Olins, D.E. and Olins, A.L. 2003. Chromatin history: our view from the bridge. *Nat Rev Mol Cell Biol* **4**(10): 809-814.

Ooi, S.K., Qiu, C., Bernstein, E., Li, K., Jia, D., Yang, Z., Erdjument-Bromage, H., Tempst, P., Lin, S.P., Allis, C.D. et al. 2007. DNMT3L connects unmethylated lysine 4 of histone H3 to de novo methylation of DNA. *Nature* **448**(7154): 714-717.

Osley, M.A. 2006. Regulation of histone H2A and H2B ubiquitylation. *Briefings in functional genomics & proteomics* **5**(3): 179-189.

Oswald, J., Engemann, S., Lane, N., Mayer, W., Olek, A., Fundele, R., Dean, W., Reik, W., and Walter, J. 2000. Active demethylation of the paternal genome in the mouse zygote. *Curr Biol* **10**(8): 475-478.

Paithankar, K.R. and Prasad, K.S. 1991. Precipitation of DNA by polyethylene glycol and ethanol. *Nucleic Acids Res* **19**(6): 1346.

Papait, R., Pistore, C., Negri, D., Pecoraro, D., Cantarini, L., and Bonapace, I.M. 2007. Np95 is implicated in pericentromeric heterochromatin replication and in major satellite silencing. *Mol Biol Cell* **18**(3): 1098-1106.

Pavri, R., Zhu, B., Li, G., Trojer, P., Mandal, S., Shilatifard, A., and Reinberg, D. 2006. Histone H2B monoubiquitination

REFERENCES

functions cooperatively with FACT to regulate elongation by RNA polymerase II. *Cell* **125**(4): 703-717.

Pfeifer, G.P., Grünwald, S., Palitti, F., Kaul, S., Boehm, T.L., Hirth, H.P., and Drahovsky, D. 1985. Purification and characterization of mammalian DNA methyltransferases by use of monoclonal antibodies. *J Biol Chem* **260**(25): 13787-13793.

Pham, A.D. and Sauer, F. 2000. Ubiquitin-activating/conjugating activity of TAFII250, a mediator of activation of gene expression in Drosophila. *Science* **289**(5488): 2357-2360.

Pieper, A.A., Verma, A., Zhang, J., and Snyder, S.H. 1999. Poly (ADP-ribose) polymerase, nitric oxide and cell death. *Trends Pharmacol Sci* **20**(4): 171-181.

Pósfai, J., Bhagwat, A.S., Pósfai, G., and Roberts, R.J. 1989. Predictive motifs derived from cytosine methyltransferases. *Nucleic Acids Res* **17**(7): 2421-2435.

Pradhan, M., Estève, P.O., Chin, H.G., Samaranayke, M., Kim, G.D., and Pradhan, S. 2008. CXXC Domain of Human DNMT1 Is Essential for Enzymatic Activity. *Biochemistry*.

Pradhan, S., Bacolla, A., Wells, R.D., and Roberts, R.J. 1999. Recombinant human DNA (cytosine-5) methyltransferase. I. Expression, purification, and comparison of de novo and maintenance methylation. *J Biol Chem* **274**(46): 33002-33010.

Pradhan, S. and Esteve, P.O. 2003. Mammalian DNA (cytosine-5) methyltransferases and their expression. *Clin Immunol* **109**(1): 6-16.

Pradhan, S. and Estève, P.O. 2003. Allosteric activator domain of maintenance human DNA (cytosine-5) methyltransferase and its role in methylation spreading. *Biochemistry* **42**(18): 5321-5332.

Pradhan, S. and Kim, G.D. 2002. The retinoblastoma gene product interacts with maintenance human DNA (cytosine-5) methyltransferase and modulates its activity. *Embo J* **21**(4): 779-788.

Pugh, B.F. 1995. Preparation of HeLa nuclear extracts. *Methods Mol Biol* **37**: 349-357.

Qian, Y.W., Wang, Y.C., Hollingsworth, R.E., Jones, D., Ling, N., and Lee, E.Y. 1993. A retinoblastoma-binding protein related to a negative regulator of Ras in yeast. *Nature* **364**(6438): 648-652.

Qiu, C., Sawada, K., Zhang, X., and Cheng, X. 2002. The PWWP domain of mammalian DNA methyltransferase Dnmt3b defines a new family of DNA-binding folds. *Nat Struct Biol* **9**(3): 217-224.

Rainier, S., Dobry, C.J., and Feinberg, A.P. 1995. Loss of imprinting in hepatoblastoma. *Cancer Res* **55**(9): 1836-1838.

Ratnam, S., Mertineit, C., Ding, F., Howell, C.Y., Clarke, H.J., Bestor, T.H., Chaillet, J.R., and Trasler, J.M. 2002. Dynamics of Dnmt1 methyltransferase expression and intracellular localization during oogenesis and preimplantation development. *Dev Biol* **245**(2): 304-314.

Rea, S., Eisenhaber, F., O'Carroll, D., Strahl, B.D., Sun, Z.W., Schmid, M., Opravil, S., Mechtler, K., Ponting, C.P., Allis, C.D. et al. 2000. Regulation of chromatin structure by site-specific histone H3 methyltransferases. *Nature* **406**(6796): 593-599.

Reik, W. 1989. Genomic imprinting and genetic disorders in man. *Trends Genet* **5**(10): 331-336.

Reik, W., Dean, W., and Walter, J. 2001. Epigenetic reprogramming in mammalian development. *Science* **293**(5532): 1089-1093.

Reinhart, B.J. and Bartel, D.P. 2002. Small RNAs correspond to centromere heterochromatic repeats. *Science* **297**(5588): 1831.

Rhee, I., Bachman, K.E., Park, B.H., Jair, K.W., Yen, R.W., Schuebel, K.E., Cui, H., Feinberg, A.P., Lengauer, C., Kinzler, K.W. et al. 2002. DNMT1 and DNMT3b cooperate to silence genes in human cancer cells. *Nature* **416**(6880): 552-556.

Rhee, I., Jair, K.W., Yen, R.W., Lengauer, C., Herman, J.G., Kinzler, K.W., Vogelstein, B., Baylin, S.B., and Schuebel, K.E. 2000. CpG methylation is maintained in human cancer cells lacking DNMT1. *Nature* **404**(6781): 1003-1007.

Rhodes, D. and Laskey, R.A. 1989. Assembly of nucleosomes and chromatin in vitro. *Meth Enzymol* **170**: 575-585.

Richmond, T.J. and Davey, C.A. 2003. The structure of DNA in the nucleosome core. *Nature* **423**(6936): 145-150.

Ringrose, L. and Paro, R. 2007. Polycomb/Trithorax response elements and epigenetic memory of cell identity. *Development* **134**(2): 223-232.

Rippe, K., Schrader, A., Riede, P., Strohner, R., Lehmann, E., and Langst, G. 2007a. DNA sequence- and conformation-directed positioning of nucleosomes by chromatin-remodeling complexes. *Proc Natl Acad Sci U S A* **104**(40): 15635-15640.

Rippe, K., Schrader, A., Riede, P., Strohner, R., Lehmann, E., and Längst, G. 2007b. DNA sequence- and conformation-directed positioning of nucleosomes by chromatin-remodeling complexes. *Proc Natl Acad Sci USA* **104**(40): 15635-15640.

Robertson, A.K., Geiman, T.M., Sankpal, U.T., Hager, G.L., and Robertson, K.D. 2004. Effects of chromatin structure on the enzymatic and DNA binding functions of DNA methyltransferases DNMT1 and Dnmt3a in vitro. *Biochem Biophys Res Commun* **322**(1): 110-118.

Robertson, K.D. 2002. DNA methylation and chromatin - unraveling the tangled web. *Oncogene* **21**(35): 5361-5379.

Robertson, K.D., Ait-Si-Ali, S., Yokochi, T., Wade, P.A., Jones, P.L., and Wolffe, A.P. 2000a. DNMT1 forms a complex with Rb, E2F1 and HDAC1 and represses transcription from E2F-responsive promoters. *Nat Genet* **25**(3): 338-342.

Robertson, K.D., Keyomarsi, K., Gonzales, F.A., Velicescu, M., and Jones, P.A. 2000b. Differential mRNA expression of the human DNA methyltransferases (DNMTs) 1, 3a and 3b during the G(0)/G(1) to S phase transition in normal and tumor cells. *Nucleic Acids Res* **28**(10): 2108-2113.

Robertson, K.D., Uzvolgyi, E., Liang, G., Talmadge, C., Sumegi, J., Gonzales, F.A., and Jones, P.A. 1999. The human DNA methyltransferases (DNMTs) 1, 3a and 3b: coordinate mRNA expression in normal tissues and overexpression in tumors. *Nucleic Acids Res* **27**(11): 2291-2298.

Robinson, P.J., An, W., Routh, A., Martino, F., Chapman, L., Roeder, R.G., and Rhodes, D. 2008. 30 nm chromatin fibre decompaction requires both H4-K16 acetylation and linker histone eviction. *J Mol Biol* **381**(4): 816-825.

Robinson, P.J. and Rhodes, D. 2006. Structure of the '30 nm' chromatin fibre: a key role for the linker histone. *Curr Opin Struct Biol* **16**(3): 336-343.

Rodríguez-Campos, A. and Azorín, F. 2007. RNA is an integral component of chromatin that contributes to its structural organization. *PLoS ONE* **2**(11): e1182.

Roll, J., Rivenbark, A., Jones, W., and Coleman, W. 2008. DNMT3b overexpression contributes to a hypermethylator phenotype in human breast cancer cell lines. *Mol Cancer* **7**: 15.

Rollins, R.A., Haghighi, F., Edwards, J.R., Das, R., Zhang, M.Q., Ju, J., and Bestor, T.H. 2006. Large-scale structure of genomic methylation patterns. *Genome Res* **16**(2): 157-163.

Ross, P.L., Huang, Y.N., Marchese, J.N., Williamson, B., Parker, K., Hattan, S., Khainovski, N., Pillai, S., Dey, S., Daniels, S. et al. 2004. Multiplexed protein quantitation in Saccharomyces cerevisiae using amine-reactive isobaric tagging reagents. *Mol Cell Proteomics* **3**(12): 1154-1169.

Rougier, N., Bourc'his, D., Gomes, D.M., Niveleau, A., Plachot, M., Pàldi, A., and Viegas-Péquignot, E. 1998. Chromosome

REFERENCES

methylation patterns during mammalian preimplantation development. *Genes Dev* **12**(14): 2108-2113.

Rountree, M.R., Bachman, K.E., and Baylin, S.B. 2000. DNMT1 binds HDAC2 and a new co-repressor, DMAP1, to form a complex at replication foci. *Nat Genet* **25**(3): 269-277.

Routh, A., Sandin, S., and Rhodes, D. 2008. Nucleosome repeat length and linker histone stoichiometry determine chromatin fiber structure. *Proc Natl Acad Sci USA* **105**(26): 8872-8877.

Rusche, L.N., Kirchmaier, A.L., and Rine, J. 2003. The establishment, inheritance, and function of silenced chromatin in Saccharomyces cerevisiae. *Annu Rev Biochem* **72**: 481-516.

Santoro, R. and Grummt, I. 2005. Epigenetic mechanism of rRNA gene silencing: temporal order of NoRC-mediated histone modification, chromatin remodeling, and DNA methylation. *Mol Cell Biol* **25**(7): 2539-2546.

Santoro, R., Li, J., and Grummt, I. 2002. The nucleolar remodeling complex NoRC mediates heterochromatin formation and silencing of ribosomal gene transcription. *Nat Genet* **32**(3): 393-396.

Santos-Rosa, H., Schneider, R., Bernstein, B.E., Karabetsou, N., Morillon, A., Weise, C., Schreiber, S.L., Mellor, J., and Kouzarides, T. 2003. Methylation of histone H3 K4 mediates association of the Isw1p ATPase with chromatin. *Mol Cell* **12**(5): 1325-1332.

Schalch, T., Duda, S., Sargent, D.F., and Richmond, T.J. 2005. X-ray structure of a tetranucleosome and its implications for the chromatin fibre. *Nature* **436**(7047): 138-141.

Schermelleh, L., Haemmer, A., Spada, F., Rösing, N., Meilinger, D., Rothbauer, U., Cristina Cardoso, M., and Leonhardt, H. 2007. Dynamics of Dnmt1 interaction with the replication machinery and its role in postreplicative maintenance of DNA methylation. *Nucleic Acids Res*.

Schermelleh, L., Spada, F., Easwaran, H.P., Zolghadr, K., Margot, J.B., Cardoso, M.C., and Leonhardt, H. 2005. Trapped in action: direct visualization of DNA methyltransferase activity in living cells. *Nat Methods* **2**(10): 751-756.

Schnitzler, G.R. 2008. Control of nucleosome positions by DNA sequence and remodeling machines. *Cell Biochem Biophys* **51**(2-3): 67-80.

Schuettengruber, B., Chourrout, D., Vervoort, M., Leblanc, B., and Cavalli, G. 2007. Genome regulation by polycomb and trithorax proteins. *Cell* **128**(4): 735-745.

Schwartz, Y.B., Kahn, T.G., Nix, D.A., Li, X.Y., Bourgon, R., Biggin, M., and Pirrotta, V. 2006. Genome-wide analysis of Polycomb targets in Drosophila melanogaster. *Nat Genet* **38**(6): 700-705.

Scolnick, D.M. and Halazonetis, T.D. 2000. Chfr defines a mitotic stress checkpoint that delays entry into metaphase. *Nature* **406**(6794): 430-435.

Sengupta, A.K., Kuhrs, A., and Müller, J. 2004. General transcriptional silencing by a Polycomb response element in Drosophila. *Development* **131**(9): 1959-1965.

Shahbazian, M.D. and Zoghbi, H.Y. 2002. Rett syndrome and MeCP2: linking epigenetics and neuronal function. *Am J Hum Genet* **71**(6): 1259-1272.

Shao, Z., Raible, F., Mollaaghababa, R., Guyon, J.R., Wu, C.T., Bender, W., and Kingston, R.E. 1999. Stabilization of chromatin structure by PRC1, a Polycomb complex. *Cell* **98**(1): 37-46.

Sharif, J., Muto, M., Takebayashi, S., Suetake, I., Iwamatsu, A., Endo, T.A., Shinga, J., Mizutani-Koseki, Y., Toyoda, T., Okamura, K. et al. 2007. The SRA protein Np95 mediates epigenetic inheritance by recruiting Dnmt1 to methylated DNA. *Nature* **450**(7171): 908-912.

Shi, Y., Lan, F., Matson, C., Mulligan, P., Whetstine, J.R., Cole, P.A., Casero, R.A., and Shi, Y. 2004. Histone demethylation mediated by the nuclear amine oxidase homolog LSD1. *Cell* **119**(7): 941-953.

Shi, Y.J., Matson, C., Lan, F., Iwase, S., Baba, T., and Shi, Y. 2005. Regulation of LSD1 histone demethylase activity by its associated factors. *Mol Cell* **19**(6): 857-864.

Shikauchi, Y., Saiura, A., Kubo, T., Niwa, Y., Yamamoto, J., Murase, Y., and Yoshikawa, H. 2009. SALL3 interacts with DNMT3A and shows the ability to inhibit CpG island methylation in hepatocellular carcinoma. *Mol Cell Biol* **29**(7): 1944-1958.

Shilatifard, A. 2006. Chromatin modifications by methylation and ubiquitination: implications in the regulation of gene expression. *Annu Rev Biochem* **75**: 243-269.

Sleutels, F., Zwart, R., and Barlow, D.P. 2002. The non-coding Air RNA is required for silencing autosomal imprinted genes. *Nature* **415**(6873): 810-813.

Smit, A.F. 1999. Interspersed repeats and other mementos of transposable elements in mammalian genomes. *Curr Opin Genet Dev* **9**(6): 657-663.

Spada, F., Haemmer, A., Kuch, D., Rothbauer, U., Schermelleh, L., Kremmer, E., Carell, T., Längst, G., and Leonhardt, H. 2007. DNMT1 but not its interaction with the replication machinery is required for maintenance of DNA methylation in human cells. *J Cell Biol* **176**(5): 565-571.

Spahn, L. and Barlow, D.P. 2003. An ICE pattern crystallizes. *Nat Genet* **35**(1): 11-12.

Sparmann, A. and Van Lohuizen, M. 2006. Polycomb silencers control cell fate, development and cancer. *Nat Rev Cancer* **6**(11): 846-856.

Stewart, C.L., Stuhlmann, H., Jähner, D., and Jaenisch, R. 1982. De novo methylation, expression, and infectivity of retroviral genomes introduced into embryonal carcinoma cells. *Proc Natl Acad Sci USA* **79**(13): 4098-4102.

Stock, J.K., Giadrossi, S., Casanova, M., Brookes, E., Vidal, M., Koseki, H., Brockdorff, N., Fisher, A.G., and Pombo, A. 2007. Ring1-mediated ubiquitination of H2A restrains poised RNA polymerase II at bivalent genes in mouse ES cells. *Nat Cell Biol* **9**(12): 1428-1435.

Strahl, B.D. and Allis, C.D. 2000. The language of covalent histone modifications. *Nature* **403**(6765): 41-45.

Strohner, R., Nemeth, A., Jansa, P., Hofmann-Rohrer, U., Santoro, R., Längst, G., and Grummt, I. 2001. NoRC--a novel member of mammalian ISWI-containing chromatin remodeling machines. *Embo J* **20**(17): 4892-4900.

Strohner, R., Nemeth, A., Nightingale, K.P., Grummt, I., Becker, P.B., and Längst, G. 2004a. Recruitment of the nucleolar remodeling complex NoRC establishes ribosomal DNA silencing in chromatin. *Mol Cell Biol* **24**(4): 1791-1798.

Strohner, R., Németh, A., Nightingale, K.P., Grummt, I., Becker, P.B., and Längst, G. 2004b. Recruitment of the nucleolar remodeling complex NoRC establishes ribosomal DNA silencing in chromatin. *Mol Cell Biol* **24**(4): 1791-1798.

Suetake, I., Miyazaki, J., Murakami, C., Takeshima, H., and Tajima, S. 2003. Distinct enzymatic properties of recombinant mouse DNA methyltransferases Dnmt3a and Dnmt3b. *J Biochem* **133**(6): 737-744.

Suetake, I., Shinozaki, F., Miyagawa, J., Takeshima, H., and Tajima, S. 2004. DNMT3L stimulates the DNA methylation activity of Dnmt3a and Dnmt3b through a direct interaction. *J Biol Chem* **279**(26): 27816-27823.

Sun, Z.W. and Allis, C.D. 2002. Ubiquitination of histone H2B regulates H3 methylation and gene silencing in yeast. *Nature* **418**(6893): 104-108.

Swigut, T. and Wysocka, J. 2007. H3K27 demethylases, at long last. *Cell* **131**(1): 29-32.

Tachibana, M., Sugimoto, K., Nozaki, M., Ueda, J., Ohta, T., Ohki, M., Fukuda, M., Takeda, N., Niida, H., Kato, H. et al. 2002.

REFERENCES

G9a histone methyltransferase plays a dominant role in euchromatic histone H3 lysine 9 methylation and is essential for early embryogenesis. *Genes Dev* **16**(14): 1779-1791.

Takeshima, H., Suetake, I., Shimahara, H., Ura, K., Tate, S., and Tajima, S. 2006. Distinct DNA Methylation Activity of Dnmt3a and Dnmt3b towards Naked and Nucleosomal DNA. *J Biochem (Tokyo)* **139**(3): 503-515.

Takeshima, H., Suetake, I., and Tajima, S. 2008. Mouse Dnmt3a Preferentially Methylates Linker DNA and Is Inhibited by Histone H1. *Journal of Molecular Biology*.

Tatematsu, K.I., Yamazaki, T., and Ishikawa, F. 2000. MBD2-MBD3 complex binds to hemi-methylated DNA and forms a complex containing DNMT1 at the replication foci in late S phase. *Genes Cells* **5**(8): 677-688.

Taunton, J., Hassig, C.A., and Schreiber, S.L. 1996. A mammalian histone deacetylase related to the yeast transcriptional regulator Rpd3p. *Science* **272**(5260): 408-411.

Thåström, A., Bingham, L.M., and Widom, J. 2004a. Nucleosomal locations of dominant DNA sequence motifs for histone-DNA interactions and nucleosome positioning. *J Mol Biol* **338**(4): 695-709.

Thåström, A., Gottesfeld, J.M., Luger, K., and Widom, J. 2004b. Histone-DNA binding free energy cannot be measured in dilution-driven dissociation experiments. *Biochemistry* **43**(3): 736-741.

Thompson, N.E., Steinberg, T.H., Aronson, D.B., and Burgess, R.R. 1989. Inhibition of in vivo and in vitro transcription by monoclonal antibodies prepared against wheat germ RNA polymerase II that react with the heptapeptide repeat of eukaryotic RNA polymerase II. *J Biol Chem* **264**(19): 11511-11520.

Treier, M., Staszewski, L.M., and Bohmann, D. 1994. Ubiquitin-dependent c-Jun degradation in vivo is mediated by the delta domain. *Cell* **78**(5): 787-798.

Tsukiyama, T. 2002. The in vivo functions of ATP-dependent chromatin-remodelling factors. *Nat Rev Mol Cell Biol* **3**(6): 422-429.

Turner, B.M. 2002. Cellular memory and the histone code. *Cell* **111**(3): 285-291.

-. 2007. Defining an epigenetic code. *Nat Cell Biol* **9**(1): 2-6.

Uchida, K., Suzuki, H., Maruta, H., Abe, H., Aoki, K., Miwa, M., and Tanuma, S. 1993. Preferential degradation of protein-bound (ADP-ribose)n by nuclear poly(ADP-ribose) glycohydrolase from human placenta. *J Biol Chem* **268**(5): 3194-3200.

Uemura, T., Kubo, E., Kanari, Y., Ikemura, T., Tatsumi, K., and Muto, M. 2000. Temporal and spatial localization of novel nuclear protein NP95 in mitotic and meiotic cells. *Cell Struct Funct* **25**(3): 149-159.

Unoki, M., Bronner, C., and Mousli, M. 2008. A concern regarding the current confusion with the human homolog of mouse Np95, ICBP90/UHRF1. *Radiat Res* **169**(2): 240-244.

Unoki, M. and Nakamura, Y. 2003. Methylation at CpG islands in intron 1 of EGR2 confers enhancer-like activity. *FEBS Lett* **554**(1-2): 67-72.

Unoki, M., Nishidate, T., and Nakamura, Y. 2004. ICBP90, an E2F-1 target, recruits HDAC1 and binds to methyl-CpG through its SRA domain. *Oncogene* **23**(46): 7601-7610.

Van De Wetering, M., Oving, I., Muncan, V., Pon Fong, M., Brantjes, H., Van Leenen, D., Holstege, F.C., Brummelkamp, T., Agami, R., and Clevers, H. 2003. Specific inhibition of gene expression using a stably integrated, inducible small-interfering-RNA vector. *EMBO Rep* **4**(6): 609-615.

Van De Wetering, M., Sancho, E., Verweij, C., de Lau, W., Oving, I., Hurlstone, A., van der Horn, K., Batlle, E., Coudreuse, D., Haramis, A.P. et al. 2002. The beta-catenin/TCF-4 complex imposes a crypt progenitor phenotype on colorectal cancer cells. *Cell* **111**(2): 241-250.

van der Horst, A., de Vries-Smits, A.M., Brenkman, A.B., van Triest, M.H., van den Broek, N., Colland, F., Maurice, M.M., and Burgering, B.M. 2006. FOXO4 transcriptional activity is regulated by monoubiquitination and USP7/HAUSP. *Nat Cell Biol* **8**(10): 1064-1073.

van der Knaap, J.A., Kumar, B.R., Moshkin, Y.M., Langenberg, K., Krijgsveld, J., Heck, A.J., Karch, F., and Verrijzer, C.P. 2005. GMP synthetase stimulates histone H2B deubiquitylation by the epigenetic silencer USP7. *Mol Cell* **17**(5): 695-707.

Vaquero, A., Loyola, A., and Reinberg, D. 2003. The constantly changing face of chromatin. *Science of aging knowledge environment : SAGE KE* **2003**(14): RE4.

Varga-Weisz, P.D. and Becker, P.B. 2006. Regulation of higher-order chromatin structures by nucleosome-remodelling factors. *Curr Opin Genet Dev* **16**(2): 151-156.

Vassilev, A.P., Rasmussen, H.H., Christensen, E.I., Nielsen, S., and Celis, J.E. 1995. The levels of ubiquitinated histone H2A are highly upregulated in transformed human cells: partial colocalization of uH2A clusters and PCNA/cyclin foci in a fraction of cells in S-phase. *J Cell Sci* **108 (Pt 3)**: 1205-1215.

Verona, R.I., Mann, M.R., and Bartolomei, M.S. 2003. Genomic imprinting: intricacies of epigenetic regulation in clusters. *Annu Rev Cell Dev Biol* **19**: 237-259.

Vilkaitis, G., Suetake, I., Klimasauskas, S., and Tajima, S. 2004. Processive methylation of hemimethylated CpG sites by mouse Dnmt1 DNA methyltransferase. *J Biol Chem* **280**(1): 64-72.

Viré, E., Brenner, C., Deplus, R., Blanchon, L., Fraga, M., Didelot, C., Morey, L., Van Eynde, A., Bernard, D., Vanderwinden, J.M. et al. 2005. The Polycomb group protein EZH2 directly controls DNA methylation. *Nature* **439**(7078): 871-874.

Vissers, J., Nicassio, F., Van Lohuizen, M., Di Fiore, P.P., and Citterio, E. 2008. The many faces of ubiquitinated histone H2A: insights from the DUBs. *Cell Div* **3**: 8.

Vos, L.J., Famulski, J.K., and Chan, G.K. 2006. How to build a centromere: from centromeric and pericentromeric chromatin to kinetochore assembly. *Biochem Cell Biol* **84**(4): 619-639.

Wang, H., Wang, L., Erdjument-Bromage, H., Vidal, M., Tempst, P., Jones, R.S., and Zhang, Y. 2004a. Role of histone H2A ubiquitination in Polycomb silencing. *Nature* **431**(7010): 873-878.

Wang, L., Brown, J.L., Cao, R., Zhang, Y., Kassis, J.A., and Jones, R.S. 2004b. Hierarchical recruitment of polycomb group silencing complexes. *Mol Cell* **14**(5): 637-646.

Wang, R.Y., Huang, L.H., and Ehrlich, M. 1984. Human placental DNA methyltransferase: DNA substrate and DNA binding specificity. *Nucleic Acids Res* **12**(8): 3473-3490.

Wei, Y., Yu, L., Bowen, J., Gorovsky, M.A., and Allis, C.D. 1999. Phosphorylation of histone H3 is required for proper chromosome condensation and segregation. *Cell* **97**(1): 99-109.

Welchman, R.L., Gordon, C., and Mayer, R.J. 2005. Ubiquitin and ubiquitin-like proteins as multifunctional signals. *Nat Rev Mol Cell Biol* **6**(8): 599-609.

Wigler, M.H. 1981. The inheritance of methylation patterns in vertebrates. *Cell* **24**(2): 285-286.

Wilkinson, K.D., Urban, M.K., and Haas, A.L. 1980. Ubiquitin is the ATP-dependent proteolysis factor I of rabbit reticulocytes. *J Biol Chem* **255**(16): 7529-7532.

Woo, H., Pontes, O., Pikaard, C., and Richards, E. 2007. VIM1, a methylcytosine-binding protein required for centromeric heterochromatinization. *Genes Dev* **21**(3): 267-277.

Wood, A., Krogan, N.J., Dover, J., Schneider, J., Heidt, J., Boateng, M.A., Dean, K., Golshani, A., Zhang, Y., Greenblatt, J.F. et

al. 2003a. Bre1, an E3 ubiquitin ligase required for recruitment and substrate selection of Rad6 at a promoter. *Mol Cell* **11**(1): 267-274.

Wood, A., Schneider, J., Dover, J., Johnston, M., and Shilatifard, A. 2003b. The Paf1 complex is essential for histone monoubiquitination by the Rad6-Bre1 complex, which signals for histone methylation by COMPASS and Dot1p. *J Biol Chem* **278**(37): 34739-34742.

Woodcock, C.L. 2006. Chromatin architecture. *Curr Opin Struct Biol* **16**(2): 213-220.

Woodcock, C.L. and Dimitrov, S. 2001. Higher-order structure of chromatin and chromosomes. *Curr Opin Genet Dev* **11**(2): 130-135.

Woodcock, C.L. and Horowitz, R.A. 1995. Chromatin organization re-viewed. *Trends Cell Biol* **5**(7): 272-277.

Woodcock, C.L., Skoultchi, A.I., and Fan, Y. 2006. Role of linker histone in chromatin structure and function: H1 stoichiometry and nucleosome repeat length. *Chromosome Res* **14**(1): 17-25.

Wu, R.S. and Bonner, W.M. 1981. Separation of basal histone synthesis from S-phase histone synthesis in dividing cells. *Cell* **27**(2 Pt 1): 321-330.

Wu, X., Gong, Y., Yue, J., Qiang, B., Yuan, J., and Peng, X. 2008. Cooperation between EZH2, NSPc1-mediated histone H2A ubiquitination and Dnmt1 in HOX gene silencing. *Nucleic Acids Research* **36**(11): 3590-3599.

Wutz, A. and Barlow, D.P. 1998. Imprinting of the mouse Igf2r gene depends on an intronic CpG island. *Mol Cell Endocrinol* **140**(1-2): 9-14.

Wyce, A., Xiao, T., Whelan, K.A., Kosman, C., Walter, W., Eick, D., Hughes, T.R., Krogan, N.J., Strahl, B.D., and Berger, S.L. 2007. H2B ubiquitylation acts as a barrier to Ctk1 nucleosomal recruitment prior to removal by Ubp8 within a SAGA-related complex. *Mol Cell* **27**(2): 275-288.

Wysocka, J., Swigut, T., Xiao, H., Milne, T.A., Kwon, S.Y., Landry, J., Kauer, M., Tackett, A.J., Chait, B.T., Badenhorst, P. et al. 2006. A PHD finger of NURF couples histone H3 lysine 4 trimethylation with chromatin remodelling. *Nature* **442**(7098): 86-90.

Xi, S., Zhu, H., Xu, H., Schmidtmann, A., Geiman, T.M., and Muegge, K. 2007. Lsh controls Hox gene silencing during development. *Proc Natl Acad Sci USA* **104**(36): 14366-14371.

Xie, S., Wang, Z., Okano, M., Nogami, M., Li, Y., He, W.W., Okumura, K., and Li, E. 1999. Cloning, expression and chromosome locations of the human DNMT3 gene family. *Gene* **236**(1): 87-95.

Xie, S.Q., Martin, S., Guillot, P.V., Bentley, D.L., and Pombo, A. 2006. Splicing speckles are not reservoirs of RNA polymerase II, but contain an inactive form, phosphorylated on serine2 residues of the C-terminal domain. *Mol Biol Cell* **17**(4): 1723-1733.

Xin, H., Yoon, H.G., Singh, P.B., Wong, J., and Qin, J. 2004. Components of a pathway maintaining histone modification and heterochromatin protein 1 binding at the pericentric heterochromatin in Mammalian cells. *J Biol Chem* **279**(10): 9539-9546.

Yang, X.J. 2005. Multisite protein modification and intramolecular signaling. *Oncogene* **24**(10): 1653-1662.

Yoder, J.A., Walsh, C.P., and Bestor, T.H. 1997. Cytosine methylation and the ecology of intragenomic parasites. *Trends Genet* **13**(8): 335-340.

Yoder, J.A., Yen, R.W., Vertino, P.M., Bestor, T.H., and Baylin, S.B. 1996. New 5' regions of the murine and human genes for DNA (cytosine-5)-methyltransferase. *J Biol Chem* **271**(49): 31092-31097.

Yokochi, T. and Robertson, K.D. 2002. Preferential methylation of unmethylated DNA by Mammalian de novo DNA methyltransferase Dnmt3a. *J Biol Chem* **277**(14): 11735-11745.

Yoo, H.Y., Noshari, J., and Lapeyre, J.N. 1987. Subunit and functional size of human placental DNA methyltransferase involved in de novo and maintenance methylation. *J Biol Chem* **262**(17): 8066-8070.

Zapata, J.M., Pawlowski, K., Haas, E., Ware, C.F., Godzik, A., and Reed, J.C. 2001. A diverse family of proteins containing tumor necrosis factor receptor-associated factor domains. *J Biol Chem* **276**(26): 24242-24252.

Zhan, S., Shapiro, D.N., and Helman, L.J. 1994. Activation of an imprinted allele of the insulin-like growth factor II gene implicated in rhabdomyosarcoma. *J Clin Invest* **94**(1): 445-448.

Zhang, X.Y., Pfeiffer, H.K., Thorne, A.W., and McMahon, S.B. 2008a. USP22, an hSAGA subunit and potential cancer stem cell marker, reverses the polycomb-catalyzed ubiquitylation of histone H2A. *Cell Cycle* **7**(11): 1522-1524.

Zhang, X.Y., Varthi, M., Sykes, S.M., Phillips, C., Warzecha, C., Zhu, W., Wyce, A., Thorne, A.W., Berger, S.L., and McMahon, S.B. 2008b. The putative cancer stem cell marker USP22 is a subunit of the human SAGA complex required for activated transcription and cell-cycle progression. *Mol Cell* **29**(1): 102-111.

Zhang, Y. 2003. Transcriptional regulation by histone ubiquitination and deubiquitination. *Genes Dev* **17**(22): 2733-2740.

Zhang, Y., Ng, H.H., Erdjument-Bromage, H., Tempst, P., Bird, A.P., and Reinberg, D. 1999. Analysis of the NuRD subunits reveals a histone deacetylase core complex and a connection with DNA methylation. *Genes Dev* **13**(15): 1924-1935.

Zhao, Q., Rank, G., Tan, Y., Li, H., Moritz, R., Simpson, R., Cerruti, L., Curtis, D., Patel, D., Allis, C.D. et al. 2009. PRMT5-mediated methylation of histone H4R3 recruits DNMT3A, coupling histone and DNA methylation in gene silencing. *Nat Struct Mol Biol* **16**(3): 304-311.

Zhao, Y., Lang, G., Ito, S., Bonnet, J., Metzger, E., Sawatsubashi, S., Suzuki, E., Le Guezennec, X., Stunnenberg, H.G., Krasnov, A. et al. 2008. A TFTC/STAGA module mediates histone H2A and H2B deubiquitination, coactivates nuclear receptors, and counteracts heterochromatin silencing. *Mol Cell* **29**(1): 92-101.

Zhou, Q., Agoston, A., Atadja, P., Nelson, W., and Davidson, N. 2008a. Inhibition of Histone Deacetylases Promotes Ubiquitin-Dependent Proteasomal Degradation of DNA Methyltransferase 1 in Human Breast Cancer Cells. *Molecular Cancer Research* **6**(5): 873-883.

Zhou, W., Zhu, P., Wang, J., Pascual, G., Ohgi, K.A., Lozach, J., Glass, C.K., and Rosenfeld, M.G. 2008b. Histone H2A monoubiquitination represses transcription by inhibiting RNA polymerase II transcriptional elongation. *Mol Cell* **29**(1): 69-80.

Zhu, B., Zheng, Y., Pham, A.D., Mandal, S.S., Erdjument-Bromage, H., Tempst, P., and Reinberg, D. 2005. Monoubiquitination of human histone H2B: the factors involved and their roles in HOX gene regulation. *Molecular Cell* **20**(4): 601-611.

Zhu, H., Geiman, T.M., Xi, S., Jiang, Q., Schmidtmann, A., Chen, T., Li, E., and Muegge, K. 2006. Lsh is involved in de novo methylation of DNA. *Embo J* **25**(2): 335-345.

Zhu, P., Zhou, W., Wang, J., Puc, J., Ohgi, K., Erdjumentbromage, H., Tempst, P., Glass, C., and Rosenfeld, M. 2007a. A Histone H2A Deubiquitinase Complex Coordinating Histone Acetylation and H1 Dissociation in Transcriptional Regulation. *Molecular Cell* **27**(4): 609-621.

Zhu, P., Zhou, W., Wang, J., Puc, J., Ohgi, K.A., Erdjument-Bromage, H., Tempst, P., Glass, C.K., and Rosenfeld, M.G. 2007b. A histone H2A deubiquitinase complex coordinating histone acetylation and H1 dissociation in transcriptional regulation. *Mol Cell* **27**(4): 609-621.

G APPENDIX

G.1 Curriculum vitae

Name: Felle

First name: Max

Nationality: German

Date of birth: December 5th, 1978

Place of birth: Bruxelles, Belgium

Marital status: Single

Scientific education:

April 2006-present   PhD at the Institute of Biochemistry III, University of Regensburg
                     '*DNA methylation in chromatin – complexes and mechanisms'*.
                     Supervisor: Prof. Dr. G. Längst

2000-2005   Undergraduate and Graduate Studies in Biochemistry at the
                     University of Regensburg

April-Dec. 2005   Diploma-thesis: ,*Establishment of an in vitro Polymerase I*
                     Transcriptions Assay using quantitative PCR'
                     Lab group of Joachim Griesenbeck; Department of Biochemistry III,
                     Professor H. Tschochner

March 2005   Diploma-examinations: Biochemistry, Molecular Cell Biology,
                     Organic Chemistry

1999   High School Diploma (Abitur)

Internships

Sept. – Dec. 2004   Scientific Assistant at the Clinic of the University of Regensburg,
                     Department of Ophthalmogenetics, Lab group of Dr. M. Preising,
                     molecular genetics

March – June 2004   CNRS Marseille (Centre National de Recherche Scientifique), Lab
                     group of Dr. W. Nitschke, bioenergetics and the evolution of proteins

Oct. – Dec. 2003   NOVARTIS Basel, Department of Biotechnology and Development,
                     Lab group of Dr. D. Perl, physical-chemical analytics

Max Felle   --------------------------------

G.2 List of publications

Fellinger, K., Rothbauer, U., Felle, M., Längst, G., and Leonhardt, H. 2009. Dimerization of DNA methyltransferase 1 is mediated by its regulatory domain. *J Cell Biochem* **106**(4): 521-528.

Max Felle, Josef H. Exler, Rainer Merkl, Karoline Dachauer, Alexander Brehm, Ingrid Grummt and Gernot Längst (2009). 'A nucleosomal switch regulates the activity of rRNA genes'. *Submitted*

G.3 Conferences

June 26th – 29th 2007, Network of Excellence (NOE) Symposium in Stockolm/ Sweden; Epigenetics
Title of poster: 'Comparative analysis of DNA methyltransferase complexes from native tissue and tumor cells'

March 27th – 29th 2008, 59th Mosbacher Kolloquium in Mosbach/Baden Germany, Epigenetics – Molecular principles and mechanisms

Eidesstattliche Erklärung

Hiermit erkläre ich, Max Fabian Felle, geboren am 5. Dezember 1978 in Brüssel, an Eides statt, dass ich die vorliegende Arbeit mit dem Titel

‚DNA methylation in chromatin – complexes and mechanisms'

ohne unzulässige Hilfe Dritter und ohne Benutzung anderer als der angegebenen Hilfsmittel angefertigt habe. Die aus anderen Quellen direkt oder indirekt übernommenen Daten und Konzepte sind unter Angabe des Literaturzitats gekennzeichnet.

Die Arbeit wurde bisher weder im In- noch im Ausland in gleicher oder ähnlicher Form einer anderen Prüfungsbehörde vorgelegt.

Ich versichere an Eides statt, dass ich nach bestem Wissen die reine Wahrheit gesagt und nichts verschwiegen habe.

Regensburg, ...

(Max Felle)

Danksagung

Meinem Doktorvater Prof. Dr. Gernot Längst danke ich herzlichst für die Vergabe dieser Arbeit, die vielfältigen Anregungen und die fachliche Betreuung. Besonders bedanke ich mich für die Freiheiten und die Großzügigkeit, die mir gewährt wurden, und dass ich stets in meinem Handeln unterstützt wurde. Ich hätte mir keinen besseren Betreuer wünschen können. (and mac rules!)

Mein Dank gilt gleichermaßen Prof. Dr. Herbert Tschochner für die Bereitstellung der Arbeitsmittel und die sehr angenehme Atmosphäre am Institut. Danke auch, dass wir gemeinsam den Malgrübler – die beste Skitour Tirols – erzwungen haben. Ich hoffe, dass wir noch ein paar schöne Bergabenteuer erleben werden.

Bei Prof. Dr. Sterner bedanke ich für die bereitwillige Übernahme des Zweitgutachtens und bei Prof. Dr. Seufert für die Übernahme des dritten Prüfers.

Elisabeth Silberhorn danke ich from the very bottom of my heart für die grossartige Zusammenarbeit, die enorme Unterstützung und die vielen netten Stunden.

Meinen Dank richte ich auch Regina Gröbner-Ferreira für die stets perfekten Chromatin Rekonstitutionen und Sucrose-Gradienten.

Ein besonderes Dankeschön richtet sich an alle Mitarbeiter des Lehrstuhls für Biochemie III, für das angenehme Arbeitsklima, anregende Diskussionen und die stets gewährte Hilfsbereitschaft.

Für die mühevolle und geduldige Unterstützung danke ich Tom Schubert, Josef Exler, Karina Zillner und Spiderpig, denn sie machten was die vier eben so machten.

Dankbar bin ich meiner Familie, meinen Freunden und der Brunnleite 8 für das stets offene Ohr und den wunderbaren Ausgleich.